Mycobacterial Fatty Acid Metabolism: Identification of Novel Drug Targets and Chemotherapeutics

A thesis submitted to the

UNIVERSITY OF BIRMINGHAM

for the degree of

Doctor of Philosophy

September 2011

Rebecca Clare Taylor, B.Sc. (Hons)

Abstract

Tuberculosis has been a deadly human pathogen for thousands of years and is as prevalent and lethal now as it was in the pre-antimicrobials era. With new challenges continually being presented in the form of multidrug resistant strains evolving and the implications of the HIV epidemic, it is imperative that every effort is made to understand the causative agent, *Mycobacterium tuberculosis*, and develop new effective and affordable drugs to treat the disease.

With this in mind, the first part of this project tests novel drugs that have been identified using different approaches. The desired targets for all the compounds were the fatty acid and mycolic acid biosynthesis systems in *M. tuberculosis*, *Mycobacterium bovis* BCG and *Mycobacterium smegmatis*. Some promising compounds were identified, which inhibited enzymes of the prokaryotic FAS-II system, whilst not affecting the mammalian FAS-I system.

As well as identifying new drugs, it is equally important to recognise the essential genes of *M. tuberculosis*, which could be novel drug targets. Whilst the fatty acid biosynthesis pathway has been well studied, a lot less is known about fatty acid degradation. *M. tuberculosis* has an abundance of *fad* genes, yet it is only recently that they have started to be explored. Here, the functions and roles of the *fadB* genes in *M. tuberculosis*, *M. bovis* BCG and *M. smegmatis* have been explored. By producing purified recombinant protein and generating gene deletion mutants, it has been possible to fully characterise *Mt*-FadB2 and provide preliminary information regarding *fadB3*, *fadB4* and *fadB5*.

Declaration

The work carried out in this thesis was carried out in the School of Biosciences at the University of Birmingham, Birmingham, UK, B15 2TT during the period October 2007 to September 2011. The work in this thesis is original except where acknowledged by reference.

No portion of the work is being, or has been submitted for a degree, diploma or any other qualification at any other University.

Acknowledgments

Firstly I would like to thank Prof. G. Besra for accepting me as a PhD student and giving me this fantastic opportunity. For always having faith in me and providing a boost of confidence when I most needed it. I must also thank Dr. A. Bhatt for always being so calm and patient, readily offering explanations and advice whenever required.

Secondly, I would like to acknowledge the collaborators who have entrusted their ideas and work with me. Primarily Dr. R. Veyron-Churlet and colleagues, for allowing me to contribute a small portion to their paper and to help understand the effects of FabH phosphorylation (Chapter 3). All the experiments in this chapter, apart from *Mt*-FabH protein preparation and the *in vitro Mt*-FabH assays, were performed by Veyron-Churlet *et al*. Thank you to Dr. Q. Al-Balas and the group from Strathclyde University for the opportunity to test all the thiolactomycin deriviatives and Dr. A. Pathak from the Southern Research Institute, Birmingham, Alabama, for providing the indole compounds (Chapter 2). Thank you, also, to Dr. L. Kremer and co-workers for providing so many vectors. I would like to thank all the other people who have provided their expertise so willingly – Dr. K. Fütterer for the much-needed help and advice with regard to protein crystallisation and X-ray diffraction. I really appreciate all the time you spent on my work and also for giving me the opportunity to supervise a project student. Dr. T. Dafforn for the help using the CD machine and analysing the data, and Rosemary Parslow for so patiently teaching me how to use the AUC.

Thirdly, a big thank you to the others in the Besra lab who have taught me so much and made the past four years such an enjoyable experience. Ali especially, for teaching me so many essential lab techniques from making buffers to designing my own experiments. Hemza and Sarah deserve a special mention for all their help with protein purification and crystallisation, and for helping me pick up the pieces when things didn't go to plan. Luke for all his handy time-saving advice and always having so many problem-solving ideas. Vee for so kindly making me compounds against his will, Albel for the technological aid, Arun for the words of wisdom regarding writing-up, Usha for help with the spec, George for always being there and knowing exactly what to say and kindly proofreading for me ☺, and of course Helen for keeping me sane.

Final thank yous go to all my fabulous friends from ringing, uni and school for providing an indispensable escape from lab work. To Matt for providing so much love and support along the way, and lastly to my mum and dad for all their invaluable words of encouragement, love and unwavering belief in me.

This thesis is dedicated
to my family, my friends
and all those suffering
from tuberculosis.

Table of contents

List of figures

Chapter 1.

Chapter 2.

Chapter 3.

Chapter 4.

List of tables

List of abbreviations

::	in complex
%	per cent
±	plus or minus standard error
2D	two-dimensional
α	alpha
A	adenine
A	amp(s)
Å	Ångstrom
aa	amino acid(s)
ABC transporter	ATP-binding cassette transporter
ACP	acyl carrier protein
AcpM	mycobacterial acyl carrier protein
Ac_xPIM_x	acylated PIM(s)
AD	*anno domini*
AES	allelic exchange substrate
AG	arabinogalactan
Ag85	antigen 85
AMP	adenosine monophosphate
Amy	nalidixic acid
APS	ammonium persulfate
Ara*f*	arabino*furanose*
ATP	adenosine triphosphate
AU	absorbance units
AUC	analytical ultracentrifuge *or* ultracentrifugation
β	beta
BC	before Christ
BCA	bicinchoninic acid
BCG	Bacille Calmette-Guérin
BCIP	5-bromo-4-chloro-3-indolyl phosphate
BLAST	Basic Local Alignment Search Tool

bp	base pair(s)
BSA	bovine serum albumin
°C	degrees Celsius
C	cytosine
c.	circa
CAPS	*N*-cyclohexyl-3-aminopropanesulfonic acid
CD	circular dichroism
CFU/ml	colony-forming units per ml
Ci	Curies
cm	centimeter(s)
Cm	chloramphenicol
CoA	coenzyme A
CoA-SH	coenzyme A
cpm *or* CPM	counts per minute
CSPD	disodium 3-(4-methoxyspiro{1,2-dioxetane-3,2′-(5′-chloro)tricyclo[3.3.1.1^{3,7}]decan}-4-yl) phenyl phosphate
δ	delta
Δ	delta
d	deionised
D	dextrorotatory
Da	Daltons
DAG	diacyl glycerol
(*meso*)-DAP	(*meso*)-diaminopimelic acid
DAT	diacyl trehalose
DIG	digoxygenin
DMSO	dimethyl sulfoxide
DNA	deoxyribonucleic acid
DNase	deoxyribonuclease
DOTS	directly observed therapy, short-course
DTT	dithiothreitol
dUTP	deoxyuridine triphosphate
E1-FAS-II	FAS-II elongation phase 1

E2-FAS-II	FAS-II elongation phase 2
EB	Tris·HCl buffer
EC	Enzyme Commission number
e.g.	for example
Ec	*E. coli*
EDTA	ethylenediaminetetraacetic acid
Em	emission
etc.	*et cetera*; and so forth
Ex	excitation
F	Farad(s)
F^-	devoid of F plasmid
FAD	flavin adenine dinucleotide (fully oxidised)
$FADH_2$	flavin adenine dinucleotide (hydroquinone)
FAMEs	fatty acid methyl esters
FAS	fatty acid synthase
FDA	Food and Drug Administration
FHA	forkhead associated
FMN	flavin monomucleotide
γ	gamma
g	gram(s)
g	force of gravity
G	guanine
Gal	galactose
Gal*f*	galacto*furanose*
gDNA	genomic DNA
GlcNAc	*N*-acetylglucosamine
GMM	glucose monomycolate
GPL	glycopeptidolipid
GST	glutathione S-transferase
h	hour(s)
HAD	β-hydroxyacyl-AcpM dehydratase
HEPES	4-(2-hydroxyethyl)-1-piperazineethanesulfonic acid

His-tag *or* His_6	His-His-His-His-His-His
HIV-1	human immunodeficiency virus-1
hyg	hygromycin
IC_{50}	half maximal inhibitory concentration
i.e.	*id est*
IPTG	isopropyl β-D-1-thiogalactopyranoside
KAS	β-ketoacyl-ACP synthase
kb	kilobase(s)
kBq	kilo Becquerel(s)
k_{cat}	turnover number
kDa	kilo Dalton(s)
K_M	Michaelis constant
λ	lambda prophage
l	litre
L	levorotatory
LAM	lipoarabinomannan
LB	Luria-Bertani
LM	lipomannan
µ	micro
m	milli
M	molar
mAG	arabinogalactan with attached mycolic acids
MALDI-TOF	matrix-assisted laser desorption/ionisation – time-of-flight
MAMEs	mycolic acid methyl esters
manLAM	LAM with capping monooligosaccharides
Mb	megabase(s)
Mb	*M. bovis* BCG
MDR	multidrug-resistant
MIC	minimum inhibitory concentration
min	minute(s)
µm	micrometer(s)
mm	millimeter(s)

MM	minimal medium
mol	moles
MOPS	3-(*N*-morpholino)propaneulfonic acid
MP	Tris/salt phage buffer
MPD	2-methyl-2,4-pentanediol
MPI	mannosyl-phosphatidyl-*myo*-inositol
mRNA	messenger RNA
Ms	*M. smegmatis*
MS/MS	tandem mass spectrometry
Mt	*M. tuberculosis*
MurNGlyc	*N*-glycolyl muramic acid
myc-PL	6-*O*-mycolyl-β-D-mannopyranosyl-1-phosphoheptaprenol
m/z	mass to charge ratio
n	nano
N	molar in relation to acids or alkalis
N3	high salt, acidic neutralisation buffer
N-AC	*N*-acetylcysteamine
NAD^+	nicotinamide adenine dinucleotide
NADH	reduced NAD^+
$NADP^+$	nicotinamide acenine dinucleotide phosphate
NADPH	reduced $NADP^+$
NDH	NADH dehydrogenase
nm	nanometers
NMR	nuclear magnetic resonance
NQO	NADPH:quinone oxidoreductase(s)
dNTP	deoxyribonucleotide triphosphate
Ω	Ohm(s)
$\omega^2 r$	rotational velocity
(O)ADC	(oleic acid), bovine albumin, dextrose, catalase
OD_x	optical dentisty at *x* nm
p	pico
p	*para*

P	phosphate group, $[PO_4]^{3-}$
P1	Tris/EDTA/RNase A buffer
P2	SDS lysis buffer
PAGE	polyacrylamide gel electrophoresis
PAT	polyacyl trehalose
PB	DNA wash buffer
PBS	phosphate-buffered saline
PCR	polymerase chain reaction
PDB	Protein Data Bank
PDIM	phthiocerol dimycocerosate
PE	ethanolic wash buffer
PEG	polyethylene glycol
PG	peptidoglycan
pH	power of hydrogen
pI	isoelectric point
PI	phosphatidylinositol
PILAM	LAM with phosphoinositide units
PIM	phosphatidyl-*myo*-inositol-mannoside
PL	phospholipid
PLT	platensimycin
RhaP	rhamnose-phosphate
RNA	ribonucleic acid
RND	resistance, nodulation and cell division
rpm	revolutions per minute
rRNA	ribosomal RNA
SDS	sodium dodecyl sulfate
SE	sedimentation equilibrium
sec	second(s)
SL	sulfolipid
S_N2	bimolecular nucleophilic substitution
STPK	serine/threonine protein kinase(s)
Str	streptomycin

SV	sedimentation velocity
T	thymine
T-FAS-II	FAS-II termination phase
TAE	Tris·acetate/EDTA buffer
TB	tuberculosis
TBAH	tetrabutylammonium hydroxide
TBS	Tris/NaCl buffer
TBS-T	TBS buffer with added Tween®-20
TCA	tricarboxylic acid
TDM	trehalose 6,6′-dimycolate (cord factor)
TEMED	tetramethylethylenediamine
Tet	tetracycline
THF	tetrahydrofuran
TLC	thin-layer chromatography
TMM	trehalose monomycolate
TNF-α	tumour necrosis factor-α
Tris	tris(hydroxymethyl)aminomethane
tRNA	transfer RNA
TSB	tryptic soy broth
UV	ultra-violet
V	volt(s)
V_{max}	maximum reaction rate
v/v	volume to volume ratio
WHO	World Health Organisation
WT	wild-type
w/v	weight to volume ratio
XDR	extensively drug-resistant

Published work associated with this thesis

Al-Balas Q, Anthony NG, Al-Jaidi B, Alnimr A, Abbott G, Brown AK, Taylor RC, Besra GS, McHugh TD, Gillespie SH, Johnston BF, Mackay SP, Coxon GD (2009) Identification of 2-aminothiazole-4-carboxylate derivatives active against *Mycobacterium tuberculosis* H_{37}Rv and the beta-ketoacyl-ACP synthase *mt*FabH. **PLoS One** 4: e5617

Brown AK, Taylor RC, Bhatt A, Fütterer K, Besra GS (2009) Platensimycin activity against mycobacterial beta-ketoacyl-ACP synthases. **PLoS One** 4: e6306

Taylor RC, Brown AK, Singh A, Bhatt A, Besra GS (2010) Characterization of a β-hydroxybutyryl-CoA dehydrogenase from *Mycobacterium tuberculosis*. **Microbiology** 156: 1975–1982

Veyron-Churlet R, Molle V, Taylor RC, Brown AK, Besra GS, Zanella-Cléon I, Fütterer K, Kremer L (2009) The *Mycobacterium tuberculosis* beta-ketoacyl-acyl carrier protein synthase III activity is inhibited by phosphorylation on a single threonine residue. **Journal of Biological Chemistry** 284: 6414–6424

CHAPTER 1

General Introduction

1.1. *Mycobacterium tuberculosis* and Mycobacteriaceae

Tuberculosis (TB) is one of the world's most lethal diseases caused by a single infectious agent (Kremer *et al*. 2002a). The vast majority of cases are due to infection by the species *Mycobacterium tuberculosis*, a highly aerobic, non-motile, rod-shaped bacterium of approximately 2 μm in length, with no known host other than man (Glickman & Jacobs 2001). The disease is highly contagious due to the air-borne nature of bacterial transmission and as such is estimated to affect one third of the world's population. The World Health Organisation (WHO) has stated that someone in the world is newly infected with *M. tuberculosis* every second (WHO 2010).

M. tuberculosis belongs to the family Mycobacteriaceae. The prefix "myco" in Latin can mean "fungus" or "waxy" and here it refers to the waxy nature of the cell wall.

Kingdom: Bacteria

Phylum: Actinobacteria

Order: Actinomycetales

Suborder: Corynebacterineae

Family: Mycobacteriaceae

Genus: *Mycobacterium*

Species: *M. tuberculosis*

FIGURE 1-1. Images of *Mycobacterium tuberculosis*. *Left:* Scanning electron micrograph of *M. tuberculosis* cells (Tuberculosis Research Section). *Right*: Colonies of *M. tuberculosis* on Lowenstein-Jensen medium (Kubica 1976).

All mycobacteria share similar cell wall characteristics, which classes them separately as acid-fast Gram-positive bacilli. Acid-fast, or acid-resistant, refers to the inability of certain biological structures to decolourise upon acid treatment once stain, such as Ziehl-Neelsen carbol fuschin, has been taken up (Pommerville 2007). *Nocardia*, endospores, the head of sperm and all mycobacteria are acid-fast due to the high lipid content and waxy nature of their cell walls (Gaud & Gupta 2008). The species that cause disease are described as the *M. tuberculosis* complex, and include *M. tuberculosis*, *Mycobacterium bovis*, *Mycobacterium microti*, *Mycobacterium africanum*, *Mycobacterium pinnipedii* and *Mycobacterium caprae*. Between these species there is only 0.01–0.03 % nucleotide variation, a remarkably low percentage compared with most bacterial species, which show much less genetic homogeneity of 1 % or more (Gutierrez *et al*. 2006).

1.1.1. Using surrogates to study *M. tuberculosis*.

The rate at which species within the Mycobacteriaceae family grow differs greatly; some are fast-growing while others are slow-growing and fastidious to culture. *M. tuberculosis* and

Mycobacterium leprae fall into the latter category: *M. tuberculosis* has a doubling time of 15–20 hours. To-date it has not been possible to culture *M. leprae*, the bacillus that causes leprosy, *in vitro* at all. Similarly, another species, *Mycobacterium genavense*, has only been identified by molecular means (Colston & Cox 1999). Due to the slow growth rate of *M. tuberculosis* and its highly infectious nature (*M. tuberculosis* is a Category 3 human pathogen), other species of the family are often used to study shared elements.

The most closely related surrogate used is *M. bovis* strain Bacille Calmette-Guérin (BCG). Although also slow growing, it is an attenuated form of *M. bovis*, classed as Category 2, and is thus non-infective. *M. bovis* causes active tuberculosis in cattle (bovine TB) but is also well known to cause tuberculosis in humans (De la Rua-Domenech 2006). Zoonotic transmission is usually through ingestion or inhalation and is indistinguishable from disease caused by *M. tuberculosis*. Wild-type *M. bovis* BCG colonies can be seen following 3 weeks of incubation at 37 °C, and in liquid medium a film of cells appears after 5–7 days.

Another species used to replace *M. tuberculosis* is *Mycobacterium smegmatis*, a soil-dwelling saprophyte (Shiloh & DiGiuseppe Champion 2009). Approximately 30 % of *M. tuberculosis* genes lack conserved orthologues in *M. smegmatis*, compared to only 3 % in *M. bovis*, but, although a much more distant relative, *M. smegmatis* has been a major tool in the development of plasmid transformation in mycobacteria (Altaf *et al*. 2010, Shiloh & DiGiuseppe Champion 2009, Snapper *et al*. 1990). The doubling time is roughly 3 hours, visible colonies can be seen after 3–4 days of incubation and it is considered generally non-pathogenic.

One final model species is *Mycobacterium marinum*, which was first isolated from fish in 1926 (Aronson 1926). It is an opportunistic human pathogen that has been seen to infect *via*

swimming pools and fish tanks (Beran *et al*. 2006, Linell & Norden 1954). Infection mainly affects the cooler extremities (hands, arms and feet) because incubation at 37 °C inhibits *M. marinum* cell growth. *M. marinum* can be cultured at 30 °C and has a doubling time of 6–10 hours. The genome is larger than that of *M. tuberculosis* by 2.2 Mb, reflecting the greater number of environmental niches *M. marinum* can occupy (Tobin & Ramakrishnan 2008). For example, *M. marinum* has a gene encoding β-carotene, *crtB*, which protects the bacilli from photo-oxidative damage when living outside a host. This gene has been lost in *M. tuberculosis* (Ramakrishnan *et al.* 1997). Despite this and the fact that orthologous regions of the two genomes share only 85 % identity, the granulomas resulting from infection of either species are often indistinguishable, making this a good surrogate for studying infection (Tobin & Ramakrishnan 2008).

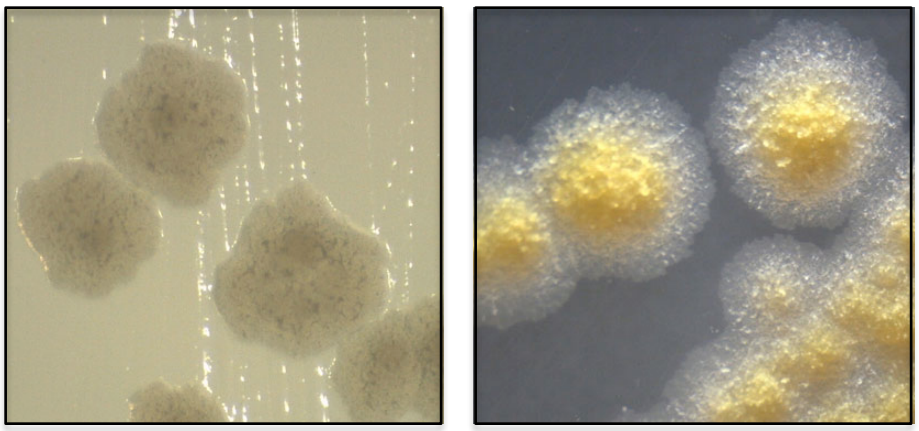

FIGURE 1-2. Surrogate mycobacterial species used in the laboratory. *Left*: *M. smegmatis* colonies on trypticase soy agar (Bryan MacDonald, Christopher Adams, and Kyle Smith, Brigham Young University, Provo, UT). *Right*: *M. marinum* colonies on 7H11 agar with oleic acid-albumin-dextrose-catalase enrichment (Richard A. Robison, Gable Moffitt, Neal Thomson, and Marissa Cohen, Brigham Young University, Provo, UT).

1.2. Evolutionary history of tuberculosis and its discovery

The most ancient evidence of tuberculosis has come from fossil remains of an estimated 500,000-year-old *Homo erectus* skeleton in Turkey (Kappelman *et al*. 2008). The skull

revealed small lesions that are distinctive to the *Leptomeningitis tuberculosa* form of TB. During the migration out of Africa, early dark-skinned hominins were experiencing new conditions, including reduced UV exposure. The group who made the discovery hypothesised that these human ancestors would have been immunocompromised from vitamin D deficiency and thus more likely to succumb to disease.

It has been widely suggested that tuberculosis was transmitted to humans from cattle infected with *M. bovis* during the time of animal domestication roughly 15,000 years ago. Indeed, there is much evidence of TB infection in mummies from Egypt, China and South America. One such study of ancient Egyptian mummies, however, suggests that modern *M. tuberculosis* may have originated from a *M. africanum*-like species (Zink *et al*. 2003). The ancient DNA was extracted and analysed by spoligotyping, a method that compares polymorphisms in the direct repeat locus of mycobacterial chromosomes. None of the spoligotypes found reflected those of *M. bovis*; mummies dating from 2050–1650 BC showed a *M. africanum*-like pattern and later mummies (circa 500 BC) showed typical *M. tuberculosis* patterns.

Due to the lack of genetic variation between *M. tuberculosis* species, it has previously been estimated that the modern-day *M. tuberculosis* originated around 35,000 years ago after clonal expansion following an evolutionary bottleneck (Hughes *et al*. 2002). A more recent report from 2005, however, has pushed the date of the progenitor species from which *M. tuberculosis* evolved back much further by studying the DNA of current tubercle bacilli from East Africa (Gutierrez *et al*. 2006). Knowing how closely related the *M. tuberculosis* complex species are and using phylogenetic analysis, the group estimated that the common ancestor is 3 million years old. It is therefore likely to have infected early *Homo* species and undergone genetic diversification as early hominins moved out of Africa.

Although TB had been mentioned in literature of Hippocrates and Aristotle dating from as early as 400 BC, the first accurate description of the disease came from the Roman doctor, Caelius Aurelianus in the 5th century AD, making detailed observations of his patients. It was not until the early 18th century when the English physician Benjamin Marten (c.1690–1756) correlated the consumptive 'phthisis' as it was then called with small 'animalcules' that lived in the lungs and caused lesions. Writing in his book "A New Theory of Consumptions" of 1720, he also recognised the highly contagious nature of the disease, opposing the theory that it was hereditary (Doetsch 1978). He stated that eating, drinking or conversing with an infected person so that expired air of the diseased may enter the lungs of the healthy person may produce disease.

In 1834, the term 'tuberculosis' was coined by Johann Lukas Schönlein (1793–1864) as a disease associated with tubercles. He did not, however, see it as the same disease as phthisis or scrofula: TB was thought of as tumerous, like cancer. The contagiousness of TB was first demonstrated experimentally by Philipp Klencke (1813–1881) in 1843, whereby a rabbit injected with material from a tubercle contracted the same disease and subsequently died. Marten's animalcule remained anonymous until 1882, when Robert Koch (1843–1910) identified a single bacterium within tubercles. He also extracted tuberculin from dead *M. tuberculosis* cells and went on to develop the tuberculin skin test for identifying people with the disease, work for which he was awarded the Nobel Prize in 1905 (Herzog 1998).

1.3. TB epidemiology

In 2009, the World Health Organisation published a report based on worldwide data collected in 2007 (WHO 2009). This information revealed the extent of the TB epidemic, estimating 9.27 million new cases (139 per 100,000 population) and 1.6 million deaths during that one year alone. India and China have the highest incidence of new TB cases, with Asia as a

whole contributing 55 % to the global occurrence. Of total TB occurrences, old and new per country, of the top fifteen highest countries, thirteen are in Africa, of which most are sub-Saharan (Figure 1-3). With the vast majority of cases occurring in the developing world, problems arise with regard to affording such large quantities of antibiotics and logistically dispensing the drugs.

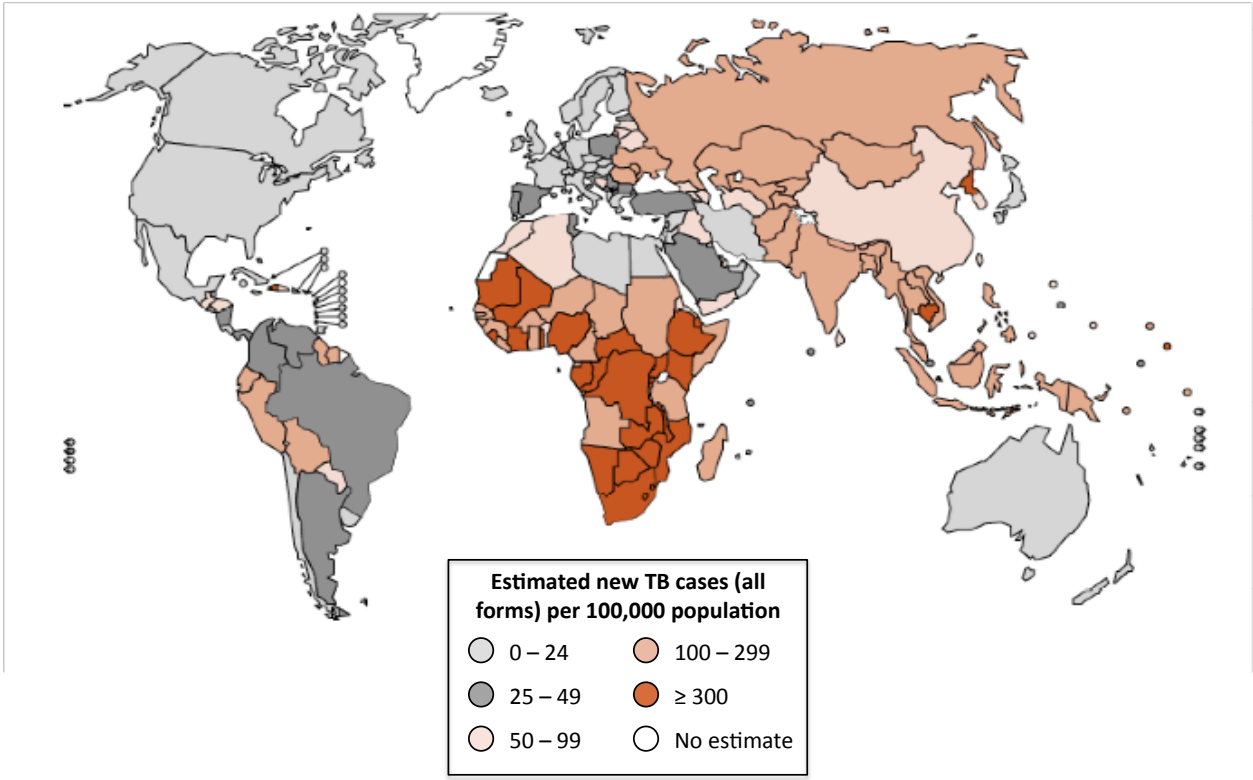

FIGURE 1-3. Tuberculosis epidemiology in 2009. World map of prevalence of all forms of TB per 100,000 inhabitants (WHO 2009).

During the 18th and 19th centuries, respiratory tuberculosis by far caused the most deaths compared with other contagious diseases such as typhus, scarlet fever and cholera (Table 1-1, Figure 1-4). The natural decline in mortality from TB has been attributed to improving nutrition throughout the 19th century and natural selection but, according to Davies *et al.* (1999), cannot be explained by the bettering of social conditions (Health Protection Agency 2009, McKeown & Lowe 1977).

TABLE 1-1. Cases of tuberculosis in the nineteenth century. Statistics for England and Wales comparing the deaths recorded due to infectious diseases during two decades in the 19th century (McKeown & Lowe 1977).

Cause		1851 – 1860	1891 – 1900
Tuberculosis	Respiratory	2,772	1,418
	Other forms	706	603
	Total	3,478	2,021
Diarrhoea, dysentery, cholera		990	715
Typhus, enteric fever, other fever		891	184
Scarlet fever		779	152
Whooping cough		433	363
Measles		357	398
Smallpox		202	13
Diphtheria		99	254

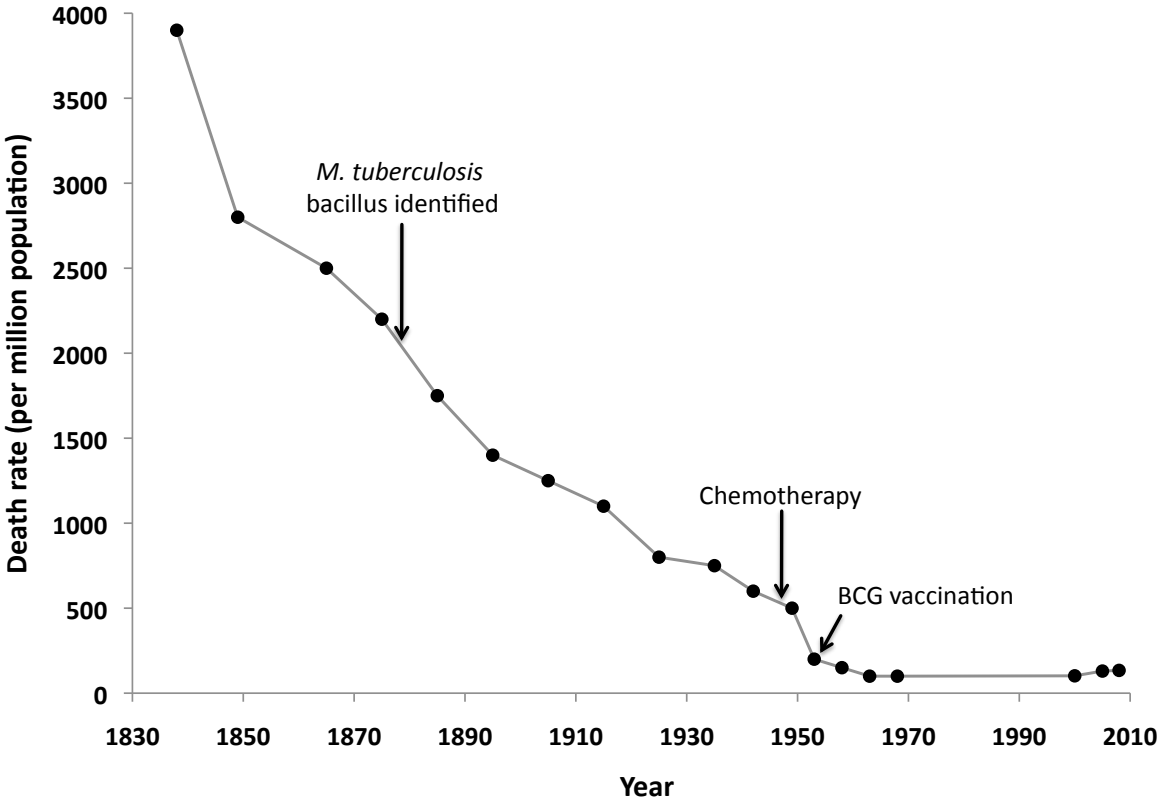

FIGURE 1-4. Cases of tuberculosis in England and Wales, 1840 – today. Graph showing the decline in mortality due to *M. tuberculosis* infection in England and Wales from 1840 to today (Health Protection Agency 2009, McKewon & Lowe 1977, WHO 2009).

Having been largely overlooked for a period of twenty years, the global threat caused by TB was brought to the fore once again in the late 1980s. A clear correlation is seen between regions of high TB and HIV-1 prevalence. The 2009 WHO report estimated that 14.8 % of total TB cases were coincident with HIV-1 infection and nearly 80 % of these occurred in Africa. This has added to the current epidemic since the probability of TB infection is greatly increased in immunocompromised people. Research has shown that there is a distinct synergy between TB and HIV-1: Specifically, *M. tuberculosis* infection modifies chemokine and cytokine concentrations, as well as their receptors, in such a way that not only permits but also boosts viral replication (Hanna *et al.* 2005, Toossi 2003).

1.4. Mechanisms of disease and immunological response

1.4.1. Overview of TB disease.

Tuberculosis is a disease primarily of the lungs; in patients that suffer from active TB, 75 % of cases are pulmonary. However, the disease can affect many organs and systems in the body, in which case it is referred to as extrapulmonary TB. Most commonly this occurs in the lymphatic system, pleura, bones and joints (most often the spine), the nervous system, liver and spleen. Miliary TB is disease that is widely disseminated throughout the body. Symptoms of tuberculosis can include a prolonged cough (for more than 2 weeks), purulus sputum that can contain blood, chest pain, fever, fatigue, weight loss and sweats (Miller *et al*. 2000). In addition to this, symptoms can occur that are not related to the site of infection, for instance haematological abnormalities such as anaemia, as well as electrolyte imbalance and psychological effects (Chung & Hubbard 1969, Ebrahim *et al*. 2009, Sukhova 2004).

1.4.2. Diagnosing TB.

Correct and rapid diagnosis is essential in the battle against TB. Accurate early diagnosis can halt the spread of disease and treatment can be started, especially in cases with HIV-1/TB co-infection. However, the method of diagnosis also needs to be cost-effective, particularly since the vast majority of cases are found in developing countries. More recently, studies have emerged comparing the various methods with respect to cost. TB is normally detected through a tuberculin skin test, chest X-ray and/or microscopy, culturing and biopsy of the affected tissue. The WHO has firmly advocated sputum smear tests as the preferred method of diagnosis. Based on the Ziehl-Neelsen staining technique and direct microscopy, it is cheap and very quick but is less sensitive than culturing, where active disease can be detected from as few as 10 cells (API Consensus Expert Committee 2006). The main problem with culturing, however, is the extensive time required, normally 3–6 weeks, although this method can be used to detect extra-pulmonary disease as well and more data can be obtained such as drug resistance.

More recently, PCR has been employed to diagnose TB, where the IS*6110* insertion element is used to amplify DNA of any *M. tuberculosis* complex species (API Consensus Expert Committee 2006). A recent study comparing Ziehl-Neelsen staining with PCR found that the latter technique is approximately 60 % more sensitive and has a quicker turn-around but is more expensive and 25 % less specific (Ani *et al*. 2009).

One final *in vitro* diagnostic method currently used, which is capable of indentifying both active and latent disease, is a blood test. One such test is QuantiFERON®-TB Gold, approved by the FDA in 2005 (Mazurek *et al*. 2005). Based on the enzyme-linked immunosorbent assay (ELISA), QuantiFERON®-TB Gold detects the release of interferon-g from immune cells within whole blood when they come into contact with mycobacteria-

specific antigens. The blood is incubated with synthetic antigens that imitate early secretory antigenic target-6 (ESAT-6) and culture filtrate protein-10 (CFP-10), proteins that are expressed in *M. tuberculosis* and *M. bovis* but not in *M. bovis* BCG, the attenuated strain used in vaccines. This technique is therefore more specific than the tuberculin skin test, which can present false positive results in people that have been vaccinated with BCG. One recent report compared the effectiveness of the tuberculin test with that of ELISpot-Plus, a test similar to QuantiFERON®-TB Gold, but which uses a novel antigen, Rv3879c, alongside ESAT-6 and CFP-10 (Dosanjh *et al*. 2008). Results showed that ELISpot-Plus was 89 % sensitive compared to 79 % for the tuberculin test. Combined sensitivity of the two diagnostic procedures was 99 %, showing that using both techniques would greatly reduce the likelihood of false positives.

1.4.3. *M. tuberculosis* infection.

Infection is initially and primarily of the lungs, more specifically, the alveolar macrophages. As such, the bacteria are almost exclusively transmitted by the inhalation of aerosol droplets expelled in the cough or sneeze of an infected patient. It is estimated that each person with untreated active TB will infect 10 to 15 people each year (WHO 2010). The smallest droplet nuclei are the most infectious, measuring approximately 5 mm and containing a maximum of three bacilli, since these are able to travel through the narrow passages to the alveoli (Rastogi 2003). Alveolar macrophages act as the main defence against respiratory pathogens (Rubins 2003). An essential part of the innate immune system, these cells clear the respiratory tract of infectious, toxic and allergic particles by ingestion. It is thought that the bacteria in the droplet also make contact initially with alveolar epithelial type II pneumocytes. These cells are found in larger numbers than macrophages in the alveoli and it has been shown that *M. tuberculosis* is capable of infecting and subsisting in them *ex vivo* (Birkness *et al*. 1999).

The tubercle bacilli that reach the alveoli make contact with the macrophages and are ingested *via* various cell surface receptors (Ernst 1998). The process is initiated by bacterial contact with macrophage mannose and/or complement receptors. Surfactant protein-A, a glycoprotein on alveolar macrophage surfaces, enhances the binding and uptake of bacteria by up-regulating mannose receptor expression (Beharka *et al*. 2002). It has been reported that cholesterol is also vital for the uptake of *M. tuberculosis*, particularly at sites of steroid-rich lipid rafts, and depletion of cholesterol actually reduces bacilli internalisation (Gatfield & Pieters 2000, Muñoz *et al*. 2009). Macrophages take up the bacteria non-specifically and at this stage do not become activated.

M. tuberculosis and other intracellular pathogens initially reside in the phagosome, an endocytic vacuole that provides the bacteria with a semi-protected environment where they are capable of logarithmic growth until bursting. When faced with highly virulent microbes, such as *M. tuberculosis*, the macrophages also secrete a plethora of cytokines, chemokines and arachidonic acid metabolites to recruit further macrophages and neutrophils to the site of infection. This leads to the development of an early tubercle. Once T-cells are chemotactically attracted to the site and presented with and activated by *M. tuberculosis* antigen, interferon-g is released, activating the macrophages. Once activated, the macrophage is able to subject the phagocytosed microbes to a variety of killing mechanisms, including a decrease in pH from phagosome-lysosome fusion, as well as reactive oxygen and nitrogen intermediates. It has been shown, however, that *M. tuberculosis* is able to prevent pH reduction and the phagocytic vacuole remains at a pH of approximately 6.5 (Sturgill-Koszycki *et al*. 1994). The precise mechanism of this has yet to be elucidated, however several suggestions have been proposed, and it is likely that the process is multi-factorial (Pethe *et al*. 2004). One mechanism is the poor recruitment of vesicular proton-ATPase, a known agent for phagosomal acidification, by pumping H^+ ions into the vacuolar space

(Sturgill-Koszycki *et al*. 1994, Xu *et al*. 1994). Another is the production of ammonia and other weak bases by the infecting *M. tuberculosis* through the degradation of urea by urease (Sinai & Joiner 1997). Non-acidification arrests the phagosome maturation cycle thereby preventing phagolysosome formation. A third, more recently identified phagosome modulator, is isotuberculosinol (also called edaxadiene), which the product of a five-gene operon including *Rv3377c* and *Rv3378c*. Although the mechanism of action is currently unknown, Mann *et al*. (2009) provided evidence that this molecule is both enzymatically biosynthesised and is able to prevent the intraphagaosomal pH from dropping below 5.5, compared to pH 5.0 in a control with no isoprene. A further study by the same group showed that it is the reduction in Mg^{2+} experienced by bacilli upon engulfment into macrophage phagosomes that induces the expression of this operon, rather than just macrophage entry (Mann *et al*. 2011). Another report has shown, however, that membrane-associated diterpenes are found in membranes of *M. tuberculosis* cells cultured outside macrophages. Having isoprenoid molecules already present in the cell membrane would be a great advantage for *M. tuberculosis*, considering that phagolysosome fusion occurs rapidly once a bacillus has been ingested, leaving little time to synthesise new proteins and lipids (Prach *et al*. 2010).

Later events in infection include the development of granulomatous focal lesions. These are composed of macrophage-derived giant cells and lymphocytes, which form when macrophages at the centre of tubercles die and release the contained bacteria. This efficiently aids the spread of bacteria, since they are then taken up by other macrophages and monocytes arriving from the blood stream (Skeiky & Sadoff 2006). As cellular immunity develops, the macrophages loaded with bacilli are killed. This results in the formation of a caseous necrosis at the centre of the granuloma, surrounded by a zone of fibroblasts, lymphocytes and

monocytes. Although unable to multiply in these harsh conditions, the tubercle bacilli can persist in a dormant, or latent state for extended periods (Colston & Cox 1999).

One feature of the granuloma environment is anoxia. In order for *M. tuberculosis* to survive without oxygen it uses the 'glyoxylate shunt', a mechanism of generating glucose independently of the O_2-consuming steps of the TCA cycle (Bishai 2000). Here, acetyl-CoA from lipid catabolism is used as the substrate for malate, which is subsequently fed into the citrate cycle to generate glucose, its carbon source (Figure 1-5).

In patients with an efficient cell-mediated immunity, infection may be permanently halted at the granuloma stage. At this point the granulomas subsequently heal, or resolve. This process forms fibrous calcified lesions by an accumulation of fibrin and collagen, which seals the granuloma thus confining infection (Porth & Matfin 2010). The patient displays a positive tuberculin skin test but shows no symptoms of active TB. Conversely, if the patient is unable to control the initial infection or the immune system becomes weakened, for example by HIV-1, ageing or malnutrition, the centre of the granuloma becomes liquefied. The liquid environment, possibly caused by an excess of lytic enzymes (Lawn & Griffin 2008), provides a rich medium for reactivating the bacilli enabling them to replicate uncontrollably. The bacteria can also now multiply extracellularly for the first time allowing them to spread to other tissues *via* the lymphatic and blood systems. There is also the risk of the granuloma bursting into neighbouring bronchi allowing the cells to disseminate through the airways to not only other parts of the lungs but also outside the patient (Rastogi 2003). The disease is then referred to as extrapulmonary or miliary TB.

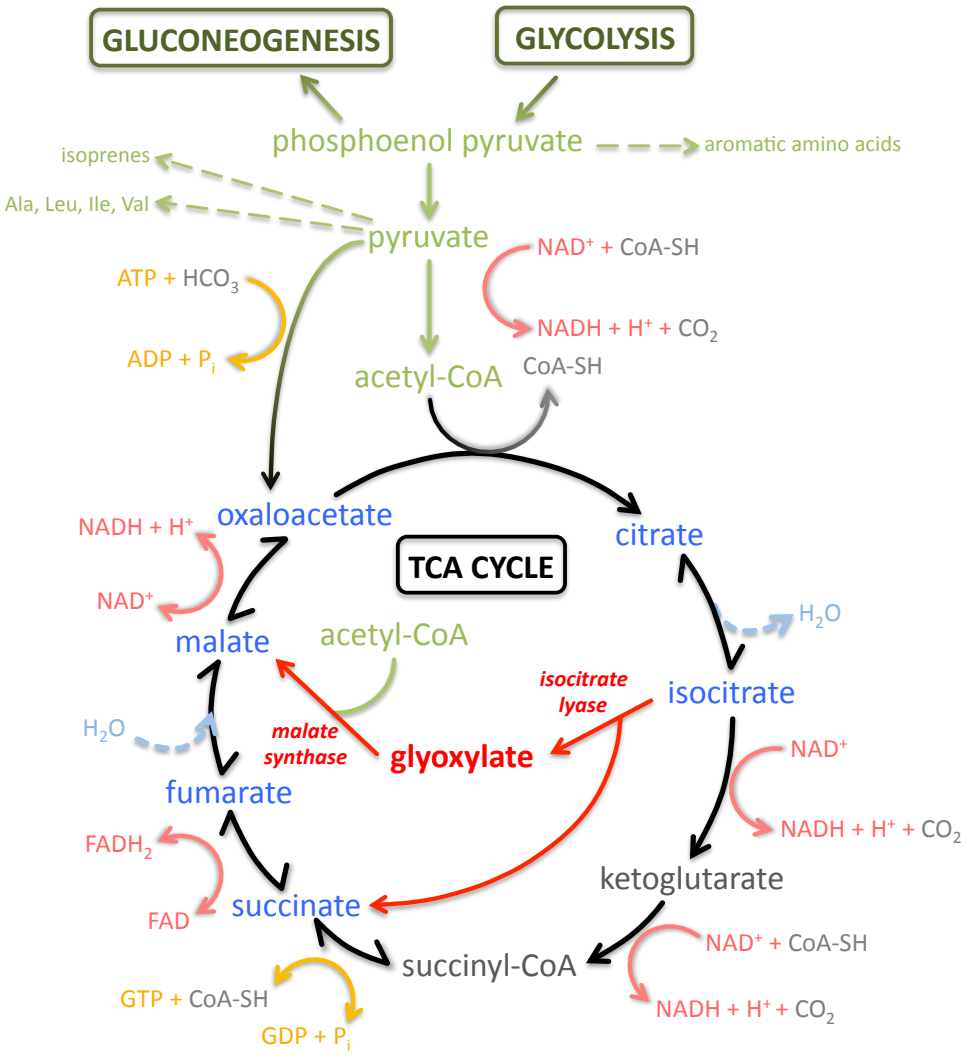

FIGURE 1-5. The glyoxylate shunt. In anoxic conditions, *M. tuberculosis* generates glucose without the O_2-dependent steps of the TCA cycle. The carbon atoms normally lost as CO_2 are retained, thus with the use of two acetyl-CoA molecules, a C_4 product, malate, can be made. Adapted from Lorenz & Fink (2001).

Reactivation is dependent not only on the environment but also on the secreted resuscitation promotion factor (*rpf*) proteins. The *rpf* genes encode *c*-type lysozyme-like enzymes, which possibly remodel the peptidoglycan cell wall throughout growth (Cohen-Gonsaud *et al*. 2005). *M. tuberculosis* has five *rpf* genes (A–E), which all produce proteins of the same function demonstrating their importance. Indeed, without them the bacteria remain in the latent state (Kana *et al*. 2008).

1.5. The mycobacterial cell wall

1.5.1. General structure and functions.

M. tuberculosis is a rod-shaped bacterium with a cell envelope that sets it apart from the well-established Gram-positive and Gram-negative classifications. All species of the mycobacteria genus are acid-fast; they are resistant to staining by acids in conventional Gram-staining techniques (Wheeler & Ratledge 1994). The cell wall of mycobacteria is unique among prokaryotes and, as well as causing acid fastness, acts as a major virulence factor (Bhatt *et al*. 2007a) (Figure 1-6). It is thought that the characteristic pathogenesis of *M. tuberculosis* is closely related to the complex lipids and polysaccharides within the cell wall (Minnikin *et al*. 2002). Generally, the cell envelope consists of three main components: (i) the plasma membrane, (ii) a covalently linked structure of a thin peptidoglycan layer connected to arabinogalactan, which is in turn linked to mycolic acids, and (iii) an outer protein-, lipid- and carbohydrate-rich layer (Crick *et al*. 2001). The cell wall also acts as a protective shell around the bacterium, providing endogenous resistance to both the host's immune system and anti-TB drugs (Takayama *et al*. 2005).

1.5.2. Peptidoglycan-arabinogalactan.

The principal structural constituent of the cell wall in mycobacteria is the insoluble cross-linking peptidoglycan (PG) (Alderwick *et al*. 2007). The glycan component consists of alternating β(1→4)-linked *N*-acetylglucosamine (GlcNAc) and *N*-glycolyl muramic acid (MurNGlyc) residue strands. Oligopeptide chains of between three and five amino acids, usually D-alanine, D-glutamate, meso-diaminopimelic acid (DAP) and occasionally glycine, are connected to the muramic acid components (Figure 1-7). These molecules can cross-link the glycan by DAP-ala and DAP-DAP covalent interactions (Crick *et al*. 2001).

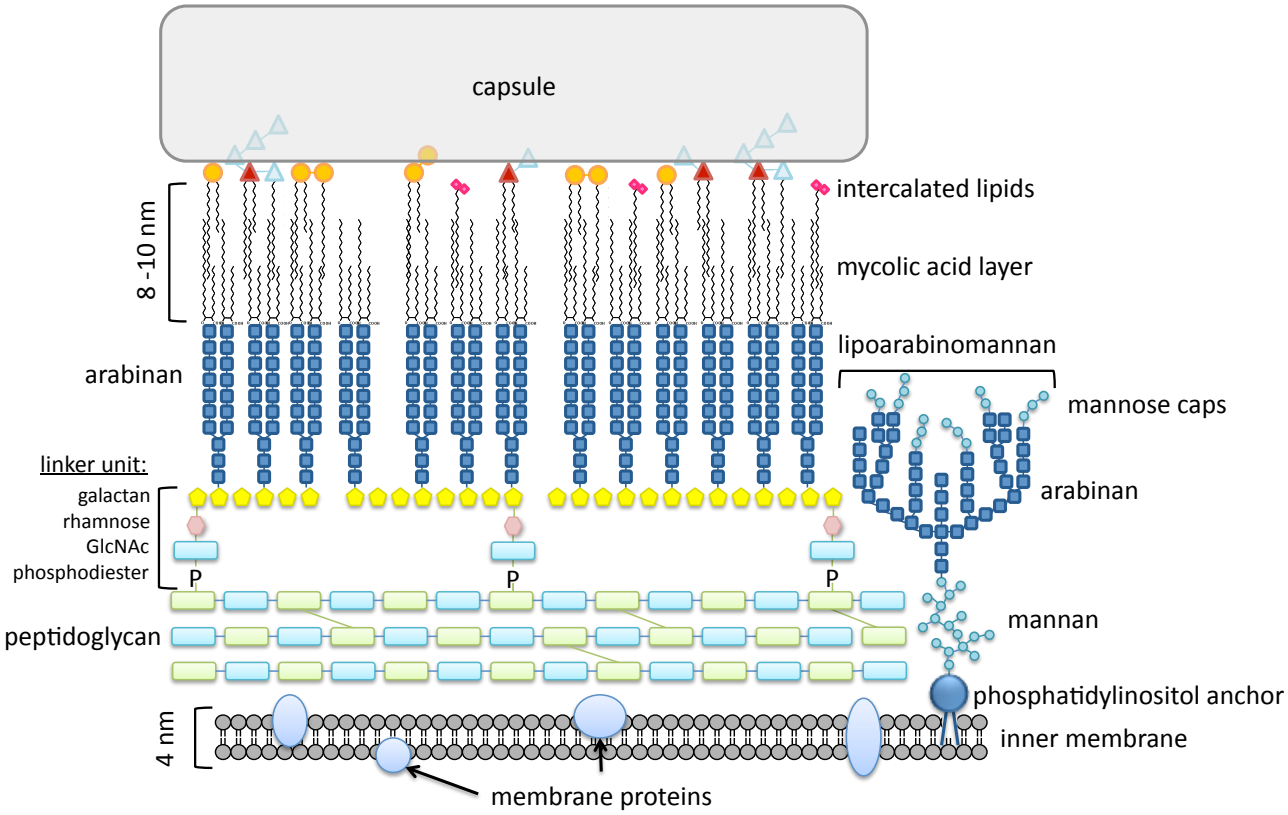

FIGURE 1-6. The *M. tuberculosis* cell wall. Peptidoglycan forms the main constituent of the cell wall. Arabinogalactan with attached mycolic acids (mAG) is connected directly to the peptidoglycan by a galactan linker. The outer-most complex free lipids, comprising sulfatides, diacyltrehalose, phthiocerol dimycocerosates and polyacyltrehalose, are thought to intercalate with the mycolates attached to the mAG. Lipoarabinomannan and phosphatidyl-*myo*-inositol hexamannoside are anchored to the plasma membrane by their fatty acyl chains (adapted from Abdallah *et al*. 2007, Esko *et al*. 2009, Hoffmann *et al*. 2008).

The PG layer is not anchored to the cell membrane but is covalently linked by a linker unit consisting of a rhamnose and *N*-acetylglucosamine molecule, [L-Rha*p*-(1→4)-D-GlcNAc-PO^{4-}], through the muramic acid residues of PG in a phosphodiester bond (Amar & Vilkas 1973, McNeil *et al*. 1990). Linear galactan, made of approximately 30 D-galactofuranose (Gal*f*) residues alternately linked β(1→5), β(1→6) by the enzyme GlfT, further extends the linker unit (Bhamidi *et al*. 2008, Kremer *et al*. 2001a, Mikusova *et al*. 2000). The arabinan domain consists of 31 arabinofuranose (Ara*f*) residues, made up of distinct structured motifs

consisting of α(1→5), α(1→3) and β(1→2) linkages. Three arabinan chains are connected to each galactan chain (Bhamidi *et al*. 2008). The more recent development and use of MALDI-TOF mass spectrometry and NMR have allowed a detailed model of the cell wall mAG to be described, showing that the Ara*f* chains are attached to the O5 of Gal*f* residues 8, 10 and 12 (from the reducing end) and that the mycolic acid chains are esterified to the 5 position of both the terminal β-D-Araf and penultimate α-D-Ara*f* residues (Bhamidi *et al*. 2008).

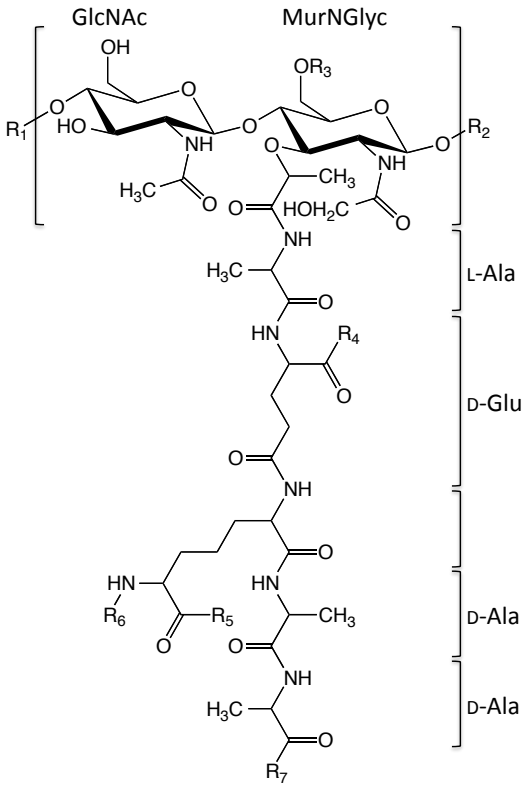

Figure 1-7. The structure of peptidoglycan before peptide trimming. R_1 and R_2, *N*-glycolylmuramic acid residue of another monomer; R_3, H or the linker unit of AG; R_4, OH, NH_2 or glycine; R_5, OH or NH_2; R_6, H or cross-linked to penultimate D-Ala or to the D-centre of another *meso*-DAP residue; R_7, OH or NH_2. Adapted from Mahapatra *et al*. (2005).

1.5.3. Lipids.

Mycobacteria are unusual in that over 60 % of the cell wall may consist of lipids. These lipids are large, complex and highly distinctive and are arranged so that some are covalently

linked to the PG-AG domain, and some are 'free' (Figure 1-6). Families of lipids include mycolic acids, trehalose-based glycolipids and phthiocerol dimycocerosate waxes.

Mycobacteria are also unusual in that they employ two fatty acid synthase (FAS) systems – named I and II – to generate lipids (Figure 1-8). The FAS-I enzyme is found in both eukaryotes and prokaryotes, whereas FAS-II is only seen in prokaryotes, Archaea and plants (Bhatt *et al*. 2007a). Atypically, the protozoan parasite *Plasmodium falciparum*, which causes malaria in humans, uses the FAS-II system to generate its fatty acids, a finding which has since awarded it with much attention with regard to creating specific anti-malarial drugs (Surolia & Surolia 2001).

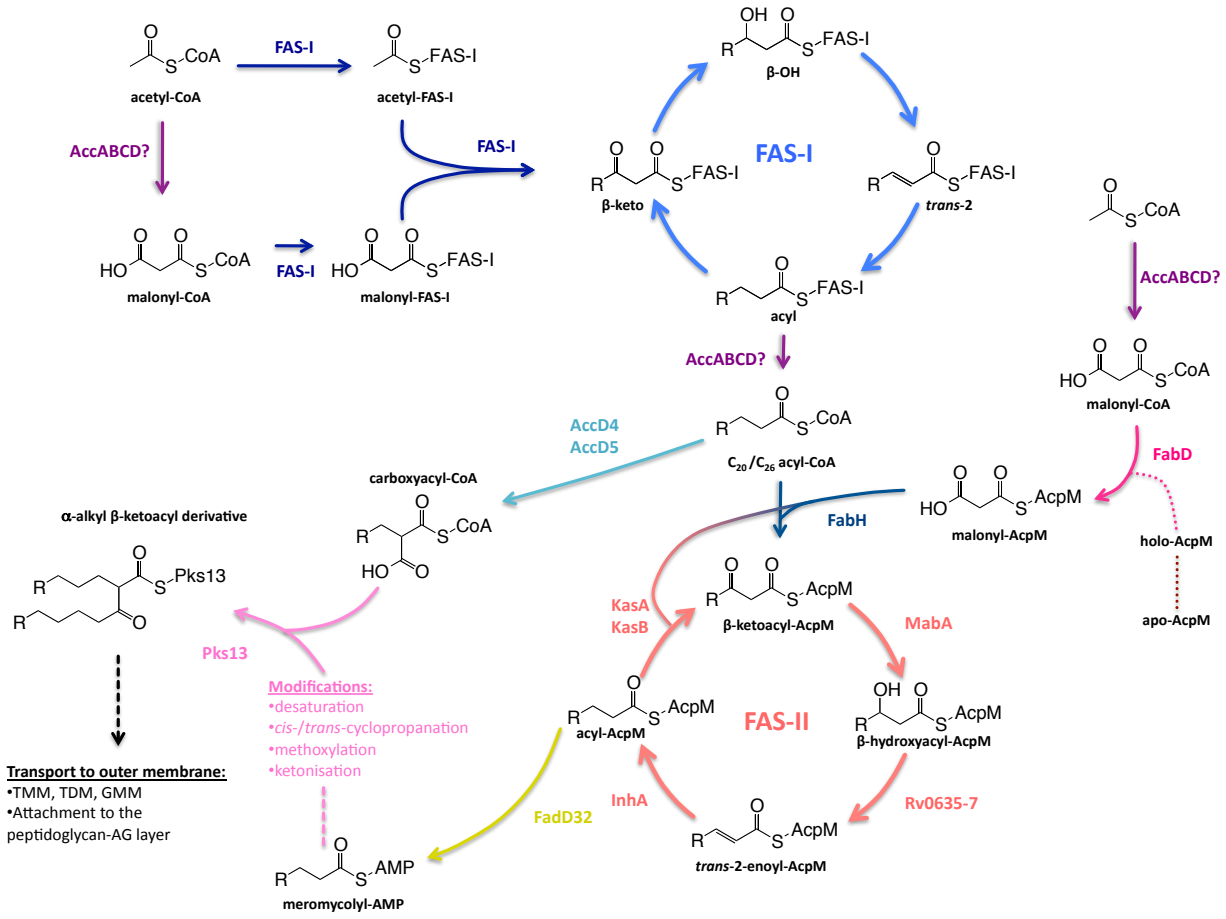

FIGURE 1-8. An overview of fatty acid and mycolic acid biosynthesis in *M. tuberculosis*. Assembled from Bhatt *et al*. (2007a) and Takayama *et al*. (2005).

1.5.3.1. FAS-I.

In mycobacteria, FAS-I catalyses *de novo* fatty acid synthesis using acetyl-CoA primers and passes the C_{20}-S-CoA product to the FAS-II cycle for continuous elongation. In both *M. smegmatis* and *M. tuberculosis*, FAS-I is a single multi-enzyme complex that shuttles the growing fatty acid around its subunits.

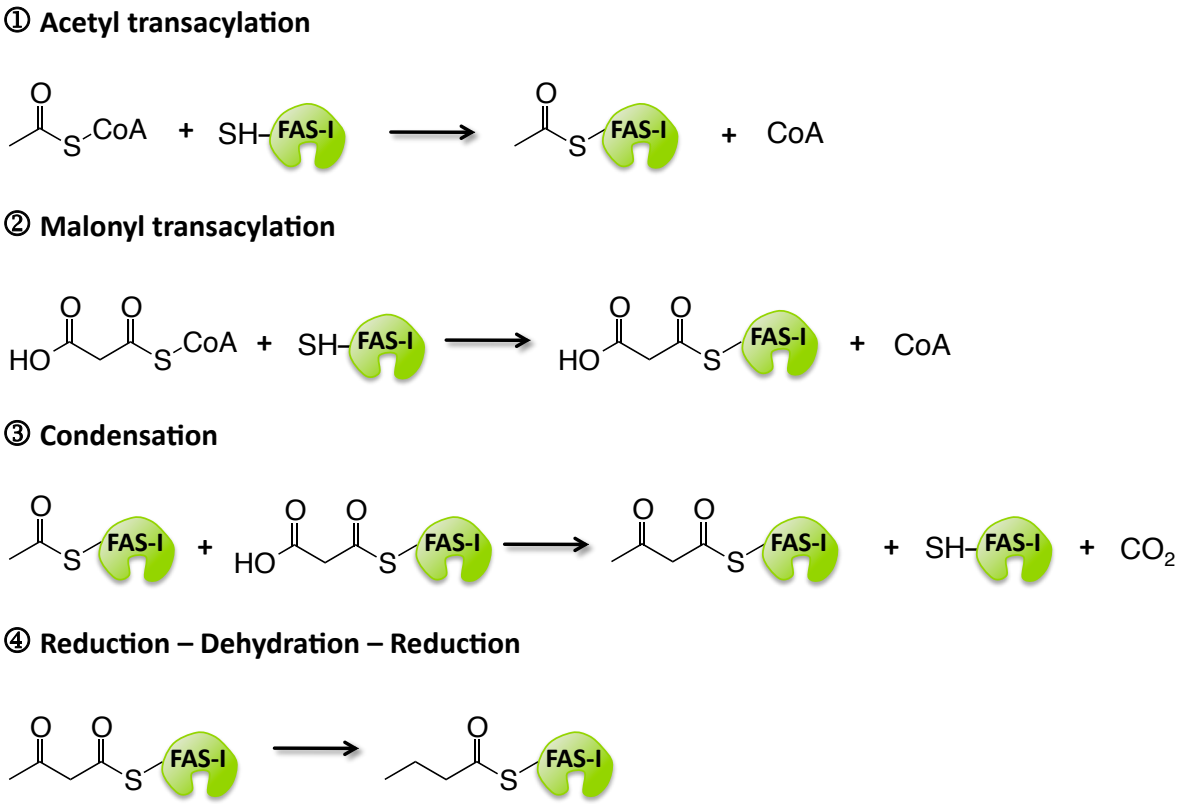

FIGURE 1-9. The initial four FAS-I reactions. (**1**) The acetyl-CoA starter unit is transacylated to the AcpM-like domain of the FAS-I multi-functional enzyme. (**2**) Similarly, the malonyl-CoA substrate also covalently binds to the same FAS-I enzyme. (**3**) A condensation reaction occurs between the two substrates to yield the β-ketobutyryl-S-FAS-I product. (**4**) Three further reactions in the cycle, β-keto reduction, dehydration and enoyl reduction, produce the saturated butyryl-S-FAS-I molecule. Recycling of this C_4-acyl chain 9 and 12 times leads to C_{20}- and C_{26}-chains respectively, which are believed to be the main precursors of mycolic acids (Takayama *et al*. 2005).

Once the acetyl-CoA and malonyl-CoA have been transacylated to the enzyme, the elongation process commences by a condensation reaction between these two starter units to

yield β-ketobutyryl that is still covalently linked to the FAS-I enzyme *via* a -S- bond (Figure 1-9). This intermediate undergoes reduction, dehydration and reduction to remove the unsaturated bonds and give the butyryl-S-enzyme product. This C_4 chain undergoes more cycles of fatty acid synthesis to yield long-chain products. It is thought that the C_{16}- and C_{18}-CoA fatty acids are channelled into membrane phospholipid synthesis, whereas the C_{20}- and C_{26}-CoA products are precursors of mycolic acids and thus fed into the FAS-II cycle (Takayama *et al*. 2005).

1.5.3.2. Mycolic acids and their biosynthesis.

It was during the 1930s that the strongly hydrophobic lipid components of the *M. tuberculosis* cell wall were first studied and the mycolic acids, which make up approximately half of the lipids, were identified (Minnikin *et al*. 2002). Mycolic acids are long-chain (C_{30}–C_{90}) α-alkyl, β-hydroxy fatty acids that are found in all species of the *Corynebacterineae* suborder (Figure 1-10).

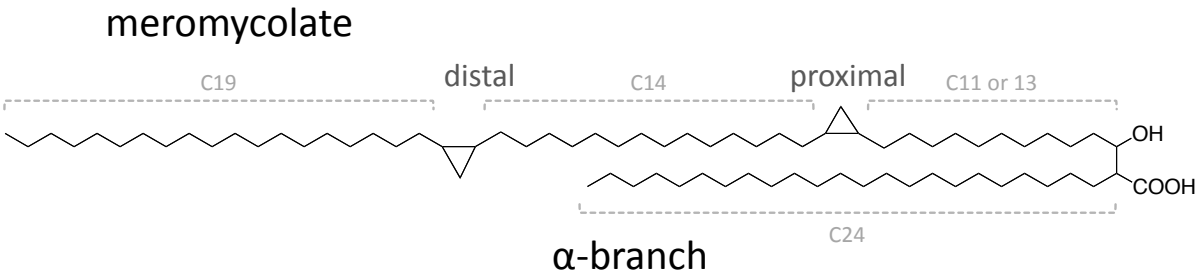

FIGURE 1-10. α-Mycolic acid from *M. tuberculosis*. The meromycolate chain is longer and contains proximal and distal cyclopropane modifications.

Within this group, the mycolic acids vary in both modifications and chain length, for example the "corynomycolic acids" of *Corynebacterium glutamicum* are 32 to 36 carbons long, whereas the "eumycolic acids" of *M. tuberculosis* are 60 to 90 carbons long (Watanabe *et al*. 2001, 2002). The mycolates of *M. tuberculosis* account for many of its features,

including drug and chemical resistance, virulence and persistence (Bhatt *et al*. 2007a). There are five known types of mycolic acid in *M. tuberculosis*. All have the same general structure of an α-branch of C_{22-26} and a longer, very hydrophobic meromycolate chain of C_{54-63}, but modifications to this give rise to α-, methoxy- and keto-mycolates (Figure 1-11). The α-mycolic acid, which is a *cis*, *cis*-dicyclopropyl fatty acid, is the most abundant in the *M. tuberculosis* cell wall (~50 %; Wanatabe *et al*. 2002) and is widespread amongst mycobacterial species. Of the keto- and methoxy-mycolates, which are found in both the *cis* and *trans* configuration, the keto-mycolic acids are present in many mycobacteria whereas, to-date, methoxy-mycolates have only been isolated from a small number of species (Yuan & Barry 1996).

Mycobacteria employ a second fatty acid synthase cycle, FAS-II, to generate mycolic acids. Unlike FAS-I, FAS-II is only able to extend already long-chain fatty acids made by FAS-I; it is incapable of *de novo* synthesis. Also unlike FAS-I, the system consists of four discrete enzymes and employs an acyl carrier protein (ACP, termed AcpM in *M. tuberculosis*) to shuttle the substrates between each enzyme active site (Kremer *et al*. 2001b) (Figure 1-8, 1-12).

❍ 1.5.3.2.1. AcpM.

AcpM is a small protein of 115 amino acid residues (14 kDa) and exists in three forms, apo, holo and palmitoylated, each of which can be over-expressed when in certain culturing conditions (Kremer *et al*. 2001b). Kremer and co-workers (2001b) showed by electrospray mass spectrometry that the apo-AcpM form refers to the inactive native enzyme, whereas holo-AcpM is the active form occurring after ligation with 4′-phosphopantetheine. A high amount of the palmitoylated form was always present, which the group attributed to the holo-form having a great affinity for this fatty acid.

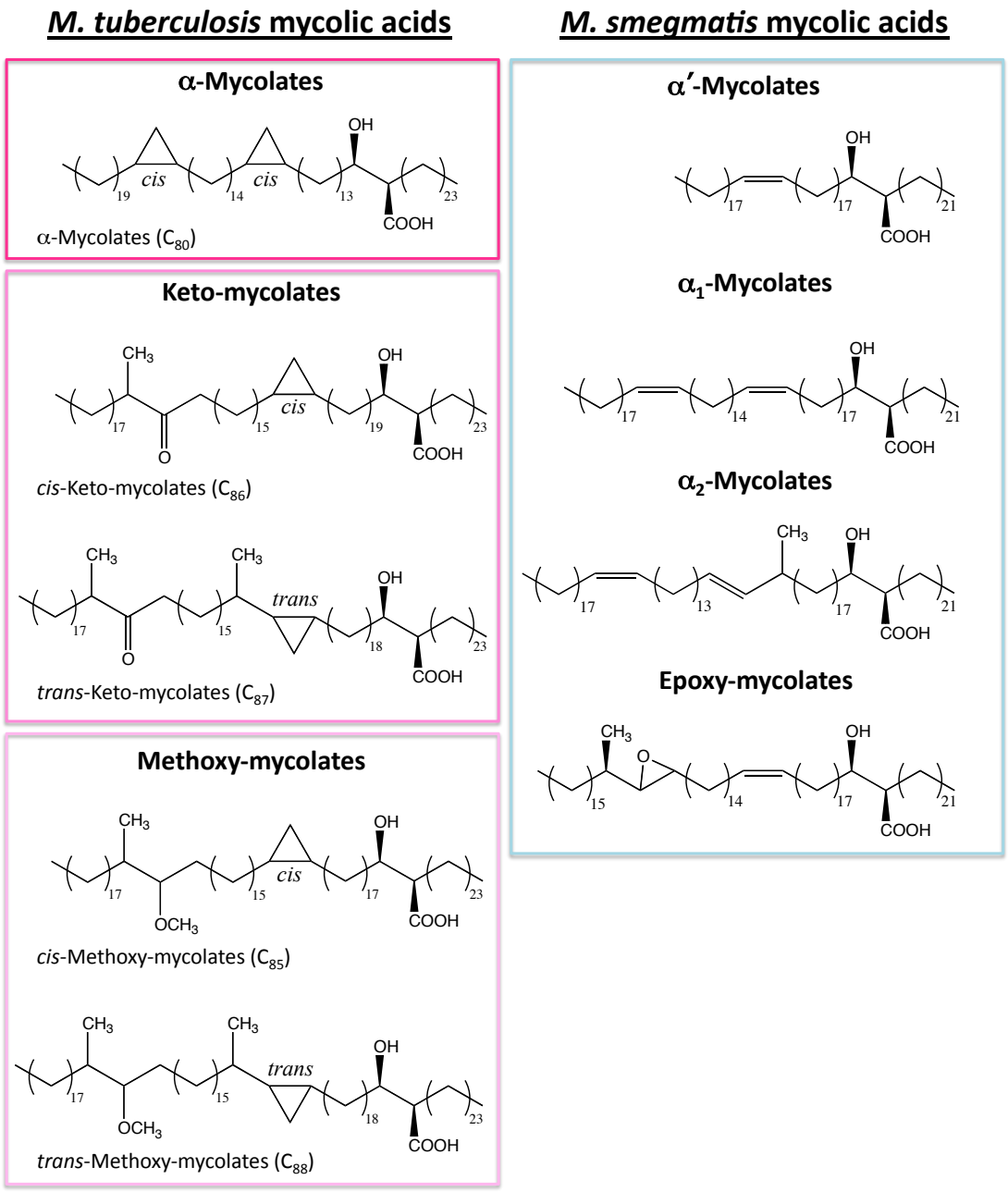

FIGURE 1-11. Structures of the main mycolic acids of *M. tuberculosis* H_{37}Rv and *M. smegmatis* mc²155. Assembled from Brown *et al*. (2009), Watanabe *et al*. (2002) and Minnikin (1982).

1.5.3.2.2. *Mt*-FabD.

The initial mycolic acid biosynthesis reaction requires the substrate malonyl-AcpM. This is made in the transacylation reaction of holo-ACP with malonate and is catalysed by the enzyme *Mt*-FabD (malonyl-CoA:ACP transacylase). The crystal structure of *Mt*-FabD revealed that the protein has two sub-domains: one large, one small (Ghadbane *et al*. 2007, Li

et al. 2007). The active site is located in a cleft between the two domains, with the small sub-domain forming a lid-like structure. The key catalytic residues were found to be Ser-91, Arg-116 and His-194. A salt bridge is thought to form between the malonyl carboxyl group and the guanido group of the arginine, helping to position the substrate. The *M. tuberculosis* genome also encodes a second *fabD* gene, *fabD2* (*Rv0649*). However, the two protein products share only a 28 % identity and FabD2 does not have the G-X-S-X-G active site motif of FabD that is common to all serine-dependent acyl-hydrolases (Takayama *et al*. 2005). More recently, Huang *et al*. (2006) have shown that FabD2 does have malonyl-CoA:ACP transacylase activity, albeit to a lesser extent than FabD. Expression of both genes was monitored under stress conditions and, although *fabD* showed higher expression when in acid conditions and at 42 °C, *fabD2* had greater expression in the untreated cells. The authors speculated that FabD2 is initially expressed during chronic infection and once the cell is engulfed by a macrophage, expression of FabD increases and takes over during persistence.

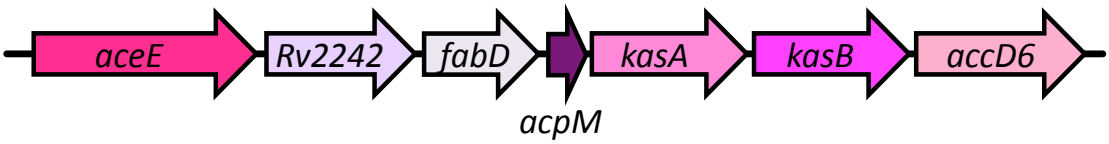

FIGURE 1-12. Map of the *M. tuberculosis* FAS-II enzyme-encoding genome region.

1.5.3.2.3. *Mt*-FabH.

Once the malonyl-AcpM substrate has been produced by *Mt*-FabD, it can then undergo a condensation reaction with the acyl-CoA primer from FAS-I, catalysed by the enzyme *Mt*-FabH (β-ketoacyl-ACP synthase III). The product is then channelled into the FAS-II system and, as such, *Mt*-FabH is thought to act as a critical link between the two fatty acid synthase systems.

The importance of *Mt*-FabH has awarded it much attention and, as a result, a good deal is known about the enzyme. Studies have shown that saturated, unbranched acyl-CoA (rather than acyl-AcpM) substrates of intermediate chain length (C_{12}–C_{20}) are preferred, with lauroyl-CoA being processed most proficiently (Choi *et al*. 2000). The acyl-CoA accepted by *Mt*-FabH is, however, disputed due to the impracticalities of testing longer chain CoA-linked fatty acids; chains of more than twenty carbons are difficult to purify and difficult to introduce into an aqueous enzyme assay. Choi *et al*. (2000) also over-expressed *Mt*-FabH in *M. bovis* BCG, which resulted in certain complex lipids, including PDIMs and multi-acylated trehaloses, being up- or down-regulated. This suggests that expression of *Mt*-FabH is crucial in the production of cell wall lipids.

The crystal structure of the *Mt*-FabH homodimer has been solved and provides insight into the substrate specificity of the enzyme (Scarsdale *et al*. 2001). Although *Mt*-FabH has 46.8 % similarity to *Escherichia coli* FabH (*Ec*-FabH) and the active site residues (Cys-112, His-244 and Asn-274) are conserved, *Ec*-FabH uses much shorter acyl-CoA primers of two to six carbons. The difference occurs at the substrate-binding pocket: whereas *Ec*-FabH has a small acyl-binding domain adjacent to the pantetheinate-binding channel, *Mt*-FabH has an "L"-shaped binding channel in each monomer (Sachdeva *et al*. 2008a). Upon solving the crystal structure of a Cys-112-Ala *Mt*-FabH mutant with bound lauroyl-CoA, it became clear that the CoA binds weakly at the pantetheinate arm of the "L", the acyl group occupies the elongated, hydrophobic arm of the "L", and the catalytic triad lies at the junction of the two arms (Musayev *et al*. 2005, Sachdeva *et al*. 2008a). It is the closed acyl channel that provides the substrate specificity; the chain length is limited to a maximum of sixteen carbons by a capping α-helix (Sachdeva *et al*. 2008b). The energetically expensive route taken by the acyl group through the pantetheinate channel and past the hydrophilic active site residues implied by the binding pocket structure has led to a new hypothesis in *Mt*-FabH conformation. It has

been proposed that the enzyme assumes an "open" conformation allowing the acyl substrate to bind directly and not *via* the solvent portal (Sachdeva *et al*. 2008a).

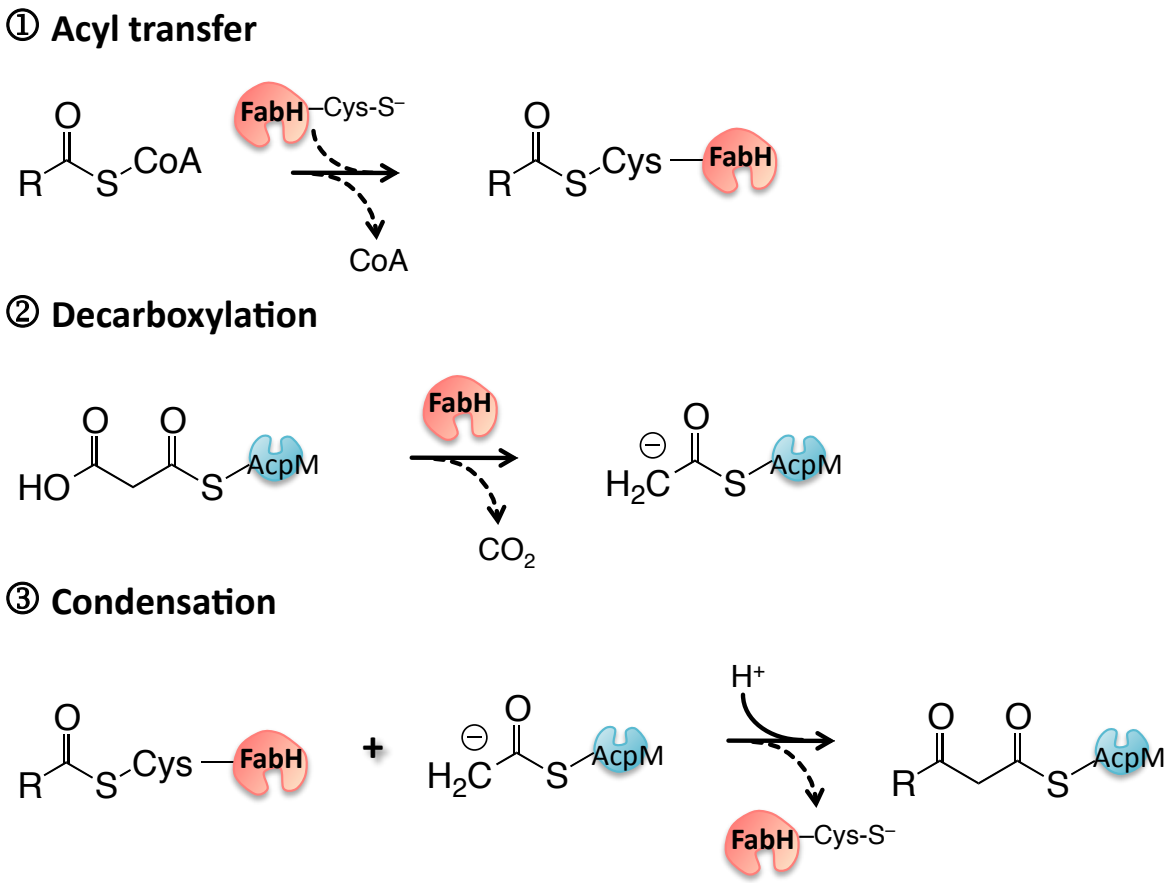

FIGURE 1-13. *Mt*-FabH reactions. (**1**) The acyl-CoA chain covalently attaches to the FabH active site cysteine. (**2**) Malonyl-CoA is decarboxylated leaving a reactive carbon atom. (**3**) FabH catalyses the condensation of the malonyl-CoA extender unit with the fatty acyl chain and releases the β-ketoacyl-AcpM product. Based on Davies *et al*. (2000).

It is thought that *Mt*-FabH performs two half reactions of transacylation and decarboxylation (Davies *et al*. 2000) (Figure 1-13). Firstly, an acetyl-enzyme intermediate is formed, substituting the CoA group for AcpM. During this reaction, a thiolate anion is produced on Cys-122 of the *Mt*-FabH active site (Davies *et al*. 2000). The nucleophilicity of this residue is also increased by the α-helix dipole effect since the active site is near the N-terminus of the helix; a phenomenon caused by the collective effect of all the carbonyl group dipoles in the helix. The thiolate, now being more chemically reactive than the thiol, can attack the acetyl-

CoA substrate. The negatively charged tetrahedral transition state is stabilised by the "oxyanion hole", which is thought to involve the residues Phe-87, Cys-122, Gly-305 and Gly-306. The second reaction is the decarboxylation of malonyl-ACP. His-244 and Asn-274 are involved in this reaction by interacting with malonyl-ACP to stabilise the negative charge on the carbonyl oxygen. It is this reactive carbanion that attacks the acetyl linked to the thiolate on Cys-122.

❍ 1.5.3.2.4. *Mt*-KasA and *Mt*-KasB.

β-Ketoacyl-ACP-synthases A and B (KasA and KasB) of mycobacterial FAS-II catalyse the mero-chain elongation condensation reactions. These enzymes, which are from the same operon (Figure 1-12), share 67 % sequence homology and are therefore thought to have overlapping functions (Figure 1-14). Current opinion suggests, however, that *Mt*-KasA may perform the early stages of mycolate chain elongation, to be taken over later by *Mt*-KasB (Slayden & Barry 2002, Takayama *et al*. 2005).

The first study to purify and characterise mycobacterial KasA and KasB identified that the enzymes preferentially accept long-chain acyl-AcpMs of at least 16 carbons atoms (Schaeffer *et al*. 2001). This finding contrasted with other β-ketoacyl-ACP-synthase (KAS) enzyme homologues, for example that of *E. coli*, which accepts C_6 to C_{12} acyl-ACP_{Ec} primers, and is therefore consistent with *Mt*-KasA and *Mt*-KasB being involved in FAS-II mycolate biosynthesis (Schaeffer *et al*. 2001). This study also identified the enzymes' sensitivity to the KAS inhibitors thiolactomycin and cerulenin, thus highlighting them as attractive drug targets. *Mt*-KasA was later acknowledged as a FAS-II component by Kremer and co-workers (2002a). The group over-expressed *Mt-kasA* in *M. smegmatis* using the pMV261 vector and saw a significant decrease in α′-mycolates and a compensatory increase in α- and epoxy-mycolates (Figure 1-11), suggesting a role for KasA in elongating mycolic acid intermediates

to full-length α-mycolic acids. A later study demonstrated the essentiality of KasA by the inability to knock out the gene and how conditional depletion of KasA results in cell lysis in *M. smegmatis* (Bhatt *et al*. 2005). Lipid profiles of *kasA*-depleted mutant strains showed a decrease in α- and epoxy mycolic acids and an accrual of α′-mycolates. In contrast, *Mt*-KasB is non-essential and it has been shown that gene deletion results in persistence of mutant bacilli in mice without causing disease for up to 600 days (Bhatt *et al*. 2007b). Altered colony morphology of the Δ*kasB* strain suggested that the cell wall was affected. Indeed, a shift was seen in the ratio of mycolic acid classes: more α- and less keto-mycolates were being made in the mutant compared to the wild-type, and those being made were shorter than wild-type mycolates by two to six carbon atoms (Bhatt *et al*. 2007b).

The homodimeric structure of *Mt*-KasB was solved in 2007 where the active site was identified as being composed of the highly conserved residues Cys-170, His-311 and His-346 (Sridharan *et al*. 2007). The structure of dimeric *Mt*-KasA was solved more recently (Luckner *et al*. 2009), although a hypothetical model had been suggested based on that of *Mt*-KasB (Sridharan *et al*. 2007). The binding and catalytic mechanisms suggested are comparable to those of *Mt*-FabH (Sachdeva *et al*. 2008a), where a gate formed by residues 115–147 opens and closes to allow direct and less energetically costly access to the acyl channel and the active site.

❍ 1.5.3.2.5. *Mt*-MabA.

MabA, also known as FabG1, is an essential enzyme that catalyses the second step of the FAS-II cycle, the NADPH-dependent reduction of the β-keto functional group to β-hydroxy (Parish *et al*. 2007). It is thought to form an operon with the downstream *inhA* gene and, although they are both β-ketoacyl-ACP-reductases with similar substrates, the two genes share only 20 % similarity.

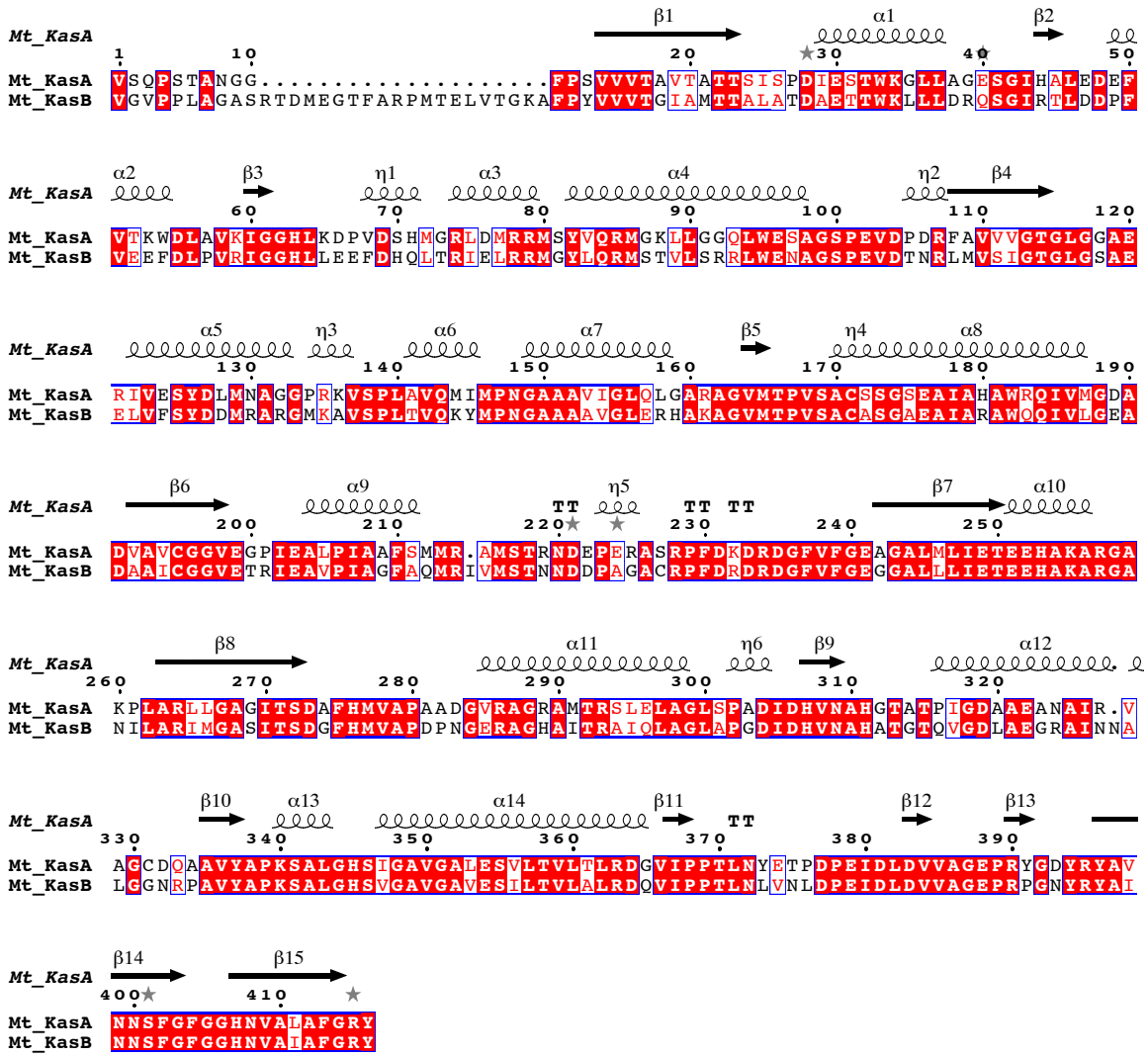

FIGURE 1-14. Sequence alignment of *Mt*-KasA and *Mt*-KasB. Data for the corresponding secondary structure for *Mt*-KasA were obtained from the Protein Data Bank (entry 2WGD; Luckner *et al*. 2009). *Red-filled boxes* indicate conserved residues and *blue boxes* are those of high similarity.

MabA has been shown to preferentially accept long-chain substrates (C_8–C_{20}) and displays little activity with C_4 chains, supporting the hypothesis that it is involved in FAS-II (Cohen-Gonsaud *et al*. 2002). The crystal structure was solved shortly after identification of the enzyme, and revealed a tetrameric conformation and a conserved fold found in all short-chain dehydrogenases/reductases (Cohen-Gonsaud *et al*. 2002). When compared with the structure of β-ketoacyl-ACP-reductases from *E. coli* and *Brassica napus*, the Ile-147 residue in MabA

was suggested as that which recognised substrates with long acyl chains. This residue is a hydrophilic asparagine in other species, which would not favour long hydrophobic chains. Indeed, an Ile-147-Asn MabA mutant showed much less affinity for long acyl-chain substrates (Cohen-Gonsaud *et al*. 2002). There are a further four *fabG* genes with putative β-ketoacyl-ACP-reductase activity in *M. tuberculosis*, named *fabG2–5*. Currently, only *fabG1* (*mabA*) and *fabG4* (*Rv0242c*) have been described as essential in *M. tuberculosis* and *M. bovis* BCG, respectively (Gurvitz 2009, Parish *et al*. 2007). Interestingly, *fabG4* is located upstream of the β-hydroxyacyl-AcpM dehydratase gene *htdX* (*Rv0241c*) (Gurvitz *et al*. 2009). It could be that these two genes form an operon of long-chain fatty acid biosynthetic enzymes. There is little further data published regarding the other *fabG* genes. The crystal structure of FabG3 has been solved but there is no information regarding its activity or function (Yang *et al*. 2002).

❍ 1.5.3.2.6. β-hydroxyacyl-AcpM dehydratase(s).

Several proteins have been proposed to catalyse the β-hydroxyacyl-AcpM dehydratase (HAD) step of the FAS-II cycle, including Rv0098 (Takayama *et al*. 2005) and Rv0216 (Castell *et al*. 2005). Bioinformatic data have shown that there are no enzymes homologous to FabZ or FabA, the dehydratase and dehydratase/isomerase enzymes found in other bacterial and protozoan species, such as *E. coli* and *P. falciparum* (Sacco *et al*. 2007). Both of these well-characterised enzymes possess a 'hotdog fold', an evolutionary conserved structural motif found in a wide range of dehydratases and thioesterases (Dillon & Bateman 2004). A bioinformatic search for this motif in *M. tuberculosis* revealed seven such proteins, of which Rv3538 and Rv0636 had previously been annotated as essential and, of these, only Rv0636 has a homologue in *M. leprae*, a closely related mycolate-producing organism (Castell *et al*. 2005, Sassetti *et al*. 2003). Subsequently, two separate concurrent publications identified the *Rv0635-Rv0636-Rv0637* gene cluster (later named HadA-HadB-HadC) as

potentially encoding the HAD proteins in *M. tuberculosis* (Sacco *et al*. 2007) and in the *M. smegmatis* homologue *MSMEG1341* (Brown *et al*. 2007a). Importantly, both *Rv0636* and *MSMEG1341* were found to be essential, as are the other genes of the FAS-II cycle. Protein-protein interaction experiments showed that two heterodimers were formed, HadAB and HadBC (Sacco *et al*. 2007). HadAB was more active in the presence of C_{16}-chains and HadBC in the presence of C_{20}-chains, with both being AcpM-dependent. From this data it has been suggested that, akin to KasA and KasB, HadAB and HadBC preferentially accept medium- and long-chain molecules respectively. Three further enzymes from *M. tuberculosis* that have been characterised as physiologically functional β-hydroxyacyl-thioester dehydratases are Rv0241c (HtdX), Rv3389c (HtdY) and Rv0130 (HtdZ) (Gurvitz *et al*. 2008, 2009). All three of these enzymes were capable of complementing dehydratase activity in a *Saccharomyces cerevisiae* mutant devoid of mitochondrial FAS-II β-hydroxyacyl-thioester dehydratase (Htd2).

❍ 1.5.3.2.7. *Mt*-InhA.

The final reaction in the fatty acid elongation pathway is reduction of 2-*trans*-enoyl-AcpM to yield the acyl-AcpM, an essential step in the FAS-II cycle. Although isoniazid had been used as a front-line drug since 1952, its target within the cell was not identified as InhA until the 1990s (Banerjee *et al*. 1994). Studies since have shown that the enzyme preferentially catalyses long-chain molecules (C_{12}–C_{24}), in accordance with its involvement in mycolate biosynthesis (Quémard *et al*. 1995), and is a prodrug that requires activation before being capable of inhibition (Zhang *et al*. 1992). In 2000, *inhA* was proven to be an essential gene, with inactivation causing inhibition of mycolic acid biosynthesis, accumulation of saturated fatty acids and cell lysis (Vilchèze *et al*. 2000). The product, a fatty acyl-AcpM with two more carbons added, is then repeatedly fed back into the FAS-II cycle to elongate the meromycolate chain to a maximum of around 56 carbons.

1.5.3.2.8. Modifications to the meromycolate chain.

Modifications to the meromycolic acid chain are made before the Pks13-mediated condensation reaction, which produces the mature mycolic acid (Qureshi *et al*. 1984). This involves the introduction of cyclopropane rings, desaturation, hydroxylation, methoxylation or ketonisation. The suggested effects of these modifications include cell wall permeability, resistance to reactive oxygen species and cell wall fluidity (Liu *et al*. 1996, Yuan *et al*. 1995). The first step, which is necessary for all further modifications, is desaturation, where a position-specific double bond is introduced in the chain. It is thought that in *M. tuberculosis* this reaction is catalysed by DesA1, DesA2 and DesA3. DesA1 and A2 are homologous to the stearoyl-ACP desaturase enzymes found in plants, where over 75 % of lipids are unsaturated. This indicates that the enzymes in *M. tuberculosis* process acyl carrier protein-attached fatty acyl chains (Ohlrogge & Browse 1995, Raman *et al*. 2007). The reaction involves the conversion of stearoyl-AcpM to oleoyl-AcpM by introducing a *cis*-Δ^9 double bond. Oleic acid is the most abundant unsaturated fatty acid in mycobacterial species and is essential for correct cell membrane physiology (Phetsuksiri *et al*. 2003). The Δ^9 desaturase found in the plant kingdom is soluble, a supposedly unique feature since all others are thought to be membrane-bound (Ohlrogge & Browse 1995). Interestingly, although *Mt*-DesA1 has been found to be insoluble, *Mt*-DesA2 was not and the homodimeric structure has been solved (Dyer *et al*. 2005). Despite being unrelated species, when *Mt*-DesA2 is compared with the structure of stearoyl-ACP desaturase from castor seed (Lindqvist *et al*. 1996) an excellent correlation is evident, such as the arrangement of a nine-α-helical portion and and certain conserved metal-binding residues (Dyer *et al*. 2005). Two potentially crucial differences in *Mt*-DesA2, however, which could imply alternative functions, are found in the di-iron metal binding site, a consistent feature within the acyl-ACP desaturase family, and the arrangement of the intersubunit region.

DesA3 is annotated as a possible linoleoyl-CoA desaturase, a widely-found enzyme that introduces *cis*-Δ^6 double bonds and has a close sequence similarity to Δ^6 acyl-lipid desaturases in plants and cyanobacteria (Phetsuksiri *et al*. 2003). DesA3 is an essential membrane-spanning enzyme in *M. tuberculosis* and has previously been shown to be the target of the drug isoxyl (Phetsuksiri *et al*. 2003). Interestingly, over-expression of DesA3 but not A1 or A2 resulted in increased production of oleic acid and an increase in the minimum inhibitory concentration (MIC) of isoxyl.

Once the double bond has been introduced, it can be converted into other functional groups. Cyclopropane ring-containing lipids are a widespread phenomenon across bacterial genera, such as *Enterobacter*, *Lactobacillus* and *Streptococcus*, as well as mycobacteria, but also in the oils of some subtropical plants (Buist 2007, Grogan & Cronan 1997). The *cma1* gene encodes CMAS-1, which Yuan *et al.* (1995) identified as introducing distal *cis*-cyclopropane rings. The *cma2* protein product introduces proximal *cis*- and *trans*-cyclopropane rings of both methoxy- and keto-mycolates (Glickman *et al*. 2001). PcaA is a *cis*-cyclopropane synthase, an enzyme that is essential for *M. tuberculosis* persistence in the mouse infection model (Glickman *et al*. 2000). This result indicates that mycolate cyclopropanation is a key factor in *M. tuberculosis* pathogenesis.

Four further genes that have been identified as modifying mycolic acids are *mmaA1*, *mmaA2*, *mmaA3* and *mmaA4*. These genes are adjacent in the genome and are thought to function together in the methoxy-mycolic acid biosynthetic pathway (Figure 1-15) (Yuan & Barry 1996). MmaA4 converts the distal *cis*-double bond to a secondary alcohol, which MmaA3 then methylates. In mutant strains without *mma4*, no oxygenated mycolates are produced and pathogenicity is highly attenuated (Yuan & Barry 1996). MmaA2 then introduces a *cis*-cyclopropane ring at the proximal position. MmaA1 is thought not to be part of this pathway,

but instead converts *cis*-olefins to the *trans* conformation and catalyses the addition of an allylic methyl branch (Yuan & Barry 1996).

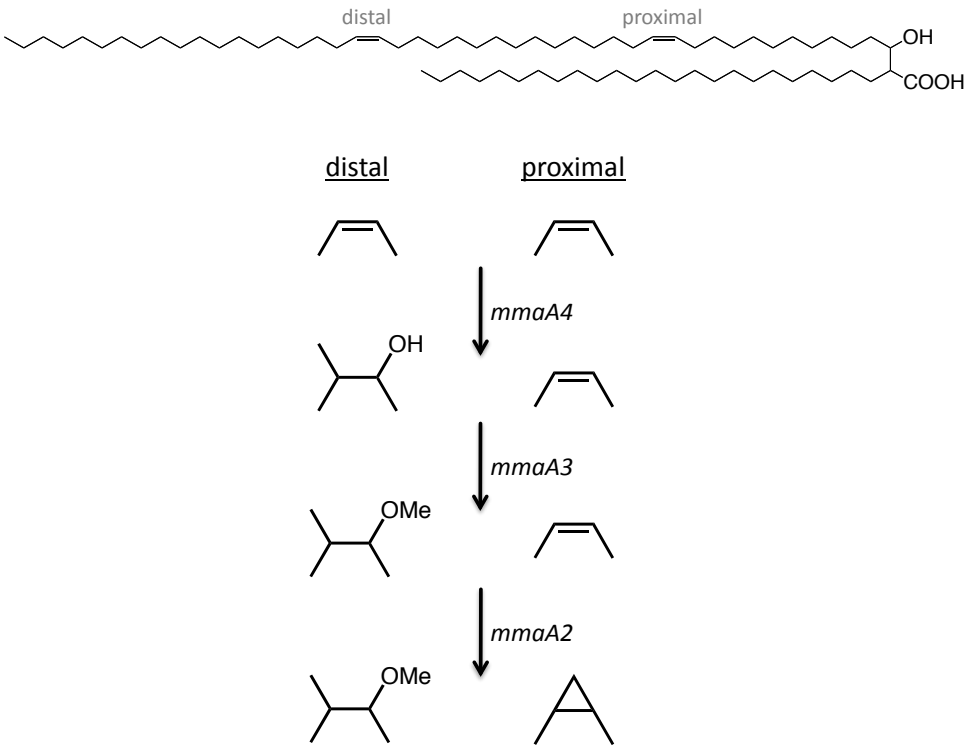

FIGURE 1-15. The proposed biosynthetic pathway of methoxy-mycolic acids. Adapted from Yuan & Barry (1996).

1.5.3.2.9. *Mt*-Pks13 and the ACC complex.

One of the final steps in mycolic acid biosynthesis is the Claisen-type condensation reaction catalysed by Pks13, a large polyketide synthase type I enzyme of 1,733 amino acid residues. This enzyme catalyses the condensation of the α-branch from FAS-I ($C_{20–26}$ acyl-CoA) with the meromycolate from FAS-II (C_{56} acyl-AcpM) to produce an α-alkyl, β-keto acid, which is then reduced to give the final mycolic acid product. Pks13 was only identified as the main candidate for this reaction over the other nine shared by *M. tuberculosis* and *M. leprae* by means of its location adjacent to *accD4* and *fadD32*, a then hypothetical acyl-CoA carboxylase and acyl-CoA synthase respectively, and that homologous genes are found in other mycolate-producing species (Figure 1-16 A) (Portevin *et al*. 2004).

Pks13 was shown to have four catalytic domains required to catalyse the reaction: ketosynthase, acyl-transferase, acyl carrier protein and thioesterase (Figure 1-16 B) (Portevin *et al*. 2004). The gene is essential in mycobacteria because mutants deficient in mycolic acids are non-viable, but a *C. glutamicum pks13*-deletion mutant was achievable and analysis revealed that the strain was deficient of mycolic acids, although was able to produce fatty acid precursors (Bhatt *et al*. 2005, Portevin *et al*. 2004, Vilchèze *et al*. 2000). *Pks13* is located in the genome downstream of *fadD32*, which has recently been shown to encode a protein that provides the substrate, a meromycolyl-AMP from meromycolic acid plus ATP (Figure 1-16 B) (Gavalda *et al*. 2009).

After being released from the FAS-I enzyme and before it can be a substrate for the condensation reaction, the $C_{20–26}$ acyl-S-CoA molecule is carboxylated to produce 2-carboxyl-$C_{20–26}$-S-CoA (Takayama *et al*. 2005). It is thought that the biotin-dependent acyl-CoA carboxylase (ACC) enzyme is formed by the complexing of different sub-units, a system that is found in bacteria and most plant chloroplasts. In contrast, mammals and fungi employ a large single multi-functional polypeptide (Cronan & Waldrop 2002). The ACC complex catalyses a two-step reaction, firstly biotin carboxylation by the α-subunit (*accA1-3* in *M. tuberculosis*) and secondly carboxyl transfer by the β-subunit (encoded by *accD1-6*) (Cole *et al*. 1998, Daniel *et al*. 2007). From whole genome analysis, it was suggested that the AccA1-AccD1 and AccA2-AccD2 complexes are involved in conversion of propionyl-CoA to succinyl-CoA (Cole *et al*. 1998), whereas more recently AccD4 and AccD5 have been implicated in the pre-Pks13 carboxylation reaction (Figure 1-8). Protein purification and complex reconstitution experiments by Oh and co-workers (2006) identified four peptides that had biotin-dependent acyl-CoA carboxylase activity when complexed in certain combinations: AccA3, AccD4, AccD5 and the novel Rv3281 (named the ε subunit).

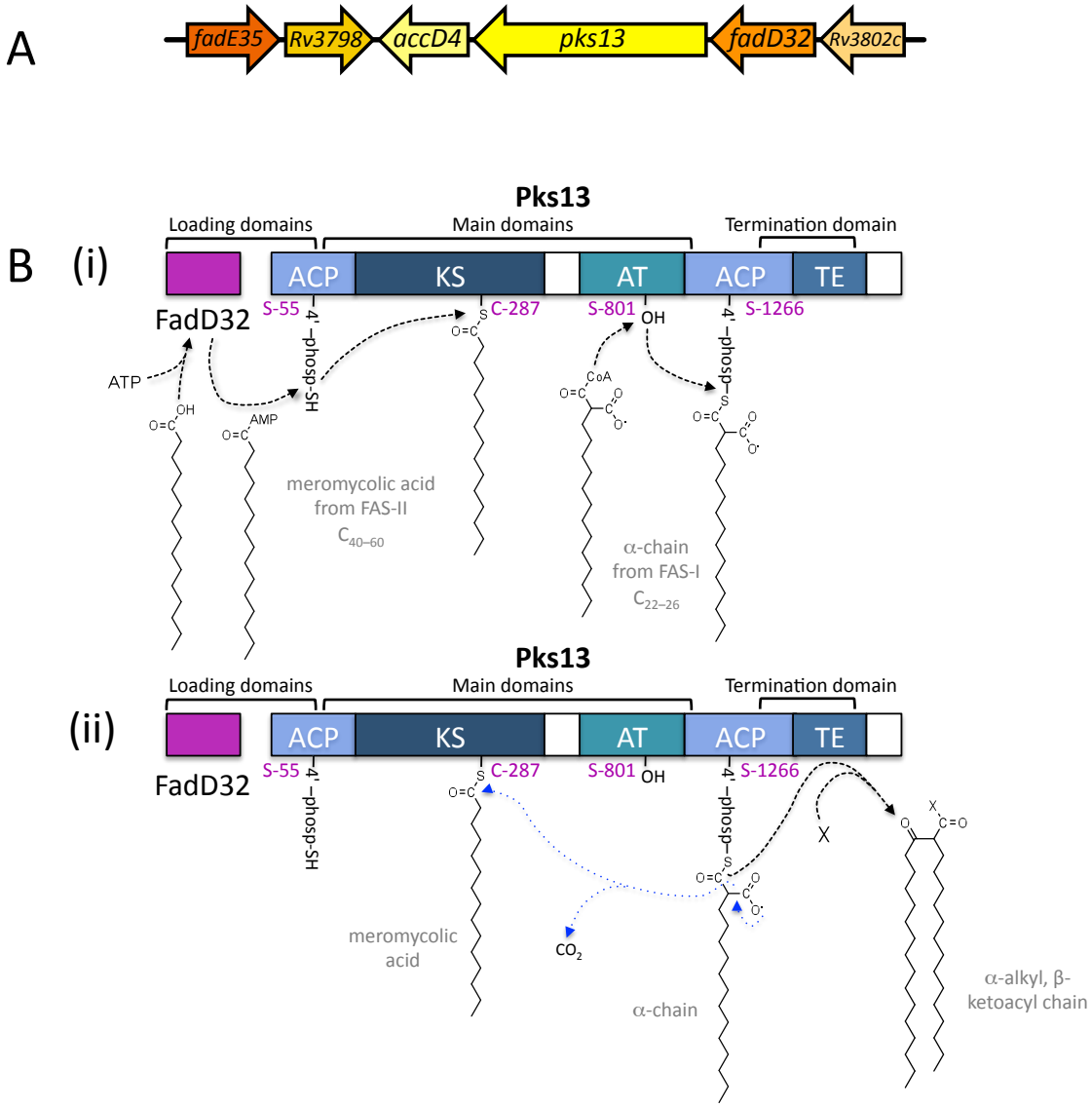

FIGURE 1-16. The FadD32 / Pks13-mediated condensation reaction. (**A**) Map of the genomic region of *M. tuberculosis* H_{37}Rv *pks13*. (**B**) The proposed system for the Claisen-type condensation between the α-branch and meromycolate chain, one of the final steps in mycolic acid biosynthesis (**i**) loading, (**ii**) condensation reaction. For clarity, shorter C16 acyl chains are drawn; actual chain lengths for *M. tuberculosis* mycolate precursors are noted alongside in **B** (**i**). *ACP*, acyl-carrier protein; *KS*, ketosynthase; *AT*, acyl-transferase; *TE*, thioesterase. Adapted from Gavalda *et al*. (2009).

The AccA3-AccD4 combination showed very little activity when acetyl-CoA or propionyl-CoA were provided as the substrates but would actively carboxylate long-chain acyl-CoAs. This would support the hypothesis that AccD4 is involved in mycolic acid biosynthesis. More recently, the AccD6 subunit has been purified and synthetically complexed with

AccA3 (Daniel *et al*. 2007). The enzyme preferentially accepts acetyl-CoA over propionyl-CoA and, along with its location in the same operon as other FAS-II enzymes, a role in providing malonyl-CoA for the FAS-I and FAS-II systems was deduced (Figure 1-12).

❍ 1.5.3.2.10. Transport and further processing.

The majority of the mycolic acid product is then esterified to arabinogalactan of the PG-AG layer (see section 1.5.2.). It is thought that approximately two-thirds of the arabinan is mycolylated (Bhamidi *et al*. 2008). Some mycolates remain as extractable 'free lipids', that is, covalently bound to trehalose or glucose to form trehalose monomycolate (TMM), trehalose 6,6′-dimycolate (TDM) and glucose monomycolate (GMM). The latter of these is also known as cord factor, which is toxic to humans (Minnikin *et al*. 2002). It is thought that these three mycolate derivatives intercalate with the mycolates attached to the PG-AG layer (Figure 1-6). Trehalose is a disaccharide of two α-glucose units covalently bonded by an α,α-1,1-glucosidic bond. It has been proposed that attachment of the mycolic acid to trehalose occurs *via* the carrier molecule 6-*O*-mycolyl-β-D-mannopyranosyl-1-phosphoheptaprenol (Myc-PL). Then, at the site of an ABC transporter in the cell membrane, the mycolyl residue is attached to trehalose in a reaction catalysed by a mycolyltransferase (Takayama *et al*. 2005). The authors note that the product being transported across the cell membrane immediately avoids accumulation of TMM inside the cell and the inevitable conversion to TDM before being ejected from the cytoplasm.

Three fibronectin-binding proteins belonging to the antigen 85 complex, Ag85A, Ag85B and Ag85C (also known as FbpA, FbpB and FbpC, respectively), are thought to be involved in this last step of cell wall assembly (Kremer *et al*. 2002c). Ag85 proteins are major secretory proteins of *M. tuberculosis* and *M. leprae*, although some members of the complex are found attached to the cell surface (Wiker & Harboe 1992). All have been shown to have

mycolyltransferase activity *in vitro*, forming TMM and TDM (Belisle *et al*. 1997), and, with transposon mutagenesis data, Jackson *et al*. (1999) provided evidence for Ag85C catalysing mycolate-attachment to arabinogalactan. As well as having a role in cell wall biosynthesis, the proteins induce intense cell-mediated and humoral immune responses in the host, and as such are being developed as new TB vaccines (see section 1.7.1.).

❍ 1.5.3.2.11. Interaction of FAS-II enzymes.

Two successive papers by Veyron-Churlet *et al*. (2004, 2005) have explored the interactions between the proteins of the FAS-II system using the yeast two-hybrid method. The protein-protein interactions observed are summarised in Table 1-2.

TABLE 1-2. **Interactions between the FAS-II enzymes of *M. tuberculosis*** (adapted from Veyron-Churlet *et al*. 2005). The more '+' signs indicates greater interaction. No protein-protein interaction is indicated by '–'. *NT*, not tested.

	FabD	FabH	KasA	KasB	MabA	InhA	MmaA1	MmaA2	MmaA3	MmaA4	Pks13
FabD	+++	+++	+++	+++	–	++	+++	+++	+++	++	*NT*
MmaA1	+++	+	+++	+++	–	–	+++	++	–	+++	*NT*
MmaA2	+++	–	+++	+	–	+	+++	+	+	+	*NT*
MmaA3	–	–	++	++	–	–	+++	++	–	+++	*NT*
MmaA4	++	–	++	++	–	–	++	++	–	–	*NT*
Pks13	++	+	+	++	–	+	+	+	++	++	+++

The results suggest that FabD, InhA, MabA and the dehydratase enzymes, HadA, HadB and HadC, form a central core that interacts with KasA, KasB and Pks13 for the sequential phases of meromycolate chain extension (Veyron-Churlet *et al*. 2004). Initially, the group identified four specialised complexes and coined names for each phase. The 'initiation-FAS-II' allows the acyl-CoA transition from FAS-I to FAS-II *via* FabH. The second elongation

phase is E1-FAS-II ('type 1 elongation-FAS-II'), made up of the core enzymes plus KasA. Similarly, the final phase is E2-FAS-II ('type 2 elongation-FAS-II'), which comprises the same core enzymes plus KasB. The speculative fourth, 'termination', complex involving Pks13 catalysed the condensation reaction between the product of E2-FAS-II and the acyl-CoA from initiation-FAS-II. This model was modified in the later report and is reviewed in Figure 1-17.

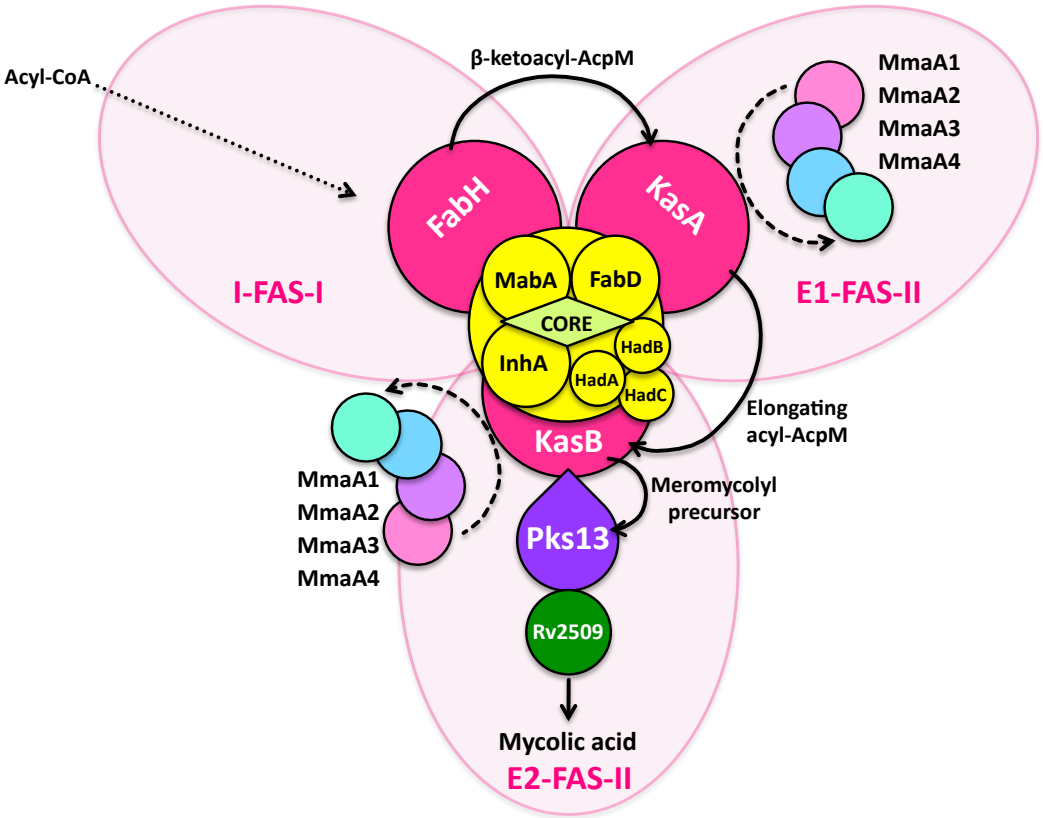

FIGURE 1-17. Model of FAS-II enzyme interactions. The specialised complexes first identified by Veyron-Churlet *et al*. (2004) are circumscribed by a pink bubble. I-FAS-II ('initiation FAS-II'), E1-FAS-II ('type 1 elongation FAS-II') and E2-FAS-II ('type 2 elongation FAS-II'). The core is thought to comprise FabD, InhA, MabA and the dehydratases HadA, HadB and HadC (Rv0635, Rv0636 and Rv0637 respectively). Solid black arrows indicate the putative route taken by intermediates from one complex to another. Dashed arrows indicate the binding of MmaA proteins with KasA and KasB. Adapted from Veyron-Churlet *et al*. (2005).

1.5.3.3. Other lipids.

The mycobacterial cell wall also contains complex lipids that have multiple methyl branched-fatty acids esterified to their backbone and various large molecules based on trehalose and phthiocerol. Examples of the latter include phenolphthiocerol and phthiocerol dimycocerosates, whereas members of the trehalose family include sulfatides, diacyltrehaloses, triacyltrehaloses and polyacyltrehaloses (Jackson *et al*. 2007, Minnikin *et al*. 2002). All of these molecules are thought to form a link between the mycolic acids (*via* the acyl chains) and the outer capsule of the bacterium.

1.5.4. Lipoarabinomannan and phosphatidyl-*myo*-inositol mannosides.

In addition to the lipids described above, another component of the mycobacterial cell wall, lipoarabinomannan (LAM), also contains fatty acyl groups. LAM is found in both pathogenic and non-pathogenic mycobacteria and is composed of three sections: a mannosyl-phosphatidyl-*myo*-inositol (MPI) anchor, a polysaccharide backbone and various capping units, which are used to distinguish between LAM types. The anchor connects the LAM to the plasma membrane by long-chain fatty acyl groups esterified to the phosphate, usually palmitic (C_{16}) and 10-methyl-octadecanoic (C_{19}) acids (Nigou *et al*. 2003). The main portion of LAM is the backbone, comprising the polysaccharides D-mannan and D-arabinan. The branched mannan section is made up of 30–35 α(1→6)-linked mannopyranose residues while the arabinan is composed of ~60 α(1→5)-linked Ara*f* residues, with occasional branches (Nigou *et al*. 2003). The precise linkage between the domains has, as yet, not been elucidated. Generally, with regard to the capping motifs, slow-growing mycobacteria, including *M. tuberculosis*, possess ManLAMs (with capping mannooligosaccharides), whereas the fast-growing species, such as *M. smegmatis*, have PILAMs, or phosphoinositide units. LAM of the fast-growing species *M. chelonae*, however, is devoid of any capping unit, either mannose or inositol phosphate (Guérardel *et al*. 2002). LAM is a major

immunomodulatory virulence factor that is involved in macrophage deactivation (Sibley *et al*. 1988), repression of T cell proliferation (Moreno *et al*. 1988) and removal of free radicals (Anthony *et al.* 1994, Chan *et al*. 1991). The cap is an important feature in this immune response and there is evidence suggesting that polysaccharides lacking a cap, as found in *M. chelonae*, having increased ability to induce TNF-α release (Guérardel *et al*. 2002).

Other members of the glycolipid family include the phosphatidyl-*myo*-inositol mannosides (PIMs). The soluble lipoglycans, lipomannans (LMs), are closely related to LAMs in their biosynthetic pathway; it is thought that the enzyme PimA, an α-mannosyltransferase, converts phosphatidyl-*myo*-inositol into PIM. Further enzymes then attach more mannose units to produce $PIMs_{2\text{-}6}$. It is thought that the LMs are subsequently produced from PIM_4 by the addition of branching mannose residues and that the LAMs are the result of an arabinan domain being introduced (Mishra *et al*. 2011).

1.5.5. The mycobacterial 'outer cell membrane'.

Numerous models have been proposed for the outer most section of the mycobacterial cell wall. Although technically described as Gram-positive, the *Corynebacterineae* suborder have what has been described as an 'outer permeability barrier' similar to the lipid bi-layer outer membranes of Gram-negative species (Zuber *et al*. 2008). Gram-positive bacteria possess an inner plasma membrane, a thin periplasmic space and an outer peptidoglycan layer. Gram-negative bacteria have an outer membrane comprising a phospholipid bi-layer with lipopolysaccharides and proteins, in addition to the other layers shared by Gram-positive species. Minnikin (1982) first postulated that mycobacteria have an asymmetrical outer membrane bi-layer, whereby mycolic acids function as the inner leaflet and extractable lipids such as TMM, TDM and GPL act as the outer leaflet (Figure 1-6; Liu *et al*. 1995, Zuber *et al*. 2008). Nevertheless, it is not until recently that visual evidence supporting the hypothesis has

become available. Zuber *et al*. (2008) and Hoffmann *et al*. (2008) have lately provided a wealth of information using cryo-electron microscopy, which allows the ultrastructure of hydrated cell samples to be visualised. Both groups provided tangible proof for the existence of a lipid bi-layer in mycobacteria (Figure 1-18).

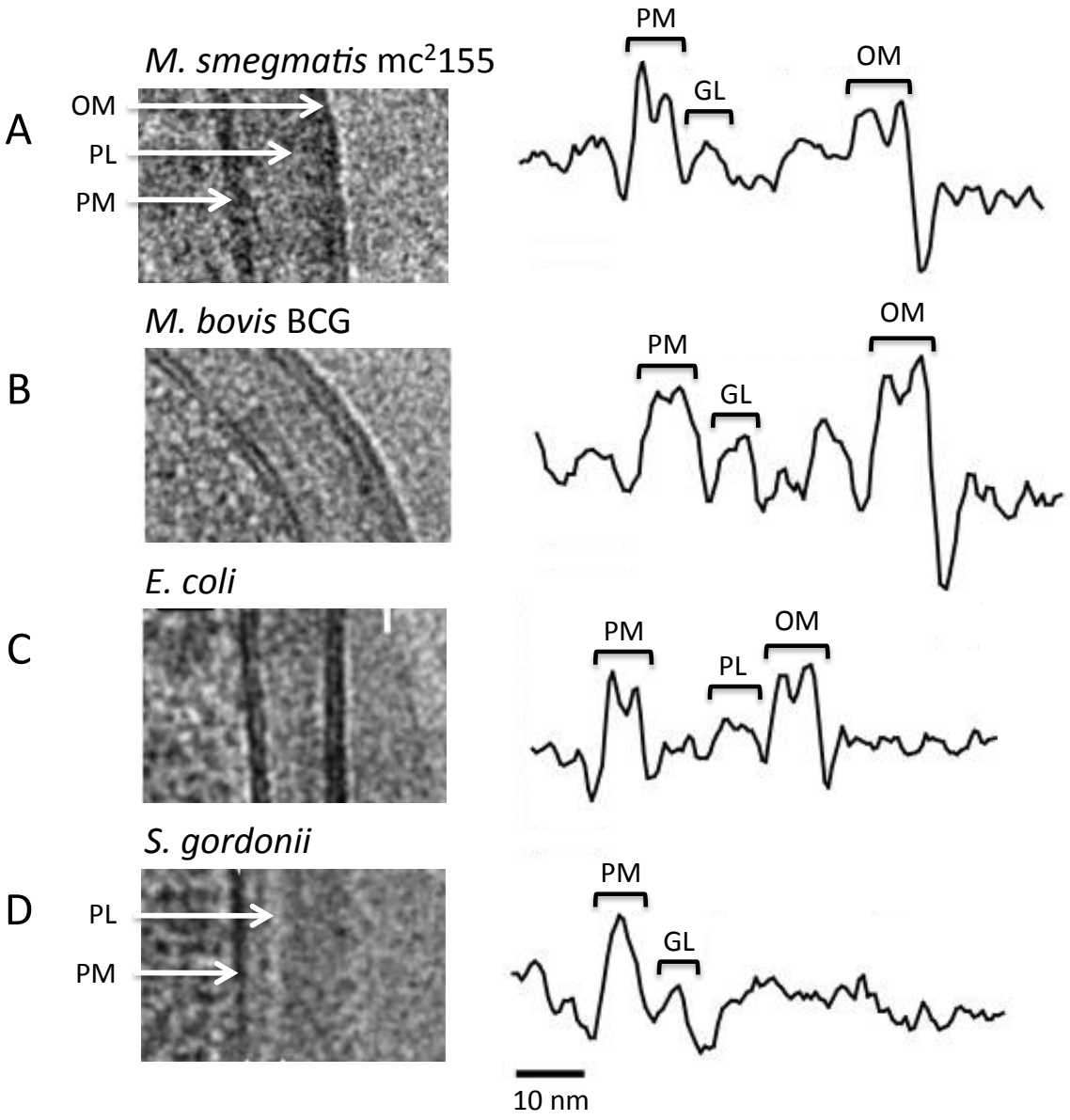

FIGURE 1-18. **The cell envelope of Gram-negative and Gram-positive bacteria.** The cell envelopes were visualised by Zuber and co-workers (2008) using cryo-electron microscopy of vitreous sections (*left panels*) and the electron density profiles were subsequently obtained from the microscopy results (*right panels*) (**A**) *M. smegmatis* mc^{2}155, (**B**) *M. bovis* BCG, (**C**) the characteristic Gram-negative bacterium *E. coli*, and (**D**) the Gram-positive species *Streptococcus gordonii*. *OM*, outer membrane; *PL*, peptidoglycan layer; *PM*, plasma membrane; *GL*, granular layer. Adapted from Zuber *et al*. (2008).

1.5.6. Regulation of the cell wall.

The cell wall is an incredibly important feature of *M. tuberculosis* but surprisingly little is known about the molecular mechanisms underlying the regulation of its biosynthesis. There is a growing pool of evidence suggesting that many fundamental cellular processes are regulated by eukaryotic-like serine/threonine protein kinases not only in *M. tuberculosis*, such as cell division and virulence, but also by the pathogen to alter signalling in the infected host cell (Molle *et al*. 2010, Scherr & Pieters 2009, Wehenkel *et al*. 2008). Phosphorylation is a reversible post-translational modification that introduces negative charges through addition of a $[PO_4]^{3-}$ group. This causes a conformational change in the target protein, thus switching the activity on or off. The usual residues to undergo phosphorylation are serine, threonine and tyrosine, although in prokaryotes histidine, arginine and lysine may also be modified (Marks 1996). The majority of kinases are membrane-bound, thus providing a mechanism for the cell to respond to external environmental stimuli.

The *M. tuberculosis* genome (Cole *et al*. 1998) highlighted eleven genes encoding two-component systems and eleven genes encoding Ser/Thr protein kinases. The former system is mainly found in prokaryotes and is a coupling mechanism usually involving a histidine kinase. The Ser/Thr kinases are found in various numbers across mycobacterial species, for example there are four in *M. leprae* but twenty-four in *M. marinum* (Wehenkel *et al*. 2008). The reduced genome of *M. leprae* (Cole *et al*. 2001) suggests that the four kinases present, PknA, PknB, PknG and PknL, are essential and are implicated in key physiological functions. Of the eleven kinases in *M. tuberculosis*, nine are membrane-bound, as indicated by their receptor-like transmembrane domains. The other two, PknG and PknK, are presumed to be cytosolic (Cole *et al*. 1998).

It is not surprising that enzymes involved in the biosynthesis of cell wall components are regulated by phosphorylation. Being closely related to cell division, these enzymes are indirectly affected by the environment *via* kinase signalling. Stress conditions can therefore alter mycolate biosynthesis allowing the cell to adapt to external conditions (Tyagi *et al*. 2008). KasA, KasB and FabH were the first enzymes of the FAS-II system to be identified as being regulated by phosphorylation, indeed part of this project explores the role of phosphorylation on *Mt*-FabH activity (Chapter 3; Molle *et al*. 2006, Veyron-Churlet *et al*. 2009). The activity of KasA and FabH is reduced by phosphorylation but that of KasB is increased, suggesting a complex mechanism of cellular adaptation. Neither KasA, KasB nor FabH have the characteristic phosphorylation recognition domains (forkhead-associated domains; FHA) but have 11-stranded β-sandwiches that mediate phosphorylation-dependent protein-protein interaction (Pallen *et al*. 2002). KasA, KasB and FabH are phosphorylated by *M. tuberculosis* PknA, PknB, PknE, PknF and PknH and are dephosphorylated by Ser/Thr phosphatase PstP (Molle *et al*. 2006, Veyron-Churlet *et al*. 2009).

Similarly, the activities of both InhA and MabA are controlled by phosphorylation. With both genes being in the same operon and both having important roles in mycolate biosynthesis, this may not be unexpected. InhA is a substrate for PknA, PknB, PknE and PknL, as is MabA, which can also phosphorylated by PknD. Phosphorylation occurs at Thr-266 on InhA and was found to deactivate the enzyme (Molle *et al*. 2010). Point mutations at Thr-266 that mimic phosphorylation by adding a negative charge (T266D and T266E) severely reduced reductase activity. MabA is phosphorylated at three sites, Thr-21, Thr-114 and Thr-191, of which the latter is the principal phosphoacceptor. A similar phosphomimicary mutant was made (T191D) and, from activity studies compared to the wild-type, it could be inferred that phosphorylation deactivates MabA (Veyron-Churlet *et al*. 2010). Phosphorylation of these

enzymes therefore may well be another way of allowing *M. tuberculosis* to control mycolate production.

Most recently, a study by Slama *et al*. (2011) has identified that the FAS-II dehydratase enzyme complexes, HadAB and HadBC, are also regulated by phosphorylation. Each of the HadA, B and C subunits were phosphorylated *in vitro* and *in vivo* at least to some degree by all the Ser/Thr protein kinases tested (PknA, B, D, E, F, H and L). Interestingly, the group found that phosphorylation down-regulates dehydratase activity and occurs mainly during stationary growth phase. From this, it was hypothesised that the bacilli switch off meromycolate chain production when not replicating as a means of controlling dormancy (Slama *et al*. 2011).

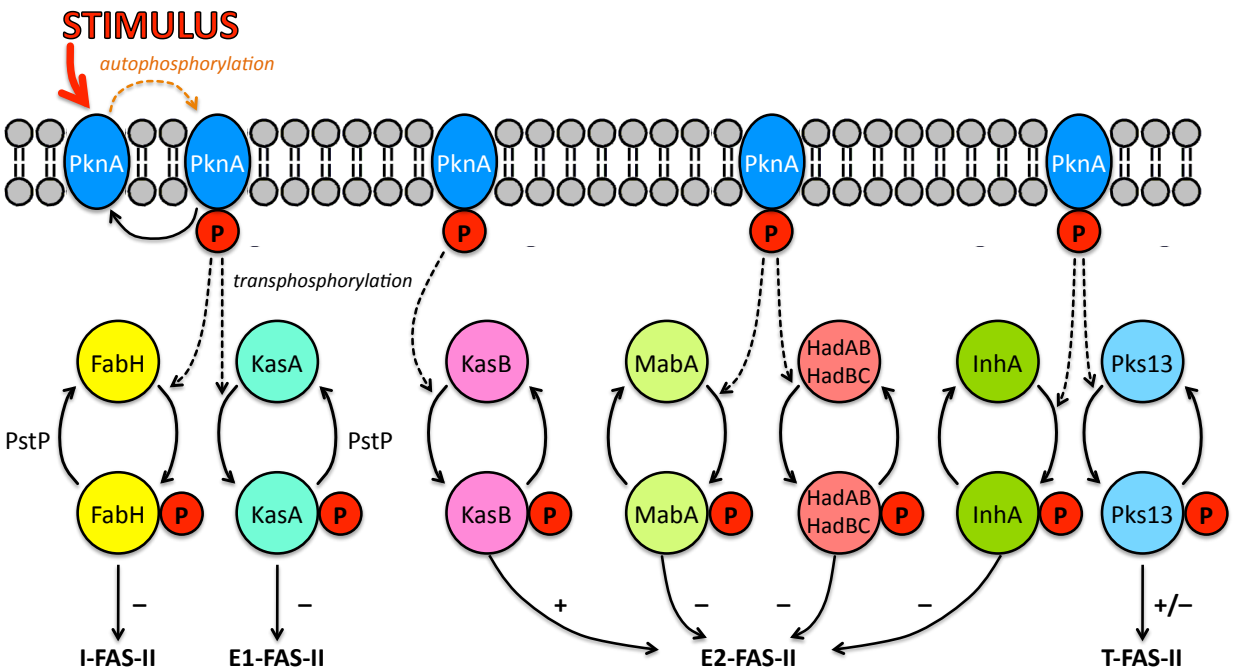

FIGURE 1-19. *M. tuberculosis* FAS-II phosphorylation. Schematic representation of how phosphorylation is used to activate and de-activate FAS-II enzymes. '-' indicates protein de-activation; '+' indicates protein activation. Based on Bhatt *et al*. (2007a) and Slama *et al*. (2011).

Another cell wall enzyme under the control of protein kinases is EmbR, a transcriptional regulator of arabinosyl transferases EmbC, EmbA and EmbB, which is activated by PknA, PknB and PknH phosphorylation (Molle *et al*. 2003a, Sharma *et al*. 2006). Activation promotes arabinan biosynthesis by inducing transcription of the *embCAB* operon. Both EmbR and the Pkn kinases are therefore directly implicated in virulence and pathogenesis of *M. tuberculosis*, since it is well known that LAM and LM are modulators of the host immune response (Chatterjee & Khoo 1998, Nigou *et al*. 2003). PknH may also be involved in the response to nitric oxide stress. Evidence from Papavinasasundaram and co-workers (2005) have shown that a *M. tuberculosis* Δ*pknH* mutant was hypervirulent and displayed higher resistance to acidified nitrite stress. It could be that this environmental stimulus triggers PknH activation. Indeed, it has been found that the kinase is up-regulated in macrophages (Sharma *et al*. 2006). Mycobacterial MurD, a cytoplasmic UDP-*N*-acetylmuramoyl-L-alanine:D-glutamate-ligase involved in peptidoglycan synthesis, is also a substrate for PknA (Thakur & Chakraborti 2008).

There are several pieces of evidence that together support the idea that PknA and PknB are involved in cell shape and cell division. Firstly, as described above, many of the substrates are enzymes of cell wall biosynthesis. Other substrates include FtsZ, a GTPase homologous to eukaryotic tubulin involved in septum formation, Wag31, a cell shape/cell division and septum formation regulation protein essential for cell growth (Kang *et al*. 2008a, Nguyen *et al*. 2007), and penicillin binding proteins (PBPs), which are involved in cell wall expansion, cell shape maintenance, septum formation and cell division (Dasgupta *et al*. 2006). Secondly, both kinases are expressed during the exponential growth phase and are down-regulated during periods of starvation. Thirdly, in experiments where PknA and PknB are over-expressed or partially deleted (deletion mutants are non-viable), cells were found to be abnormally narrow, elongated, branched and sometimes di-nucleoidal, as well as having

noticeably reduced growth rates compared to the wild-type (Kang *et al*. 2005). Finally, evidence comes from their location in the *M. tuberculosis* genome. *pknA* and *pknB* are in an operon with *pstP*, a Ser/Thr phosphatase, *pbpA*, a penicillin binding protein and *rodA*, which encodes a cell division enzyme that works with PbpA to switch between peptidoglycan synthesis and septum formation.

Other mycobacterial Pkn kinases are thought to be involved in transport across the cell membrane. PknD is co-transcribed with *pstS*, which encodes one of four membrane-bound phosphate-specific transporters (Av-Gay & Everett 2000, Vanzembergh *et al*. 2010). Another putative substrate for PknD is MmpL7, one of thirteen MmpL proteins in *M. tuberculosis* (Perez *et al*. 2006). MmpL7 transports phthiocerol dimycocerosate (PDIM) and sulfolipids to the cell wall and as such is essential for virulence. The PknD of *M. bovis*, however, has lost the transmembrane domain (Peirs *et al*. 2000), but it is able to phosphorylate the FHA domain of the ABC transporter encoded by *Rv1747*. PknF, which is only found in pathogenic mycobacteria, also interacts with this enzyme. Evidence from Curry *et al*. (2005) suggests that PknF regulates environment-dependent transport of solutes, including glucose uptake (Deol *et al*. 2005). In the case of PknG, one of the assumed cytoplasmic kinases, its genetic locus may suggest a role in glutamine uptake. The *pknG* gene is part of an operon with *glnH*, which encodes a membrane-bound extracellular glutamine binding protein and, although PknG is not essential, it is only found in *M. tuberculosis* complex species, thus implying a role in pathogenicity (Av-Gay & Everett 2000). Indeed, Walburger *et al*. (2004) identified that PknG inhibits phago-lysosome fusion, a key tool in mycobacterial survival in the host. Deletion of *pknG* had no effect *in vitro*, however, in macrophages, mutant cells were quickly transferred to lysosomes and killed.

1.6. Fatty acid β-oxidation

As with other bacteria, mycobacteria also carry out the β-oxidation of lipids (Figure 1-20). Indeed, it is thought that they are principally lipolytic and not lipogenic due to the lipid-rich nature of their host tissues. It is thought that, *in vivo*, the lipids of the cell wall are largely derived from incorporated host fatty acids, and it has been demonstrated that mycobacteria do favour using host cell lipids over *de novo* synthesis (Wheeler *et al*. 1990, Wheeler & Ratledge 1994). A similar observation is made in *Pseudomonas aeruginosa* lung infections in cystic fibrosis patients (Kang *et al*. 2008b, 2010, Son *et al*. 2007). The highly virulent and pathogenic cells replicate rapidly inside the lungs and the fatty acid degradation pathways are thought to be key in maintaining this. *P. aeruginosa* adapts to the environment and induces a number of genes to exploit its surroundings. Lung surfactant is thought to be a main source of nutrients, 80 % of which being phosphatidylcholine. The phospholipid is cleaved by lipases and subsequently metabolised by degradation enzymes, including those encoded by the *fadBA* operon.

The *E. coli* β-oxidation pathways are well studied and understood in contrast to studies investigating the equivalent in mycobacteria. In *E. coli*, the FadR protein globally regulates fatty acid metabolism at transcription level; it is able to repress and induce all *fad* and *ace* genes (the latter of which are involved in the glyoxylate shunt) as well as *fabA*, an unsaturated fatty acid biosynthesis gene (Black & DiRusso 1994). It is known that FadR is in turn regulated directly by acyl-CoA molecules (DiRusso *et al*. 1992). FadR binds long-chain acyl-CoAs with high affinity when they are in high concentrations, which changes the conformation of the protein allowing its induction. In *E. coli*, the FadB and FadA activities, which together catalyse at least five steps required for fatty acid oxidation, are collectively found as a single multi-enzyme complex with an α2β2 structure (DiRusso 1990). This same arrangement is seen in *M. leprae*, which possesses a single multi-functional FadB-FadA

enzyme, although this is likely to be a result of its extreme reductive evolution. Interestingly, the oldest known organism to process fatty acids by β-oxidation, the archaeon *Archeoglobus fulgidus*, does not have a multi-functional enzyme like *E. coli*, but discrete mono-functional enzymes, like *M. tuberculosis* (Klenk *et al*. 1997). As such, it is thought that the multi-functional enzyme evolved from non-covalent interactions between these mono-specific proteins and/or gene fusion rather than dissociation of a large multi-domain protein (Winkler *et al.* 2003).

M. tuberculosis possesses a huge abundance of enzymes involved in lipid metabolism; where in *E. coli* there are around 50 enzymes, there are at least 250 in *M. tuberculosis* (Côtes *et al*. 2008). *M. tuberculosis* has multiple homologues of the fatty acid degradation (Fad) enzymes, whereas in *E. coli* there is only one. For example, there are 36 FadD enzymes alone (Black and DiRusso 1993, Cole *et al*. 1998, Fujita *et al*. 2007). Approximately 52 % of the genes in *M. tuberculosis* have been created by gene duplication, which has resulted in massive functional redundancy. The reason for this could be the huge diversity of lipids in mycobacteria – certain homologues catalyse normal β-oxidation reactions, some may be involved in the recycling of complex lipids unique to the genus and others may have unrelated functions. An example of this is FadD33, now renamed MbtM, which, although being homologous to a lipid metabolism protein, has recently been shown to convert fatty acids into acyl-adenylates (Krithika *et al*. 2006). A similar finding has also been reported for the FadD15 homologue. Trivedi and co-workers (2004) demonstrated that the protein was able to catalyse the production of acyl-adenylates from long-chain fatty acids or, with the inclusion of CoA-SH, the corresponding fatty acyl-CoA. These activated metabolites are not only used for lipid metabolism but also as substrates in biosynthetic pathways.

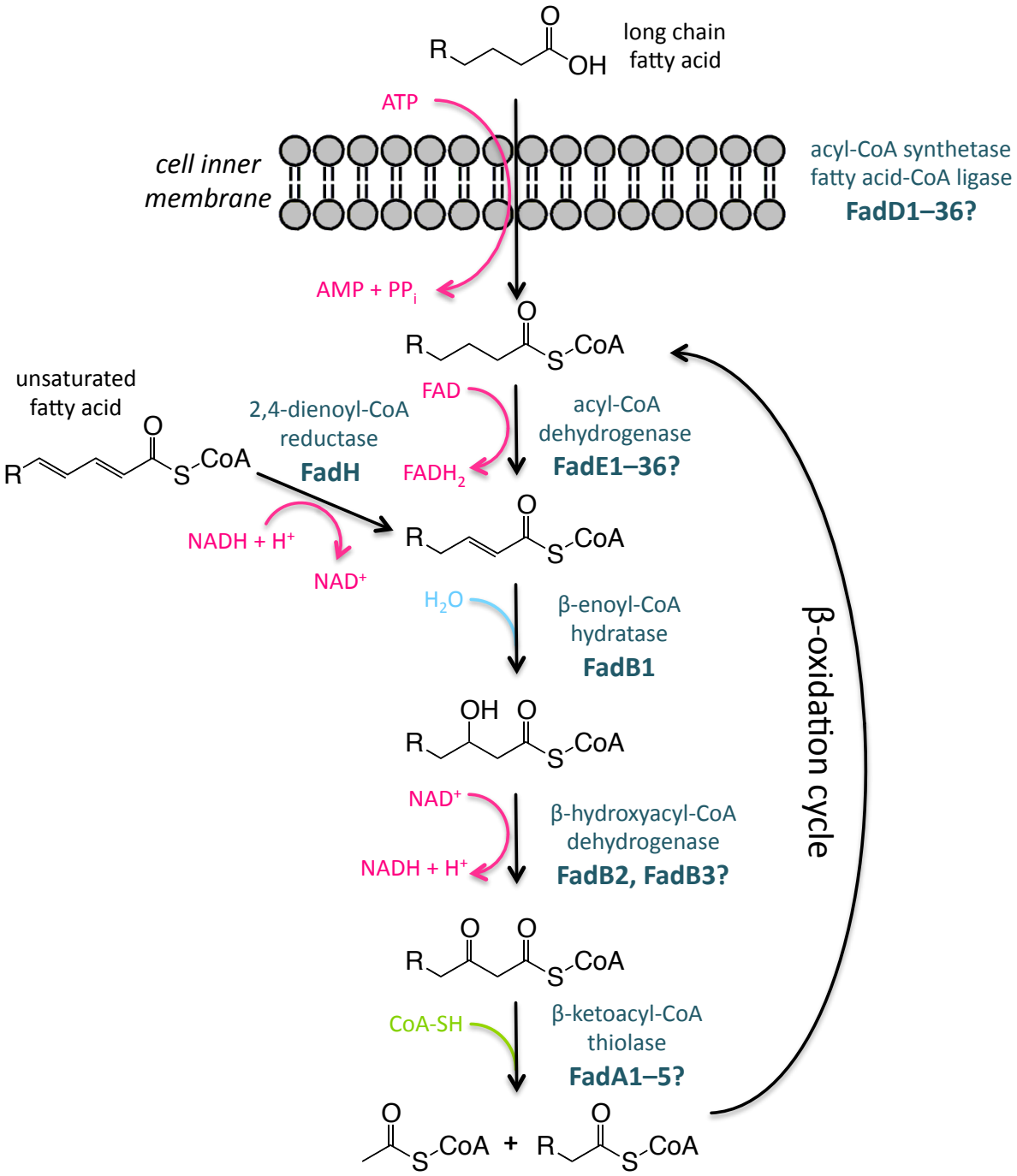

FIGURE 1-20. The β-oxidation pathway in *M. tuberculosis*. Extracellular fatty acids are first activated by CoA-attachment and translocated across the cell membrane by an acyl-CoA synthetase, possibly encoded by one or more of the *fadD* genes. An acyl-CoA dehydrogenase catalyses the first oxidation step, currently annotated as 36 *fadE* genes. It is thought the hydration step is catalysed by FadB1, the second oxidation step converting the β-hydroxy group to a β-keto by FadB2, and the thiolysis step by one or more of the FadA enzymes. Further enzymes are required to process unsaturated fatty acids, possibly including FadH, currently annotated as a 2,4-dienoyl-CoA reductase. Based on Fujita *et al.* (2007).

In complete contrast, all gene families in *M. leprae* have undergone a massive reduction in number resulting in the species possessing approximately 74 % of the genes found in *M. tuberculosis*, of which only about half encode proteins (Cole *et al*. 2001). The remaining genes are either regulatory or are pseudogenes. This is a sharp contrast to *M. tuberculosis*, where over 90 % of the genome is protein-encoding (Scherr & Pieters 2009). Despite this, *M. leprae* is also an extremely successful pathogen and it is believed that it retained the minimum genetic functionality required for pathogenicity and intracellular survival (Cole *et al*. 2001).

The FadB and FadA enzymes of *M. tuberculosis* are thought to catalyse the last three steps in the β-oxidation pathway (Figure 1-20). FadB1, a non-essential gene according to Sassetti *et al*. (2003), is thought to be a β-enoyl-CoA hydratase, converting the *trans* double bond into a OH functional group. FadB1 is a large protein of 720 amino acids and is located in the genome downstream of *fadA*, a β-ketoacyl-CoA thiolase that is thought to catalyse the final step in β-oxidation, and *far*, a fatty acid-CoA racemase, which is involved in the β-oxidation of branched fatty acids (Figure 1-21) (Rhee *et al*. 2005). It could be speculated that FadB1 is a multi-functional enzyme much like the single, multi-domain FadB protein in *E. coli*. This could further augment the degeneracy between the putative five *Mt*-FadB enzymes.

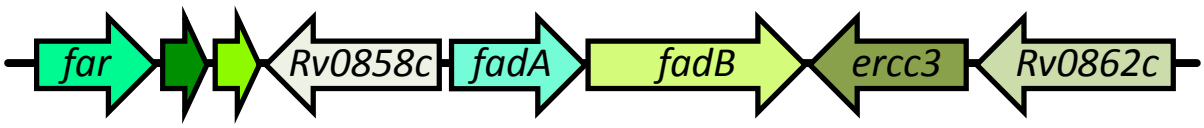

FIGURE 1-21. Map of the *M. tuberculosis* genome region encoding the β-oxidation enzymes *fadA* and *fadB*. It is thought *fadA* catalyses the last step in the pathway, thiolysis, whereas *fadB* catalyses the hydration of the β-enoyl double bond to a β-hydroxy group. The upstream gene *far* encodes a fatty acid-CoA racemase, which is involved in the β-oxidation of branched fatty acids.

FadB2 (β-hydroxyacyl-CoA dehydrogenase), also non-essential, is thought to subsequently reduce the hydroxyl group to a keto function. There are three additional FadB enzymes (FadB3–5), whose function(s) are as yet unknown. The genes may be involved in β-oxidation, but it is equally likely, as found with the *fadD* homologues, that they catalyse different steps of lipid metabolism or have an unrelated function. Regarding FadA, there are six known genes in *M. tuberculosis* numbered 1 to 6. In *E. coli*, FadA is a β-ketoacyl-CoA thiolase, which completes the β-oxidation process using CoA-SH to produce acetyl-CoA and a new acyl-CoA chain that is shorter by two carbons. Recently, *fadA5* (*Rv3546*) has been shown to be involved in cholesterol β-oxidation and is essential for utilisation of cholesterol as the cells' sole carbon source (Nesbitt *et al.* 2010). These studies demonstrated that the reaction catalysed by FadA5 was thiolysis using acetoacetyl-CoA, which they found to be consistent with β-ketoacyl-CoA thiolysis in cholesterol metabolism.

Two further enzymes are required for the metabolism of unsaturated fatty acids in order to remove the *cis* double bond (Figure 1-22). The first is a 2,4-dienoyl-CoA reductase, named FadH in *E. coli*, which yields the *trans* bond (3-enoyl-CoA), and the second is enoyl-CoA isomerase, which moves the double bond to an even carbon (*e.g.* $\Delta^3 \rightarrow \Delta^2$) to resume normal β-oxidation (van Roermund *et al*. 1998). FadH is a strictly NADPH-dependent flavoprotein (1 mol FAD/mol enzyme), which occurs as a monomer with a calculated molecular weight of 70,000 kDa (Dommes & Kunau 1984). Studies performed on the substrate specificity of *E. coli* FadH (*Ec*-FadH) have demonstrated that it is capable of reducing both 2-*trans*,4-*trans*-enoyl-CoA and 2-*trans*,4-*cis*-enoyl-CoA, but has no activity on either *cis*- or *trans*-monounsaturated acyl-CoA esters (Dommes & Kunau 1984). The *Ec*-FadH enzyme reaction is thought to occur in two half reactions (He *et al*. 1997):

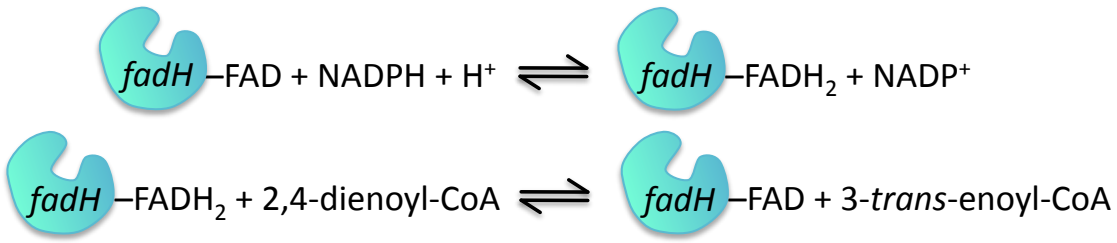

The importance of the genes involved in lipid metabolism is evident from the high percentage of the *M. tuberculosis* genome dedicated to the task; altogether, around 250 enzymes are implicated in fatty acid metabolism (Cole *et al*. 1998). Taking all this into consideration, it is clear that the enzymes of these essential pathways could offer excellent drug targets, although overcoming the apparent redundancy may be a problem.

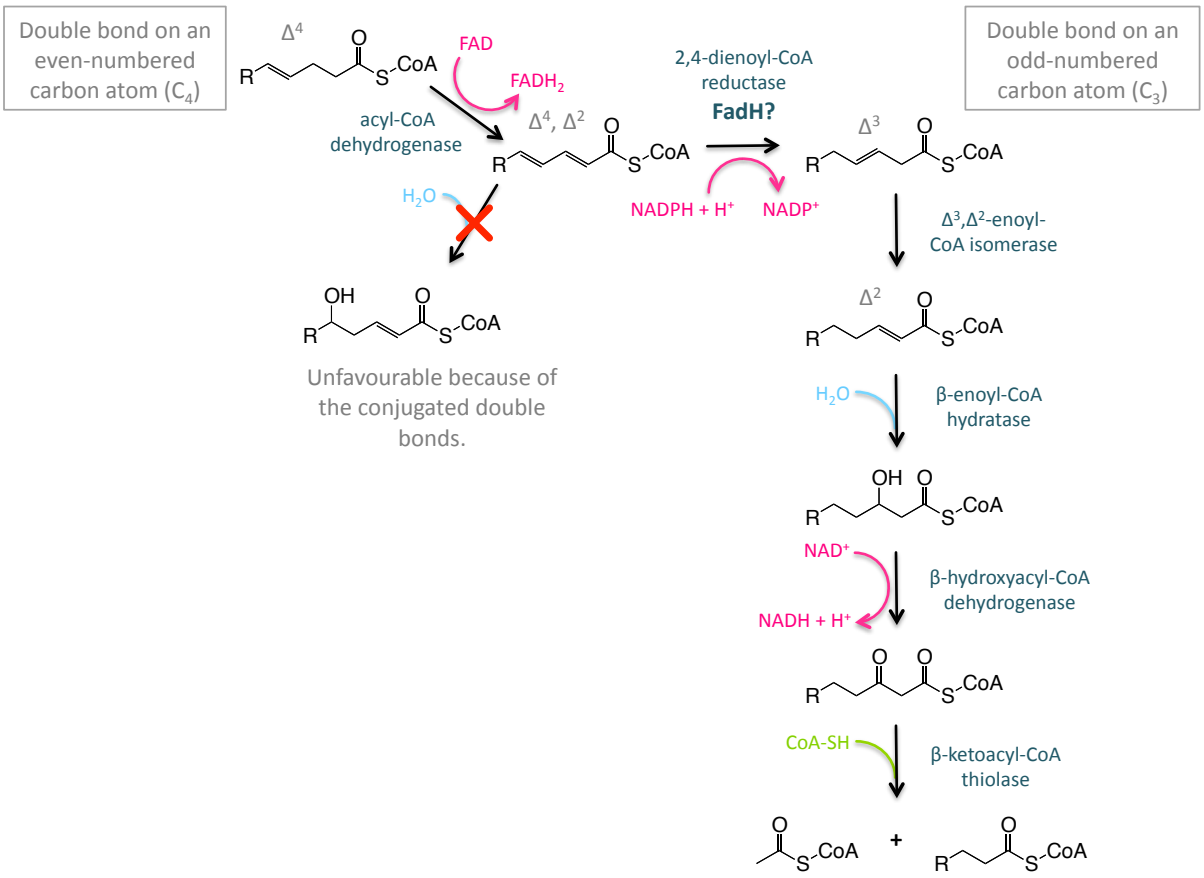

FIGURE 1-22. The β-oxidation of unsaturated fatty acids. Two further enzymes are required for the metabolism of unsaturated fatty acids in order to remove the *cis* double bond. The first is NADPH-dependent 2,4-dienoyl CoA reductase (FadH), which yields the *trans* bond and the second is enoyl CoA isomerase, which moves the double bond to an even carbon to resume normal β-oxidation. Adapted from van Roermund *et al*. (1998).

1.7. Control of tuberculosis

1.7.1. Vaccines.

Currently, the only vaccine against TB is the attenuated form of *M. bovis*: Bacille Calmette-Guérin (BGC). This BCG vaccine is part of a collaborative project with organisations such as WHO, UNICEF and GAVI called the Expanded Programme on Immunization. Established in 1974, the project aimed to immunise every child in the world against a variety of lethal diseases, including TB, by 1990 (UNICEF 2010). It has been shown that the vaccine is most effective in newborns and children, reducing the risk of TB by an average of 50 % (Colditz *et al*. 1995). However, the report showed that in adults this protection has been found to range from 0–83 %.

It is because of this limited protection that new vaccines are being developed. Two such examples are the recBCG vaccine and the MVA85A booster vaccine. The recombinant Δ*ureC hly*$^{+}$ BCG, or recBCG, vaccine is aimed at replacing the current BCG vaccine. This strain is deficient in the urease enzyme *ureC* and expresses the listeriolysin O protein of *Listeria monocytogenes*, a pore-forming hemolysin (Geoffroy *et al*. 1987). Compared to the normal BCG vaccine, the recBCG reduced bacterial load in the lungs and spleen of mice challenged with *M. tuberculosis* H_{37}Rv by 1 log (Tchilian *et al*. 2009).

Another vaccine, currently being tested, is the modified vaccinia virus Ankara strain, which expresses the *M. tuberculosis* antigen 85A (MVA85A). This has been designed to work synergistically with the BCG vaccine to boost efficacy. One group has shown that co-administration of BCG and MVA85A significantly increased the 85A-specific CD4 response in the spleen. Nevertheless, this viral booster did not improve on the protection achieved with BCG or recBCG vaccine alone (Tchilian *et al*. 2009). Another group, however, has found

promising results, demonstrating enhanced protection especially in the lungs of BCG-MVA85A co-immunised cattle, reducing the median bacterial lung scores from 10.5 to 2.5 (Vordermeier *et al*. 2009).

1.7.2. WHO initiatives.

In 1991, the WHO introduced the DOTS treatment, an acronym for Directly Observed Therapy, Short-course. This follows the patient from the initial positive screen for disease through to appropriate medication and monitored outcome (Obermeyer *et al*. 2008). Although many countries have adopted the DOTS scheme, the WHO also initiated a "Stop TB" campaign in 2006 (WHO 2010). This strategy established six main aims for 2006–2015, including increasing uptake of DOTS and promoting awareness of the rising multidrug-resistant and extensively drug-resistant cases of TB. The target by 2015 is to have reduced the prevalence of TB by 50 % compared to that in 1990. During the years from 1990 to 2007, the WHO estimated the prevalence dropped from 300 to 206 per 100,000 population. By 2050, the aim is to reduce this to just 1 case per million people per year (WHO 2009).

Despite being a called a short course, DOTS chemotherapy requires a strict therapeutic regimen involving a cocktail of drugs administered over a minimum of six months. The current standard DOTS treatment involves taking rifampicin, isoniazid, ethambutol, pyrazinamide and (in some cases) streptomycin daily for the first two months, followed by isoniazid and rifampicin thrice weekly for the ensuing four months (Cox *et al*. 2006). If the cells are resistant to one or more drugs, the regimen is changed and extended (Table 1-3) (Campbell & Bah-Sow 2006). Due to this regime, one of the main reasons for relapse in TB infection is drug non-adherence, especially when in most cases the patient's symptoms are reduced within a few months. Non-completion of the DOTS course not only leaves the patient infected but also can result in drug resistance.

TABLE 1-3. Common treatment regimens for patients suffering from drug-resistant tuberculosis.

Rifampicin-resistant TB	Isoniazid-resistant TB	Multi-drug-resistant TB
• Isoniazid 18 months • Ethambutol and/or pyrazinamide 18 months	• Rifampicin 12 months • Ethambutol or pyrazinamide 12 months	• Five drugs initially, then three drugs for 18–24 months

1.7.3. Currently used drugs.

Anti-tubercular treatment involves targeting essential systems in the cell. Due to the uniqueness and vast number of genes involved in lipid metabolism, the enzymes involved in this pathway provide excellent drug targets. Some of the most successful anti-TB treatments currently used act against this aspect of *M. tuberculosis*, and much work is underway to find new drug targets and novel compounds against these essential components. Other drugs used include those that disrupt DNA replication, translation and protein synthesis.

1.7.3.1. Isoniazid, pyrazinamide and ethionamide.

These three drugs are fatty acid synthase (FAS) inhibitors. Isonicotinic acid hydrazide, or isoniazid (Figure 1-23 A), was first introduced in 1952 and today is one of the most widely prescribed and potent anti-tubercular drugs, with a minimum inhibitory concentration in drug-sensitive *M. tuberculosis* strains of <0.05 μg/ml (Herzog 1998, Kremer & Besra 2002). Isoniazid is a pro-drug that targets mycolic acid biosynthesis. It is activated by mycobacterial KatG, a catalase peroxidase, which has been shown to oxidise the drug *via* a series of highly reactive transition states (Zhang *et al*. 1992, Zhang & Young 1993). It is these electrophilic intermediates that form adducts with NAD^+, which act as competitive inhibitors of InhA in a two-step process (Ducasse-Cabanot *et al*. 2004). The *inhA* gene encodes the NADH-

dependent enoyl-AcpM reductase, which, in the last step of the FAS-II cycle, removes the Δ^2-double bond to produce the saturated fatty acid (Figure 1-8) (Bhatt *et al*. 2007a). This hypothesis is derived from evidence where mutation of the *katG* or *inhA* gene confers resistance, although mutations in other genes, for example *ahpC* and *kasA*, have the same effect (Kremer & Besra 2002, Vilchèze *et al*. 2000). Vilchèze and co-workers (2000) demonstrated that *inhA* is essential for cell viability by isolating a strain of *M. smegmatis* with a temperature-sensitive mutation in the *inhA* gene. When inactivated at 42 °C, mycolic acid biosynthesis was halted and the cells lysed, an effect seen also upon isoniazid treatment. Isoniazid has also been shown to inhibit MabA (β-ketoacyl-ACP reductase), the enzyme that catalyses the second step in the FAS-II cycle, reducing the β-keto functional group to a β-hydroxyl (Ducasse-Cabanot *et al*. 2004). The report by Ducasse-Cabanot *et al*. (2004) showed how structurally and functionally similar InhA and MabA are, and demonstrated *in vitro* that an adduct forms between the activated isoniazid drug and the NADPH co-factor, which MabA uses, binds to and obstructs the enzyme active site.

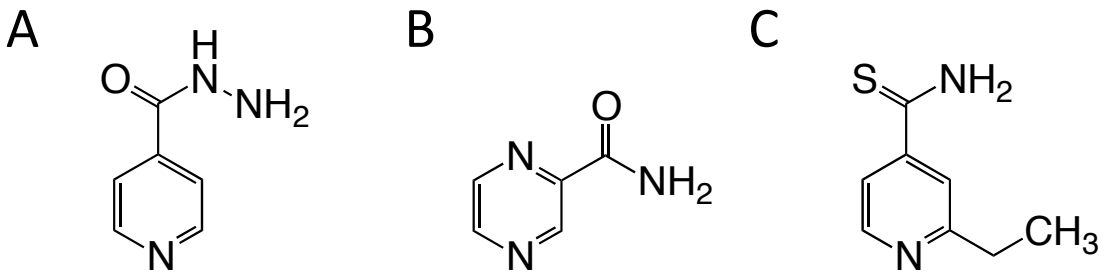

FIGURE 1-23. Currently used anti-tubercular drugs that target fatty acid biosynthesis. **(A)** Isoniazid, **(B)** Pyrazinamide, **(C)** Ethionamide.

Pyrazinamide (Figure 1-23 B) is used along with isoniazid and rifampicin to shorten the DOTS course from one year to six months. It appears to work specifically against semi-dormant bacilli *i.e.* those in the acidic conditions of the phagosome. Akin to isoniazid, pyrazinamide is a pro-drug that is activated by its conversion to pyrazinoic acid, an amide

hydrolysis reaction catalysed by the product of *pncA*, pyrazinamidase (Zimhony *et al*. 2007). The target of pyrazinoic acid is the FAS-I system, where it prevents the elongation of C_{16} to $C_{24/26}$ (Zimhony *et al*. 2000).

Ethionamide is a second-line drug and is mainly used in the treatment of drug-resistant tuberculosis (Wang *et al*. 2007a). It is the structural analogue of isoniazid (Figure 1-23 C) and consequently both compounds have been shown to target InhA. Indeed, a single Ser-94-Ala point mutation in the *inhA* gene is sufficient to cause both isoniazid and ethionamide resistance (Banerjee *et al*. 1994). Ethionamide is also similar to isoniazid in that it too is a pro-drug, although mutational studies in the *katG* gene have shown that it is not activated in the same way (Morlock *et al*. 2003). Subsequent studies identified the activator gene as *ethA*, a flavin mono-oxygenase that catalyses the cleavage of a carbon-carbon bond next to carbonyl, thus detoxifying ketones to esters and cyclic ketones to lactones *via* a Baeyer-Villiger oxidation reaction (DeBarber *et al*. 2000, Dover *et al*. 2004).

More recently, other compounds have been shown to inhibit mycolic acid biosynthesis in mycobacteria. One example of a promising anti-TB drug is platensimycin. A report by Wang *et al*. (2006) showed that the compound has good activity against *Staphylococcus aureus*, *Enterococcus faecalis* and *Streptococcoccus pneumoniae* by specifically targeting the β-ketoacyl-ACP synthases FabF and FabH of the FAS-II cycle. Part of this PhD project has been to test the activity of platensimycin against mycobacteria (see Chapter 2). Another prospective drug is thiolactomycin, which has been shown to target the mycobacterial FAS-II system with an MIC of 30 μg/ml in *M. bovis* BCG (Kremer *et al.* 2000a, Slayden *et al*. 1996). Treatment of wild-type *M. bovis* BCG with thiolactomycin alters both the α- and keto-mycolic acids, even at low concentrations (10 μg/ml). With evidence that over-expression of *Mt*-KasA and *Mt*-KasB in *M. bovis* BCG confers resistance, it appears that the drug targets

these enzymes specifically (Kremer *et al*. 2000a). The most promising aspects of developing thiolactomycin as a novel TB drug are that, because it targets FAS-II exclusively, and not FAS-I, it is unlikely to be cytotoxic and, also, it has been shown that isoniazid-resistant strains of mycobacteria are particularly sensitive to thiolactomycin treatment (Kremer *et al.* 2000a, Slayden *et al*. 1996).

Triclosan has typically been used as a non-specific microbicide in items such as deodorant, soaps and toothpaste (Bhargava & Leonard 1996). It has since been shown, however, to directly target *E. coli* FabI, the homologue of which in mycobacteria is InhA (Heath *et al*. 1998). More recently, the binding model of triclosan has been described as reversible and dependent on NAD^+ binding, indicating that it competes with the fatty acyl substrate for binding (Kuo *et al.* 2003).

Further examples of prospective drugs are those that target the β-hydroxyacyl-AcpM dehydratase enzymes of the FAS-II cycle. The FabZ and FabA dehydratase enzymes of pathogens such as *Campylobacter jejuni*, *Plasmodium falciparum*, *Pseudomonas aeruginosa* and *E. coli* have been well studied, however, there are still several candidate genes for the homologous enzymes in *M. tuberculosis* (Heath & Rock 1996a, Kimber *et al*. 2004, Kirkpatrick *et al*. 2009, Sharma *et al*. 2003). It was only recently that the enzymes encoded by the *Rv0635-Rv0636-Rv0637* gene cluster were identified in *M. tuberculosis* as the potential missing dehydratases, and their essentiality highlights them as excellent new candidates for anti-TB drugs (Brown *et al*. 2007b, Sacco *et al*. 2007). An example of a group of compounds that inhibit this activity are flavonoids, polyphenolic ketone-containing secondary metabolites found widely in the plant kingdom that are collectively known as Vitamin P. These compounds are known to help defend plants from attack by microbes, insects and fungi and have therefore attracted attention as potential anti-microbials for use in

mammals (Galeotti *et al*. 2008, Orhan *et al*. 2009). Recently, one study has shown that various flavonoids isolated from the marine sponges *Spongia* spp. and *Ircinia* spp. have *in vitro* activity against species of the parasitic protozoa *Trypanosoma*, *Leishmania* and *Plasmodium* (Orhan *et al*. 2010). Previously, Tasdemir *et al*. (2006) showed that the flavonoid targets within *P. falciparum* are enzymes of fatty acid biosynthesis, FabG, FabZ and FabI. Knowing the similarity between this fatty acid biosynthetic system and FAS-II of mycobacteria, Brown *et al.* (2007b) tested five flavonoids against *M. bovis* BCG. Two in particular, butein and isoliquirtigenin, appeared to inhibit this enzyme with MICs as low as 150 μM. Butein appeared to target FAS-II specifically, although over-expression of *Rv0636* did not afford much resistance. It is therefore likely that the flavonoid targets more than one enzyme of the cycle.

The compounds NAS-21 (4,4,4-trifluoro-1-(4-nitrophenyl)butane-1,3-dione) and NAS-91 (4-chloro-2-[(5-chloroquinolin-8-yl)oxy]phenol) have previously been shown to target the homologous enzyme, FabZ, in *P. falciparum* (Sharma *et al*. 2003). A library of NAS-21 and NAS-91 analogues was generated by Bhowruth *et al.* (2008) and the compounds were tested in a similar way to the flavonoids, against wild-type *M. bovis* BCG and the *Rv0636* over-expressing strain. Several new compounds had encouraging results, showing MIC_{99} values as low as 18 μg/ml against whole cells. One NAS-21 analogue (4,4,4-trifluoro-1-(4-ethyl)butane-1,3-dione) demonstrated FAS-II specificity with an IC_{50} of 19 μg/ml, a figure that increased 4-fold in the over-expressing strain. This provides evidence not only that Rv0636 is involved in the β-hydroxyacyl-AcpM dehydratase reaction but also that the scaffold on which the NAS analogues are based has promising anti-mycobacterial activity.

1.7.3.2. Ethambutol.

Ethambutol (Figure 1-24) was first introduced as an anti-TB drug in 1962. It is a very efficient agent and is normally used in conjunction with isoniazid. It is a bacteriostatic drug that is only active against actively dividing cells. Evidence from mutational studies has shown that ethambutol targets the *emb* locus, which encodes arabinosyltransferases, therefore acting by specifically inhibiting AG and LAM synthesis (Kremer & Besra 2002). The incorporation of D-arabinose into AG and LAM of the cell wall is prevented, thus inducing a build-up of the intermediate decaprenyl-*P*-arabinose (Takayama & Kilburn 1989). This indirectly affects the lipids of the cell wall, since disruption of the AG layer removes the 5-hydroxyl groups to which the mycolic acids are attached. This not only results in an accumulation of TMM, TDM and free mycolic acids, but also increases the permeability of the cell wall, allowing other drugs used in combination (*e.g.* isoniazid) to gain full access to the cell's cytoplasm.

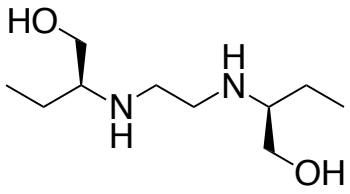

FIGURE 1-24. Ethambutol.

1.7.2.3. Rifampicin and streptomycin.

Both of these drugs inhibit protein synthesis. Rifampicin (Figure 1-25 A) was introduced as an anti-tubercular agent in 1968, significantly reducing the length of TB treatment. The compound targets DNA-dependent RNA polymerase, specifically the β-subunit of the catalytic core of prokaryotic RNA polymerase. Ezekiel and Hutchins (1968) and others have found that mutations conferring rifampicin resistance are almost solely in the *rpoB* gene, which encodes the RNA polymerase β-subunit. Rifampicin acts by blocking the second or third phosophodiester bond between nucleotides from being made (McClure & Cech 1978).

The same study showed that, once an RNA chain has been synthesised and has entered the elongation phase, the transcript and polymerase are unaffected by rifampicin, leading to the hypothesis that the compound works by steric hindrance. Evidence from co-crystallisation of the drug and the RNA polymerase core of *Thermus aquaticus* supported this theory, showing how the drug is positioned alongside a highly conserved loop domain, which is flanked by regions that contain mutations in rifampicin-resistant strains (Campbell *et al.* 2001, Zhang *et al.* 1999). The consequence of this obstruction is prevention of transcription of DNA to RNA, which subsequently provides no mRNA for protein translation.

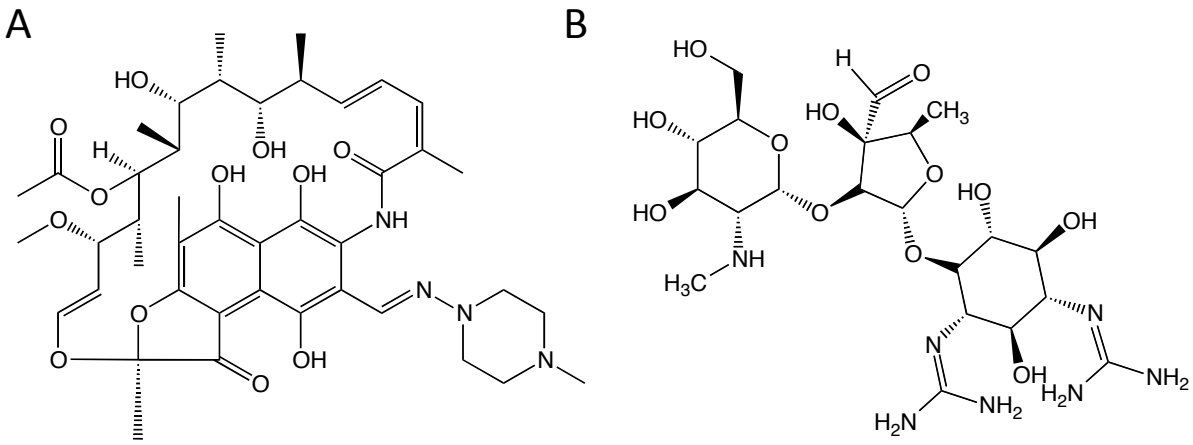

FIGURE 1-25. Currently used anti-tubercular drugs that target protein synthesis. (**A**) Rifampicin, (**B**) Streptomycin.

The antimicrobial activity of streptomycin (Figure 1-25 B), a member of the aminoglycoside group of compounds, was discovered in 1943 by Selman Waksman and co-workers (Jones *et al*. 1944) and was the first effective drug to be used against TB (Emmart 1945, Greenwood *et al*. 2007, Herzog 1998, Schatz & Waksman 1944, Smith & McClosky 1945, Wolinsky & Steenken 1947, Youmans 1945). Originally isolated from the actinomycete *Streptomyces griseus*, it is a broad-spectrum compound that is bactericidal towards Gram-positive and Gram-negative cells. Streptomycin also inhibits protein synthesis but its mechanism differs

from that of rifampicin. The drug binds irreversibly to the S12 protein of the 30S subunit of bacterial ribosomes. Resistance to streptomycin can be achieved by a single point mutation within the S12 protein, for example Lys-42-Asp/Thr/Arg or Lys-87-Arg. The drug inhibits the initiation of peptide chains by preventing the transfer of peptidyl tRNA from the A-site to the P-site. This stalls peptide synthesis because there is no space for the next formyl-methionyl-tRNA to bind. Streptomycin can stop synthesis at the start of translation as well as slowing elongation of partly completed chains. The structural differences between mammalian and bacterial ribosomes allows for target specificity. Today, because bacterial resistance is acquired so rapidly, streptomycin is used in combination with other agents to treat TB as a second-line drug and where other more expensive treatments cannot be afforded.

1.8. Drug resistance

Statistics showing an increase in multidrug-resistant (MDR) and extensively drug-resistant cases (XDR) of TB clearly demonstrate the immense necessity for new therapeutics. The 2009 WHO report estimated that, of the 10.4 million cases of TB worldwide, nearly 5 % were MDR-TB. More than half of these were in newly presenting cases, with only 1.9 % being in patients that had previously been treated for TB. It is not then surprising that the countries with the highest incidence of MDR-TB correlate with those of the highest incidence of newly diagnosed TB cases – India and China.

Resistance can be acquired through a variety of means, such as spontaneous chromosomal mutation in the target gene, gene over-expression, drug efflux or inactivation mechanisms, and preventing the drug from reaching the target (Zhang *et al*. 2005). Drug resistant TB strains first arose shortly after the introduction of streptomycin. Changes to the cell that confer resistance are selected for under the pressure of chemotherapeutics. The rationale for

combination therapy, therefore, is to reduce the probability of drug resistance developing; a cell is much more likely to acquire one mutation in a gene targeted by a drug than two or three unlinked genes. Generation of spontaneous genetic mutations is accelerated by mono-therapy, be it due to patient drug non-adherence, shortfalls in drug distribution or poor drug prescription (Zhang & Yew 2009). The genes found to have mutations in clinical isolates and the subsequent drug resistance are outlined in Table 1-4 (Zhang & Yew 2009).

Much work is underway looking at *M. tuberculosis* with a view to finding new drug targets. With the publication of the high G+C-rich *M. tuberculosis* H_{37}Rv genome in 1998, a strain originally isolated in 1905, this task has been taken to a new level and the insight into the pathogen has advanced greatly (Cole *et al*. 1998). With this and the enormous progression in molecular biology over the past decade or so, the understanding of *M. tuberculosis* – biology, mechanisms of drug action and resistance – has increased vastly.

1.9. Project aims

With the prevalence of multidrug-resistant cases of tuberculosis on the increase and reports telling of strains evolving that are resistant to all drugs currently used, the need for new, cheap and effective chemotherapy is as great now as it was 100 years ago. Therefore, there are two main aims to this PhD project:

1. To test novel compounds against known and highly effective targets such as the essential FAS-II enzymes. A combination of whole cell experiments using the well established lab surrogates, *M. bovis* BCG and *M. smegmatis*, as well as *M. tuberculosis*, and *in vitro* protein assays will be used.

2. To find new essential genes that have the potential to be novel drug targets, focussing on the little-explored β-oxidation (Fad) enzymes of *M. tuberculosis*, *M. bovis* BCG and *M. smegmatis*. Biochemical characterisation will help elucidate protein functions *in vitro*, and generating knock-out mutants using the same non-pathogenic models will aid the study of protein functionality *in vivo*.

TABLE 1-4. The mechanisms of drug resistance in *M. tuberculosis*. Based on Okamoto *et al*. 2007, Zhang *et al*. 2005 and Zhang & Yew 2009.

Drug	MIC (µg/ml)	Genes involved in resistance	Gene function	Target for inhibition	Mutation frequency (%)	Allele type
Isoniazid	0.02 – 0.2	*katG*	Catalase-peroxidase	Mycolic acid biosynthesis and other effects on lipids, DNA, carbohydrates and NAD metabolism	20 – 80	Recessive
		inhA	Enoyl-ACP reductase		15 – 43	Dominant
		ndh	NADH dehydrogenase II		10	Recessive
		ahpC	Alkyl hydroperoxidase		10 – 15	?
Rifampicin	0.5 – 2.0	*rpoB*	RNA polymerase	DNA transcription	96	Dominant
Pyrazinamide	16 – 50 (pH 5.5)	*pncA*	Nicotinamidase/pyrazinamidase	Acidification of cytoplasm and de-energised membrane	72 – 97	Recessive
Ethambutol	1 – 5	*embCAB*	Arabinosyl transferase	Arabinogalactan synthesis	47 – 65	Dominant
Streptomycin	2 – 8	*rpsL*	S12 ribosomal protein	Protein synthesis	52 – 59	Recessive
		rrs	16S ribosomal RNA		8 – 21	Dominant
		gidB	rRNA methyltransferase		33	?
Ethionamide	2.5 – 10	*etaA/ethA*	Flavin mono-oxygenase	Mycolic acid biosynthesis	37	Recessive
		inhA	Enoyl-ACP reductase		56	

CHAPTER 2

Novel compounds targeting mycobacterial fatty acid and mycolic acid biosynthesis

2.1. Introduction

Tuberculosis remains one of the foremost diseases of the world despite infection of drug-susceptible strains being almost entirely curable (Palomino *et al*. 2009). There are several well-recognised key issues that prevent TB from being eradicated, including the extensive period of time necessary for treatment and the plethora of drugs required. These factors are inextricably linked to cost of treatment, failure to complete drug courses and the evolution of drug-resistant strains, the synergistic co-infection of TB and HIV-1, and the nature of TB infection – persistent *M. tuberculosis* cells lying dormant in an asymptomatic host for potentially decades (Palomino *et al*. 2009). The drugs used today are those developed in the mid-twentieth century; no new anti-TB drugs have passed the clinical trials stage and been approved for general use since the 1960s. The need for inexpensive new drugs that are vastly more efficient is therefore imperative.

Today, several strategies are available for screening new compounds for anti-tubercular activity. The potentiality of compounds tested here have been identified and developed in the following ways:

1. From screening thousands of naturally occurring small molecules and testing against a wide range of bacterial species.

2. From *in silico* drug design, using the crystal structures of known essential *M. tuberculosis* enzymes and creating a library of pharmacophores.

3. From a chemically synthesised library of analogues based on a scaffold that has previously been identified as having anti-microbial and anti-fungal properties.

All the compounds tested here are related by targeting enzymes that are involved in mycobacterial fatty acid biosynthesis (Figure 2-1). The fatty acid synthase I (FAS-I) enzyme is found in mammals as well as bacteria meaning compounds that target this system are generally not desirable. FAS-II, however, is only found in bacteria, Archaea and plants and, although an ideal drug target would be unique to mycobacteria so as to minimise transfer of resistance factors to and from other bacteria, the system nevertheless represents an excellent pathway to block (Tripathi *et al*. 2004). Briefly, the FAS-II process in *M. tuberculosis* is initiated by the condensation of an acyl-CoA (starter unit from FAS-I) and malonyl-AcpM (extending unit), a reaction catalysed by *Mt*-FabH (Brown *et al*. 2005). AcpM then shuttles the growing fatty acyl chain between the active sites of the other FAS-II components (Kremer *et al*. 2001b). The resulting β-ketoacyl-AcpM is reduced by a β-ketoacyl-AcpM reductase (MabA) (Banerjee *et al*. 1998) to form a β-hydroxyacyl-AcpM intermediate, which is then dehydrated by the β-hydroxyacyl-AcpM dehydratase (Rv0635/Rv0636/Rv0637, named HadA, HadB and HadC respectively) to form an enoyl-AcpM intermediate (Brown *et al*. 2007a, Brown *et al*. 2007b, Sacco *et al*. 2007). Reduction to the aliphatic chain and completion of the cycle is performed by an enoyl-AcpM reductase (InhA) to yield an AcpM-bound acyl chain that is two carbons longer (Banerjee *et al*. 1994, Kikuchi & Kusaka 1984, Quémard *et al*. 1995). Two other KAS enzymes, KasA and KasB, initiate the subsequent reductive FAS-II cycles (Figure 2-1; Kremer *et al*. 2000a, Mdluli *et al*. 1998, Schaeffer *et al*. 2001). The C_{56} mero-chain is then condensed with a C_{26} fatty acid, a reaction catalysed by Pks13, to yield an oxo-mycolic acid intermediate that is then reduced to form a mature mycolic acid (Gande *et al*. 2004, Lea-Smith *et al*. 2007, Portevin *et al*. 2004, Portevin *et al*. 2005, Takayama *et al*. 2005).

The products of both FAS-I and FAS-II provide precursors for the lipid-rich cell wall, which acts as both a virulence factor and a shield against natural host killing mechanisms and

chemotherapy (Bhatt *et al*. 2007a). However, its uniqueness also provides a very attractive drug target, which has been exploited by the use of isoniazid, a front-line drug that impedes the production of essential cell wall components, such as mycolic acids. Isoniazid specifically inhibits two FAS-II cycle enzymes: primarily InhA, which catalyses the last step of the cycle, but also MabA, which catalyses the second, reduction step. To date, isoniazid is the only drug used that targets the FAS-II system, however there are many reports of newly discovered compounds that also take advantage of this system (Brown *et al*. 2007b, Slayden *et al*. 1996, Wang *et al*. 2006).

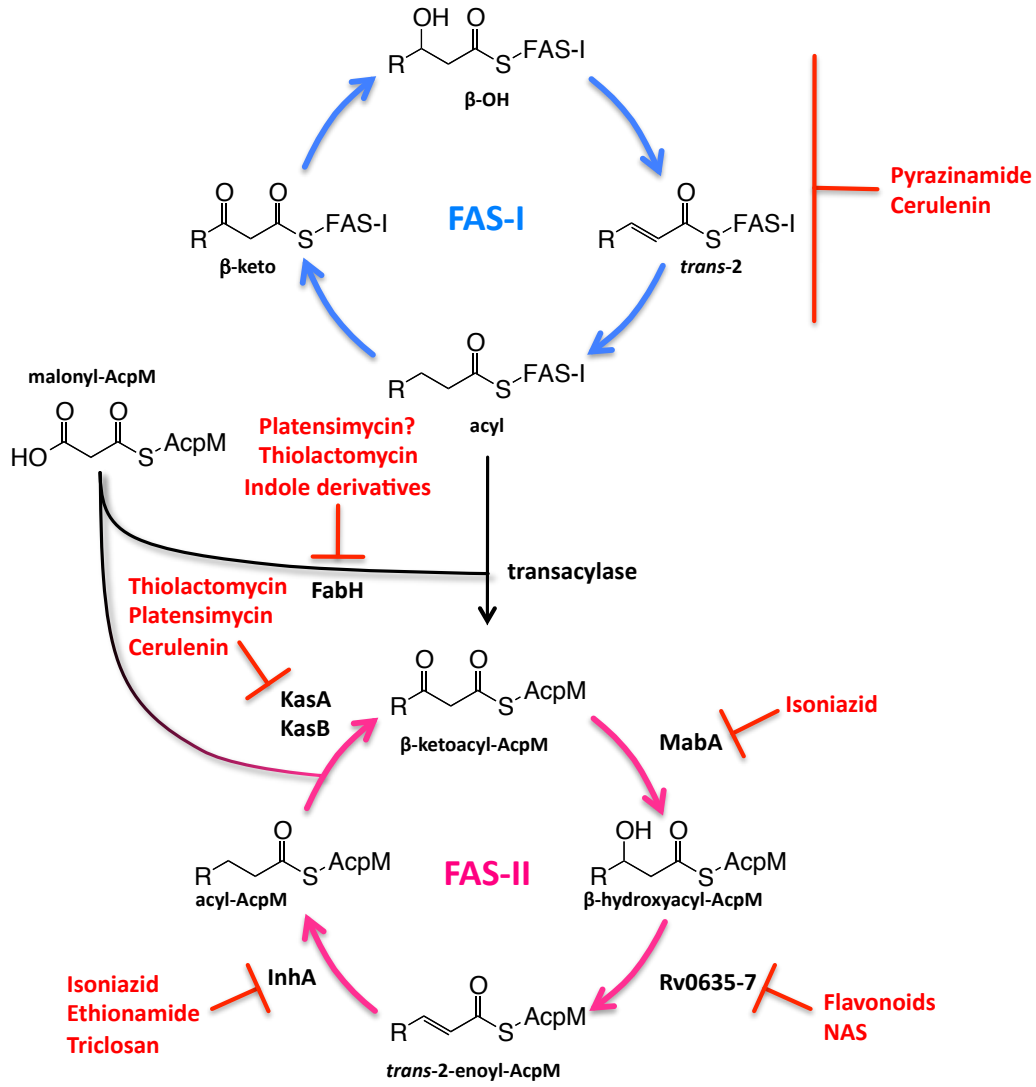

FIGURE 2-1. Fatty acid and mycolic acid biosynthetic pathways in *M. tuberculosis*. Many of the currently used drugs target enzymes of FAS-II because the system is not present in mammals. Similarly, new compounds being developed aim to inhibit these same targets. Based on Brown *et al*. (2009).

Platensimycin (Figure 2-2 A) is a small molecular weight secondary metabolite from *Streptomyces platensis* whose antibacterial activity was originally recognised after screening over 80,000 naturally occurring small molecules (Wang *et al*. 2006). It has been shown to possess potent anti-microbial activity against Gram-positive bacteria including methicillin-resistant *Staphylococcus aureus* (the hospital 'super-bug', MRSA) and vancomycin-resistant *Enterococci*. Activity against Gram-negative species, such as *E. coli*, appears to be lessened by the employment of efflux pumps. One of the main encouraging features of platensimycin is that it has minimal mammalian cytotoxicity and apparent lack of antifungal activity, indicating that platensimycin acts selectively (Wang *et al*. 2006).

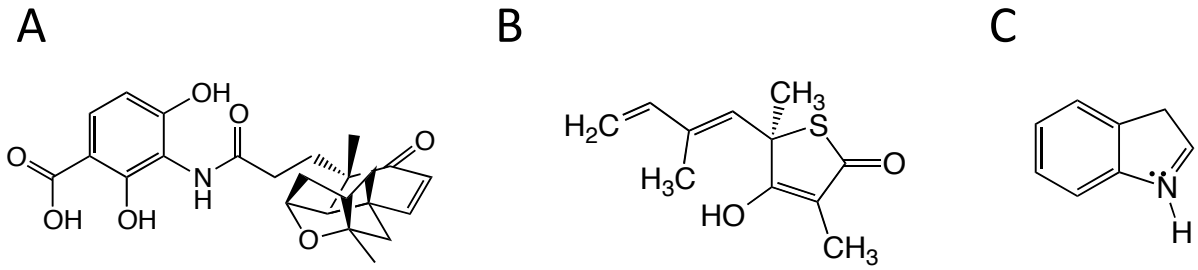

FIGURE 2-2. Novel compounds being tested for their ability to inhibit mycobacterial fatty acid biosynthesis enzymes. (**A**) Platensimycin, (**B**) Thiolactomycin, (**C**) Indole.

Platensimycin has previously been shown to target fatty acid biosynthesis by specifically inhibiting the KAS I/II enzymes, FabB and FabF, of FAS-II (Wang *et al*. 2006, Wang *et al*. 2007b). The homologous enzymes in *M. tuberculosis* are *Mt*-KasA and *Mt*-KasB, respectively (Brown *et al*. 2005, Choi *et al*. 2000). Here, the whole cell susceptibility of *M. smegmatis* and *M. bovis* BCG to platensimycin has been assessed. In addition, using discrete enzyme assays with purified *Mt*-KasA, *Mt*-KasB and *Mt*-FabH, platensimycin has been established as a promising lead compound for drug development.

Thiolactomycin (Figure 2-2 B) is also a naturally occurring compound produced by a species of *Nocardia* that was originally found in a Japanese soil sample (Oishi *et al*. 1982). The

molecule contains a unique thiolactone moiety, classing it separately from other antibiotics. Whilst demonstrating *in vivo* activity against pathogens such as malaria and trypanosomes as well as TB, the promising aspect of thiolactomycin is its specificity towards FAS-II inhibition but not against FAS-I (Jones *et al*. 2004). Indeed, thiolactomycin benefits from its low molecular weight, its high water solubility, meaning it is absorbed rapidly when administered orally, and its apparent minimal toxicity in the mouse model (de Souza 2009, Miyakawa *et al*. 1982, Oishi *et al*. 1982). Thiolactomycin has been shown to nestle very well into the FabB active site (*Mt*-KasA homologue), causing minimal structural rearrangement, where it forms reversible, non-covalent hydrogen bonds with the two active site histidine residues (Price *et al*. 2001). Slayden *et al*. (1996) tested the activity of thiolactomycin against *M. tuberculosis* and *M. smegmatis* and found that the compound targets the AcpM-dependent FAS-II system with minimum inhibitory concentrations (MICs) of 25 and 75 μg/ml, respectively. Since then, the specific targets have been identified as KasA and KasB (Kremer *et al*. 2000a) and, more recently, the structure of *Mt*-KasA has been solved complexed with thiolactomycin (Luckner *et al*. 2009). Here, a library of thiolactomycin pharmacophores was developed with cost-effectiveness of compound production in mind. A chiral centre at the 5-position of the structural scaffold means that synthesising analogues is expensive, both in terms of time and money, a fact that must be contemplated in view of drug accessibility in developing countries. The analogue library was therefore formed by simple modifications whilst basing the compound structure on that of the *Mt*-FabH active site and the reaction mechanism suggested by Sachdeva *et al*. (2008a, 2008b).

Indole-containing compounds are known to have anti-microbial properties and indeed there are several reports of compounds containing the indole ring structure dating back over 10 years (Figure 2-2 C). In 2003, a report was published showing how indole naphthyridinones act as inhibitors of the bacterial enoyl-ACP reductases FabI and FabK (Seefeld *et al*. 2003).

In the case of targeting the FAS-II enzyme InhA (the homologue of *E. coli* FabI), unlike diazoborines and triclosan, which act non-selectively, indole derivatives such as indole-5-amides act directly against the enzyme. One problem with the current front-line drug isoniazid is that it requires activation by the enzyme KatG. This immediately provides the opportunity for resistance to develop and it has been estimated by Escalante *et al*. (1998) that 50 % of clinical isoniazid-resistant cases of TB are caused by *katG* mutations. Therefore, drugs that do not require this activation are the most promising. In 2003, Kuo *et al*. undertook a high-throughput screen of approximately 500,000 compounds against *Mt*-InhA. One compound, Genz-10850, an indole-5-amide, was found to have activity against both drug-sensitive and drug-resistant *M. tuberculosis* and *P. falciparum*, the malaria-causing protozoan that also has a FAS-II system. When assayed against purified *Mt*-InhA, Genz-10850 displayed an IC_{50} of 0.16 μM and one brominated derivative had an IC_{50} of 0.12 μM. Genz-10850 was co-crystallised with *Mt*-InhA and the compound was found to occupy a larger portion of the active site than where the fatty acyl substrate or inhibitor triclosan binds (Kuo *et al*. 2003). Not only have indoles been used to target fatty acid biosynthesis but also a report from 2007 demonstrated how a novel *N*-substituted tetracyclic indole is capable of mimicking the binding of NAD^+ with the essential *M. tuberculosis* enzyme LigA, a NAD^+-dependent DNA ligase, thus acting as an inhibitor (Srivastava *et al*. 2007). A report from 2009 also highlighted azole-containing compounds that are normally used to treat fungal infection to be active against *M. tuberculosis* H_{37}Rv. The possible mechanism is inhibition of the P450-dependent sterol 14α-demethylase, perhaps through co-ordination of the azole nitrogen with the haem iron in the cytochrome (Zampieri *et al*. 2009). Most recently, the structure of *Mt*-InhA with bound Genz-10850 has been used to study the bioactive conformation of the enzyme and as a basis for identifying new hypothetical compounds (Lu *et al*. 2010).

2.2. Materials and Methods

2.2.1. Plasmids, strains and DNA manipulation.

The *E. coli* mycobacterial shuttle vector pVV16 (a gift from Varalakshmi Vissa, Colorado State University, CO, USA) containing the *hsp60* promoter and encoding a 6-histidine C-terminal tag was used for the over-expression of *Mt*-KasA and *Mt*-KasB. All DNA manipulations were performed using standard protocols, as described by Sambrook & Russell (2001). *Mt-kasA* PCR amplification was performed using the upstream primer 5′-gatcgatcaagcttgatgagtcagccttccaccg-3′ and the downstream primer 5′-gatcgatcaagcttgtaacgcccgaaggcaagc-3′, which both contain *Hin*dIII restriction sites (underlined). The 1251 bp PCR product was then digested with *Hin*dIII and ligated with similarly digested pVV16, giving rise to pVV16-*Mt-kasA*. *Mt-kasB* was cloned similarly using the upstream primer 5′-gatcgatccatatggatggggtccccccgctt-3′ and the downstream primer 5′-gatcgatcaagcttgtaccgtccgaaggcgat-3′, which contain *Nde*I and *Hin*dIII restriction sites, respectively (underlined). The 1317 bp PCR product was then digested with *Nde*I and *Hin*dIII and ligated with similarly digested pVV16, giving rise to pVV16-*Mt-kasB*. *Mt-fabH* was cloned similarly using the upstream primer 5′-gatcgatccatatggtaccgtccgaaggcgat-3′ and the downstream primer 5′-gatcgatcaagcttacccttcggcattcgca-3′, which contain *Nde*I and *Hin*dIII restriction sites, respectively (underlined). The 1033 bp PCR product was then digested with *Nde*I and *Hin*dIII and ligated with similarly digested pVV16, giving rise to pVV16-*Mt-fabH*. The pVV16-*kasAB* was constructed using the *Mt-kasA* upstream primer and the *Mt-kasB* downstream primer, the 2623 bp PCR product was then digested with *Nde*I and *Hin*dIII and ligated with similarly digested pVV16, giving rise to pVV16-*Mt-kasAB*.

The pET28b-*Mt-acpM* and pET28b-*Mt-fabD*, pET28a-*Mt-kasA* and pET28b-*Mt-kasB* over-expression plasmids for protein purification were provided by Dr. L. Kremer (Laboratoire de

Dynamique des Interactions Membranaires Normales et Pathologiques, Universités de Montpellier II et I) and the pET28a-*Mt-fabH* plasmid was constructed by Dr. A. Brown (Applied Biosciences, Northumbria University).

The *kasB*-knockout phage phAE404 was used to construct a *kasB* deletion in *M. bovis* BCG (Bhatt *et al*. 2007b). The mutant was generated by Dr. A. Bhatt using specialised transduction, as described in Bardarov *et al*. (2002). The validity of the *M. bovis* BCG Δ*kasB* was confirmed by Southern blot analysis. The coding sequences of all the recombinant genes were verified by DNA sequencing.

2.2.2. Protein over-expression and purification.

2.2.2.1. Purification of *Mt*-AcpM.

Over-expression of mycobacterial AcpM was performed as described (Kremer *et al*. 2001b). The pET28b-*Mt-acpM* over-expression plasmid was transformed into *E. coli* C41 (DE3) cells and incubated on Luria-Bertani (LB; Difco) agar supplemented with kanamycin (25 μg/ml). One colony was used to inoculate 5 ml LB broth containing kanamycin (25 μg/ml) and the culture was incubated in a rotary incubator overnight at 37 °C. The mini-culture was used to inoculate 1 l Terrific Broth containing kanamycin (25 μg/ml) and was incubated in a rotary incubator (180 rpm) at 37 °C until the OD_{600} had reached 0.6. At this point the cells were induced by adding 1 mM isopropyl β-D-1-thiogalactopyranoside (IPTG) and the culture was incubated overnight at 16 °C. The cells were harvested by centrifugation (4,500 × *g* for 15 min at 4 °C) and the pellets were stored at -20 °C for purification.

Mt-AcpM-containing pelleted cells were resuspended in buffer A (0.02 M sodium phosphate, pH 7.9, 0.5 M NaCl) and lysed twice by French press. The crude lysate was centrifuged at 27,000 × *g* for 40 min at 4 °C to remove the insoluble components and the resulting clarified

lysate was applied to a Ni^{2+}-charged 5 ml HisTrap™ HP affinity column (GE Healthcare). The column was washed with 10 column volumes of buffer A and the protein was eluted with a step-wise imidazole gradient of 10 mM, 20 mM, 30 mM, 40 mM (each of 25 ml), 50 mM (30 ml) and 150 mM (15 ml). The fractions were analysed by 14 % SDS-PAGE followed by Coomassie staining. The 150 mM fraction contained the most pure AcpM protein, where two bands were visible corresponding to holo-AcpM (14.875 kDa) and acyl-AcpM (15.135 kDa) (Kremer *et al*. 2001b). This fraction was dialysed twice against 50 mM Tris·HCl (pH 7.9), 50 mM NaCl at 4 °C. Dithiothreitol (DTT, 1.5 %) was added to the protein preparation to remove any contaminants and the acylated form of AcpM, followed by incubation in a rotary incubator at 37 °C for 36 h. Progress of the precipitation was monitored by SDS-PAGE gel and once completed, the preparation was centrifuged at 4,500 × *g* for 10 min at 4 °C. The DTT was removed by dialysing the protein twice against 50 mM Tris·HCl (pH 7.9), 50 mM NaCl at 4 °C. The AcpM may be further purified using an additional two columns. Firstly using a Q-Sepharose anion exchange column (GE Healthcare), maintained at pH 7.9, where the protein is eluted using a salt gradient (0.05–1 M NaCl). Secondly using a Thiopropyl-Sepharose 6B column (Amersham Pharmacia Biotech) equilibrated in O_2-free 50 mM Tris·HCl (pH 7.9). Here, the protein is eluted with a DTT gradient (10–25 mM).

2.2.2.2. Purification of *Mt*-FabD.

Over-expression of mycobacterial FabD was performed as described (Kremer *et al*. 2001b). The pET28b-*Mt-fabD* over-expression plasmid (provided by Dr. L. Kremer) was transformed into *E. coli* C41 (DE3) cells and incubated on LB agar supplemented with kanamycin (25 µg/ml). One colony was used to inoculate 5 ml LB broth containing kanamycin (25 µg/ml) and the culture was incubated in a rotary incubator overnight at 37 °C. The mini-culture was used to inoculate 1 l Terrific Broth containing kanamycin (25 µg/ml) and was incubated in a

rotary incubator (180 rpm) at 37 °C until the OD_{600} had reached 0.6. At this point the cells were induced by adding 1 mM IPTG and the culture was incubated for 16 h at 16 °C. The cells were harvested by centrifugation (4,500 × *g* for 15 min at 4 °C) and the pellets were stored at -20 °C for purification.

Mt-FabD-containing pelleted cells were resuspended in buffer A and lysed by French press. The crude lysate was centrifuged at 27,000 × *g* for 40 min at 4 °C to remove the insoluble components and the resulting clarified lysate was applied to a Ni^{2+}-charged 1 ml HisTrap™ HP affinity column (GE Healthcare). The column was washed with 50 ml of buffer A and the protein was eluted with a step-wise imidazole gradient of 25 mM, 50 mM, 75 mM, 100 mM, 150 mM, 250 mM and 500 mM (each of 10 ml). The fractions were analysed by 12 % SDS-PAGE followed by Coomassie staining. One band at approximately 35 kDa was visible in the 500 mM fraction. This fraction was dialysed three times against 50 mM Tris·HCl (pH 7.9), 50 mM NaCl, 1 % glycerol at 4 °C. Protein concentration was estimated using the BCA Protein Assay kit (ThermoScientific) and the fraction was stored at -80 °C.

2.2.2.3. Purification of *Mt*-FabH.

Over-expression of mycobacterial FabH was performed as described (Heath & Rock 1996b). The pET28a-*Mt-fabH* over-expression plasmid was transformed into *E. coli* C41 (DE3) cells and incubated on LB agar supplemented with kanamycin (25 µg/ml). One colony was used to inoculate 5 ml LB broth containing kanamycin (25 µg/ml) and the culture was incubated in a rotary incubator overnight at 37 °C. The mini-culture was used to inoculate 1 l Terrific Broth containing kanamycin (25 µg/ml) and was incubated in a rotary incubator (180 rpm) at 37 °C until the OD_{600} had reached 0.6. At this point the cells were induced by adding 1 mM IPTG and the culture was incubated for 3 h at 37 °C. The cells were harvested by centrifugation (4,500 × *g* for 15 min at 4 °C) and the pellets were stored at -20 °C for purification.

Mt-FabH-containing pelleted cells were resuspended in buffer A and lysed by French press. The crude lysate was centrifuged at 27,000 × *g* for 40 min at 4 °C to remove the insoluble components and the resulting clarified lysate was applied to a Ni^{2+}-charged 1 ml HisTrap™ HP affinity column (GE Healthcare). The column was washed with 50 ml of buffer A and the protein was eluted with a step-wise imidazole gradient of 25 mM, 50 mM, 110 mM and 500 mM (each of 10 ml). The fractions were analysed by 12 % SDS-PAGE followed by Coomassie staining. One band at approximately 40 kDa was visible in the 500 mM fraction. This fraction was dialysed three times against 50 mM Tris·HCl (pH 7.9), 50 mM NaCl, 1 mM EDTA, 5.6 mM β-mercaptoethanol, 1 % glycerol at 4 °C. Protein concentration was estimated using the BCA Protein Assay kit and aliquots of the fraction were stored at -80 °C.

2.2.2.4. Purification of *Mt*-KasA.

Over-expression and purification of mycobacterial KasA was adapted from Kremer *et al*. (2002a). The pET28a-*Mt-kasA* over-expression plasmid was transformed into *E. coli* Tuner™ cells and incubated on LB agar supplemented with kanamycin (25 µg/ml). One colony was used to inoculate 5 ml LB broth containing kanamycin (25 µg/ml) and the culture was incubated in a rotary incubator overnight at 37 °C. The mini-culture was used to inoculate 1 l Terrific Broth containing kanamycin (25 µg/ml) and was incubated in a rotary incubator (180 rpm) at 37 °C until the OD_{600} had reached 0.6. At this point the cells were induced by adding 1 mM IPTG and the culture was incubated for 16 h at 16 °C. The cells were harvested by centrifugation (4,500 × *g* for 15 min at 4 °C) and the pellets were stored at -20 °C for purification.

Mt-KasA-containing pelleted cells were resuspended in buffer A containing one EDTA-free complete protease inhibitor-cocktail tablet (Roche) to prevent *Mt*-KasA degradation during purification and a few grains of DNase I (New England Biolabs) to reduce the viscosity of

the lysate and remove unwanted DNA. Cell lysis was by French press and the crude lysate was centrifuged at 27,000 × *g* for 40 min at 4 °C to remove the insoluble components. The resulting clarified lysate was applied to a Ni^{2+}-charged 1 ml HisTrap™ HP affinity column (GE Healthcare). The column was washed with 50 ml of buffer A containing 50 mM imidazole and the protein was eluted in 5 ml fractions with a step-wise imidazole gradient of 100 mM, 150 mM, 200 mM, 300 mM and 500 mM. The fractions were analysed by 12 % SDS-PAGE followed by Coomassie staining. One small band at approximately 40 kDa was visible in the 150 mM and 200 mM fractions. These fractions were pooled and dialysed three times against 50 mM Tris·HCl (pH 7.5), 20 mM NaCl, and 10 % glycerol at 4 °C. The first dialysis contained 1 mM EDTA to remove any leached nickel. Protein concentration was estimated as 0.3 mg/ml using the BCA Protein Assay kit and the protein was stored at -20 °C.

2.2.2.5. Purification of *Mt*-KasB.

Over-expression of mycobacterial KasB was performed as described (Sridharan *et al*. 2007). The pET28b-*Mt-kasB* over-expression plasmid was transformed into *E. coli* C41 (DE3) cells and incubated on LB agar supplemented with kanamycin (25 µg/ml). One colony was used to inoculate 5 ml LB broth containing kanamycin (25 µg/ml) and the culture was incubated in a rotary incubator overnight at 37 °C. The mini-culture was used to inoculate 1 l Terrific Broth containing kanamycin (25 µg/ml) and was incubated in a rotary incubator (180 rpm) at 37 °C until the OD_{600} had reached 0.6. At this point the cells were induced by adding 1 mM IPTG and the culture was incubated for 16 h at 16 °C. The cells were harvested by centrifugation (4,500 × *g* for 15 min at 4 °C) and the pellets were stored at -20 °C for purification.

Mt-KasB-containing pelleted cells were resuspended in buffer A and lysed by French press. The crude lysate was centrifuged at 27,000 × *g* for 40 min at 4 °C to remove the insoluble components and the resulting clarified lysate was applied to a Ni^{2+}-charged 1 ml HisTrap™

HP affinity column (GE Healthcare). The column was washed with 50 ml of buffer A and the protein was eluted in 10 ml fractions with a step-wise imidazole gradient of 25 mM, 50 mM, 75 mM, 100 mM, 150 mM, 250 mM and 500 mM. The fractions were analysed by 12 % SDS-PAGE followed by Coomassie staining. One band at approximately 60 kDa was visible in the 100 mM fraction. This fraction was dialysed three times against 50 mM Tris·HCl (pH 7.9), 50 mM NaCl, 1 mM EDTA, 5.6 mM β-mercaptoethanol, 1 % glycerol at 4 °C. Protein concentration was estimated using the BCA Protein Assay kit and aliquots of the protein were stored at -20 °C.

2.2.3. Preparation of FAS-I and FAS-II crude cell-free extracts.

The soluble cytosolic and particulate cell wall enzyme fractions from *M. smegmatis* were prepared as described (Slayden *et al*. 1996). Wild-type *M. smegmatis* mc^2155 cultures (15 litres) were grown to an OD_{600} of 0.8 and centrifuged at 6,000 × *g* to obtain one pellet. The cells were resuspended in 30 ml buffer A (50 mM MOPS·KOH, pH 7.9, 10 mM $MgCl_2$, 5 mM β-mercaptoethanol) and lysed by probe sonication (10 cycles of 60 sec pulses followed by 90 sec cooling intervals). The crude lysate was centrifuged at 27,000 × *g* for 1 h at 4 °C. The supernatant was removed and centrifuged at 100,000 × *g* for 3 h. The resulting supernatant was decanted into a clean tube and, to precipitate the protein, 6.78 g ammonium sulfate was added initially to give a final saturation concentration of 40 % (computed using <http://www.proteinchemist.com/cgi-bin/s2.pl>). The solution was mixed at 4 °C overnight. The next day, the preparation was centrifuged at 27,000 × *g* for 1 h; the pellet being the 0–40 % fraction. Again, the supernatant was removed and 8.68 g ammonium sulfate was added to give a new final saturation concentration of 80 %. The solution was mixed for 4 h at 4 °C before pelletting the 80 % fraction by centrifugation (27,000 × *g* for 1 h at 4 °C). The supernatant was discarded and the pellet was resuspended in 5 ml buffer A. The concentration of the protein preparation, containing both FAS-I and FAS-II activity, was

determined using the BCA Protein Assay kit and the protein was stored for as little time as possible at -20 °C before use. FAS-I extracts from *C. glutamicum* were kindly provided by Dr. A. Brown.

2.2.4. Generation of the pharmacophore libraries.

The library of thiolactomycin-derivatives was produced by Al-Balas and co-workers (2009) at the Strathclyde Institute of Pharmacy and Biomedical Sciences, Strathclyde University, and the compounds were provided for *in vitro* testing. Briefly, using the structure of the *E. coli Mt*-FabH homologue *Ec*-FabB complexed with thiolactomycin, the positioning of the drug in the active site was first assessed. The computer program GOLD was then used to calculate protein-ligand docking of the thiolactomycin scaffold within the *Mt*-FabH active site. Once the key functional groups and active site residue interactions had been identified, a series of thiazole derivatives was chemically synthesised.

The series of 1,6-disubstituted indole-2-carboxylic acid analogues tested here has previously been tested against pathogenic *Francisella tularensis* bacteria (Wen *et al*. 2009). This group provided the same compounds for *in vitro* testing against *M. tuberculosis*.

2.2.5. Whole cell effects of platensimycin on *Mycobacterium spp*.

Experiments using *M. tuberculosis* CDC1551 was kindly performed by Dr. A. Bhatt. Briefly, the strain was grown in 7H9 broth supplemented with 10 % Middlebrook OADC enrichment (BBL™) and 0.05 % Tween®-80 to an OD_{600} of 0.4. Following serial 10-fold dilutions, 20 µl of each dilution was spotted on to 7H10 agar plates containing 0–128 µg/ml platensimycin. The minimum concentration of platensimycin required to inhibit growth of single colonies was noted as the MIC.

M. smegmatis-pVV16 and over-expression strains were grown in LB broth (10 ml) with 25 µg/ml kanamycin and 0.05 % Tween®-80 at 37 °C to an OD_{600} of 0.25. At this point, the minimum inhibitory concentration of platensimycin was added (14 µg/ml) and the OD_{600} was recorded over 72 h. Samples (100 µl) were taken periodically and stored at 4 °C for viable count analysis. After 72 h the cells were pelleted by centrifugation and washed with 8 ml of phosphate-buffered saline (PBS) to remove the platensimycin and the pellet was resuspended in fresh LB media. The OD_{600} was recorded over 55 h and 100 µl samples taken and viable counts determined at each time point. Briefly, the 100 µl samples were serially diluted to 10^{-7} and 10 µl samples, in triplicate, were spotted on to LB selective agar thrice. Following incubation at 37 °C, the colonies were counted and converted into colony forming units (CFU/ml).

The MICs of platensimycin against *M. smegmatis* and *M. bovis* BCG were calculated by Alamar Blue testing as previously described (Franzblau *et al*. 1998). Briefly, 200 µl of sterile deionised water was added to all outer-perimeter wells of a sterile 96-well plate (Corning Incorporated, Corning, NY, USA) to minimise evaporation of the medium in the test wells during incubation. The wells in rows B to G in columns 3 to 11 received 100 µl of 7H9 medium plus ADC (Beckton Dickinson, Sparks, MD), and contained 25 µg/ml kanamycin, 50 µg/ml hygromycin for the strains harbouring the pVV16 vector. Platensimycin was added to rows B-G in column 2 followed by 1:2 serial dilutions across the plate to column 10, and 100 µl of excess medium was discarded from the wells in column 10. A bacterial culture (100 µl) was added to the wells in rows B to G in columns 2 to 11, where the wells in column 11 served as drug-free controls. The plates were sealed with Parafilm and were incubated at 37 °C for 24 h for *M. smegmatis* strains or 5 days for *M. bovis* BCG strains. A freshly prepared 1:1 mixture of Alamar Blue (Celltiter-Blue™, Promega Corp, Madison, WI, USA) reagent and 10 % Tween®-80 (50 µl) was added to well B11 (drug-free control). The plates were re-

incubated at 37 °C for 24 h. If the well turned pink, corresponding to cell growth, the Alamar Blue mixture was added to the remaining wells, re-sealed with Parafilm and incubated at 37 °C for a further 7–12 h for *M. smegmatis* or 24 h for *M. bovis*. The colours of all the wells were recorded using a 96-well plate fluorescence reader at the wavelengths (nm) $560_{Ex}/590_{Em}$. Viable cells turned the reagent pink, whereas wells containing non-viable cells remained blue. The MIC_{99} was defined as the lowest concentration of drug that prevented a change in colour from blue to pink.

2.2.6. The *in vivo* effects of platensimycin on cell envelope lipid synthesis.

M. smegmatis cultures were grown to an OD_{600} of 0.4 in the presence of 0.25 % Tween®-80 in Sautons medium at 37 °C. Platensimycin was added at various concentrations followed by incubation at 37 °C for 16 h for *M. bovis* BCG and 8 h for *M. smegmatis* at which point 1 μCi/ml [1,2-^{14}C] acetate (57 Ci/mol, GE Healthcare, Amersham Bioscience) was added to the cultures. The *M. bovis* BCG and *M. smegmatis* cultures were further incubated at 37 °C for 24 h and 12 h, respectively. The [^{14}C]-labelled cells were harvested by centrifugation at 2,000 × *g*, washed with PBS and processed as described below.

The [^{14}C]-labelled cells were initially resuspended in methanol/0.3 % NaCl (2 ml, 100:10, v/v) and mixed with 1 ml of petroleum ether (60–80 °C) for 15 min. The upper petroleum ether layer was removed and a further 1 ml of petroleum ether added, followed by further mixing for 15 min (Dobson *et al*. 1985). The petroleum ether extracts were combined and evaporated under nitrogen using a heating block. The dried apolar lipid extract was resuspended in 200 μl of CH_2Cl_2 prior to thin-layer chromatography (TLC) and autoradiography. Polar lipids were extracted by the addition of chloroform/methanol/0.3 % NaCl (2.3 ml, 9:10:3, v/v/v) to the lower methanolic saline phase and mixed for 1 h. The mixture was centrifuged and the pellet re-extracted twice with chloroform/methanol/0.3 %

NaCl (750 µl, 5:10:4, v/v/v). Chloroform (1.3 ml) and 0.3 % NaCl (1.3 ml) were added to the combined extracts and the mixture centrifuged. The lower layer containing the polar lipids was recovered and dried (Dobson *et al*. 1985). The polar lipid extract was resuspended in chloroform/methanol (2:1, v/v). The apolar lipid extract (50,000 cpm) was applied to the corners of 6.6 × 6.6 cm plates of silica gel 60 F_{254} TLC plates (Merck 5554, Darmstadt, Germany). The plates were then developed using direction 1, chloroform/methanol/water (100:14:0.8, v/v/v), and direction 2, chloroform/acetone/methanol/water (50:60:2.5:3, v/v/v/v), to separate [^{14}C]-labelled lipids (trehalose dimycolate and glucose monomycolate). Lipids were visualised by autoradiography by overnight exposure of Kodak X-Omat AR film to the TLC plates to reveal [^{14}C]-labelled lipids and compared to known standards (Dobson *et al*. 1985).

2.2.7. The *in vivo* effects of platensimycin on mycolic acid synthesis.

The delipidated cells and whole cell pellets were similarly subjected to alkaline hydrolysis using 5 % aqueous tetrabutylammonium hydroxide (TBAH) at 100 °C overnight, followed by the addition of 4 ml CH_2Cl_2, 500 µl CH_3I, 2 ml H_2O and then followed by mixing for 30 min. The upper aqueous phase was discarded following centrifugation and the lower organic phase washed thrice with water and evaporated to dryness. The resulting fatty acid methyl esters (FAMEs) and mycolic acid methyl esters (MAMEs) were dissolved in diethyl ether and insoluble residues removed by centrifugation. The ethereal solution was evaporated to dryness and re-dissolved in 200 µl CH_2Cl_2. Equivalent volumes of the resulting solution of FAMEs and MAMEs were subjected to TLC using silica gel plates (5735 silica gel 60F_{254}; Merck), developed in petroleum ether/acetone (95:5). Autoradiograms were produced by overnight exposure of Kodak X-Omat AR film to the plates to reveal [^{14}C]-labelled FAMEs and MAMEs. Ag^{2+}-TLC was performed as described previously using Ag^{2+}-impregnated TLC plates developed twice in direction 1, hexane/ethyl acetate (95:5, v/v), and then thrice

in direction 2, petroleum ether/acetone (85:15, v/v) (Kremer *et al*. 2002b).

2.2.8. The *in vitro* effects of platensimycin, thiolactomycin analogues and indole derivatives using crude cell-free extracts.

FAS-I extracts from *M. smegmatis* and *C. glutamicum* and FAS-II cell-free extracts from *M. smegmatis* were prepared as described previously using the 40–80 % ammonium sulfate fraction (Slayden *et al*. 1996). The thiolactomycin analogues and indole derivatives were initially screened for activity against the *M. smegmatis* FAS-I system at 200 μg/ml. The thiazole derivatives were defined simply as active or not active at this concentration, whereas of the indole derivatives, those active at 200 μg/ml were then titred (0.5–100 μg/ml) into the standard reaction to obtain IC_{50} values. Platensimycin was titred into the *M. smegmatis* and *C. glutamicum* FAS-I-containing reactions from 0.1 to 150 μg/ml. The standard reaction for incorporation of radioactivity from [2-^{14}C] malonyl-CoA into C_{16}–C_{24} fatty acids catalysed by FAS-I contained: 100 mM Tris·HCl (pH 7.9), 5 mM EDTA, 5 mM DTT, 300 μM acetyl-CoA, 100 μM NADPH, 100 μM NADH, 1 μM flavin mononucleotide, 500 μM α-cyclodextrin, 300 μM CoA-SH, 20 μM malonyl-CoA, 100,000 cpm of [2-^{14}C] malonyl-CoA (specific activity 53 Ci/mol; GE Healthcare, Amersham Biosciences) and 1 mg of the cytosolic enzyme preparation in a total volume of 500 μl. The activity of the thiolactomycin analogues and the indole derivatives against mycobacterial FAS-II enzymes was tested using a cell-free extract rather than in discrete assays using purified proteins. The thiazole derivatives were again defined as active or not active at 200 μg/ml, whereas the indole derivatives that were active at 200 μg/ml were titred (0.5–100 μg/ml) into the standard reaction to monitor incorporation of radioactivity from [2-^{14}C] malonyl-CoA into C_{24}–C_{30} fatty acids catalysed by FAS-II: 100 mM potassium phosphate buffer (pH 7.0), 5 mM EDTA, 5 mM DTT, 10 μM palmitoyl-CoA, 140 μM NADPH, 140 μM NADH, 100 μg AcpM, 40 μM malonyl-CoA, 200,000 cpm of [2-^{14}C] malonyl-CoA (specific activity 53 Ci/mol) and

200 mg of cytosolic enzyme preparation in a total volume of 250 µl. In both FAS-I and FAS-II experiments, reactions were performed in triplicate at 37 °C for 1 h and terminated by the addition of 500 µl of 20 % potassium hydroxide in 50 % methanol at 100 °C for 30 min. Following acidification with 300 µl of 6 N HCl, the resultant [^{14}C]-labelled fatty acids were extracted three times with petroleum ether. The organic extracts were pooled, washed once with an equal volume of water and dried in a scintillation vial prior to counting using 5 ml of EcoScintA (National Diagnostics, Hull, UK).

2.2.9. The *in vitro* effects of platensimycin, thiolactomycin analogues and indole derivatives using purified proteins.

Mt-KasA, *Mt*-KasB and *Mt*-FabH proteins were purified and assayed as described previously (Brown *et al*. 2005, Kremer *et al*. 2002a, Sridharan *et al*. 2007). Platensimycin was titred into all three discrete enzymatic reactions (0.1–150 µg/ml), whereas the thiolactomycin analogues and indole derivatives were only tested for *Mt*-FabH inhibition. The *Mt*-KasA and *Mt*-KasB reactions were performed as follows: Holo-AcpM (40 µg) was incubated on ice for 30 min with β-mercaptoethanol (0.5 µmol) in a total volume of 40 µl. [2-^{14}C] malonyl-CoA (100,000 cpm, 6.78 nmol, 1.66 kBq), *Mt*-FabD (40 ng) and 25 µl of 1 M potassium phosphate buffer (pH 7.0) were added followed by incubation at 37 °C for 30 min. C_{16}-AcpM/holo-AcpM heterogeneous mix (22.5 µg) was added to obtain a final volume of 89 µl. *Mt*-KasA or *Mt*-KasB (0.25 µg) was added to initiate the reaction and was held at 37 °C for 1 h. The reaction was quenched by the addition of 2 ml of a $NaBH_4$ reducing solution (5 mg/ml $NaBH_4$ in 0.1 M K_2HPO_4, 0.4 M KCl and 30 % (v/v) THF). The reaction was kept at 37 °C for a further 1 h followed by two extractions with 2 ml of water-saturated toluene. The combined organic phases were pooled and washed using 2 ml of toluene-saturated water. The organic layer was removed and dried under a stream of nitrogen in a scintillation vial. The [$^{14}C_{18}$]-1,3-diol product was then quantified by liquid scintillation counting using 5 ml of EcoScintA.

The activity of *Mt*-FabH was determined as previously described (Brown *et al*. 2005). As for the cell-free extracts experiments, the thiolactomycin analogues and indole derivatives were initially tested at 200 μg/ml and those active at this concentration were titred (0.5–100 μg/ml) into the standard reaction. Platensimycin (0.1–150 μg/ml) was titred similarly into the following standard reaction to observe inhibition of the condensing activity of *Mt*-FabH: 50 μM holo-ACP/AcpM, 1 mM β-mercaptoethanol, 0.1 M sodium phosphate buffer (pH 7.0) were initially mixed and incubated at 4 °C for 30 min to ensure complete reduction of AcpM. To this, 50 μM malonyl-CoA, 45 nCi of [2-^{14}C] malonyl-CoA (specific activity 53 Ci/mol), 12.5 μM palmitoyl-CoA primer and 0.3 μg purified *Mt*-FabD were added and mixed in a volume of 50 μl and incubated at 37 °C for 30 min. *Mt*-FabD was added to generate the malonyl-AcpM reaction substrate from malonyl-CoA and AcpM *in situ*. The reaction was initiated by the addition of 0.5 μg of *Mt*-FabH followed by incubation at 37 °C for 40 min. The *Mt*-FabH assays were quenched and processed as described for the *Mt*-KasA/B assays.

2.3. Results

2.3.1. Activity of platensimycin against slow-growing mycobacteria.

Platensimycin has previously been shown to be an effective inhibitor of Gram-positive bacteria with MIC values as low as 1 μg/ml for *S. aureus*, *E. faecalis* and *S. pneumoniae* (Wang *et al*. 2006). To test the anti-mycobacterial potency of platensimycin against slow-growing mycobacteria, the activity of the antibiotic was tested against *M. tuberculosis* strains CDC1551 and H_{37}Rv. The MIC of platensimycin required to inhibit the growth of 99 % of both *M. tuberculosis* strains on solid medium was 12 μg/ml, indicating a comparable potency for this drug against this slow growing pathogen (Table 2-1). Surprisingly, the growth of the vaccine strain *M. bovis* BCG in the presence of platensimycin was different to that of *M. tuberculosis* and the strain grew normally in medium containing up to 128 μg/ml

platensimycin. The insensitivity of *M. bovis* BCG to platensimycin may be attributed to a yet unknown efflux system present in *M. bovis* but not in *M. tuberculosis*. Wang *et al*. (2006, 2007b) previously showed that a tolC efflux-negative *E. coli* strain was sensitive to platensimycin whereas the wild-type was not, indicating that the efflux of the compound plays a major role in species resistance.

TABLE 2-1. Influence of *Mt*-KasA, *Mt*-KasB and *Mt*-FabH over-expression on platensimycin in whole cell inhibition of *M. tuberculosis*, *M. smegmatis* and *M. bovis* BCG.

Strain	MIC_{99} (µg/ml)
M. tuberculosis CDC1551	12
M. tuberculosis H_{37}Rv	12
M. smegmatis	14
M. smegmatis pVV16	14
M. smegmatis pVV16-*kasA*	30
M. smegmatis pVV16-*kasB*	124
M. smegmatis pVV16-*kasAB*	126
M. smegmatis pVV16-*fabH*	16
M. bovis BCG	>128
M. bovis BCG pVV16	>128
M. bovis BCG pVV16-*kasA*	>128
M. bovis BCG pVV16-*kasB*	>128
M. bovis BCG Δ*kasB*	61

In an effort to investigate the apparent resistance of BCG to platensimycin, we sought to test the effects of increased membrane permeability by generating a *M. bovis* BCG Δ*kasB* mutant (Figure 2-3). It had previously been shown that a Δ*kasB* null mutant in *M. tuberculosis* synthesised shorter mycolic acids with an almost complete loss of *trans*-cyclopropanation of oxygenated mycolic acids that resulted in increased susceptibility to lipophilic antibiotics (Bhatt *et al*. 2007b). Interestingly, the *M. bovis* BCG Δ*kasB* mutant was sensitive to

platensimycin (MIC 61 μg/ml) suggesting that the increased permeability in comparison to the parental *M. bovis* BCG strain has indeed increased the sensitivity of *M. bovis* BCG to platensimycin (Table 2-1). The increased levels of platensimycin able to penetrate the cell may overwhelm any potential efflux protection system therefore killing the cell by cessation of FAS-II and mycolate biosynthesis. However, the high MIC of the mutant BCG strain in comparison to that of *M. tuberculosis* indicates that it is still unclear whether the resistance of BCG to platensimycin was solely due to decreased permeability to the drug.

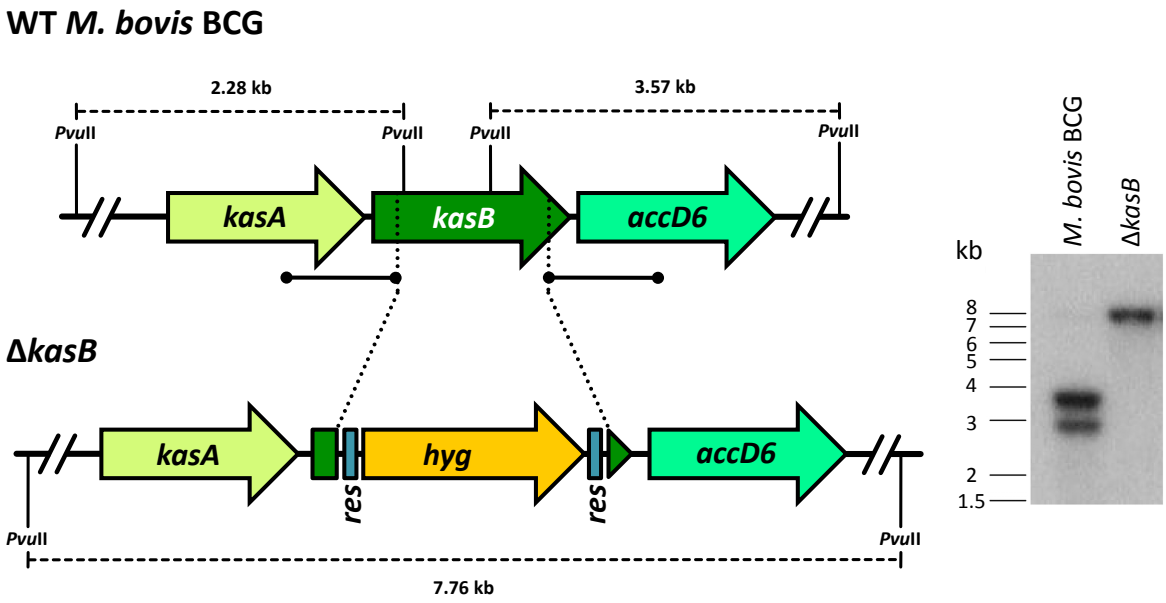

FIGURE 2-3. Generation of a *M. bovis* BCG Δ*kasB* mutant. Maps of the *kasB* region in the *M. bovis* BCG genome and its corresponding region in the conditional mutant Δ*kasB* are shown on the *left*, with the corresponding Southern blot on the *right* (produced by Dr. A. Bhatt). The regions used as probes are indicated by solid lines with round ends, while the expected bands are indicated by broken lines (with sizes indicated). *hyg*, hygromycin resistance gene from *Streptomyces hygroscopicus*; *res*, γδ resolvase recognition sites.

To facilitate further studies of the effects of platensimycin on MIC, growth and *in vivo* fatty acid biosynthesis, the non-pathogenic mycobacteria *M. bovis* BCG and *M. smegmatis* mc^2155 were used in place of *M. tuberculosis*. Not only are these species safer to use, but both have a

much faster doubling time than *M. tuberculosis* and have been shown to be equally effective in testing anti-tubercular agents (Shiloh & DiGiuseppe Champion 2009).

2.3.2. Whole cell activity of platensimycin against *M. smegmatis*.

Platensimycin was tested for inhibitory properties against the non-pathogenic, fast-growing *M. smegmatis* mc^2155. The MIC of this strain in liquid medium was found to be 14 µg/ml (Table 2-1). The growth of *M. smegmatis* was then monitored in LB broth in the presence or absence of 14 µg/ml platensimycin for a period of 72 h (Figure 2-4).

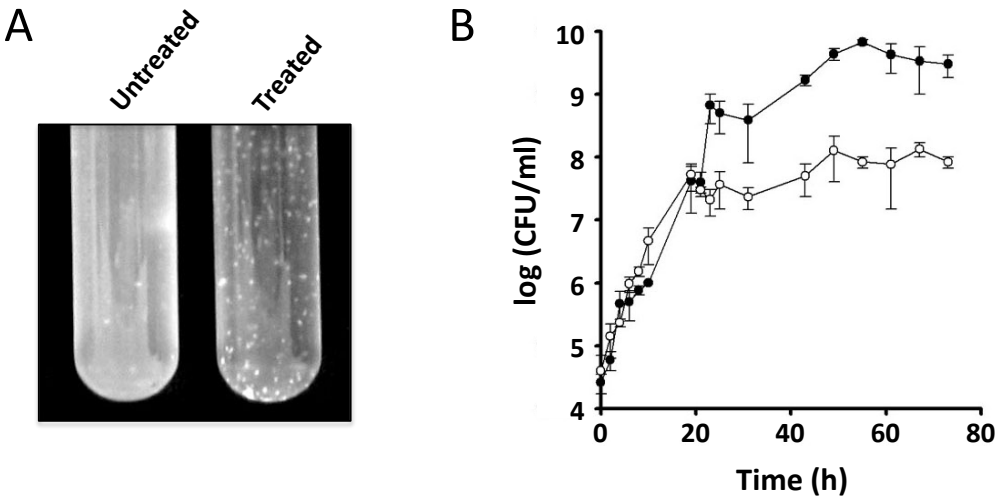

Figure 2-4. *In vivo* effect of platensimycin against *M. smegmatis*. (**A**) Clarification of cultures due to clumping and cellular lysis at time point 72 h. (**B**) Cultures were grown to an OD_{600} of 0.4 upon which 14 µg/ml of platensimycin was added. Samples were taken over a 72 h period and viable counts were calculated as *per* the methods where the mean CFU *per* ml from three independent experiments was calculated. ● *M. smegmatis*; ○ *M. smegmatis* + platensimycin.

While *M. smegmatis* grew normally in medium devoid of platensimycin, the culture in the presence of platensimycin showed a decrease in OD_{600} values with time resulting in clumping after 24 h of incubation (Figure 2-4 A). Monitoring of viable colony forming units (CFU) demonstrated that the culture grown in medium with platensimycin possessed a 2-log

decrease in CFU (Figure 2-4 B). The plateau shape observed with the treated cells would suggest that platensimycin is bacteristatic in nature. Further experimentation utilising cells exposed to platensimycin for 72 h showed that, after washing and re-inoculating into fresh media, treated cultures could be revived. This furthers the notion that platensimycin is bacteristatic against *M. smegmatis*.

2.3.3. Platensimycin inhibits the biosynthesis of fatty acids and mycolic acids.

To study the biochemical effects of platensimycin treatment, cultures of *M. smegmatis* were metabolically labelled with [^{14}C] acetate following exposure to platensimycin. Fatty acids and mycolic acids were extracted from [^{14}C]-labelled cells and methylated using phase-transfer catalysis and iodomethane. Extracts of total fatty acid methyl esters (FAMEs) and mycolic acid methyl esters (MAMEs) from untreated and platensimycin treated cultures (5–60 μg/ml) were analysed by TLC-autoradiography. Biosynthesis of fatty acids and α- and epoxy-mycolic acids was significantly inhibited upon platensimycin treatment (20–40 μg/ml) (Figure 2-5 A, B). Interestingly, an accumulation of α′-MAMEs was observed at lower concentrations of platensimycin (10–20 μg/ml). This is similar to studies observed upon thiolactomycin treatment of *M. smegmatis*, a known inhibitor of FAS-II enzymes KasA and KasB (Figure 2-5 B) (Slayden *et al*. 1996). The inhibition of fatty acids is in contrast to studies involving the FAS-II inhibitor isoniazid where inhibition of mycolic acid biosynthesis leads to an accumulation of fatty acids (Baulard *et al*. 2000). These results suggest that platensimycin also inhibits fatty acid biosynthesis *via* inhibition of mycobacterial FAS-I.

Further analysis of the same samples by 2D-Ag^{2+} TLC reinforced these findings and revealed more clearly that synthesis of α- (α_1 and α_2) and epoxy-mycolic acids (Figure 1-11) was abolished at lower concentrations (Figures 2-6 A), in comparison with the initial accumulation and then cessation of α′-mycolic acid biosynthesis (Figure 2-5 A). Futhermore,

extracts of cell wall-bound mycolic acids afforded similar profiles upon platensimycin treatment (Figure 2-6 B). In addition, analysis of [^{14}C]-labelled lipids extracted from platensimycin-treated cultures also revealed that the synthesis of mycolate containing lipids glucose monomycolate and trehalose dimycolate were reduced (Figure 2-6 C). These results demonstrated that platensimycin targeted fatty acid and mycolic acid biosynthesis in *M. smegmatis*.

2.3.4. Platensimycin resistance of *M. smegmatis* strains over-expressing *Mt*-KasA, *Mt*-KasB or *Mt*-FabH.

The use of gene over-expression to identify cellular targets of anti-mycobacterial drugs has been highly successful (Belanger *et al*. 1996, Kremer *et al*. 2000a, Larsen *et al*. 2002). Given that the targets of platensimycin in other bacteria were β-ketoacyl synthases, the effects of over-expression of *Mt*-KasA, *Mt*-KasB or *Mt*-FabH on platensimycin resistance in *M. smegmatis* were tested. The three β-ketoacyl-ACP synthases, cloned into the *E. coli-Mycobacterium* shuttle vector pVV16, were introduced into *M. smegmatis* by electroporation. Multiple copies and constitutive expression driven by the *hsp60* promoter ensures over-expression of the cloned genes in the host Mycobacterium. First, levels of each recombinant protein were assessed by Western blot to confirm that any observed change in resistance could be attributed to increased levels of the target protein. Over-expression of *Mt*-KasA conferred a modest 2-fold increase in resistance to platensimycin, increasing the MIC from 14 to 30 μg/ml (Table 2-1). Conversely, *Mt*-KasB over-expression resulted in a substantial 9-fold increase in the MIC to 124 μg/ml (Table 2-1). A combination of *Mt*-KasA/B over-expression failed to enhance resistance to platensimycin further and possessed a MIC of 126 μg/ml. Interestingly, although platensimycin was previously shown to target FabH in other bacteria (Wang *et al*. 2007b), over-expression of *Mt*-FabH failed to confer resistance to platensimycin; the MIC only increased to 16 μg/ml (Table 2-1).

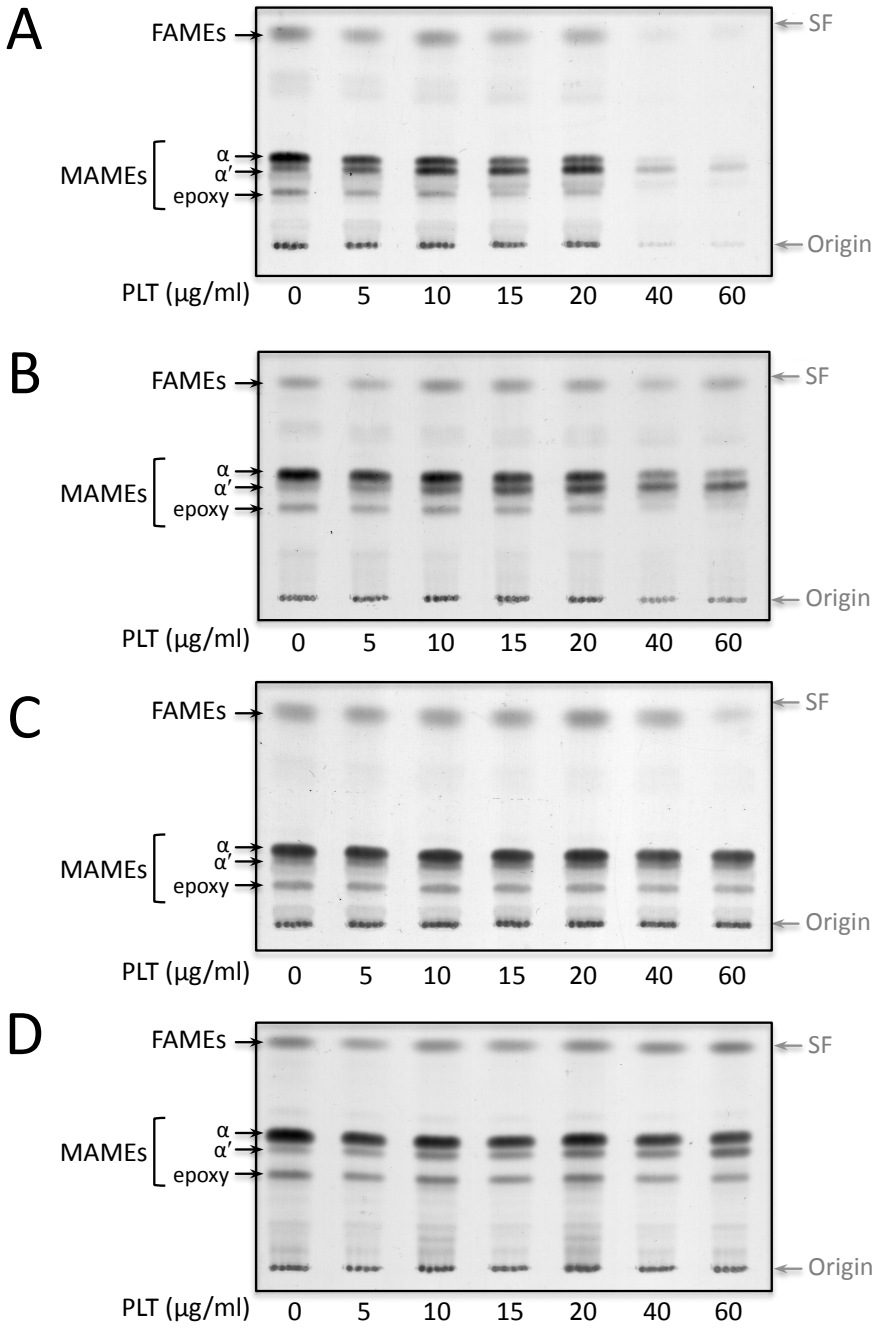

FIGURE 2-5. TLC-autoradiography of FAMEs and MAMEs from *M. smegmatis* strains over-expressing *Mt*-KasA, *Mt*-KasB and *Mt*-FabH following platensimycin treatment. Platensimycin (0–60 µg/ml) was titred into *M. smegmatis* cultures at an OD_{600} of 0.4 prior to labelling with 1 µCi/ml [1,2-^{14}C] acetate for 12 h. [^{14}C]-FAMEs and MAMEs were extracted and resolved by TLC. An equivalent aliquot of the resulting solution of FAMEs and MAMEs was subjected to TLC using silica gel plates developed twice in petroleum ether/acetone (95:5). Autoradiograms were produced by overnight exposure to Kodak X-Omat film to reveal [^{14}C]-labelled FAMEs and MAMEs. (**A**) *M. smegmatis* pVV16, (**B**) *M. smegmatis* pVV16-*Mt-kasA*, (**C**) *M. smegmatis* pVV16-*Mt-kasB* and (**D**) *M. smegmatis* pVV16-*Mt-kasAB*. *SF*, solvent front; *FAMEs*, fatty acid methyl esters; *MAMEs*, mycolic acid methyl esters; *PLT*, platensimycin.

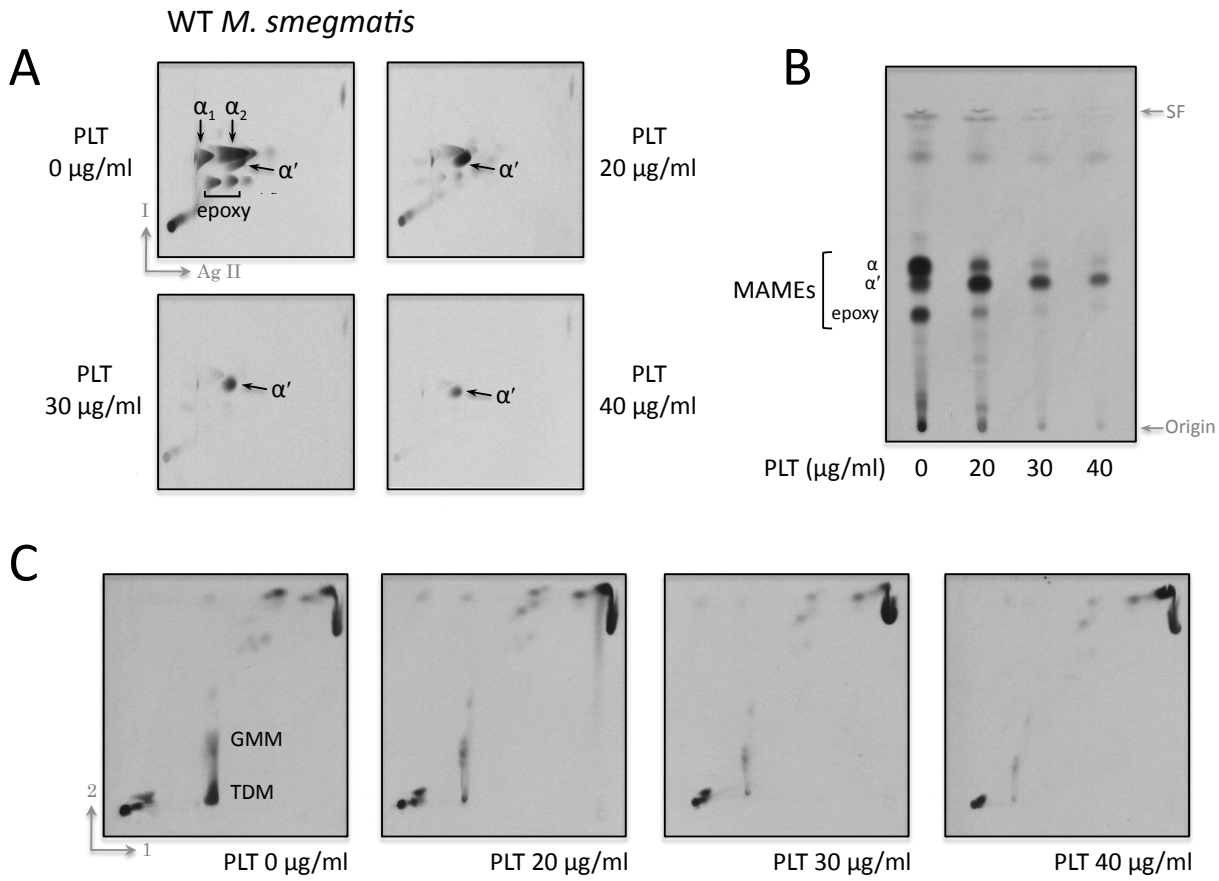

FIGURE 2-6. TLC-autoradiography of *M. smegmatis* lipid extracts and cell wall bound mycolates following platensimycin treatment. Platensimycin (0, 20, 30, 40 µg/ml) was added to *M. smegmatis* cultures at an OD_{600} of 0.4 for 8 h prior to labelling with 1 µCi/ml [1,2-^{14}C] acetate for 12 h. (**A**) 2D-Ag^{2+} TLC using silica gel plates developed twice in hexane/ethyl acetate (95:5) (*direction 1*) then thrice in petroleum ether/diethyl ether (85:15) (*direction 2*, Ag^{2+}). (**B**) Cell wall bound mycolate profiles were revealed following development twice in petroleum ether-acetone (95:5). (**C**) [^{14}C]-Polar lipids were extracted and resolved by TLC; *direction 1*, chloroform/methanol/water (100:14:0.8); *direction 2*, chloroform/acetone/methanol/water (50:60:2.5:3). Autoradiograms were produced by overnight exposure to film to reveal [^{14}C]-labelled lipids. *PLT*, platensimycin; *MAMEs*, mycolic acid methyl esters; *GMM*, glucose monomycolate; *TDM*, trehalose dimycolate.

These observations were similar to resistance studies conducted with thiolactomycin and strains over-expressing *Mt*-FabH (Choi *et al*. 2000). The 9-fold increase in resistance to platensimycin by *M. smegmatis* over-expressing *Mt*-KasB suggests that platensimycin preferentially targets KasB.

To further confirm the targeting of mycobacterial KasA and KasB enzymes by platensimycin, the ability of the recombinant KAS over-expressing *M. smegmatis* strains to incorporate [^{14}C] acetate into fatty acids and mycolic acids was examined. TLC analysis of FAMEs and MAMEs extracted from different strains treated with platensimycin revealed that, whilst mycolic acid biosynthesis was only partially restored in the *Mt*-KasA over-producing strain, over-expression of either *Mt*-KasB or *Mt*-KasAB fully restored fatty acid and mycolic acid biosynthesis (Figure 2-5 B–D).

2.3.5. *In vitro* activity of platensimycin, thiolactomycin analogues and indole derivatives against FAS-I and FAS-II extracts.

To date, no crystal structure of *Mt*-FabH has been solved complexed with an inhibitor, so the ligand docking used to synthesise the thiolactomycin analogues here was based on the interaction between thiolactomycin and the homologous enzyme in *E. coli*, FabF (Price *et al*. 2001). The key interactions identified are outlined in Table 2-2.

TABLE 2-2. The key interactions between *E. coli* FabF (homologous to *Mt*-FabH) and the ligand thiolactomycin (Al-Balas *et al*. 2009).

Ligand	Active site interaction
C3 methyl group	Hydrophobic pocket defined by Phe-229 and Phe-392
5-isoprenoid moiety	Wedged between Val-271 / Phe-272 and Gly-391 / Phe-392
2-carbonyl group oxygen	Two H bonds with the active site histidines, His-298 and His-333
4-hydroxy group	Network of H_2O molecules positioned by the carbonyl O of Val-271 and amide NH of Gly-305

Taking these interactions into consideration, the achiral scaffold of 2-amino thiazole-5-carboxylate was chosen and derivatives were chemically synthesised by Al-Balas and co-workers (2009) using the methods described by Barton *et al*. (1982) (Figure 2-7).

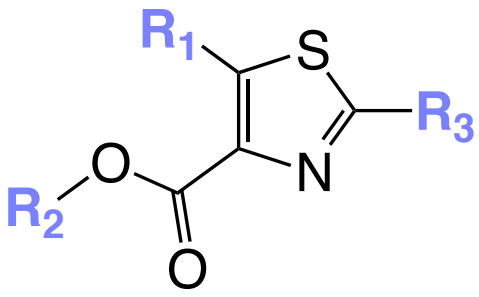

FIGURE 2-7. The structure of 2-amino thiazole-5-carboxylate. The scaffold on which the thiolactomycin pharmacophore library was based.

The effects of all the compounds on the FAS-I and FAS-II systems *in vitro* were evaluated by observing the impact upon [^{14}C] malonyl-CoA incorporation into fatty acids and mycolic acids, respectively. The FAS-I systems of both *M. smegmatis* and *C. glutamicum* were used to assess the anti-FAS-I activity of platensimycin, whereas just that of *M. smegmatis* was used for the thiazole compounds and indole derivatives. For platensimycin, the mycolate-producing FAS-II system was assessed by discrete assays using pure *Mt*-KasA, *Mt*-KasB and *Mt*-FabH (see section 2.3.6.), whereas for the thiazole library and indole derivatives a crude cell-free extract with FAS-II activity was used to evaluate activity (Brown *et al*. 2005, Kremer *et al*. 2000a, Kremer *et al*. 2002a, Radmacher *et al*. 2005).

Interestingly, when platensimycin was titred into crude cell-free extracts enriched with FAS-I of either *M. smegmatis* or *C. glutamicum*, activity was inhibited at an IC_{50} value of 12 µg/ml and 6.5 µg/ml, respectively. It could be argued that this inhibition of FAS-I activity could be detrimental to the effectiveness of platensimycin as a lead compound. In the recent patent publication using human cell-free FAS-I assays, it was demonstrated that both platensimycin and platencin had activity (IC_{50}) of 0.132 µg/ml (0.3 µM) and 2.68 µg/ml (6.3 µM), respectively (Singh *et al*. 2008). However, it was previously demonstrated in whole cell assays by the patent applicants, Wang *et al.* (2006), that platensimycin had low mammalian

cell toxicity (IC_{50}) of HeLa MTT >1000 μg/ml. The authors also confirmed a lack of antifungal activity against *Candida albicans*, which synthesises fatty acids *via* a type I fatty acid synthase (>64 μg/ml).

Of the thiazole derivatives tested, all the compounds possessing a bromoacetamido group at the 2-position showed activity against FAS-I, FAS-II or both systems (Table 2-4). One compound, QAB-130a, showed *in vitro* activity against FAS-II but not FAS-I (60 % inhibition at 200 μg/ml). This would be an encouraging result since the compound appears to be specific to the bacterial system, however, when aligned with *M. tuberculosis* MIC data on the same compounds (data provided by Dr. Q. Al-Balas, University of Strathclyde), it can be seen that these compounds do not display any whole cell activity.

There were five indole derivatives that showed activity against FAS-I and six against FAS-II, of which two were active against both systems (Table 2-5). The most encouraging of these is WIUAKP-045, which inhibited only FAS-II with an IC_{50} of 3.64 ± 0.02 μg/ml. The fact that none of the FAS-II-inhibiting compounds were active against FabH indicates that some other enzyme in the cycle is being targeted.

2.3.6. *In vitro* activity of platensimycin, thiolactomycin analogues and indole derivatives against *Mt*-KasA, *Mt*-KasB and *Mt*-FabH.

In order to examine whether the compounds target mycobacterial mycolic acid biosynthesis or not, purified *Mt*-KasA, *Mt*-KasB or *Mt*-FabH (for platensimycin) or *Mt*-FabH (for the thiolactomycin analogues and indole derivatives) were assessed in discrete assays as described earlier (Brown *et al*. 2005, Kremer *et al*. 2000a, Kremer *et al*. 2002a). In these assays [^{14}C] malonyl-CoA was transacylated to AcpM *via* *Mt*-FabD prior to the addition of the relevant substrates (C_{16}-AcpM and C_{16}-CoA) and the enzyme of interest. Upon

completion and termination of the experiment the radiolabelled acyl-AcpM derivates were extracted using organic solvents. The assays were performed with a titre in triplicate and recorded as an IC_{50} value.

Platensimycin was found to be active against both *Mt*-KasA and *Mt*-KasB possessing IC_{50} values of 2.0 µg/ml and 4.2 µg/ml, respectively (Table 2-3). These results are consistent with platensimycin *in vitro* inhibition of FabF in *S. aureus* and *E. coli* (Wang *et al*. 2007b). Interestingly, the IC_{50} values obtained with platensimycin are significantly lower than those obtained with another mycobacterial KAS inhibitor thiolactomycin (KasA = 4.21 µg/ml [20 µM], KasB = 18.9 µg/ml [90 µM]) (Schaeffer *et al*. 2001). Studies by Wang *et al* (2007b) demonstrated that *S. aureus* FabH activity was inhibited by platensimycin (IC_{50} = 29.5 µg/ml [67 µM]). In contrast *Mt*-FabH over-expression failed to confer resistance (Table 2-1) and *in vitro Mt*-FabH was relatively insensitive to platensimycin (IC_{50} >150 µg/ml) in comparison to *Mt*-KasA and *Mt*-KasB (Table 2-3).

TABLE 2-3. *In vitro* inhibition (IC_{50}) of platensimycin against purified FAS-II system enzymes. Values represent the mean of three replicates ± standard error.

Protein	IC_{50} (µg/ml)
Mt-KasA	2.0 ± 0.1
Mt-KasB	4.2 ± 0.1
Mt-FabH	>150

Only three of the thiazole compounds were active against purified *Mt*-FabH, QAB-61, QAB-62a and QAB-108a, with IC_{50} values of 1.04 ± 0.2, 1.1 ± 0.1 and 79.9 ± 1.0 µg/ml, respectively. This is interesting considering the compounds were designed to target *Mt*-FabH, however, all three had the bromoacetamido group at the R3 position indicating that this is a key feature (Table 2-4). All three of these were also active against FAS-I but, unlike the other

two, QAB-61 was not found to be active against FAS-II. Similarly, of the 44 indole derivatives tested, only two were found to be active against *Mt*-FabH, WIUAKP-052 and WIUAKP-056, with IC_{50} values of 109.5 ± 1.15 and 109.1 ± 0.64 µg/ml, respectively (Table 2-5).

2.4. Discussion

Mycolic acid biosynthesis is essential for mycobacterial survival and many anti-tuberculosis drugs like isoniazid, ethionamide and thiolactomycin target enzymes of this exclusive pathway (Banerjee *et al*. 1994, Kremer *et al*. 2000a). The identification and functionality of novel lead anti-tubercular agents is essential mainly due to the emergence of MDR-TB, and more recently, XDR-TB (Kaye & Frieden 1996, Wright *et al*. 2006). In this worrying climate where untreatable strains of XDR-TB are becoming apparent, the impetus for the discovery of new anti-tubercular agents becomes crucial. The discovery and characterisation of new drugs targeting key enzymes involved in essential mycobacterial biosynthetic pathways is paramount, but without the introduction of novel lead compounds, such as platensimycin, anti-tubercular therapy will not proceed fast enough to cope with the increasing resistance observed today. Not only should drug development focus on the synthesis of active analogues of existing anti-mycobacterials, but also on identification of new classes of drugs, such as platensimycin.

2.4.1. Platensimycin.

The *Streptomyces platensis* natural product platensimycin represents a new chemical class of antibiotics (Wang *et al*. 2006). This study has shown that platensimycin is active against *M. tuberculosis* and, through the use of the *M. smegmati*s surrogate system, the mode of action of platensimycin against *Mycobacterium spp*. could be investigated and elucidated.

TABLE 2-4. The *in vitro* activity of the thiolazole-containing compounds compared to that of thiolactomycin. * Compounds were regarded as not active if <50 % inhibition was observed at 200 µg/ml, † Values obtained by Al-Balas *et al*. (2009); compounds were regarded as not active if no inhibition was observed at 200 µg/ml. a. From Kim *et al*. 2006, b. From Bhowruth *et al*. 2007.

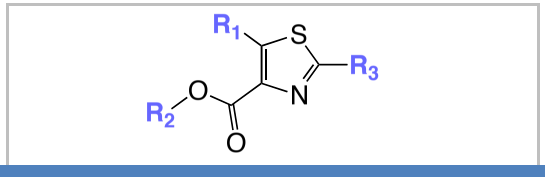

Compound	R_1	R_2	R_3	*Mt*-FabH IC_{50} (µg/ml)	*Ms*-FAS-I *	*Ms*-FAS-II *	TB MIC_{99} (µg/ml) †
Thiolactomycin	-	-	-	16.0 [a]	Not active	Active	13.0 [b]
QAB-4	CH_3	CH_3	NH_2	Not active	Not active	Not active	16.0
QAB-4a	CH_3	H	NH_2	Not active	Not active	Not active	0.06
QAB-7	C_6H_5	CH_3	NH_2	Not active	Not active	Not active	Not active
QAB-7a	C_6H_5	H	NH_2	Not active	Not active	Not active	Not active
QAB-8	$C_6H_5CH_2$	CH_3	NH_2	Not active	Not active	Not active	0.06
QAB-8a	C_6H_5CH2	H	NH_2	Not active	Not active	Not active	Not active
QAB-30	*m*-Cl-C_6H_5	CH_3	NH_2	Not active	Not active	Not active	32.0
QAB-30a	*m*-Cl-C_6H_5	H	NH_2	Not active	Not active	Not active	Not active
QAB-56	*p*-Cl-C_6H_5	CH_3	NH_2	Not active	Not active	Not active	Not active
QAB-58a	*m*-Cl-C_6H_5	H	$NHCOCH_2Br$	Not active	Active	Not active	Not active
QAB-61	*p*-Cl-C_6H_5	CH_3	$NHCOCH_2Br$	1.04 ± 0.2	Active	Not active	Not active
QAB-62a	C_6H_5	H	$NHCOCH_2Br$	1.1 ± 0.1	Active	Active	Not active
QAB-108a	$C_6H_5CH_2$	H	$NHCOCH_2Br$	79.9 ± 1.0	Active	Active	Not active
QAB-130	CH_3	CH_3	$NHCOCH_2Br$	Not active	Active	Active	Not active
QAB-130a	CH_3	H	$NHCOCH_2Br$	Not active	Not active	Active	Not active

TABLE 2-5. The *in vitro* inhibition (IC_{50}) of the indole-derivative library against *Ms*-FAS-I, *Ms*-FAS-II and *Mt*-FabH. Compounds were regarded as not active if <50 % inhibition was observed at 200 µg/ml. Values are means of three replicates ± standard error.

Compound	Structure	IC_{50} (µg/ml)		
		***Ms*-FAS-I**	***Ms*-FAS-II**	***Mt*-FabH**
WIUAKP-003	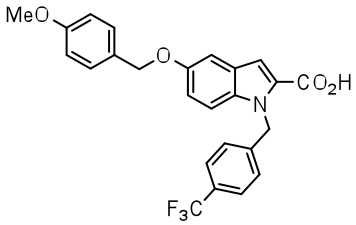	Not active	33.2 ±1.20	Not active
WIUAKP-005	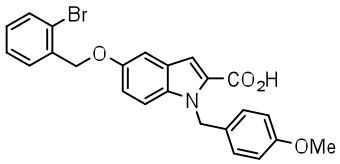	Not active	28.0 ± 0.60	Not active
WIUAKP-026	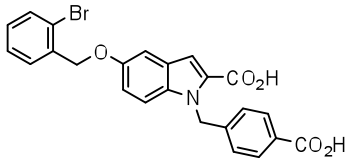	89.5 ± 8.50	Not active	Not active
WIUAKP-027	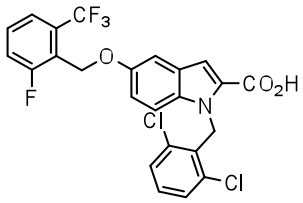	69.0 ± 4.40	Not active	Not active
WIUAKP-028	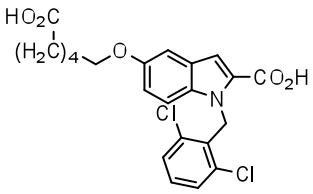	182.8 ± 9.70	Not active	Not active
WIUAKP-041	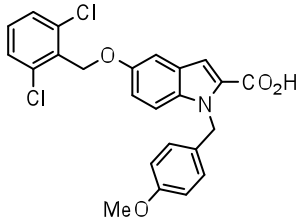	182.0 ± 9.50	19.7 ± 1.01	Not active
WIUAKP-042	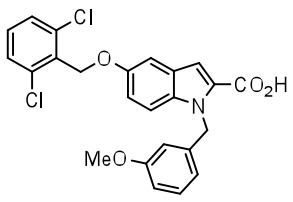	191.0 ± 3.50	5.37 ± 0.03	Not active

Compound	Structure	IC_{50} (µg/ml)		
		***Ms*-FAS-1**	***Ms*-FAS-II**	***Mt*-FabH**
WIUAKP-045	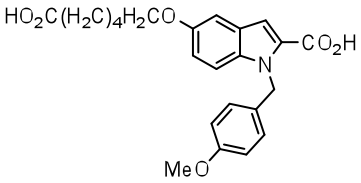	Not active	3.64 ± 0.02	Not active
WIUAKP-052	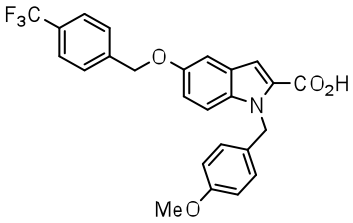	Not active	Not active	109.5 ± 1.15
WIUAKP-056	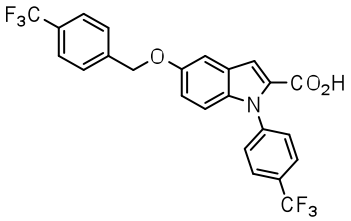	Not active	Not active	109.1 ± 0.64
WIUAKP-059	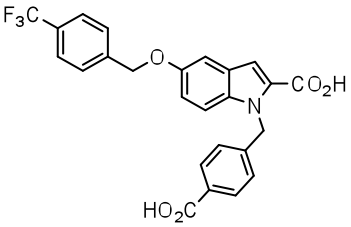	Not active	5.22 ± 0.06	Not active

The activity of platensimycin against FAS-I has previously been observed against the human and rat FAS *in vitro* (Singh *et al*. 2008) but no activity was observed against mammalian culture systems *in vivo* (Singh *et al*. 2006). Although in mycobacteria the fatty acyl-products of FAS-I provide primers for extension to meromycolate precursors of mycolic acids, the effects on FAS-II appear to be more complex than a simple deprivation of primer supply brought about *via* FAS-I inhibition. Therefore, the combination of activity observed against both FAS-I and the FAS-II components KasA/KasB contribute to the inhibitory effect of platensimycin against *M. smegmatis*. While from the point of view of drug development, FAS-II inhibition, which causes cessation of the essential mycolic acids, is desirable, inhibition of FAS-I is not since mammalian fatty acid synthases are too similar. However, in

previous studies platensimycin has been shown to possess low mammalian cell toxicity in HeLa cytotoxicity assays and to lack antifungal activity, indicating that platensimycin may not act selectively against mycobacterial FAS-I.

Despite only a moderate level of sequence identity between *Mt*-KasB and *E. coli* FabF (~36 %), the two enzymes display identical folds (Figure 2-8 A). To ascertain whether the active site of *Mt*-KasB would be compatible with the steric requirements of platensimycin, a hypothetical structural model of platensimycin-bound *Mt*-KasB was generated using the *Mt*-KasB (PDB code 2GP6) superimposed with platensimycin-bound *Ec*-FabF with a single point mutation Cys-163-Gln (PDB code 2GFX) (Figure 2-8). Subsequent conjugate-gradient energy minimisation relieved mild steric clashes between protein and ligand and resulted, compared to ligand-free *Mt*-KasB, in minor to moderate shifts of side chains located within a 4 Å-radius of platensimycin (root mean square displacement 0.93 Å for 186 main and side chain atoms, maximum displacement 3.5 Å).

The model illustrates steric compatibility between platensimycin and the active site of *Mt*-KasB, but hints at subtle differences in protein-inhibitor interactions between *Ec*-FabF and *Mt*-KasB. The benzoic acid ring faces a structural environment that is virtually identical to that in *Ec*-FabF (Figure 2-8 B). However, the ketolide group would appear to be less exposed to solvent than it is in the *Ec*-FabF::platensimycin complex (Figure 2-8 B, C). Indeed, the simulated complex structure suggests that the ketolide group makes close hydrophobic interactions with Met-212 and Ile-214 (Figure 2-8 B, C), contacts that are not seen in platensimycin-bound *Ec*-FabF, where these residues correspond to alanine side chains. Such differences provide scope for design efforts with the aim of enhancing inhibitor affinity in a species-specific manner.

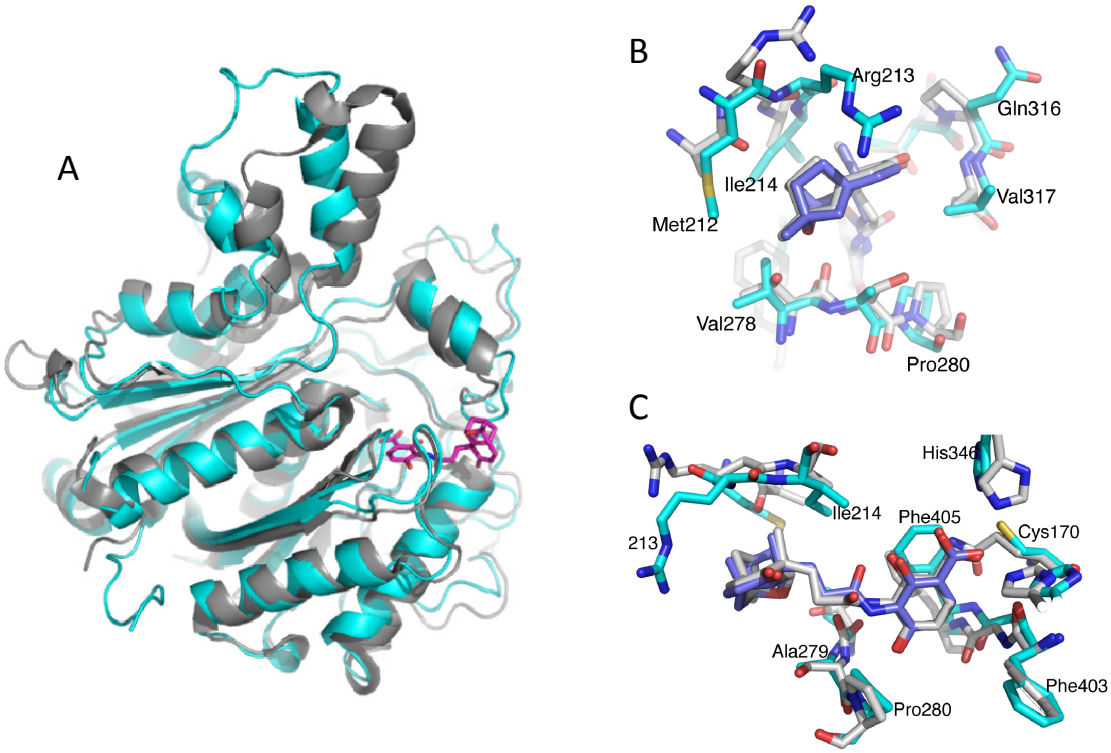

FIGURE 2-8. Comparison of *Mt*-KasB with *Ec*-FabF and simulated KasB::platensimycin complex. The structures of *E. coli* FabF(C163Q) (PBD: 2GFX) bound to platensimycin and *Mt*-KasB (PBD: 2GP6) were superimposed using CNS 1.2 (Brünger 2007). (**A**) Ribbon diagram displaying *Mt*-KasB (*cyan*) and *Ec*-FabF (*grey*) with platensimycin shown as sticks (*pink*). (**B**, **C**) Two orthogonal views of the simulated *Mt*-KasB::platensimycin complex of *Mt*-KasB with carbon atoms of the experimental FabF and simulated *Mt*-KasB complex structures in grey and cyan respectively. Residue identifiers refer to *Mt*-KasB.

Previous studies by Wang *et al.* (2007b) demonstrated that platensimycin poorly inhibited FabH in other bacteria. Interestingly, it was shown that platencin (Figure 2-9), a related antibiotic, was more active against *S. aureus* FabH (3.90 µg/ml [9.17 µM]). Platensimycin and platencin are structurally similar: Platensimycin contains a pentacyclic motif with a cyclic ether ring, whereas platencin contains a unique tetracyclic motif without the ether ring (Wang *et al*. 2007b).

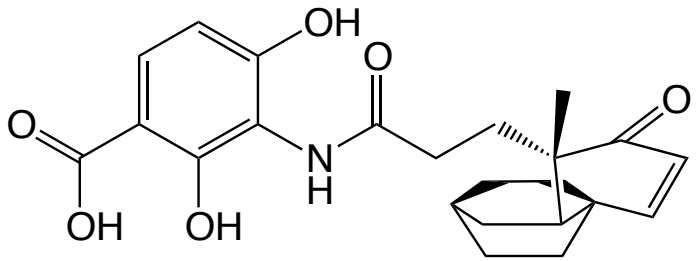

FIGURE 2-9. Platencin.

The chemical modification between platensimycin and platencin has been proposed as responsible for the change in activity against *S. aureus* FabH. Platensimycin failed to inhibit mycobacterial *Mt*-FabH as one would expect, therefore, it would be interesting to examine whether platencin is active against *Mt*-FabH. Altogether, the culture inhibition studies and *in vitro* assay data indicate that platensimycin targets *Mt*-KasA and *Mt*-KasB. Given that over-expression of *Mt*-KasA or *Mt*-KasB increased the MIC of the host *M. smegmatis* strain for platensimycin, it was surprising that platensimycin was relatively inactive against *M. bovis* BCG. Poor permeability may have been one of the factors responsible for the observed resistance. Indeed, deletion of *kasB* from *M. bovis* BCG resulted in a strain that was more `permeable to lipophilic antibiotics and thus sensitive to platensimycin (Table 2-2) (Bhatt *et al*. 2007b). This data suggests that, in order to realise the full potential of this compound as an anti-TB agent, it is imperative that any future modifications to platensimycin include designs that render it more diffusible into the lipid-rich envelope of *M. bovis* BCG. Nevertheless, the results here highlight the potential of platensimycin as an inhibitor of the essential fatty acid and mycolic acid biosynthesis pathways in mycobacteria.

The promise in this drug has awarded it much attention. More recent work on platensimycin has seen the synthesis of congeners. A report by Jang *et al*. (2010a) has shown that more potent anti-bacterial compounds can be made using the platensimycin structure as a central

scaffold. The most promising were 7-phenylplatensimycin and 11-methyl-7-phenylplatensimycin, which displayed MIC values of <0.25 μg/ml against MRSA.

2.4.2. Thiolactomycin analogues.

Despite most of the compounds not showing any activity at 200 μg/ml against *Mt*-FabH, it can be seen from the data that the three that were active have the bromoacetamido group at the R3 position. The esters QAB-61, QAB-62a and QAB-108a inhibited with IC_{50} values of 1.04 ± 0.2, 1.1 ± 0.1 and 79.9 ± 1.0 μg/ml, respectively. This functional group was designed to be able to facilitate an S_N2-type substitution between the ligand and the Cys-122 residue of the *Mt*-FabH active site. It is therefore interesting that compounds QAB-58a, QAB-130 and QAB-130a, which have the same bromo-R3 group, did not inhibit the enzyme. Here, the R1 group may have an effect. Although in the active compounds the R1 groups are different (*p*-Cl-C_6H_4-, C_6H_5- and $C_6H_5CH_2$-), they do all share the aromatic benzene ring. Compounds QAB-130 and QAB-130a both have a CH_3 group at the R1 position, which could explain their inactivity. QAB-58a however does have both the bromoacetamido and aromatic moieties, although having the Cl constituent at the *meta* rather than the *para* position may be a large enough difference to produce the results observed. Indeed, the magnitude of activity displayed by the compounds is dependent on the substituents at the 4- and 5-positions on the ring. By assuming the ligand-enzyme interaction is between the electrophilic bromomethyl and the active site cysteine, this observation could be explained by the substituents being arranged around the catalytic triad. It is known that the channels of *Mt*-FabH are lipophilic in order for the acyl-AcpM chain to be able to reach the active site. It could be that the methyl groups at R1 of compounds QAB-130 and QAB-130a are unable to make the necessary hydrophobic interactions to inhibit the enzyme, whereas QAB-61, which has a *p*-Cl-C_6H_5 group, can.

From the data obtained by Al-Balas and co-workers (2009) for this study, it can be seen that none of the bromoacetamido compounds were active against *M. tuberculosis* as a whole cell organism. One reason for this could be that these compounds are unable to access the FabH target inside the cell, in which case the physiochemical properties will need to be altered so as to cross the complex hydrophobic cell wall. Another reason could be the cell using efflux pumps, such as that encoded by *Rv2333c* (Ramón-García *et al*. 2007). Although not well understood, it is known that *M. tuberculosis* actively uses multi-drug efflux transporters as a mechanism of drug resistance, including the major front-line anti-TB drug, isoniazid (De Rossi *et al*. 2006). One final explanation could be that the cell is able to chemically or metabolically alter or degrade the bromomethyl group thus rendering it inactive. The three compounds that did display whole cell activity were inactive against the fatty acid and mycolic acid biosynthetic systems tested here. Their mechanism(s) of action must therefore involve other targets within the cell.

It is clear from the data that no inhibition of either FAS system was possible when there was an amine group at R3, regardless of the other R groups (Table 2-3). This can rule out the alternative targets for QAB-4, QAB4a, QAB-8 and QAB-30 being any of the active sites of FAS-I or the other enzymes of the FAS-II system. All the bromomethyl compounds tested were active against the FAS enzymes, although no obvious trends were seen across the series. Since there are so many potential active site targets within the FAS systems, however, this is not surprising.

Our collaborators (Dr. Q. Al-Balas, University of Strathclyde) also tested the cytotoxicity of these compounds against human foreskin fibroblast HS-27 cells (data not shown). Essentially, the results showed that only the carboxyl ester of the bromoacetamido analogues,

QAB-130, was toxic at a concentration of 100 μg/ml. One potential reason for this could be the indiscriminate alkylation of essential cellular components.

This data indicates that the 2-aminothiazole-4-carboxylate scaffold offers a promising new lead for further development. Since many of the compounds do not inhibit the target *Mt*-FabH, it is important to elucidate their actual target(s) in order to improve on them.

2.4.3. Indole derivatives.

Only two compounds were active against purified *Mt*-FabH, WIUAKP-052 and WIUAKP-056, with very similar IC_{50} values of 109.5 and 109.1 μg/ml, respectively. Both of these compounds have a *p*-CF_3-phenyl group esterified to the indole scaffold and a functional group in the *para* position on a phenyl ring attached to the indole nitrogen. It is therefore interesting that WIUAKP-009, which has the same CF_3 group and a *para*-group on the N-attached phenyl, does not show any FabH activity. WIUAKP-059 is the only other compound tested that has *para* functional groups on the aromatic rings and this compound was found to be active against both FAS-I and FAS-II. Interestingly, neither WIUAKP-052 nor WIUAKP-056 were found to be active against *F. tularensis* FabH, despite having conserved active site residues (Wen *et al*. 2009). This could indicate that either the compounds do not dock and inhibit activity competitively at the *Mt*-FabH active site, or that the *Ft*-FabH conformation is sufficiently different from *Mt*-FabH so that it cannot accommodate either compound.

Encouragingly, there were four indole-derivatives that were active against FAS-II but not FAS-I or *Mt*-FabH. It would be interesting to test these in discrete protein assays to elucidate their actual targets. The most promising compound was WIUAKP-045 with an IC_{50} of 3.64 ± 0.02 μg/ml against FAS-II. All four FAS-II-inhibiting compounds have a functional group in the *para*-position on the indole nitrogen-attached benzene, however, WIUAKP-045 differs

from the other three by having a C_6 fatty acid chain esterified to the indole rather than an aromatic group. It might be this that increases the potency. Nevertheless, it is interesting to note that none of the other compounds with an acyl chain in this position, even with an OMe group on the nitrogen-attached benzene, inhibit any of the targets tested here. It would be beneficial to test these four compounds against the whole cell to see if they are able to pass through the cell wall and still inhibit FAS-II.

2.4.4. Conclusion.

It is evident from this data, and from the literature, that the indole structure holds promise for developing new anti-tubercular drugs (Kuo *et al*. 2003, Seefeld *et al*. 2003). The aim with this and all the scaffolds presented here will be to generate more derivatives in order to increase selectivity, potency and whole cell activity. The huge advances in computer modelling and *in silico* structure design, as well as genetic engineering in *M. tuberculosis* and surrogate species used in the lab, have accelerated the synthesis and discovery of novel compounds. However, similarly to the discovery of platensimyin and thiolactomycin, naturally occurring products need to be exploited to find new classes of antibiotics. One such compound, whose structure is as of yet undisclosed, is FAS20013, which is now in pre-clinical development. It is formed from both thiolactomycin and cerulenin, a natural product of the fungus *Cephalosporium caerulens* that is a known irreversible inhibitor of β-ketoacyl synthase from FAS-I and FAS-II (Nomura *et al*. 1972, Schaeffer *et al*. 2001). Created by FASgen™ in 2005, the compound has been shown to kill both actively growing and latent mycobacteria with an MIC of 50 μg/ml (FASgen, Inc. 2005). This compound demonstrates how combining elements of naturally occurring metabolites can produce potent and highly promising new anti-tubercular chemotherapy.

CHAPTER 3

Mycobacterium tuberculosis β-ketoacyl-acyl carrier protein synthase III (*Mt*-FabH) is inhibited by phosphorylation on a single threonine residue

3.1. Introduction

Within the infected host, *M. tuberculosis* encounters numerous environmental conditions, and induces or represses a number of genes, for quick adjustment to new conditions. The infection process of *M. tuberculosis* involves complex signalling between the host and the bacterium, resulting in reprogramming of the host signalling network. Protein phosphorylation/dephosphorylation within the bacilli represents a central mechanism for distribution of signals to various parts of the cell, regulating growth, differentiation, mobility and survival (Stock *et al*. 1989). In mycobacteria, a common signal transduction pathway is transmitted through membrane-embedded sensor kinases, enabling the pathogen to modify itself for survival in this hostile environment.

Protein kinases can be classified into two families based on their similarities and enzymatic specification: (i) the histidine kinase superfamily, which relies on autophosphorylation of a conserved histidine residue and commonly occurs as part of two-component systems, and (ii) the superfamily of serine, threonine and tyrosine kinases that phosphorylate on serine, threonine and tyrosine residues respectively (Hanks *et al*. 1988, Hunter 1995, Stock *et al*. 1989). Although the two-component systems represent the classical prokaryotic mechanism for detection and response to environmental changes, the serine/threonine/tyrosine protein kinases and phosphatases are also widespread in prokaryotes. The *M. tuberculosis* genome contains 11 Ser/Thr protein kinases (STPKs) (Av-Gay & Everett 2000, Cole *et al*. 1998), most of which are being investigated for their physiological roles and potential application for future drug development to combat tuberculosis (Wehenkel *et al*. 2008). This significant number of STPKs suggests that phosphorylation may influence a wide range of biological functions, such as adaptation to various environmental conditions, stress, cell wall synthesis, cell division and pathogenicity (Cowley *et al*. 2004, Dasgupta *et al*. 2006, Deol *et al*. 2005, Fernandez *et al*. 2006, Jayakumar *et al*. 2008, Kang *et al*. 2005, Papavinasasundaram *et al*.

2005, Walburger *et al*. 2004). The cell wall of *M. tuberculosis* plays a critical role in the defence of this pathogen in the host, since environmental stimuli induce changes in the cell wall composition and thus help *M. tuberculosis* to adapt during infection (Daffé & Draper 1998, Glickman & Jacobs 2001). Several recent studies support the view that regulation of cell wall synthesis involves STPKs. For instance, PknH and PknJ phosphorylate the forkhead-associated (FHA) domain-containing protein EmbR, a putative transcriptional regulator of the EmbCAB arabinosyltransferases (Jang *et al*. 2010b, Molle *et al*. 2003a). Activation of EmbR upon phosphorylation by PknH induces transcription of the *embCAB* operon, leading to a higher LAM/LM ratio (Sharma *et al*. 2006), and regulates the synthesis of arabinan, an important component of arabinogalactan, essential for the structural integrity of the cell wall. Also, LM and LAM are major cell wall-associated lipoglycans and important modulators of the immune system (Briken *et al*. 2004). Furthermore, a recent study has shown that PknH was able to phosphorylate other substrates, such as DacB1 (Zheng *et al*. 2007). In *Bacillus subtilis*, DacB1 is a sporulation-specific protein involved in cell envelope biosynthesis. Based on homology with the *B. subtilis* orthologue, it has been postulated that PknH-dependent phosphorylation of *M. tuberculosis* DacB1 regulates the synthesis of peptidoglycan, a key component of the mycobacterial cell envelope (Zheng *et al*. 2007). A final example is MmpL7, a member of the RND (resistance, nodulation and cell division) family of transporters, which is thought to be involved in the transport of phthiocerol dimycocerosate and known to be essential for virulence (Camacho *et al*. 2001, Cox *et al*. 1999), has been shown to undergo phosphorylation. The last finding suggests that kinases could also play an important role in regulating the transport of cell wall components (Pérez *et al*. 2006).

Considering the large repertoire of polyketides and complex lipids present in *M. tuberculosis*, STPKs could play an important role in regulating the metabolism of these molecules. There

is now evidence to suggest that phosphorylation may also participate in the regulation of mycolic acids. The β-ketoacyl-ACP synthases, KasA and KasB, of the mycobacterial FAS-II system involved in fatty acid elongation, represent STPK substrates and phosphorylation of KasA and KasB differentially modulates their condensing activity *in vitro* (Molle *et al.* 2006). The present study was undertaken to address the question of whether mycolic acid synthesis in general might be influenced by STPK-dependent regulatory mechanisms. Here, *Mt*-FabH has been identified as a new substrate of the *M. tuberculosis* STPKs and defined its phosphorylation state. This has allowed the role and effect of *Mt*-FabH phosphorylation to be investigated (Veyron-Churlet *et al.* 2009).

3.2. Materials and Methods

3.2.1. Bacterial strains and growth conditions.

Strains used for cloning and expression of recombinant proteins were *E. coli* TOP10 (Invitrogen) and *E. coli* BL21(DE3)pLysS (Novagen). Strains were grown at 37 °C in LB medium supplemented with 100 µg/ml ampicillin or 25 µg/ml kanamycin when required. *M. bovis* BCG Pasteur 1173P2 strain was plated on Middlebrook 7H10 agar supplemented with OADC (Difco) and kanamycin (25 µg/ml) when required or grown in Sauton's medium containing 0.05 % Tyloxapol (Sigma).

3.2.2. Cloning, expression and purification of *Mt*-FabH and mutant proteins.

The initial cloning work was performed by Dr. R. Veyron-Churlet and co-workers (Universités de Montpellier II et I, France) and vectors were provided for over-expression and purification. The *Mt*-FabH gene was amplified by PCR using *M. tuberculosis* H_{37}Rv chromosomal DNA as a template and the primers 5′-taatagctcatatgacggagatcgccacgaccagc-3′ and 5′-taatagctgctagctcaacccttcggcattcgcac-3′ containing an *Nde*I or *Nhe*I restriction site

respectively (underlined). This 1008-bp amplified product was then digested by *Nde*I and *Nhe*I and ligated into the pETTev plasmid, a variant of pET15b (Novagen) that includes the replacement of the thrombin site coding sequence with a tobacco etch virus protease site (Cohen-Gonsaud *et al*. 2004), thus generating pETTev-*Mt-fabH*. Site-directed mutagenesis was performed directly on pETTev-*Mt-fabH* using inverse PCR amplification with the following self-complementary primers: 5′-cgtccgacgagtggatctac**g**cccgaaccggcatcaagac-3′ and 5′-gtcttgatgccggttcggg**c**gtagatccactcggacg-3′ for *Mt*-FabH(T45A) and 5′-cgtccgacgagtggatctac**ga**ccgaaccgcgatcaagac-3′ and 5′-gtcttgatgccggttcgg**tc**gtagatccactcgtcggacg-3′ for *Mt*-FabH(T45D) (the corresponding substitutions are shown in boldface type). All constructs were verified by DNA sequencing. Recombinant strains harbouring the *Mt*-FabH-expressing constructs were used to inoculate 200 ml of LB medium supplemented with ampicillin and resulting cultures were incubated at 37 °C with shaking until the OD_{600} reached 0.5. At this point, 1 mM IPTG was added and growth was continued for 3 h at 37 °C. Purifications of *Mt*-FabH(WT), *Mt*-FabH(T45A), and *Mt*-FabH(T45D) were performed as described earlier (Molle *et al*. 2006; see section 2.2.2.3).

3.2.3. Over-expression and purification of *Mt*-FabH in *M. bovis* BCG.

All *M. bovis* BCG work was performed by the lab of Veyron-Churlet at the Universités de Montpellier II et I. Briefly, the *M. tuberculosis* H_{37}Rv *Mt-fabH* gene was amplified using the following primers: pVV16-*Mt-fabH*-up (5′-gataggacgcatatgacggagatc-3′) and pVV16-*Mt-fabH*-lo (5′-aagcttacccttcggcattcgcaccac-3′) containing an *Nde*I and *Hin*dIII site, respectively. The PCR product was cut with *Nde*I/*Hin*dIII enabling direct cloning into the pVV16 expression vector cut with the same enzymes (Jackson *et al*. 2000). This plasmid harbours the *hsp60* promoter as well as a His tag for expression of C-terminal His-tagged fusion proteins. The resulting vector, pVV16-*Mt-fabH*, was used to transform *M. bovis* BCG. Purification of soluble *Mt*-FabH-His_6 was performed on Ni^{2+}-nitrilotriacetic acid-agarose

beads, as described previously (Molle *et al*. 2006).

3.2.4. *In vitro* kinase assay.

In vitro phosphorylation was performed by Dr. R. Veyron-Churlet as previously described (Molle *et al*. 2003a), with 2 µg of *Mt*-FabH in 20 µl of buffer P (25 mM Tris·HCl, pH 7.0, 1 mM DTT, 5 mM $MgCl_2$, 1 mM EDTA) with 200 Ci/ml [γ-^{33}P]-ATP corresponding to 65 nM (3000 Ci/mmol; PerkinElmer Life Sciences) and 0.6–4.2 µg of kinase in order to obtain for each specific kinase its optimal autophosphorylation activity for 30 min at 37 °C. Cloning, expression, and purification of the eight recombinant GST-tagged STPKs from *M. tuberculosis* were described previously (Molle *et al*. 2006).

3.2.5. Analysis of the phosphoamino acid content of *Mt*-FabH.

Mt-FabH samples phosphorylated *in vitro* in the presence of GST-tagged PknF (or PknA) and [γ-^{33}P]-ATP were separated by one-dimensional gel electrophoresis and electroblotted onto an Immobilon polyvinylidene difluoride membrane (performed by Veyron-Churlet and colleagues). Analysis of the phosphoamino acid content was done as reported previously (Molle *et al*. 2003a).

3.2.6. Mass spectrometry analysis.

Mass spectrometry experiments and analyses were performed by Dr. R. Veyron-Churlet. Purified *Mt*-FabH(WT) and *Mt*-FabH(T45A) proteins were subjected to *in vitro* phosphorylation by GST-tagged PknF or PknA as described above, except that [γ-^{33}P]-ATP was replaced with 5 mM cold ATP. Subsequent mass spectrometry analyses were performed as previously described (Fiuza *et al*. 2008).

3.2.7. Two-dimensional gel electrophoresis and western blot analysis.

M. bovis BCG crude lysates were prepared as described earlier (Molle *et al*. 2006) and performed by Veyron-Churlet *et al*. Approximately 150 µg of total soluble proteins were loaded onto a 7 cm immobiline strip (Bio-Rad, pH 3.9–5.1) and electrophoresed in a Protean IEF Cell (Bio-Rad) in the first dimension and on a 10 % SDS-PAGE in the second dimension. Proteins were then blotted on a polyvinylidene difluoride membrane and probed with a rabbit anti-*Mt*-FabH antibody raised against recombinant *Mt*-FabH (1 : 250 dilution). The membrane was then incubated with horseradish peroxidase-conjugated anti-rabbit antibodies (1 : 5,000 dilution), and detection of the different *Mt*-FabH isoforms was carried out using the Western Lightening Reagent (PerkinElmer Life Sciences) according to the manufacturer's instructions.

3.2.8. *Mt*-FabH condensation assay.

The condensing activity of *Mt*-FabH was assayed as described by Brown *et al*. (2005), by mixing 50 µM holo-AcpM (mycobacterial acyl carrier protein), 1 mM β-mercaptoethanol, 0.1 M sodium phosphate buffer (pH 7.0), 50 µM malonyl-CoA, 45 nCi of [2-^{14}C] malonyl-CoA (specific activity, 55 Ci/mol), 12.5 µM palmitoyl-CoA and 0.3 µg of *Mt*-FabD in a final volume of 40 µl. The *Mt*-FabD protein was added to generate the malonyl-AcpM substrate for the reaction *in situ*. A mixture of holo-AcpM containing 1 mM β-mercaptoethanol was incubated at 37 °C for 30 min to ensure complete reduction of AcpM, prior to the addition of the remaining components (except *Mt*-FabH). The reaction was initiated by the addition of 0.5 µg of *Mt*-FabH, held at 37 °C for 40 min and quenched by adding 5 mg/ml $NaBH_4$ in 100 mM K_2HPO_4, 100 mM KCl, 30 % THF. This resulted in the liberation of β-ketoacyl groups from their respective thioesters as acyl-1,3-diols, which were extracted with water-saturated toluene. The radiolabelled products were then quantified by liquid scintillation counting.

3.2.9. *Mt*-FabH transacylation assay.

Acyl transfer was assessed using [9,10-^{3}H]-myristoyl-CoA (specific activity 57.0 Ci/mmol) to follow the transacylation of the acyl chain from acyl-CoA to the active site Cys-122 of *Mt*-FabH. The reaction mixture consisted of 50 mM Tris·HCl, pH 7.5 (Buffer A), 250 pmol of [^{3}H]-myristoyl-CoA (14.6 nCi), and 4 µg of WT or mutant *Mt*-FabH (110 pmol) in a final volume of 60 µl. The reaction was held at room temperature for 15 min, and 200 µl of Ni^{2+}-charged chelating Sepharose fast flow chromatography medium (50 % slurry in buffer A) was added. After a further 5 min, the slurry was diluted by adding 300 µl of buffer A and unbound C_{14}-CoA was then removed by filtration (cellulose nitrate, 0.45 µm). The beads were washed with 20 ml of buffer A before the filters were removed to vials for liquid scintillation counting.

3.2.10. Malonyl-AcpM decarboxylation assay.

The methods used by Brown *et al.* (2005) and Shorrosh *et al.* (1996) have been combined and modified to investigate the decarboxylation of malonyl-CoA by wild-type *Mt*-FabH and mutants. Malonyl-AcpM was synthesised from malonyl-CoA and holo-AcpM *in situ* using *Mt*-FabD. The initial reaction mixture of 25 mM Tris·HCl (pH 7.5), 12 µM AcpM, and 1 mM DTT in a volume of 28 µl was held at 4 °C for 30 min. [2-^{14}C]-malonyl-CoA (160 nCi) and 0.3 µg of *Mt*-FabD were added and incubated at 37 °C for 1 h prior to the addition of 5 µg of either wild-type *Mt*-FabH or mutants. The reaction was quenched after 1.5 h at 37 °C by the addition of 900 µl of ice-cold 10 % (w/v) trichloroacetic acid at 4 °C and 50 µl of 2 mg/ml bovine serum albumin and incubated on ice for 20 min. The solution was centrifuged at 27,000 × *g* for 15 min, the protein pellets were washed with 900 µl of ice-cold 10 % (w/v) trichloroacetic acid and then centrifuged again. The pellet was dried to remove excess trichloroacetic acid and resuspended in 40 µl of 50 mM Tris·HCl (pH 7.4). Ten µl of 2 M hydroxylamine (pH 7.0) was added to form hydroxamate derivatives of malonyl-CoA and

acetyl-CoA and the reaction mixture was incubated at 37 °C for 1 h. Of the resulting mixture, 5 µl was subjected to scintillation counting, before spotting the remaining 45 µl on 10 × 20 cm Cellulose 300, F-254 glass-backed TLC plates (Fisher), where [^{14}C]-acetyl-hydroxamate and [^{14}C]-malonyl-hydroxamate were separated by butanol/acetic acid/water (8:2:3, v/v/v). Autoradiograms were obtained after exposing the plates for 7 days to Kodak X-Omat AR film.

3.3. Results

3.3.1. *Mt*-FabH is a substrate of mycobacterial STPKs.

The coupling of the acyl and malonyl groups to form β-ketoacyl derivatives is catalysed by the β-ketoacyl-ACP synthase (KAS) components of the FAS-II system (Kremer *et al*. 2000b, Takayama *et al*. 2005). Three distinct KAS enzymes, *Mt*-FabH (KAS-III), KasA and KasB, operate in the *M. tuberculosis* FAS-II pathway. The *Mt*-FabH enzyme has been reported to act as the pivotal link between FAS-I and FAS-II by initiating the biosynthesis of very long chain fatty acids used in mycolate biosynthesis (Choi *et al*. 2000). It catalyses the condensation of an acyl-CoA substrate (a FAS-I end product) with malonyl-AcpM to generate a β-ketoacyl-AcpM product (Choi *et al*. 2000). Following reduction, an acyl-AcpM with two more carbons is generated. KasA and KasB are β-ketoacyl-AcpM synthases that further elongate the growing acyl chain in the mycobacterial FAS-II system (Bhatt *et al*. 2007a, 2007b, Kremer *et al*. 2002a, Schaeffer *et al*. 2001) and have been shown to undergo post-translational modification by phosphorylation (Molle *et al*. 2006). Herein, it was investigated whether or not *Mt*-FabH would also represent a substrate for mycobacterial kinases. STPKs of *M. tuberculosis* (PknA, PknB, PknD, PknE, PknF, PknH, PknK, or PknL) were expressed as GST fusions and purified from *E. coli* as described previously (Molle *et al*. 2006). Recombinant *Mt*-FabH was expressed and purified from *E. coli* BL21(DE3)pLysS

harbouring the pETTev-*Mt-fabH* plasmid. The protein contained a N-terminal His tag, which was subsequently removed following cleavage with the tobacco etch virus protease. Interestingly, when the different STPKs were incubated in the presence of *Mt*-FabH and [γ-^{33}P]-ATP, phosphorylation of *Mt*-FabH was observed, although levels varied for different kinases. PknA and PknF were the most efficient kinases to phosphorylate *Mt*-FabH (Figure 3-1 A). PknD, PknE and PknH, which display strong autophosphorylation activity *in vitro*, phosphorylated *Mt*-FabH to a lesser extent than PknA or PknF. PknB, PknK, and PknL did not phosphorylate *Mt*-FabH, which, at least for PknK and PknL, may be due to their very low autokinase activity. STPKs usually migrate as diffuse bands, reflecting the different levels of phosphorylation for each isoform and this aberrant profile of migration of *M. tuberculosis* kinases has already been reported in earlier studies (Canova *et al*. 2008, Molle *et al*. 2003a, 2003b, Peirs *et al*. 1997). These results are consistent with the finding that PknA and PknF also efficiently phosphorylate KasA and KasB (Molle *et al*. 2006). In contrast, although PknB efficiently phosphorylates KasA and KasB, it failed to phosphorylate *Mt*-FabH *in vitro* (Figure 3-1 A). Together, these data suggest different levels of substrate specificity of the various STPKs.

3.3.2. PknF phosphorylates *Mt*-FabH *in vitro* on threonine residues.

To examine the nature of the *Mt*-FabH-phosphorylated residues, the phosphoamino acid content of PknF-phosphorylated *Mt*-FabH was analysed. The *Mt*-FabH protein (3 µg) was labelled with [γ-^{33}P]-ATP *in vitro*, separated by SDS-PAGE, excised and subjected to acid hydrolysis. *Mt*-FabH was exclusively phosphorylated on threonines (Figure 3-1 B). Similar results were obtained when *Mt*-FabH was phosphorylated with PknA. Understanding the potential regulatory role that phosphorylation of a given kinase substrate might play necessitates the identification of the specific sites undergoing phosphorylation. Although experimentally challenging, liquid chromatography/MS/MS mass spectrometry has allowed

the different phosphorylation sites to be deciphered in a sequence-specific fashion.

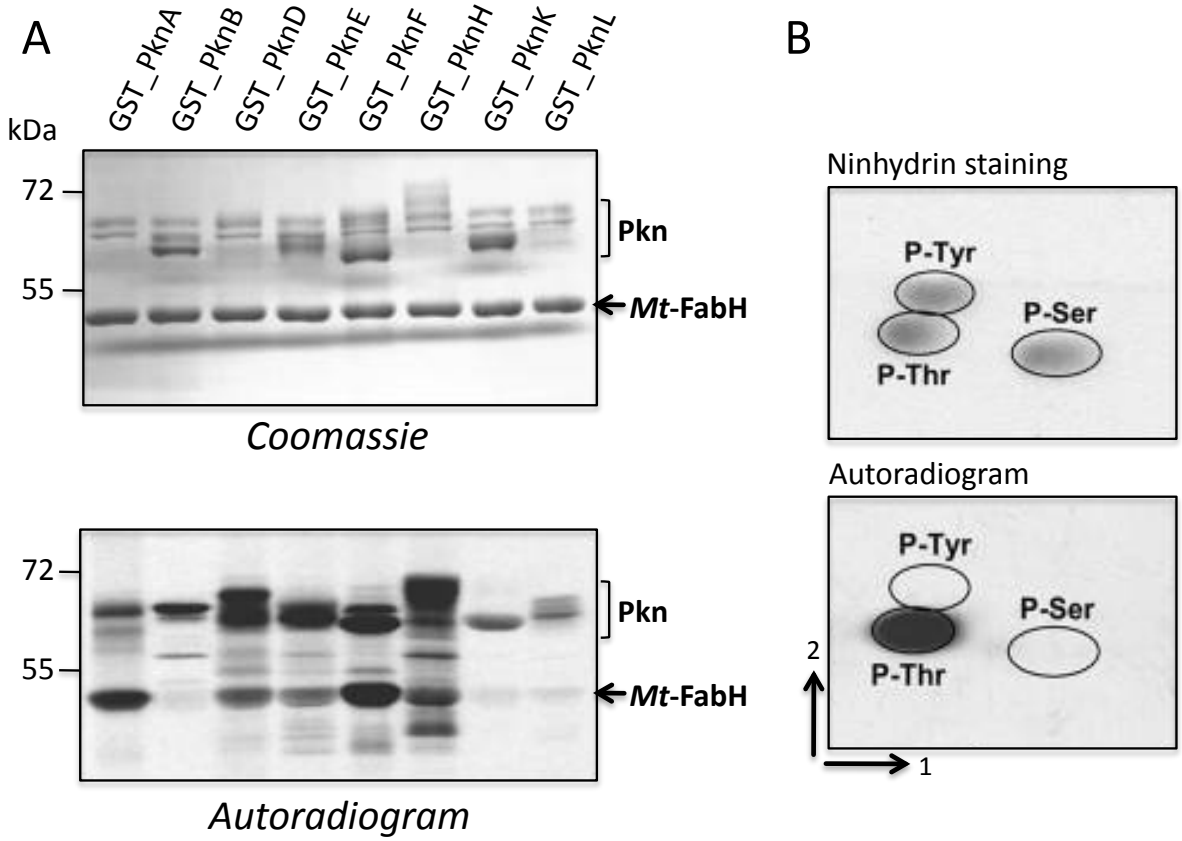

FIGURE 3-1. *In vitro* phosphorylation of *Mt*-FabH. (**A**) *In vitro* phosphorylation of *Mt*-FabH by mycobacterial STPKs. Eight recombinant STPKs (PknA-PknL) encoded by the *M. tuberculosis* genome were expressed and purified as GST fusions and incubated with purified His-tagged *Mt*-FabH and [γ-^{33}P]ATP. The quantity between the STPKs was varied from 0.6 to 4.2 μg in order to obtain for each specific kinase its optimal autophosphorylation activity. Samples were separated by SDS-PAGE (*top*) and visualised by autoradiography (*bottom*). The upper bands illustrate the autokinase activity of each STPK, whereas lower bands reflect phosphorylation of *Mt*-FabH. (**B**) Phosphoamino acid content of *Mt*-FabH. *Mt*-FabH was phosphorylated *in vitro* in the presence of PknF and [γ-^{33}P]ATP, analysed by SDS-PAGE, electroblotted onto an Immobilon polyvinylidene difluoride membrane, excised, and hydrolysed in acid. The phosphoamino acids thus liberated were separated by electrophoresis in the first dimension (*1D*) and ascending chromatography in the second dimension (*2D*). After migration, radioactive molecules were detected by autoradiography (*bottom*). Authentic phosphoserine (*P-Ser*), phosphothreonine (*P-Thr*), and phosphotyrosine (*P-Tyr*) were run in parallel as internal standard controls and visualised by ninhydrin staining (*top*). Figure produced by Veyron-Churlet *et al*. (2009).

3.3.3. *Mt*-FabH is phosphorylated on a unique threonine residue.

To identify which of the 22 threonines of *Mt*-FabH correspond to the phosphorylated site(s), recombinant *Mt*-FabH was incubated with unlabelled ATP in the presence of PknF and subjected to mass spectrometry analysis after tryptic digestion. ProteinPilot® database searching software (version 2.0; Applied Biosystems), using the Paragon method with phosphorylation emphasis, was used to detect and identify the phosphorylated peptides. The sequence coverage of the protein was 98 %, and phosphorylation occurred only on peptide 26–50 with an 80 Da mass increment from 2,978.41 to 3,058.39 Da (monoisotopic mass). The MS/MS spectrum of the corresponding triply charged ion at *m/z* 1020.47 unambiguously confirmed the presence of the phosphate group on the threonine residue Thr-45 (Figure 3-2), consistent with phosphoamino analysis (Figure 3-1 B). The absence of mass increments lower or higher than 80 Da excludes the eventuality of any other post-translational modifications on *Mt*-FabH.

Definitive identification and localisation of Thr-45 as being the unique phosphorylation site in *Mt*-FabH was achieved by site-directed mutagenesis to introduce a mutation that prevents specific phosphorylation (Thr-45-Ala replacement). This mutant was expressed, purified as a His-tagged protein in *E. coli* BL21(DE3)pLysS harbouring pETTev-*Mt-fabH(T45A)*, and used in an *in vitro* kinase assay. After cleavage of the His-tag by the tobacco etch virus protease, the recombinant *Mt*-FabH(T45A) was incubated along with [γ-^{33}P]-ATP and PknF. The mixture was separated by SDS-PAGE and analysed by autoradiography. As shown in Figure 3-3 (*left panel*), equal amounts of *Mt*-FabH(WT) or mutant *Mt*-FabH(T45A) were used. Phosphorylation of *Mt*-FabH(T45A) was completely abrogated, compared with phosphorylation of *Mt*-FabH(WT), as evidenced by the absence of a specific radioactive band (Figure 3-3, *right panel*). These results unambiguously demonstrate that *Mt*-FabH(T45A) has lost its ability to be phosphorylated by PknF.

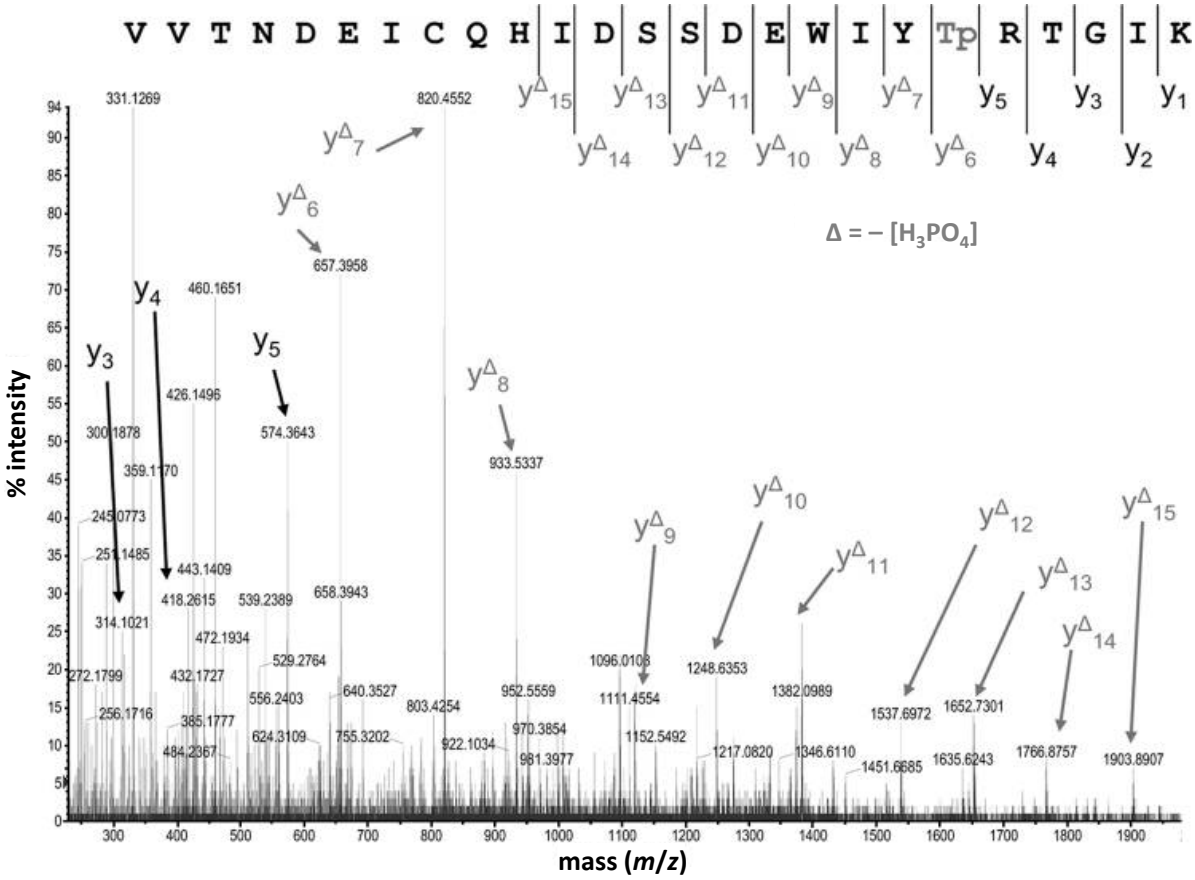

FIGURE 3-2. MS/MS spectrum of the triply charged ion $[M + 3H]^{3+}$ at *m/z* 1,020.47 of peptide 26–50 (monoisotopic mass 3,058.39 Da). The unambiguous location of the phosphate group on Thr-45 was shown by observation of the "y" C-terminal daughter ion series. Starting from the C-terminal residue, all y ions lose phosphoric acid (-98 Da) after the Thr-45 phosphorylated residue. Figure produced by Veyron-Churlet *et al*. (2009).

An additional round of mass spectrometry analysis was also performed directly on *Mt*-FabH(T45A) pretreated with ATP and PknF, which failed to identify any additional phosphate group that could eventually have arisen as a compensatory mechanism to the loss of the Thr-45 phosphorylation (data not shown).

In order to investigate whether Thr residue(s) other than Thr-45 could be phosphorylated by other STPKs, *Mt*-FabH was incubated with [γ-^{33}P]-ATP in the presence of PknA, PknD, PknE, or PknH, which are all able to phosphorylate *Mt*-FabH *in vitro* (Figure 3-1 A). In fact,

the Thr-45-Ala substitution completely abrogated *in vitro* phosphorylation of *Mt*-FabH(T45A) by PknA/D/E/H in comparison with *Mt*-FabH(WT), indicating that Thr-45 represents the unique phosphorylation site for all kinases. It is believed that this is the first demonstration that different mycobacterial kinases can interact with and phosphorylate an identical phosphorylation site in a given substrate.

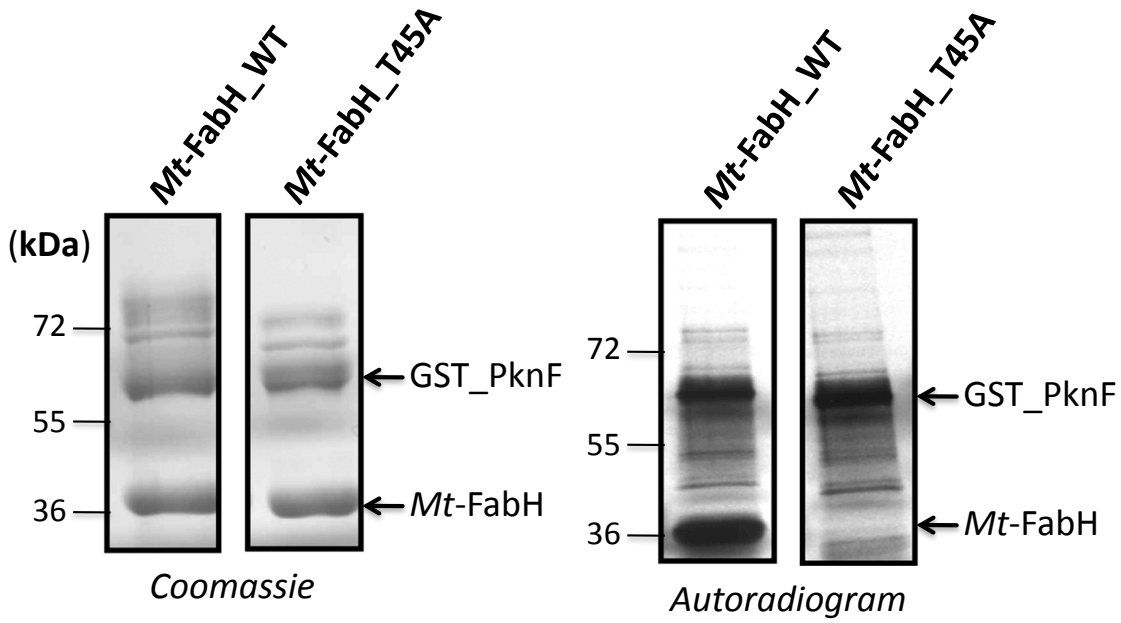

FIGURE 3-3. *In vitro* phosphorylation of the *Mt*-FabH(T45A) mutant. Purified *Mt*-FabH(WT) and *Mt*-FabH(T45A) were incubated with PknF and [γ-^{33}P]-ATP. Samples were separated by SDS-PAGE (*left*) and visualised by autoradiography (*right*). Figure produced by Veyron-Churlet *et al*. (2009).

3.3.4. *Mt*-FabH is phosphorylated *in vivo* in *M. bovis* BCG on Thr-45.

To assess the relevance of *in vitro* phosphorylation, the *in vivo* phosphorylation pattern of *Mt*-FabH in *M. bovis* BCG Pasteur was investigated. A proteomic approach was adopted in which total soluble *M. bovis* BCG proteins were resolved on a two-dimensional gel, subsequently transferred to a membrane, and probed with antibodies raised against *M. tuberculosis* FabH. Two spots were detected in a pH range close to the predicted pI of 4.8 of *Mt*-FabH (Figure 3-4 A). These spots presumably correspond to two *Mt*-FabH isoforms

differing by a translational modification of the protein. Since a phosphate group renders the total charge of a protein more negative, a phosphorylated protein is expected to migrate toward a more acidic pH on a two-dimensional gel. Thus, the two isoforms presumably correspond to the nonphosphorylated (*nP*) and the monophosphorylated (*P*) isoforms of *Mt*-FabH (Figure 3-4 A).

To further support *in vivo* phosphorylation of *Mt*-FabH, a recombinant *M. bovis* BCG strain was designed allowing the over-expression of a soluble His-tagged version of the protein. Cultures of *M. bovis* BCG harbouring the pVV16-*Mt-fabH* plasmid were collected, lysed and fractionated in order to separate the soluble cytosolic compartment from the cell envelope. Soluble *Mt*-FabH was then purified to homogeneity by affinity chromatography on nickel-containing beads under native conditions and subjected to two-dimensional gel electrophoresis. As shown in Figure 3-4 B, two spots, presumably corresponding to the nonphosphorylated form, followed in the acidic direction by a monophosphorylated form of *Mt*-FabH, were clearly detected. The more acidic spot was excised from the acrylamide gel and analysed by mass spectrometry after tryptic digestion. The MS/MS spectrum of the corresponding triply charged ion unambiguously confirmed the presence of a single phosphate group on the threonine residue 45, consistent with the phosphoacceptor identified in *in vitro* phosphorylated *Mt*-FabH (Figure 3-5). Whether the phosphorylation of *Mt*-FabH remains constant or is a growth phase-dependent phenomenon is presently not known and requires investigation. In addition, it would be particularly interesting to monitor the dynamics of *Mt*-FabH phosphorylation in cultures growing under different conditions (temperature, low oxygen concentration, etc.).

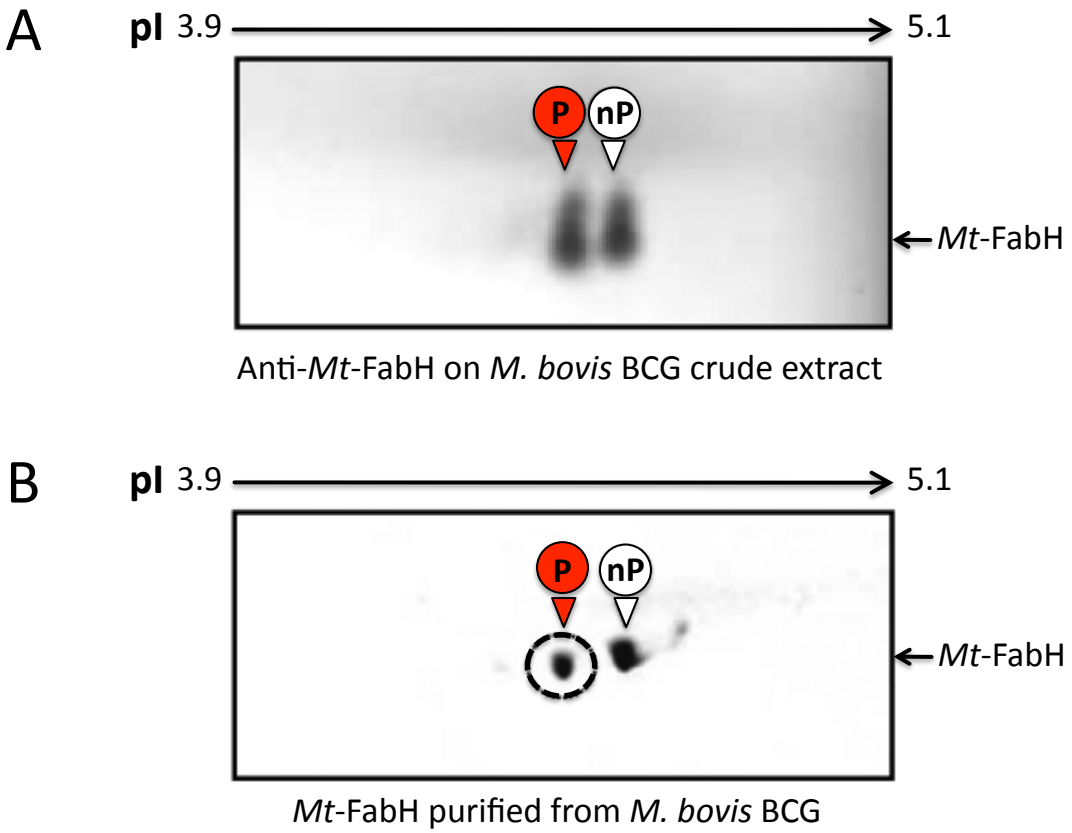

FIGURE 3-4. *In vivo* phosphorylation of *Mt*-FabH in *M. bovis* BCG. (**A**) Detection of phosphorylated *Mt*-FabH in *M. bovis* BCG crude lysates. Approximately 150 µg of total soluble proteins from *M. bovis* BCG lysate were loaded on a 7 cm immobiline strip (pH 3.9–5.1; Bio-Rad) and electrophoresed on a Protean IEF Cell (Bio-Rad) for the first dimension and on a 10 % SDS-PAGE for the second dimension. Proteins were then transferred to a polyvinylidene difluoride membrane and probed with rabbit antibodies raised against the *M. tuberculosis Mt*-FabH protein. Following incubation with Horseradish peroxidase-conjugated anti-rabbit serum as secondary antibody, detection was carried out using the Western Lightening Reagent (PerkinElmer Life Sciences). A selected portion of the membrane that strongly reacted with the antibodies, corresponding to *Mt*-FabH (34.8 kDa, pI 4.8), is represented. (**B**) Phosphorylation profile of *Mt*-FabH purified from recombinant *M. bovis* BCG carrying the pVV16-*Mt-fabH* construct. Cultures were recovered and lysed and the soluble fraction was incubated with Ni^{2+}-nitrilotriacetic acid-agarose beads in order to purify His-tagged *Mt*-FabH, which was then subjected to two-dimensional gel electrophoresis and stained with Coomassie Blue. The *dashed circle* indicates the position of the spot that was subsequently excised from the polyacrylamide gel and analysed by mass spectrometry. The *arrowheads* representing the different phosphorylated isoforms are indicated. *nP*, non-phosphorylated; *P*, monophosphorylated. Figure produced by Veyron-Churlet *et al*. (2009).

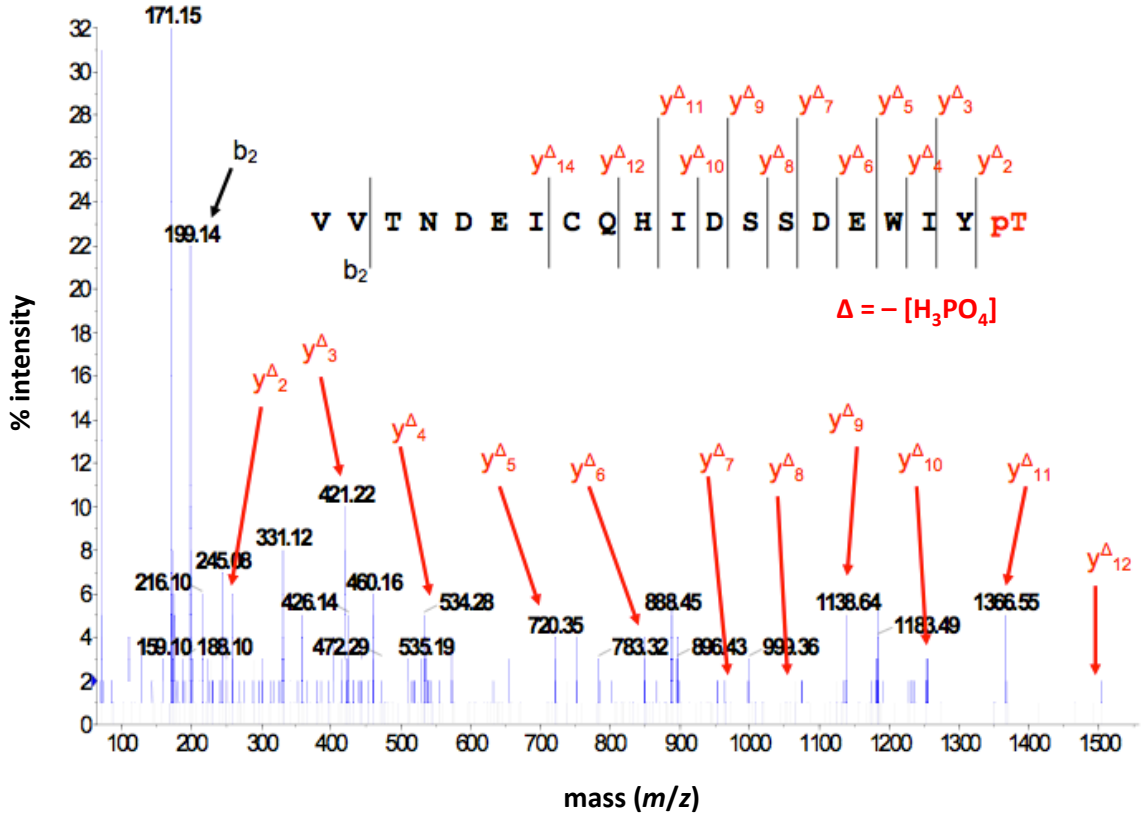

FIGURE 3-5. MS/MS spectrum of the triply charged ion at m/z 887.38 (monoisotropic mass: 2,659.13 Da). Tryptic peptide with no missed cleavage with the characteristic phosphorylation on the Thr-45 residue from *in vivo* purified *Mt*-FabH. Figure produced by Veyron-Churlet *et al*. (2009).

Overall, these results clearly indicate that (i) *Mt*-FabH is phosphorylated *in vivo*, (ii) two dominant forms of *Mt*-FabH co-exist in *M. bovis* BCG, a nonphosphorylated and a monophosphorylated form and (iii) *Mt*-FabH is phosphorylated on a unique residue (Thr-45) both *in vitro* and *in vivo*.

3.3.5. Localisation of Thr-45 on the *Mt*-FabH structure.

In order to understand the effect of Thr-45 phosphorylation on the enzymatic behavior of *Mt*-FabH, the location of this residue with respect to the substrate binding site and the catalytic residues was examined, taking advantage of the available three-dimensional structures of *Mt*-FabH (Alhamadsheh *et al*. 2007, Brown *et al*. 2005, Musayev *et al*. 2005, Scarsdale *et al*.

2001). As Figure 3-6 illustrates, solvent-exposed Thr-45 is situated more than 20 Å away from the catalytic cysteine at the surface of *Mt*-FabH. Thus, it is unlikely that a phosphoryl group on Thr-45 will have a noticeable effect on the catalytic reaction mechanism. However, in the structure of apo-*Mt*-FabH (PDB entries 1HZP (Scarsdale *et al*. 2001) and 1M1M (Brown *et al*. 2005)), Thr-45 is seen in close proximity (≤6 Å) to residues Arg-46 and Trp-42. Both residues play important roles in binding coenzyme A, the donor substrate in the ketoacyl synthase reaction; in the CoA-bound structure of *E. coli* FabH (PDB entry 1HNJ (Qiu *et al*. 2001)), Arg-46 coordinates the pyrophosphate, whereas Trp-42 stacks on top of the adenine base. The latter interaction is also seen in the methyl-CoA disulfide-bound structure of *Mt*-FabH (PDB entry 2EFT (Alhamadsheh *et al*. 2007)). Indeed, it has been shown in a previous study that alanine mutations on these sites markedly reduced (although they do not completely abrogate) β-ketoacyl synthase activity (Brown *et al*. 2005), underscoring a role of these residues in substrate binding. A phosphate group on Thr-45 would offer an alternative salt bridge interaction for Arg-46, which would require this residue to assume a rotamer conformation incompatible with simultaneous binding to the CoA-pyrophosphate. Likewise, a phosphorylated Thr-45 may influence the conformational freedom of Trp-42, impeding the stacking interaction of this residue with the adenine base. Moreover, it is conceivable that phosphorylation of Thr-45 affects the interaction of *Mt*-FabH with the acyl carrier protein AcpM, which also must bind in the vicinity of the narrow substrate binding channel of *Mt*-FabH. Thus, the structural analysis suggests that phosphorylation of Thr-45 may affect substrate binding and/or protein-protein interactions with other FAS-II partners (Veyron-Churlet *et al*. 2004). The condensing activities of wild-type *Mt*-FabH with that of point mutants, Thr-45 to alanine and aspartic acid, were assessed and compared *in vitro* in order to test this hypothesis. These point mutations prevent *Mt*-FabH phosphorylation and introduce a mimic of the negative charge of a phosphate group, respectively.

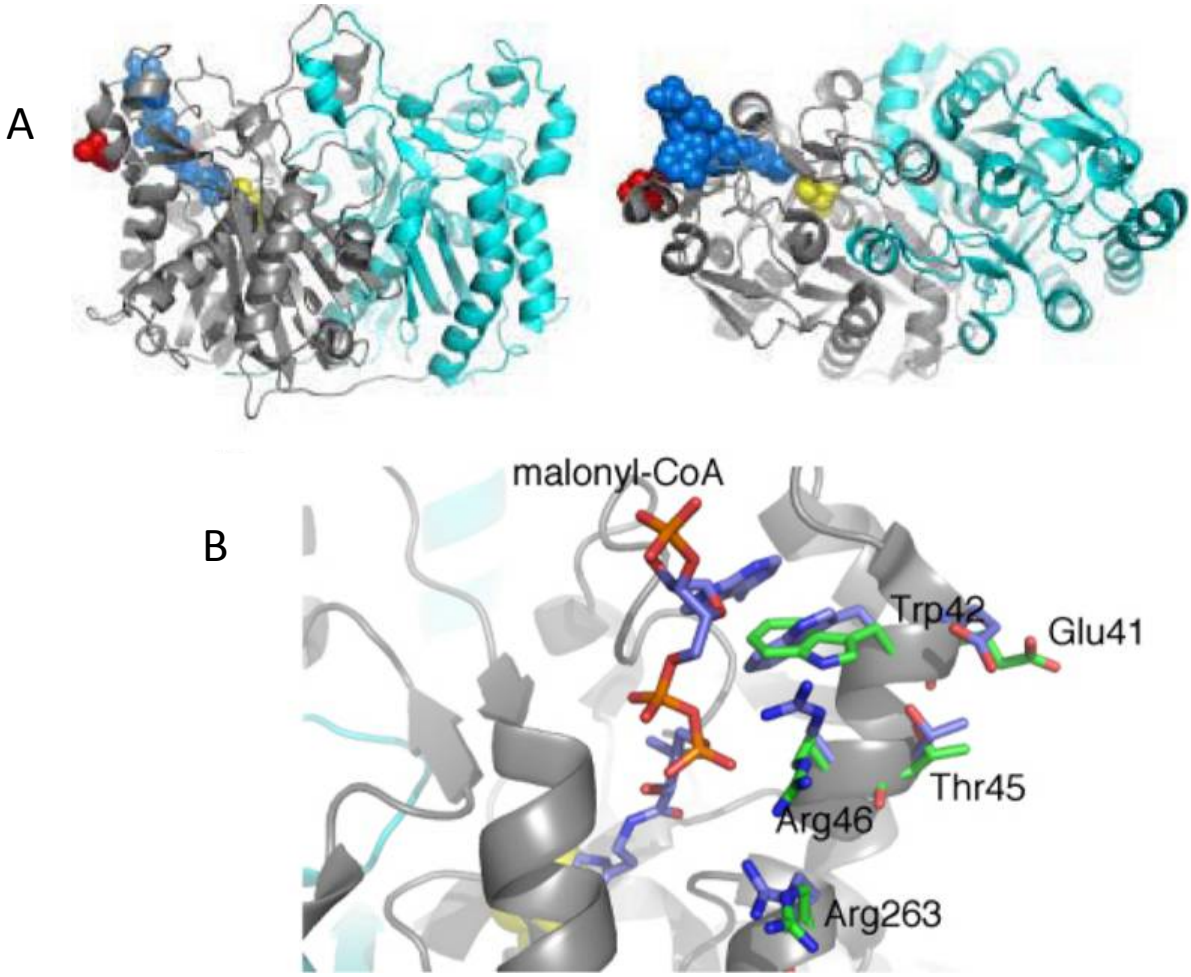

FIGURE 3-6. Location of the Thr-45 phosphorylation site on the *Mt*-FabH crystal structure. (**A**) Two orthogonal views of the *Mt*-FabH dimer (PDB entry 1M1M (Brown *et al*. 2005); *grey* and *cyan ribbon*) superimposed with malonyl-CoA-bound *E. coli* FabH (PDB entry 1HNJ (Qiu *et al*. 2001)) illustrating, for one protomer, the respective locations of the active site cysteine (*yellow spheres*), the substrate channel (malonyl-CoA in *blue spheres*), and Thr-45 (*red spheres*). (**B**) Close-up view of the *Mt*-FabH substrate channel, demonstrating surface exposure of Thr-45 and its proximity to *Mt*-FabH residues Arg-46 and Trp-42. *Blue sticks* represent residues of *E. coli* FabH bound to malonyl-CoA (PDB entry 1HNJ (*Ec*-FabH)); *green sticks* show the corresponding side chains of *Mt*-FabH (PDB entry 1M1M). Residue numbers refer to the amino acid sequence of *Mt*-FabH. Figure produced by Veyron-Churlet *et al*. (2009).

3.3.6. Enzymatic activity is negatively regulated in an *Mt*-FabH(T45D) mutant.

The reaction catalysed by the *Mt*-FabH homodimer initiates with the binding of an acyl-CoA generated by FAS-I, following transacylation of the acyl chain of the bound CoA to the

catalytic Cys-122, allowing the CoA moiety to dissociate from the protein and the malonyl-AcpM to bind to the active site liberated by CoA (Scarsdale *et al*. 2001). The malonyl-AcpM is then decarboxylated to form a carbanion, which in turn reacts with the Cys-122-bound acyl group to generate the final product of the reaction, the β-ketoacyl-AcpM. Therefore, an assessment was made as to whether or not phosphorylation could have an influence on the different activities characterising *Mt*-FabH (*i.e.* the condensation, transacylation, and malonyl-AcpM decarboxylation).

Following a strategy that has been successfully used to demonstrate that regulation of Wag31 by phosphorylation is important during active cell growth in mycobacteria (Kang *et al*. 2008a), a phosphorylation mimic of FabH, *Mt*-FabH(T45D), was expressed and purified. Previous studies have shown that acidic residues, such as Asp or Glu, qualitatively recapitulate the effect of phosphorylation with regard to functional activity (Cottin *et al*. 1999). Condensing activities of *Mt*-FabH(WT), *Mt*-FabH(T45A), and *Mt*-FabH(T45D) were determined and compared. The overall condensing activities of *Mt*-FabH(WT) and *Mt*-FabH(T45A) were similar (Figure 3-7 A). This suggests that Thr-45, unlike its neighbouring residue Arg-46 (Brown *et al*. 2005), does not play a critical role in the condensation reaction, consistent with its surface-exposed localisation (Figure 3-6). In contrast, *Mt*-FabH(T45D) expressed a 42 % reduced activity with respect to *Mt*-FabH(WT) activity. Since the Asp mutant mimics constitutive phosphorylation of *Mt*-FabH, these results suggest that the introduction of a negative charge at position 45 has a negative impact on the condensing activity of the enzyme. Phosphorylation may modulate *Mt*-FabH on a fine tuned level rather than a strict on/off mechanism, as previously proposed for Arg-46, involved in the binding of acyl-CoA substrates (Scarsdale *et al*. 2001), since decreased overall activity was observed in the *Mt*-FabH(R46A) mutant (Brown *et al*. 2005).

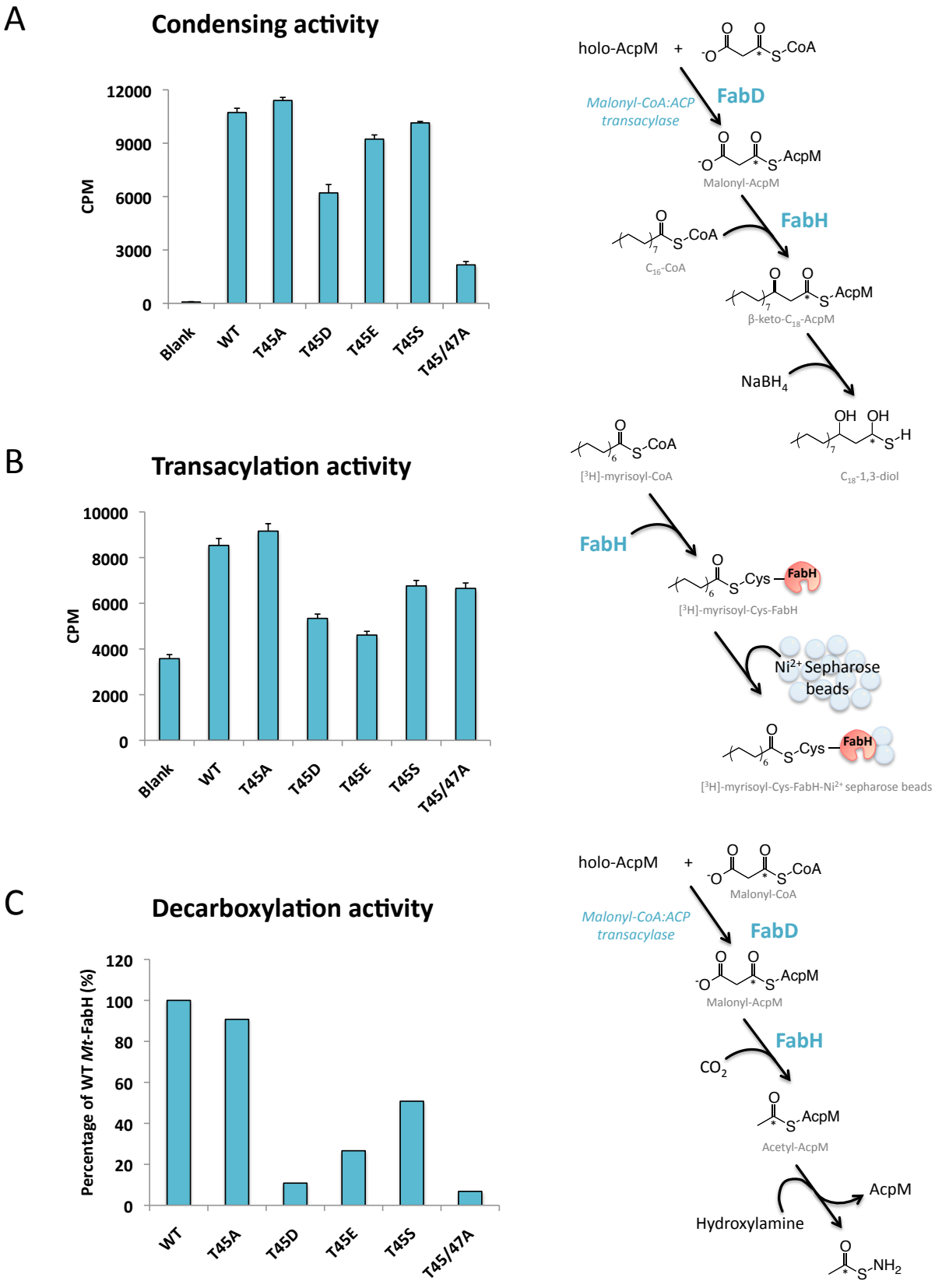

FIGURE 3-7. Comparative enzymatic activities of wild-type and mutant *Mt*-FabH proteins in KAS-III and part-reaction assays. Legend over page.

FIGURE 3-7. Comparative enzymatic activities of wild-type and mutant *Mt*-FabH proteins in KAS-III and part-reaction assays. Each part-reaction step is depicted by a schematic representation *beside* the corresponding bar charts. * Indicates the position of the radiolabelled carbon. In each schematic, the final product is shown. (**A**) Whole condensing activity. The assays were performed in triplicate on two separate protein preparations and activity was assessed by the scintillation counting method using AcpM and a palmitoyl-CoA primer. (**B**) The extent of transacylation activity of *Mt*-FabH and its mutants was determined by quantifying the binding of [^{3}H]-myristoyl-CoA to the protein after incubation by liquid scintillation counting of protein-bound radiolabelled acyl chains captured on Ni^{2+}-charged chelating Sepharose beads. Assays were performed in triplicate on two separate protein preparations. (**C**) The malonyl-AcpM decarboxylation activity was obtained from a direct densitometric reading from the autoradiogram normalised to the activity of *Mt*-FabH(WT) with AcpM and expressed as a percentage, as described in section 3.2.10., and by Brown *et al.* (2005). *WT*, wild-type.

When the transacylation reaction was examined, both *Mt*-FabH(WT) and *Mt*-FabH(T45A) behaved similarly (Figure 3-7 B). However, as for the condensing activity, the *Mt*-FabH(T45D) mutant exhibited a significant reduced transacylase activity compared with *Mt*-FabH(WT). As mentioned above, the presence of a negative charge affects part-reaction activity of *Mt*-FabH. These results are in favour of a model where the substitution of the neighbouring Arg-46 by Ala has a moderate effect on the transacylation activity of *Mt*-FabH (Brown *et al*. 2005).

In the malonyl-AcpM decarboxylation assay, the activity of *Mt*-FabH(WT) was arbitrarily fixed at 100 %. The substitution of Thr-45 by Ala only slightly affects the decarboxylation activity (Figure 3-7 C). Remarkably, the decarboxylative activity of *Mt*-FabH(T45D) was severely inhibited and was found to represent about 10 % of the wild-type activity (Figure 3-7 C). As mentioned above, mimicking the phosphorylation state of Thr-45 fits properly with the overall effects observed in the case of R46A mutant, in which the decarboxylation activity was almost completely abrogated (Brown *et al*. 2005). As with the R46A mutation, the condensation activity of the T45D mutant protein was less affected than observed in the

decarboxylation activity. This can be attributed to the enzymatic state of the protein during the decarboxylation assays, upon which no acyl chain is bound to the active site Cys, which may change the overall decarboxylation activity of the protein, since the two part-reaction assays are not true kinetic representations of the condensation activity.

3.4. Discussion

The β-ketoacyl-ACP synthase III of *M. tuberculosis* (*Mt*-FabH) links the FAS-I and FAS-II systems, catalysing the condensation of FAS-I-derived acyl-CoAs with malonyl-AcpM (Brown *et al*. 2005, Choi *et al*. 2000, Scarsdale *et al*. 2001). The first step of the reaction, catalysed by a *Mt*-FabH homodimer, involves transfer of an acyl group from acyl-CoA to the enzyme active site. This is followed by a two-carbon acyl chain extension through a Claisen-type condensation with malonyl-AcpM. The resulting β-ketoacyl-AcpM product is then reduced to acyl-AcpM by the β-ketoacyl-AcpM reductase MabA (Banerjee *et al*. 1998, Cohen-Gonsaud *et al*. 2002, Marrakchi *et al*. 2002), followed by a dehydration step carried out by the newly identified β-hydroxyacyl-AcpM dehydratases Rv0635-7 (HadA, HadB and HadC, respectively), also known as FabZ′, FabZ and FabZ″ (Brown *et al*. 2007a, Sacco *et al*. 2007), and reduced by the enoyl-AcpM reductase InhA, the primary target of isoniazid (Banerjee *et al*. 1994, Vilchèze *et al*. 2006, Zhang *et al*. 1992). In this study, *Mt*-FabH has been identified as a substrate of STPKs in mycobacteria. Phosphorylation of this enzyme occurs both *in vitro* and *in vivo* on a single and identical residue, Thr-45. It is noteworthy that, similarly to other FAS-II enzymes, *Mt*-FabH interacts with several STPKs *in vitro*, suggesting that it may be regulated by multiple environmental signals. Table 3-1 reviews the current evidence of *Mt*-FAS-II enzyme phosphorylation and highlights the fact that STPKs are selective with regard to which enzymes they phosphorylate. Identification of the Thr-45 phosphoacceptor allowed for the assessment of the role of phosphorylation on the different activities characterising *Mt*-FabH (condensation, transacylation, and malonyl-AcpM

decarboxylation). The comparative analysis of enzymatic activities in *Mt*-FabH and Thr-45 point mutants clearly demonstrates that phosphorylation on residue 45 is able to exert a marked influence on the activity of this enzyme and thus supports the hypothesis of regulation through STPK-mediated phosphorylation. Based on structural constraints, a direct effect on catalysis can be ruled out. However, the structural parameters are compatible with the assumption that Thr-45 phosphorylation regulates transacylation, decarboxylation, and condensing activities through affecting substrate binding. Precisely how this regulatory effect comes to bear remains to be elucidated. Interactions of a phosphorylated Thr-45 with adjacent residues Arg-46 and Trp-42 are likely to affect binding of CoA. Nonetheless, the enzymatic data suggest that the latter effect is less important than the interference with binding of AcpM, demonstrated by the 90 % reduction of decarboxylation activity in *Mt*-FabH(T45D) compared with wild-type. Indeed, the parallel effects on decarboxylation of the Arg-46-Ala mutation in Brown *et al*. (2005) and that of the Thr-45-Asp mutation observed here hint that the Thr-45–Arg-46 surface patch constitutes a critical element of the interaction with AcpM. Together, these data suggest that phosphorylation may fine-tune the interactions of *Mt*-FabH with the components of the FAS-II system.

Previously, it has been shown that *Mt*-FabD, KasA, and KasB are substrates of *M. tuberculosis* STPKs (Molle *et al*. 2006). There is now a strong body of evidence to suggest that several FAS-II components are phosphorylated and that STPK-dependent phosphorylation can induce either positive or negative signalling to the different interconnected FAS-II complexes. Indeed, a model based on co-existence of multiple interconnected FAS-II systems has been proposed (Veyron-Churlet *et al*. 2004). It predicts the occurrence of four FAS-II systems responsible for the initiation, elongation, and termination steps of the mycolic acid pathway, each system characterised by a common enzyme core along with a specific condensase (Figure 3-8).

TABLE 3-1. Phosphorylation of the *Mt*-FAS-II enzymes by the known serine / threonine protein kinases. × no phosphorylation; ✓ moderate phosphorylation; ✓✓ efficient phosphorylation; ? unknown, not tested. Assembled from Molle *et al*. (2006, 2007), Slama *et al*. (2011), Veyron-Churlet *et al*. (2009, 2010).

***Mt*-FAS-II enzyme**	**Ser/Thr protein kinase (Pkn)**										
	A	**B**	**D**	**E**	**F**	**G**	**H**	**I**	**J**	**K**	**L**
AcpM	×	×	×	×	×	×	×	×	×	×	×
FabD	✓✓	✓	✓	✓	✓	×	✓✓	×	×	×	✓
FabH	✓✓	?	✓	✓	✓✓	?	✓	?	?	×	×
KasA	✓✓	✓✓	✓	✓✓	✓✓	×	✓✓	×	×	×	×
KasB	✓✓	✓✓	✓✓	✓✓	✓✓	×	✓✓	×	×	×	✓
MabA	✓	✓✓	✓✓	✓✓	×	?	×	?	×	×	✓
HadAB/BC	✓	✓	✓	✓	✓	?	✓	?	?	?	×
InhA	✓✓	✓✓	×	✓✓	×	?	×	?	?	×	✓

The "initiation FAS-II" (I-FAS-II) is characterised by the condensase *Mt*-FabH, which converts an acyl-CoA from FAS-I to form β-ketoacyl-AcpM. Upon completion of the FAS-II reductive cycle, this acyl-AcpM derived product primes the "elongation-1 FAS-II" (E1-FAS-II) characterised by the condensase KasA. E1-FAS-II elongates the acyl-AcpM to longer chain acyl-AcpM products, which are then channelled into the "elongation-2 FAS-II" (E2-FAS-II), comprising KasB that completes the meromycolate precursor synthesis (Bhatt *et al*. 2007a, 2007b). Various enzymes modify this acyl product further to form the mature meromycolate (Takayama *et al*. 2005) before lastly, the polyketide synthase Pks13 (Portevin *et al*. 2004) of the "termination FAS-II" system catalyses the condensation of the meromycolate (C_{56}) with the α-branch (C_{26}) (produced by FAS-I) to generate the oxo-mycolic acid. The Rv2509 enzyme reduces this product to yield mature mycolates (Bhatt *et al*. 2008). The results here support a model in which STPK-dependent phosphorylation of the condensases can induce either positive or negative signalling to the I-FAS-II and E-FAS-II

complexes. To support this further, preliminary experiments performed by Veyron-Churlet and co-workers have demonstrated that, in addition to KasA, KasB, and *Mt*-FabH, the remaining mycobacterial condensase, Pks13, is also phosphorylated by *M. tuberculosis* STPKs (Veyron-Churlet *et al*. 2009). Thus, the differential expression of the mycobacterial STPKs in response to stress/environmental conditions may directly influence the phosphorylation profile of all four condensases, which in turn may modulate the different interconnected FAS-II systems. It is, therefore, tempting to hypothesise that phosphorylation controls critical enzymatic steps of the FAS-II pathway and, subsequently, regulation of mycolic acid biosynthesis in order to promote adaptation to environmental changes and survival within the infected host.

It is noteworthy that over-expression of *Mt*-FabH in *M. bovis* BCG leads to an unusual smooth texture of the colony morphology and is accompanied by alterations in complex lipid composition, including a decrease in phthiocerol dimycocerosate (PDIM) synthesis (Choi *et al*. 2000). These methyl-branched fatty acids are formed by unique enzymes, which utilise acyl-CoA primers rather than ACP-bound primers (Kolattukudy *et al*. 1997). Since *Mt*-FabH uses long chain acyl-CoA primers and not acyl-ACP primers (Choi *et al*. 2000), over-expression of this enzyme in mycobacteria may decrease the pool of acyl-CoA primers available for PDIM and other related complex lipid biosynthetic pathways. In addition, complex lipids, such as PDIMs, have been shown to interact with host cells and participate in the virulence and pathogenesis of *M. tuberculosis* (Camacho *et al*. 1999, Cox *et al*. 1999). This suggests that the expression level of *Mt*-FabH or regulation of its activity by phosphorylation may also be a determinant for *M. tuberculosis* virulence by controlling the pool of acyl-CoAs available for complex lipid synthesis. Supporting the view of a connection between FAS-II and PDIM biosynthetic pathways, a recent study conducted by Kruh *et al.* (2008) described a novel interaction between KasA and polyketide modules involved in the

biosynthesis of PDIM. These observations suggest that regulation of the activity of condensing enzymes, such as *Mt*-FabH (and KasA), by phosphorylation may directly participate in the control of both the FAS-II and the PDIM pathways. Further studies are needed to ascertain this hypothesis.

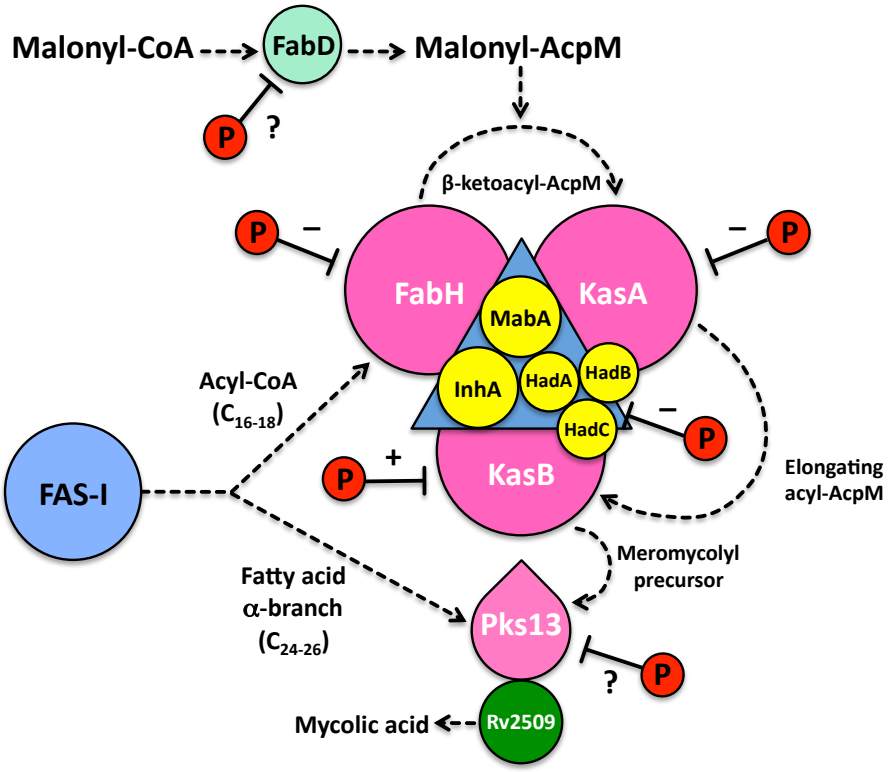

FIGURE 3-8. Proposed regulatory role of condensase phosphorylation in mycolic acid initiation, elongation and termination. Mycolic acid biosynthesis is initiated *via de novo* biosynthesis of C_{16-26}-CoA by the mycobacterial FAS-I and further extended to the meromycolate precursor by FAS-II. FAS-I provides both the initiation primer (C_{16}-CoA) for FAS-II and the C_{24-26} fatty acid utilised by the Claisen-type condensing enzyme Pks13 (belonging to the T-FAS-II system) during the formation of the non-reduced mycolic acid. The initiation primer is utilised by *Mt*-FabH (a feature of the I-FAS-II system), forming a β-ketoacyl-AcpM product, which is further modified *via* the reductive cycle of FAS-II performed by MabA, HadA, HadB, HadC and InhA. The derived aliphatic acyl-AcpM is then used as the substrate of the condensing enzymes KasA and KasB of the E-FAS-II systems. KasA is involved in the elongation of the meromycolate precursors that are further extended to their full lengths by KasB. The condensing enzymes are shown in *pink*. Experimental evidence has demonstrated phosphorylation of all four condensases. Phosphorylation can either activate (+) or inhibit (–) the condensing activity. A *question mark* indicates that the effect of phosphorylation on the enzyme activity has not yet been investigated. Based on Veyron-Churlet *et al*. (2009) and Slama *et al*. (2011).

Although this work here provides evidence for the first time that phosphorylation of *Mt*-FabH occurs *in vivo* in mycobacteria, more work is required to address whether it influences the production of mycolic acids (and PDIM synthesis) during *in vivo* growth and, eventually, if it participates in mycobacterial survival/virulence within the infected host. Using specialised transduction, it is now feasible to isolate isogenic strains of *M. tuberculosis* differing by single point mutations in the genome (Vilchèze *et al*. 2006). This technology would be particularly useful to transfer T45A or T45D point mutations that will either prevent or mimic constitutive phosphorylation of *Mt*-FabH in *M. tuberculosis* and investigate whether phosphorylation of *Mt*-FabH represents an important physiological event *in vivo*.

CHAPTER 4

Insights into mycobacterial FadB2, FadB3, FadB4 and FadB5

4.1. Introduction

4.1.1. *Mt*-FadB2 and *Mt*-FadB3.

Despite lipid biosynthesis having been well studied in mycobacteria (Bhatt *et al.* 2007a, Heath & Rock 2004, Takayama *et al.* 1972, Takayama *et al*. 2005), the extensive field of lipid degradation has not yet been investigated with equal intensity. The chemistry of the β-oxidation pathway is similar to the reverse of lipid biosynthesis. Saturated long-chain fatty acids are first activated by CoA attachment and subsequently undergo oxidation by an acyl-CoA dehydrogenase. This is followed by hydration catalysed by an enoyl-CoA hydratase to produce β-hydroxyacyl-CoA. The hydroxy group is further oxidised to form a β-ketoacyl-CoA, which is then finally cleaved by a β-ketoacyl-CoA thiolase releasing acetyl-CoA and a saturated fatty acid that is two carbons shorter (Black & DiRusso 1994). While playing a general role in fatty acid turnover, in mycobacteria fatty acid β-oxidation may have a specific relevance for the physiology of the bacterium during survival within the hypoxic niche of a granuloma, a critical site of chronic infection. The glyoxylate cycle, which utilises acetyl-CoA (produced by β-oxidation) to generate glucose by conserving the two carbon atoms lost as 2 CO_2 in the TCA cycle, is crucial for the persistence of *M. tuberculosis* in the mouse model of infection (McKinney *et al.* 2000). Additionally, several studies have indicated that host-derived fatty acids could be a key source of carbon to the bacteria (Bishai 2000, Bloch & Segal 1956, Sassetti & Rubin 2003) suggesting that infecting mycobacteria favour exploiting the lipid-rich environment of host tissues over synthesising their own lipids *de novo* (Wheeler *et al.* 1990, Wheeler & Ratledge 1994).

The third step in β-oxidation is catalysed by a β-hydroxyacyl-CoA dehydrogenase [EC 1.1.1.35], which converts the β-hydroxy group to a β-keto using $NAD(P)^+$ as a co-factor (Figure 4-1). There are many genes annotated as acyl-CoA dehydrogenases in the *M.*

tuberculosis genome, including *fadE1-36*. There are two *fadB* genes, however, described specifically as β-hydroxybutyryl-CoA dehydrogenases, *fadB2* and *fadB3*. In *E. coli*, the *fadA* and *fadB* genes form a single operon encoding the two proteins of the β-oxidation multi-enzyme complex (DiRusso 1990). In *M. tuberculosis* there are five discrete *fadB* genes and six *fadA* genes. Recently, the function of *Mt*-FadA5 has been shown to catalyse the thiolysis of cholesterol, although the function(s) of the other five *fadA* genes are yet to be elucidated (Nesbitt *et al.* 2010). FadB1 is thought to perform the second step in the pathway, involving conversion of the *trans*-2-enoyl to the β-hydroxy, but despite having putative functions assigned, the actual function(s) of FadB2, B3, B4 and B5 remain unknown. The number of *fadB* genes may suggest a certain degree of redundancy amongst the FadB enzymes, especially as only FadB3 has been described as essential (Sassetti *et al.* 2003), but there is no evidence yet to show this. It is possible that the FadB enzymes are chain length-specific, like the short-, medium- and long-chain β-hydroxyacyl-CoA dehydrogenases found in mammalian mitochondria (El-Fakhri & Middleton 1982, McGuire *et al.* 1990).

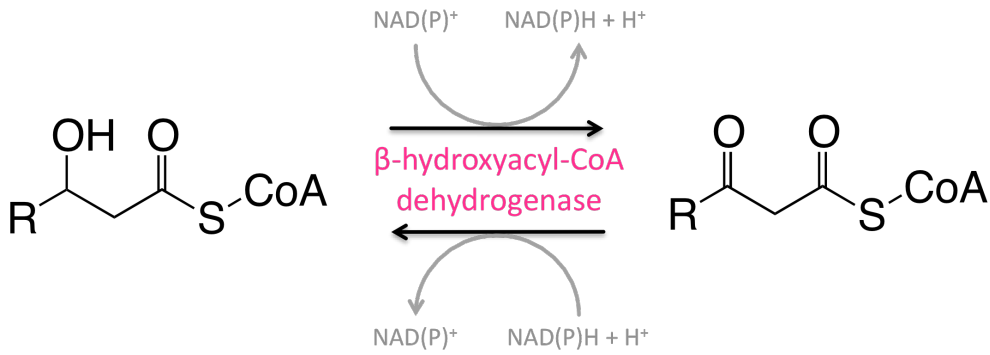

FIGURE 4-1. The proposed *Mt*-FadB2 and *Mt*-FadB3 reaction scheme. Mycobacterial β-hydroxyacyl-CoA dehydrogenase catalyses the $NAD(P)^+$-dependent reduction of β-hydroxyacyl-CoA to β-oxoacyl-CoA.

The *Mt*-FadB2 (Rv0468) sequence is homologous to the products of the *M. smegmatis* gene *MSMEG0912* (91.6 % sequence similarity), the *M. leprae* gene *Ml*_2461 (94.4 % sequence similarity) and sections of the *E. coli* and *Psuedomonas fragi* FadB enzymes (Figure 4-2 A,

B). The *fadB2* gene is interesting because it is conserved across mycobacteria, and also is located in the genome adjacent to *icl1* (Figure 4-2 B). This gene encodes the glyoxylate shunt enzyme, isocitrate lyase, which has been shown to promote persistence of *M. tuberculosis* cells in an infected host (McKinney *et al.* 2000). Unlike *fadB2*, *fadB3* is not conserved across mycobacteria. There is much less homology between *Mt*-FadB3 (Rv1715) and the closest *M. smegmatis* protein, MSMEG6791, sharing only 45.6 % sequence similarity (Labarga *et al*. 2007). A similar homology is found between *Mt*-FadB2 and *Mt*-FadB3 (44.8 %). Interestingly, there is no homologue for *Mt*-FadB3 in *M. leprae*, which could suggest that the gene is not essential at all, given the vastly reduced genome of *M. leprae* (Cole *et al*. 2001). The *M. bovis fadB3* gene is identical to that of *M. tuberculosis*, apart from a single point mutation (g→a) that has split the gene into two parts, *Mb1742* and *Mb1743*, annotated as *fadB3a* and *fadB3b* respectively (Tuberculist).

Prior to sequencing the first *M. tuberculosis* genome, a β-hydroxyacyl-CoA dehydrogenase enzyme from *M. smegmatis* had been characterised using a purified protein fraction containing β-hydroxyacyl-CoA dehydrogenase activity (Shimakata *et al.* 1979). This, and a previous study by the same group, found that the enzyme was involved in the acetyl-CoA-dependent elongation of fatty acids, but failed to provide evidence for its involvement in fatty acid β-oxidation (Shimakata *et al.* 1977).

4.1.2. *Mt*-FadB4 and *Mt*-FadB5.

Two further *M. tuberculosis fadB* genes, *fadB4* and *fadB5*, are also investigated here, albeit in not so much detail. The functions of mycobacterial FadB4 and FadB5 are unknown, although both are described as NADPH:quinone oxidoreductases (NQOs) [EC 1.6.5.5], enzymes that essentially catalyse the one-electron reduction of quinones (Lechat *et al*. 2008).

A

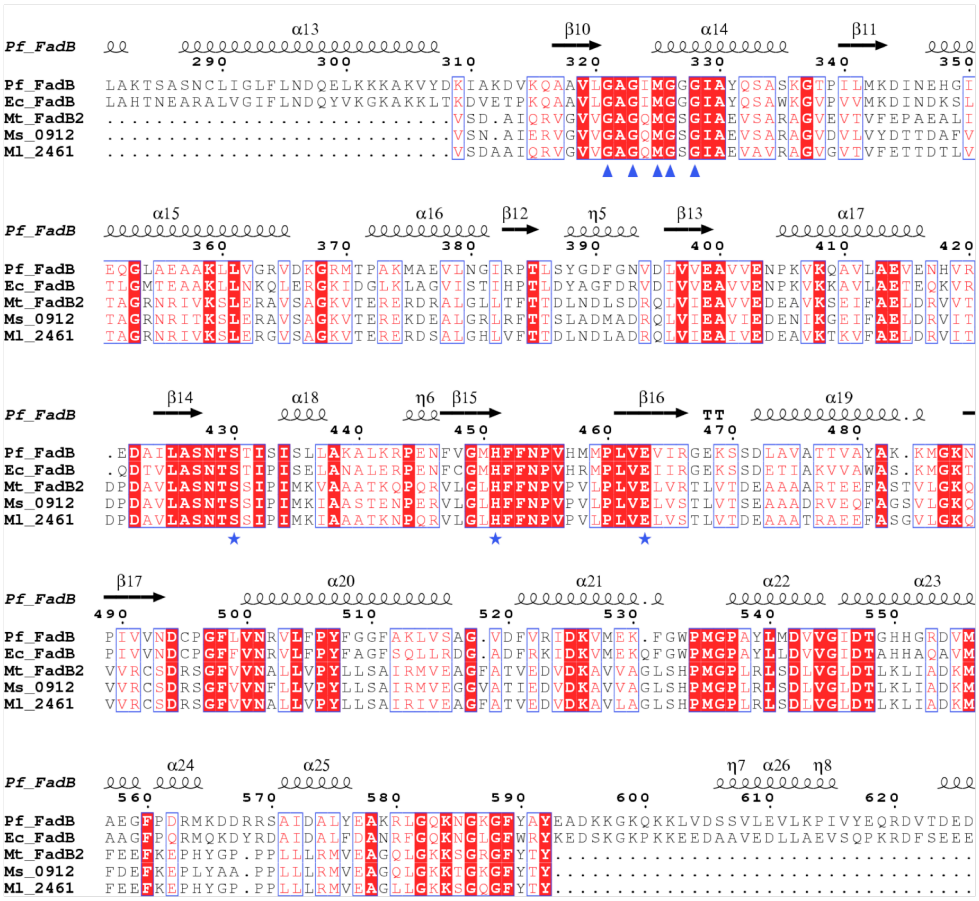

B

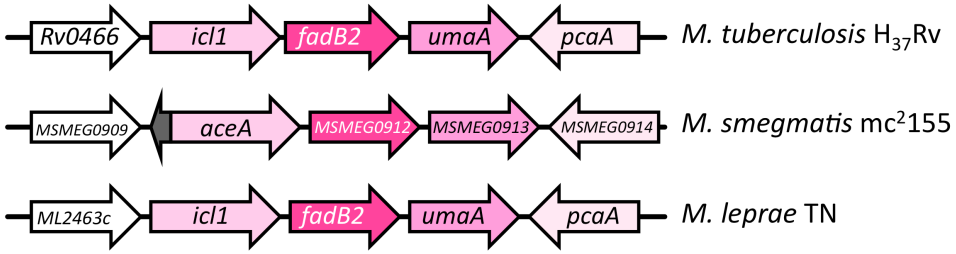

FIGURE 4-2. Sequence alignments. (**A**) Multiple sequence alignment of *M. tuberculosis* FadB2 with mycobacterial homologues and other *M. tuberculosis* Fad proteins**.** The amino acid sequences of *M. tuberculosis* FadB2 (Mt_FadB2, accession number CAA17423) and FadB3 (Mt_FadB3, accession number CAE55415) are compared with the amino acid sequence of homologues in *M. smegmatis* (Ms_0912, accession number ABK71785), *M. leprae* (Ml_2461, accession number CAC31978), *E. coli* (Ec_FadB, accession number AAC76849 residues 297–624) and *Psuedomonas fragi* (Pf_FadB accession number 2D3T_A residues 297–624). The figure was generated using Clustal W and ESPript (available from http://expasy.ch/) and data for the corresponding secondary structure for *Psudomonas fragi* FadB (residues 297–624) was obtained from the Protein Data Bank. *Red-filled boxes* indicate residues conserved across all the species aligned and *blue-boxed* residues are those of high similarity. The *triangles* indicate the putative NAD^+-binding site and the *stars* highlight residues of the hypothetical catalytic triad. (**B**) Maps of the genomic regions of *M. tuberculosis* H_{37}Rv *fadB2*, *M. smegmatis* mc^2155 *MSMEG0912* and *M. leprae* TN *fadB2*.

There is much evidence from other bacterial species and eukaryotes that these NQOs have an antioxidant or detoxifying function (Itoh *et al*. 1997, Shimada 2006, Triccas *et al*. 1999, Tumminia *et al*. 1993). Oxidative molecules are not only a bi-product of aerobic respiration but are also produced by macrophages and other lymphocytes to aid the killing of phagocytosed bacteria. It is therefore interesting to note that *fadB4* is known to be up-regulated during intracellular growth, which could be one of the many defence mechanisms mycobacteria have evolved in order to allow them to reside and multiply within the macrophage (Triccas *et al*. 1999). As such, FadB4 is a virulence factor and therefore demands attention.

E. coli NQO enzymes 1 and 2 are membrane-bound. Membrane-bound quinone oxidoreductases are well studied in bacteria and are essential constituents of the respiratory chain. These insoluble proteins are NADH-dependent, require either FMN or FAD for activity, and some have iron-sulfur clusters as co-factors. Mycobacterial FadB4 and FadB5 are, however, annotated as members of a distinct group of soluble NQOs, of which there are far fewer examples. There is one example of a soluble NQO in *E. coli* encoded by the gene *qor*. FadB4 and Qor share 44.5 % sequence similarity and FadB5 and Qor share 45.3 % sequence similarity. Thorn and co-workers (1995) determined the structure of this protein complexed with NADPH but were unable to elucidate a function. Later, Søballe & Poole (1999) found that Qor maintains ubiquinone in its reduced state thereby promoting its antioxidant function. *Streptococcus gordonii* has an oxidative stress response operon comprising three genes *nosX*, *qor1* and *qor2*, the latter two being quinone oxidoreductases. The operon responds to environmental oxygen levels and oxidative stress and is important in biofilm formation (Loo *et al*. 2004). A similar finding was made in *Staphylococcus aureus* by Maruyama *et al*. (2003). The team identified that gene *SA1989* encoded a protein with NQO-

activity that was capable of the one-electron reduction of quinone to semiquinone and was more highly expressed when under oxidative stress conditions (Figure 4-3).

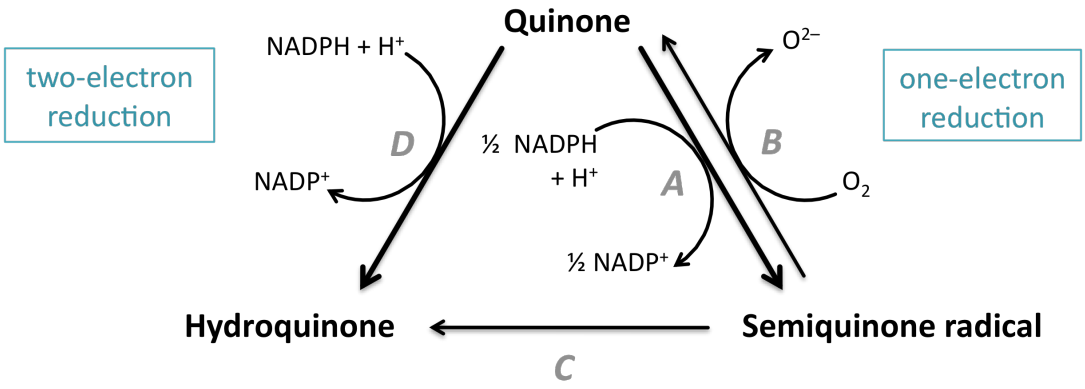

FIGURE 4-3. Quinone metabolism. (**A**) The one-electron reduction of quinone to the semiquinone radical. (**B**) Oxidation of the semiquinone radical and generation of a superoxide anion (O^{2-}). (**C**) Conversion of accumulated semiquinone radical to hydroquinone and (**D**) the two-electron reduction of quinone. Adapted from Maruyama *et al*. (2003).

In eukaryotes, there are two types of soluble NQOs, DT-diaphorase and zeta-crystallin (Maruyama *et al*. 2003). The former, a flavoenzyme, detoxifies quinone by catalysing the NAD(P)H-dependent reduction of quinone with two electrons to produce hydroquinone. The latter, zeta-crystallin, does not require FMN or FAD and catalyses the NADPH-dependent one-electron reduction of quinone to produce the semiquinone radical. The radical is highly unstable and is thus readily oxidised back to quinone in the presence of oxygen to produce superoxide anions (Figure 4-3). Zeta-crystallin is a highly conserved protein, found in bacteria, plants and animals (Shimomura *et al*. 2003). There are three zeta-crystallin homologues in *Arabidopsis thaliana* of which P1-zeta-crystallin has been very well studied (Mano *et al*. 2000a, 2000b, 2002). P1 is oxidative stress-induced, it catalyses the NADPH-dependent reduction of quinones, diamides and 2-alkenals of carbon chain C_3-C_9. The protein has highest specificity for 4-hydroxy-(2*E*)-nonenal, a major toxic product from lipid

peroxides. The P1 enzyme catalyses the hydrogenation of α,β-unsaturated bonds (but not the reduction of the aldehyde moiety) to give saturated aldehydes (Mano *et al*. 2002). Giving the importance of lipids to *M. tuberculosis* and the annotation of *fadB4* and *fadB5* as being involved in fatty acid degradation, the genes may have a role in lipid peroxide detoxification.

The location of *fadB4* in the genome may also suggest a role in detoxification. The gene is downstream of *fadE23* and *fadE24*, both of which encode putative acyl-CoA dehydrogenases. These two genes were found to be induced upon isoniazid treatment. It was concluded that, rather than being directly linked to the isoniazid response, FadE23 and FadE24 may be involved in mechanisms related to the toxic effects of the drug (Wilson *et al*. 1999). Speculatively, *fadE24*, *fadE23* and *fadB4* could form a detoxification operon that is induced during periods of toxic stress.

The function of *M. tuberculosis* FadB4 was explored in a single study in 2008 (Scandurra *et al*. 2008). A Δ*Mt-fadB4* deletion mutant was created and the effects were observed in a mouse model of infection. The mutant was found to be hypervirulent: cells replicated faster in the host than the wild-type strain and induced less TNF-α secretion in macrophages. As a result, mice infected with the mutant died sooner than those infected with wild-type *M. tuberculosis*. Several hypervirulent deletion mutants have been described in *M. tuberculosis* (Rousseau *et al.* 2003, Shimono *et al*. 2003) and other pathogens such as *Cryptococcus* (Nelson *et al.* 2001) and *Shigella* (Hachani *et al*. 2008). One reason for this is that the deletions are removing toxic protein products, thereby giving an advantage in the host, but confer reduced growth outside the host, therefore are not retained (Scandurra *et al*. 2008). An alternative explanation for mutations involving the pathogen's cell wall, cell surface proteins or secreted factors, is that the disruption alters the interaction with the host immune cells (Rousseau *et al.* 2003, Saint-Joanis *et al*. 2006).

FadB5 (Rv1912c) is non-essential according to Sassetti *et al*. (2003) and has been found wholly or partially deleted in some clinical isolates of *M. tuberculosis* (TubercuList; Lechat *et al*. 2008). The protein shares a 44.1 % sequence similarity with FadB4 and it too is annotated as a putative oxidoreductase containing a zeta-crystallin signature. *Bacillus cereus* has a *fadB5* gene described as a zinc-binding oxidoreductase and, although a homologue has been identified in *M. leprae*, there is no close match to FadB5 in *M. smegmatis*. The closest 'homologue' is MSMEG6362, which is annotated as a putative quinone oxidoreductase but only shares 45.3 % sequence similarity.

This works describes the cloning of *M. tuberculosis* β-hydroxyacyl-CoA dehydrogenases, *Mt*-FadB2 and *Mt*-FadB3, and the putative NQO *Mt*-FadB4, their over-expression in *E. coli* and purification, which in the case of FadB2, has allowed for detailed protein characterisation and kinetic studies. In parallel, mutants of the *fadB2*, *fadB3* and *fadB4* homologues in the surrogate species *M. smegmatis*, and *M. bovis* BCG Δ*fadB3* and Δ*fadB5* strains, were generated, in order to explore the functional role of these genes *in vivo*.

4.2. Materials and Methods

4.2.1. *In silico* analysis of the FadB proteins.

The Rv0468 (*Mt*-FadB2), Rv1715 (*Mt*-FadB3), Rv3141 (*Mt*-FadB4) and Rv1912c (*Mt*-FadB5) nucleotide and protein sequences were obtained from TubercuList (Lechat *et al*. 2008; http://genolist.pasteur.fr/TubercuList/). Homologous genes in *M. bovis* BCG and *M. smegmatis* were identified using the BLAST feature on the *x*BASE server (Chaudhuri *et al*. 2008). EMBOSS-Needle and ClustalW from the EMBL-EBI server (Labarga *et al.* 2007) and ESPript (Gouet *et al.* 1999) were used to produce the pair-wise and multiple sequence alignments of β-hydroxyacyl-CoA dehydrogenase from various species respectively. The

ProtParam tool from the Swiss Institute of Bioinformatics ExPASy Server was used for primary sequence analysis (Gasteiger *et al*. 2005), and GOR IV and TMHMM were used to predict the secondary protein structure (Garnier *et al*. 1996).

4.2.2. Plasmids and DNA manipulation.

The *E. coli* compatible vector pET28b (Novagen) containing a T7 promoter and encoding both 6-histidine N- and C-terminal tags was used for the over-expression of *Mt*-FadB2 and *Mt*-FadB3, and the pET28a plasmid for *Mt*-FadB4. The *Mt*-FadB2 PCR amplifications were executed using Vent$_R$® DNA polymerase (New England Biolabs) and the *Mt*-FadB3 and *Mt*-FadB4 PCR reactions executed using Phusion® DNA polymerase (Finnzymes). Chromosomal DNA from *M. tuberculosis* strain H_{37}Rv was used as the template. *Mt*-FadB2 PCR amplification was performed using the upstream primer 5′-gatcgatccatatggtgagcgatgcgatccagcgg-3′ and the downstream primer 3′-gatcgatcaagcttgtacgtgtagaaacctcgacc-5′, which contain *Nde*I and *Hin*dIII restriction sites respectively (underlined). The 858 bp PCR product was then doubly digested with *Nde*I/*Hin*dIII and ligated into a similarly cut pET28b plasmid, yielding pET28b-*Mt-fadB2*. *Mt*-FadB3 PCR amplification was performed using the upstream primer 5′-gatcgatccatatgctgacctcgcacgggttctcc-3′ and the downstream primer 3′-gatcgatcaagctttgtccccttcctttttcgtt-5′, which also contain *Nde*I and *Hin*dIII restriction sites respectively (underlined). The 912 bp PCR product was then doubly digested with *Nde*I/*Hin*dIII and ligated into a similarly cut pET28b plasmid to give pET28b-*Mt-fadB3*. *Mt*-FadB4 PCR amplification was performed using the upstream primer 5′-gatcgatccatatgcgcgcggtacgggtgactgcc-3′ and downstream 3′-gatcgatcaagcttgtcgcgcacgcgtagtacgac-5′, which contain *Nde*I and *Hin*dIII restriction sites respectively (underlined). The 969 bp PCR product was then doubly digested with

*Nde*I/*Hin*dIII and ligated into a similarly cut pET28a plasmid, yielding pET28a-*Mt-fadB4*. DNA sequencing was used to verify the recombinant genes.

4.2.3. Construction of the *Mt*-FadB2 S122A mutant.

The Stratagene QuikChange® Multi Site-Directed Mutagenesis Kit was used to create a pET28b-*Mt-fadB2*(S122A) plasmid. The following primers were used to introduce the mutation into the pET28b-*Mt-fadB2* plasmid template: 5′-tggcgtcgaatacc**gcc**agcatcccgatc-3′ and 5′-gatcgggatgctgg**cgg**tattcgacgcca-3′. The ensuing PCR and transformation were performed as per the kit manual. Sequencing was used to confirm that the mutation had been made.

4.2.4. Over-expression of wild-type and S122A *Mt*-FadB2, *Mt*-FadB3 and *Mt*-FadB4.

The wild-type and S122A-mutated proteins were over-expressed using the same protocol. pET28b-*Mt-fadB2* and pET28b-*Mt-fadB2*(S122A) plasmids were independently transformed into *E. coli* C43 (DE3) cells and incubated on LB agar containing 25 μg/ml kanamycin overnight at 37 °C. One colony of each was used to inoculate LB broth (5 ml) containing kanamycin (25 μg/ml) and cultures were incubated in a rotary incubator at 37 °C overnight. These mini-cultures were used separately to inoculate Terrific Broth (1 l) containing kanamycin (25 μg/ml) and incubated in a rotary incubator (180 rpm) at 37 °C until the OD_{600} had reached 0.6. At this point, the cultures were induced by the addition of 1 mM IPTG and incubated with shaking for 16 h at 16 °C. The cells were harvested by centrifugation at 4,500 × *g* for 12 min and stored at -20 °C for purification. Over-expression of the his-tagged *Mt*-FadB2 was confirmed by Western blot analysis using mouse monoclonal Penta-His™ Antibody (Qiagen).

The pET28b-*Mt-fadB3* plasmid was similarly transformed into *E. coli* C43 (DE3) cells and incubated on LB agar containing 25 µg/ml kanamycin overnight at 37 °C. One colony was used to inoculate LB broth (5 ml) containing 25 µg/ml kanamycin and 1 % glucose and cultures were incubated in a rotary incubator at 37 °C overnight. This mini-culture was used to inoculate 1 l Terrific Broth containing kanamycin (25 µg/ml) and was incubated in a rotary incubator (180 rpm) at 37 °C until the OD_{600} had reached 0.6. At this point, the culture was induced by the addition of 0.25 mM IPTG and incubated with shaking at 37 °C for 3.5 h. The cells were harvested by centrifugation at 4,500 × *g* for 12 min and stored at -20 °C for purification. Over-expression of the His-tagged *Mt*-FadB3 was visualised by Western blot analysis using mouse monoclonal Penta-His™ Antibody.

The pET28a-*Mt-fadB4* plasmid was co-transformed into *E. coli* BL21 (DE3) cells along with plasmids harbouring the GroES and CPN 60.2 chaperones (kindly donated by Dr S. Batt, University of Birmingham). Cells were incubated on selective LB agar containing 25 µg/ml kanamycin and 100 µg/ml ampicillin overnight at 37 °C. One colony was used to inoculate LB broth (5 ml) containing the same antibiotics and 1 % glucose, and the culture was incubated in a rotary incubator at 37 °C overnight. This mini-culture was used to inoculate 1 l Terrific Broth containing the same selective antibiotics and incubated at 37 °C with shaking until the OD_{600} had reached 0.6. At this point, the culture was induced by the addition of 0.25 mM IPTG and incubated similarly at 16 °C for 16 h. The cells were harvested by centrifugation at 4,500 × *g* for 12 min and stored at -20 °C for purification. Over-expression of the His-tagged protein was confirmed by Western blot analysis using mouse monoclonal Penta-His™ Antibody.

4.2.5. Purification of wild-type and S122A *Mt*-FadB2 proteins, *Mt*-FadB3 and *Mt*-FadB4.

The same purification method was applied to both wild-type and S122A-mutated *Mt*-FadB2 proteins. Pelleted cells were resuspended in buffer A (0.02 M sodium phosphate, pH 7.9, 0.5 M NaCl) and lysed by probe sonication (10 cycles of 30 second pulses followed by 30 second cooling intervals). The crude lysate was centrifuged at 27,000 × *g* for 40 min at 4 °C to remove the insoluble components and the resulting clarified lysate was applied to a Ni^{2+}-charged 5 ml HisTrap™ HP affinity column (GE Healthcare). The column was washed with 10 column volumes of buffer A and the protein was eluted with a step-wise gradient of 50 mM (50 ml), 130 mM (10 ml) and 1 M (10 ml) imidazole. The fractions were analysed by 12 % SDS-PAGE followed by Coomassie staining. A large single band at 30 kDa on the gel demonstrated the purity of the protein and *Mt*-FadB2 was correctly identified by a trypsin digest and mass spectrometry. The fractions containing pure *Mt*-FadB2 protein were dialysed, first against 50 mM potassium phosphate (pH 7.9), 50 mM NaF, with 1 mM EDTA added to remove any leached Ni^{2+}, and then twice against 50 mM potassium phosphate (pH 7.9), 50 mM NaF at 4 °C. The potassium phosphate/NaF buffer was chosen because it provided optimal conditions for circular dichroism experiments. The purified protein concentration was estimated using the BCA Protein Assay kit and protein aliquots were stored at -80 °C both with and without the addition of 10 % glycerol.

Mt-FadB3-containing pelleted cells were resuspended in buffer A containing one EDTA-free complete protease inhibitor-cocktail tablet (Roche) and a few grains of DNase I (New England Biolabs) and lysed by probe sonication as for *Mt*-FadB2. The crude lysate was centrifuged at 27,000 × *g* for 45 min at 4 °C to remove the insoluble components and the resulting clarified lysate was applied to a Ni^{2+}-charged 5 ml HisTrap™ HP affinity column. The column was washed with 5 column volumes of buffer A and the protein was eluted with

a step-wise imidazole gradient: thrice each of 25 mM and 50 mM (all 10 ml fractions), twice each of 75 mM, 100 mM and 150 mM (all 10 ml) and once each of 250 mM, 500 mM and 1 M (all 10 ml). The fractions were analysed by 12 % SDS-PAGE followed by Coomassie staining. A large single band at 30 kDa was visible demonstrating the purity of the protein. The second 150 mM and 250 mM fractions containing pure *Mt*-FadB3 were dialysed, first against 50 mM Tris·HCl (pH 7.9), 50 mM NaCl, with 1 mM EDTA added to remove any leached Ni^{2+}, and then twice against 50 mM Tris·HCl (pH 7.9), 50 mM NaCl at 4 °C. After determining the concentration (as before), the purified protein was stored in aliquots at -80 °C or -20 °C both with and without the addition of 10 % glycerol.

The *E. coli* cells containing *Mt*-FadB4 were resuspended in buffer A containing an EDTA-free complete protease inhibitor-cocktail tablet and a few grains of DNaseI and lysed by probe sonication as above. The crude lysate was centrifuged at 27,000 × *g* for 45 min at 4 °C to remove the insoluble components and the resulting clarified lysate was applied to a Ni^{2+}-charged 1 ml HisTrap™ HP affinity column. The column was washed with 5 column volumes of buffer A and the protein was eluted with a step-wise imidazole gradient: twice each of 25 mM, 50 mM, 75 mM, 100 mM, 150 mM and 250 mM (all 10 ml fractions) and once each of 500 mM and 1 M (both 10 ml). The fractions were analysed by 12 % SDS-PAGE followed by Coomassie staining. The strongest bands at around 35 kDa on the gel corresponding to *Mt*-FadB4 were visible in the 75 mM imidazole fractions, much weaker bands were visible in the 100 mM and 150 mM fractions. All six fractions containing protein were pooled and dialysed three times against 20 mM Tris·HCl (pH 7.5), 10 mM NaCl, 0.1 mM DTT and 10 % glycerol, with 1 mM EDTA added to remove any leached Ni^{2+} in the first buffer, at 4 °C. Attempts were made to remove the contaminants by loading the dialysed protein onto a QHP anion-exchange column (GE Healthcare) equilibrated with dialysis buffer. The protein was eluted with an increasing salt (Cl^-) concentration from 50 mM to 400

mM NaCl in 1.5 ml fractions. Those containing the purest protein were pooled and dialysed as before. The protein concentration was estimated using the BCA Protein Assay kit as 0.23 mg/ml and the protein was stored at -20 °C.

4.2.6. Enzyme assay for wild-type and S122A *Mt*-FadB2.

The activity assay for *Mt*-FadB2 was based on that previously described (Nemeria *et al.* 2001). The forward *Mt*-FadB2-dependent reduction of NAD^+ to NADH was monitored spectrophotometrically at 340 nm using a Jenway 6710 UV/Vis spectrophotometer. The standardised 1 ml reaction contained 100 mM *N*-cyclohexyl-3-aminopropanesulfonic acid (CAPS) buffer (pH 9.5), 50 µM NAD^+, 50 µM β-hydroxybutyryl-CoA and 7 µg purified *Mt*-FadB2 protein. The reaction mixture minus the protein was incubated for 2 minutes at 30 °C before adding the enzyme to start the reaction. The reverse reaction was observed similarly. The standard 1 ml reaction contained 100 mM potassium phosphate buffer (pH 7.0), 50 µM NADH, 50 µM acetoacetyl-CoA and 7 µg pure *Mt*-FadB2 protein. All controls were performed to ensure neither the potassium phosphate/NaF buffer nor any of the assay buffers or substrates interfered with the assay results. The initial velocity of each reaction was measured and the kinetic parameters, K_M, V_{max} and k_{cat}, for each substrate and co-factor were ascertained by varying their concentration and fitting the data to the Michaelis-Menten equation using SigmaPlot 8.0. Each reaction was performed in triplicate.

4.2.7. Circular dichroism spectroscopy of wild-type and S122A *Mt*-FadB2.

All circular dichroism (CD) far UV spectra were obtained at 25 °C using a JASCO J-715 spectropolarimeter and a 0.01 cm pathlength cell. The wild-type and S122A-mutant *Mt*-FadB2 proteins were made to 1.1 mg/ml as determined by the BCA Protein Assay kit. To compare the folding of the wild-type and mutant protein, 50 mM potassium phosphate (pH 7.9), 50 mM NaF buffer was used. To assess protein folding at different pH values, 50 mM

potassium phosphate (pH 6, pH 7 or pH 8), 50 mM NaF or 50 mM CAPS (pH 9, pH 10 or pH 11), 50 mM NaF was used. Each condition was scanned eight times over a wavelength of 197–245 nm and a bandwidth of 2 nm. The results were normalised by subtracting the baseline buffer spectrum from each.

4.2.8. Analytical ultracentrifugation of wild-type *Mt*-FadB2.

Analytical ultracentrifuge (AUC) experiments were performed using an 8-piece An60Ti rotor in a Beckman-Optima XL-I using interference optics. The protein was analysed separately with substrate, product and co-factors as well as native. Sedimentation velocity was executed at 4 °C, 40,000 rpm and data were processed using the continuous c(s) distribution method in the SEDFIT program.

4.2.9. *Mt*-FadB2 crystallisation trials.

Mt-FadB2 was purified, dialysed and concentrated to 30 mg/ml. Native protein was incubated overnight at 4 °C with 8 mM NAD^+, NADH, β-hydroxybutyryl-CoA or acetoacetyl-CoA prior to trials. The Molecular Dimensions optimised sparse matrix screens JCSG-*plus*™ and Structure Screen™ were used initially to identify conditions that were most permissible for crystal growth. The sitting drop vapour diffusion method was employed using a 96-well plate and a Mosquito nano-drop crystallisation robot. Conditions were optimised and the best crystals were cryoprotected, frozen and diffracted.

4.2.10. Construction of the *fadB2* (*MSMEG0912*), *fadB3* (*MSMEG6791*) and *fadB4* (*MSMEG2033*) deletion mutants in *M. smegmatis* and the *fadB3* (*Mb1742-1743*) and *fadB5* (*Mb1947c*) deletion mutants in *M. bovis* BCG.

All five mycobacterial deletion mutants were generated using the specialised transduction method previously described by Bardarov *et al*. (2002). All initial PCR amplifications for the *M. smegmatis* mutants were performed using *M. smegmatis* mc^2155 genomic DNA and Phusion® DNA polymerase. For Δ*Ms-fadB2*, a 1000 bp sequence of the upstream region of *Ms-fadB2* and an 800 bp sequence of the downstream region of the gene were PCR amplified using the following primers, each containing a *Dra*III restriction site at the 5′ end (underlined): *Ms-fadB2*_LL (5′-tttttttt<u>cacaaagtg</u>ctggagccctgcatcgcgcg-3′), *Ms-fadB2*_LR (5′-tttttttt<u>cacttcgtg</u>cgggatgctcgacgtgttcg-3′), *Ms-fadB2*_RL (5′-tttttttt<u>cacagagtg</u>ctgctctcggcaatccgcat-3′) and *Ms-fadB2*_RR (5′-tttttttt<u>caccttgtg</u>cttcccaaccctgcaggcgg-3′). For the *M. smegmatis fadB3* null-mutant, an 861 bp sequence of the upstream region of *Ms-fadB3* and a 974 bp sequence of the downstream region of *Ms-fadB3* were PCR amplified using the following primers, each containing a *Dra*III restriction site at the 5′ end (underlined): *Ms-fadB3*_LL (5′-tttttttt<u>cacaaagtg</u>ggcttcatgcaggcgctaac-3′), *Ms-fadB3*_LR (5′-tttttttt<u>cacttcgtg</u>acggcctccatcacgtagtc-3′), *Ms-fadB3*_RL (5′-tttttttt<u>cacagagtg</u>tcgcataccgcaacaagg-3′) and *Ms-fadB3*_RR (5′-tttttttt<u>caccttgtg</u>aggcgtgaaagctggaag-3′). For the *Ms-fadB4* deletion mutant, a 1000 bp sequence of the upstream region of *Ms-fadB4* and a 900 bp sequence of the downstream region of the gene were amplified by PCR using the following primers, each containing a *Dra*III restriction site at the 5′ end (underlined): *Ms-fadB4*_LL (5′-tttttttt<u>cacaaagtg</u>cccaactcggtggccagcgc-3′), *Ms-fadB4*_LR (5′-tttttttt<u>cacttcgtg</u>acaccggccacctcggcgcc-3′), *Ms-fadB4*_RL (5′-tttttttt<u>cacagagtg</u>tcggcgcgggttggggtgcg-3′) and *Ms-fadB4*_RR (5′-

tttttttt<u>caccttgtg</u>ccgtcaacacgcgaatcggc-3′). The PCR fragments for each gene were cloned independently into the appropriate p0004S vector to generate the allelic exchange plasmids pΔ*Ms-fadB2*, pΔ*Ms-fadB3* and pΔ*Ms-fadB4*. The plasmids were then *Pac*I-digested and packaged separately into the mycobacteriophage phAE159 to generate the knock-out phages, phΔ*Ms-fadB2*, phΔ*Ms-fadB3* and phΔ*Ms-fadB4*. High titre phage particles were produced for each knock-out and transduced into wild-type *M. smegmatis* mc^2155 cells, as previously described (Bardarov *et al*. 2002). True hygromycin-resistant colonies obtained after transduction were confirmed as *Ms-fadB2*-, *Ms-fadB3*- and *Ms-fadB4*-deletion mutants by Southern blot.

The initial PCR amplifications for the *M. bovis* BCG mutants were performed using *M. bovis* BCG genomic DNA as the template and Phusion® DNA polymerase. For the *M. bovis* BCG *fadB3* null-mutant, an 802 bp sequence of the upstream region of *Mb-fadB3* and an 853 bp sequence downstream of *Mb-fadB3* were PCR amplified using the following primers, each containing a *Bst*API restriction site at the 5′ end (underlined): *Mb-fadB3*_LL (5′-tttttttt<u>gcataaattgc</u>ccgtttggacggagtgttg-3′), *Mb-fadB3*_LR (5′-tttttttt<u>gcatttcttgcg</u>ccgttcgaagagttcctg-3′), *Mb-fadB3*_RL (5′-tttttttt<u>gcatagattgc</u>acatcgggttggacctcac-3′) and *Mb-fadB3*_RR (5′-tttttttt<u>gcatcttttgc</u>gaagtcgtcgagcaccttg-3′). For the Δ*Mb-fadB5* mutant, a 994 bp sequence upstream of *Mb-fadB5* and an 821 bp sequence downstream of the gene were PCR amplified using the following primers: *Mb-fadB5*_LL (5′-tttttttt<u>cacaaagtg</u>atcgcaagtacccgatcaag-3′) and *Mb-fadB5*_LR (5′-tttttttt<u>cacttcgtg</u>tagccaccaaatcgtgtacc-3′) both containing a *Dra*III restriction site, underlined, and *Mb-fadB5*_RL (5′-tttttttt<u>ccatagattggc</u>gaagctcctgaagcacatc-3′) and *Mb-fadB5*_RR (5′-tttttttt<u>ccatcttttgg</u>ttggagaagccagggtttcg-3′) both containing a Van91*i* restriction site, underlined. Allelic exchange substrates were generated as described for the *M.*

smegmatis mutants and packaged similarly. High titre phage particles were transduced into wild-type *M. bovis* BCG cells and genuine mutant colonies were verified by Southern blot.

4.2.11. Construction of the complemented knock-out strains.

The *E. coli–Mycobacterium* shuttle vector pMV261 was used for all complementation experiments (Stover *et al*. 1991). The *M. tuberculosis* genes *Rv0468* (*fadB2*), *Rv1715* (*fadB3*), *Rv3141* (*fadB4*) and *Rv1912c* (*fadB5*) were PCR amplified using H_{37}Rv chromosomal DNA, and the homologous *M. smegmatis* genes *MSMEG0912* (*fadB2*), *MSMEG6791* (*fadB3*), *MSMEG2033* (*fadB4*) and *MSMEG6362* (*fadB5*) were amplified from *M. smegmatis* mc^2155 chromosomal DNA, all using Phusion® DNA polymerase. The following primers were used, all restriction sites are underlined with the restriction endonuclease in parentheses: *Mt-fadB2* upstream 5′-gatcgatcggatccagtgagcgatgcgatccagcgg-3′ (*Bam*HI), *Mt-fadB2* downstream 3′-gatcgatcaagcttatcagtacgtgtagaaacctcg-5′ (*Hin*dIII), *Mt-fadB3* upstream 5′-gatcgatcggatccaatgctgacctcgcacgggttc-3′ (*Bam*HI), *Mt-fadB3* downstream 3′-gatcgatcaagcttctatgtccccttccttttttcgtt-5′ (*Hin*dIII), *Mt-fadB4* upstream 5′-gatcgatcggatccaatgcgcgcggtacgggtgact-3′ (*Bam*HI), *Mt-fadB4* downstream 3′-gatcgatcaagctttttagtcgcgcacgcgtagtac-5′ (*Hin*dIII), *Mt-fadB5* upstream 5′-gatcgatcggatccatgcgagcagtggtcatcacc-3′ (*Bam*HI), *Mt-fadB5* downstream 5′-gatcgatcaagcttacacggtaccagcaccacctt-3′ (*Hin*dIII), *Ms-fadB2* upstream 5′-gatcgatcggatccagtgagcaatgcaatcgaacga-3′ (*Bam*HI), *Ms-fadB2* downstream 3′-gatcgatcaagctttcagtaggtatagaagccctt-5′ (*Hin*dIII), *Ms-fadB3* upstream 5′-gatcgatcggatccaatgctgacctcgcacgggttc-3′ (*Bam*HI), *Ms-fadB3* downstream 3′-gatcgatcaagcttctatgtccccttccttttttcgtt-5′ (*Hin*dIII), *Ms-fadB4* upstream 5′-gatcgatcggatccaatgcgcgctgcactgataac-3′ (*Bam*HI), *Ms-fadB4* downstream 3′-gatcgatcaagctttcagcgcagtttgagcacca-5′ (*Hin*dIII), *Ms-fadB5* upstream 5′-gatcgatcggatccaatgtctcctgccgtgcgtcc-3′ (*Bam*HI), *Ms-fadB5* downstream 5′-

gatcgatcaagctttcattcggagacgcgcagca-3′ (*Hin*dIII). The PCR products were then digested with *Bam*HI and *Hin*dIII and each ligated into a similarly cut pMV261 plasmid, yielding pMV261-*Mt-fadB2*, pMV261-*Mt-fadB3*, pMV261-*Mt-fadB4*, pMV261-*Mt-fadB5*, pMV261-*Ms-fadB2*, pMV261-*Ms-fadB3,* pMV261-*Ms-fadB4* and pMV261-*Ms-fadB5*. DNA sequencing was used to verify the recombinant genes. Electrocompetent Δ*Ms-fadB2* cells were electroporated with pMV261-*Ms-fadB2*, pMV261-*Mt-fadB2* or pMV261 plasmid, electrocompetent Δ*Ms-fadB3* and Δ*Mb-fadB3* cells were electroporated with pMV261-*Mt-fadB3*, pMV261-*Ms-fadB3* or pMV261 plasmid. Electrocompetent Δ*Ms-fadB4* cells were electroporated with pMV261-*Ms-fadB4*, pMV261-*Mt-fadB4* or pMV261 plasmid, and electrocompetent Δ*Mb-fadB5* cells were electroporated with pMV261-*Mt-fadB5*, pMV261-*Ms-fadB5* or pMV261 plasmid. Transformants were selected for using hygromycin- (100 µg/ml for *M. smegmatis* mutants, 75 µg/ml for *M. bovis* BCG mutants) and kanamycin- (25 µg/ml) containing agar plates.

4.2.12. Growth analysis of the deletion mutants.

4.2.12.1. Growth on different carbon sources.

The *fadB2* and *fadB4* deletion mutants were analysed for growth on different carbon sources. Wild-type *M. smegmatis*, Δ*Ms-fadB2*, Δ*Ms-fadB4*, the complemented strains (pMV261-*Ms-fadB2*, pMV261-*Mt-fadB2*, pMV261-*Ms-fadB4* and pMV261-*Mt-fadB4*) and *M. smegmatis* containing an empty pMV261 plasmid were grown to saturation in minimal medium (MM) plus 0.1 % glucose. The MM used was based on that of Chang *at al*. (2009), containing (per litre) 1.5 g KH_2PO_4, 1.0 g NH_4Cl, 0.2 g $MgSO_4{\cdot}7H_2O$, 20.0 mg $CaCl_2{\cdot}2H_2O$, 1.2 mg ferric ammonium citrate, 0.85 g NaCl and 8.99 g $Na_2HPO_4{\cdot}12H_2O$. The cultures were then washed and resuspended in PBS before streaking on MM agar plates supplemented with either 0.1 % glycerol, glucose, acetate or propionate, or 0.002 % caprylic acid, capric acid, lauric acid, myristic acid, palmitic acid, oleic acid or linoleic acid, and, in the case of Δ*Ms-fadB2*, 0.2

mM cholesterol. Growth of the Δ*Ms-fadB2* strains was also monitored in liquid MM containing cholesterol (0.2 mM) as the sole carbon source: cells were grown in 7H9 to an OD_{600} of 0.6 before being washed and resuspended in MM+cholesterol. The OD_{600} was monitored over 90 h. Cholesterol was prepared for medium supplementation as described by Chang *et al*. (2009), where a 100 mM stock was made in a 1:1 (v/v) tyloxapol:ethanol solution and the cholesterol was dissolved by heating to 70 °C and with vortexing.

4.2.12.2. Lipid analysis.

See sections 2.2.6. and 2.2.7. for lipid, FAMEs and MAMEs extraction and analysis procedures.

4.2.12.3. Sensitivity to oxidative and SDS stress.

The Bauer-Kirby disc diffusion method was used to test the sensitivity of *M. smegmatis* Δ*Ms-fadB2* cells to oxidative stress and Δ*Ms-fadB3* and Δ*Ms-fadB4* cells to oxidative and SDS stress (Bauer *et al*. 1966). Wild-type, mutant and complemented cells were grown to OD_{600} 1.0 in 7H9 with 0.05 % Tween®-80 and the appropriate antibiotic(s). Cells were washed, resuspended in fresh medium and 200 µl was used to inoculate 4 ml 7H9 soft (0.75 %) agar. Sterile filter paper discs (6 mm in diameter), saturated with 6 µl of 30 % H_2O_2, 10 % SDS or H_2O (control), were applied to the overlaid plates in duplicate and incubated at 37 °C for 3 days. The diameters of the zones of inhibition surrounding the discs were then measured.

4.2.12.4. Sensitivity to acid stress.

The sensitivity of the Δ*Ms-fadB2* mutant to acid stress was also tested by monitoring the survival of strains in 7H9 medium at pH 2, 3, 4, 5, 6 and 7 over 24 h. At 3 h intervals 50 µl

samples were taken, pelleted by centrifugation and washed with PBS before being stored at 4 °C for viable count analysis. Briefly, the 50 µl samples were diluted to 10^{-7} and 10 µl aliquots were spotted onto 7H11 (+OADC) agar in triplicate. Following incubation at 37 °C for 2 days, colonies were counted and converted to colony-forming units (CFU/ml). Growth was similarly monitored in SDS stress conditions in liquid medium. Strains were grown in 7H9 medium to an OD_{600} of 0.4 before adding sterile 0.05 % SDS at t = 0 h. Samples were stored and cell viability was monitored as for acid stress.

4.2.12.5. Sensitivity to isoniazid.

Sensitivity to isoniazid of wild-type *M. smegmatis* mc^2155 compared to the Δ*Ms-fadB2* and Δ*Ms-fadB3* mutants and the complemented strains was assessed using the agar dilution method. TSB agar plates were supplemented with isoniazid at concentrations ranging from 0–20 µg/ml in duplicate. *M. smegmatis* strains were grown in TSB with 0.05 % Tween®-80 and appropriate antibiotic(s) until OD_{600} ~0.6. The cells were then resuspended in fresh medium, serially diluted to 10^{-7} and spotted (10 µl) on the plates. After incubation at 37 °C for 3–4 days, the colonies were counted and converted to log(CFU/ml).

4.2.12.6. Ability to utilise amino acids.

The ability of the Δ*Ms-fadB4* mutant to utilise amino acids was evaluated using MM agar supplemented with alanine, asparagine, lysine, leucine, valine or threonine (20 µg/ml and 100 µg/ml) or 0.1 % glucose (control). Cells were initially grown to OD_{600} 1.0 in 7H9 with 0.05 % Tween®-80 and then washed and used to inoculate MM broth containing 0.1 % glucose. Cells were serially diluted to 10^{-7}, spotted (10 µl) on the plates and incubated at 37 °C for one week. The colonies were counted and converted into units of log(CFU/ml).

4.3. Results

4.3.1. *In silico* analysis of Mt-FadB2 and *Mt*-FadB3.

Mt-FadB2 has a higher than average proportion of charged amino acids (24.1 %) compared to the entire *M. tuberculosis* proteome (20.0 %), the majority of which being negatively charged (Asp + Glu, 13.3 %) (Luthra *et al.* 2008). Similarly, there are more polar residues (42.3 %) than hydrophobic residues, which is also found for *Mt*-FadB3. The high percentage of charged and polar residues suggests that the protein is soluble and therefore not an integral cell membrane protein. The theoretical pI of native *Mt*-FadB2 protein is calculated as 5.2, whereas for the recombinant protein used here it is calculated as 6.1 (Gasteiger *et al*. 2005).

Alignment of β-hydroxyacyl-CoA dehydrogenases from mycobacteria and other species highlights the conserved residues of the hypothetical catalytic triad as identified by Barycki *et al*. (1999) (Figure 4-2 A). The residues annotated with triangles are consistent with the sequence of a Rossmann fold, a structural motif known to bind nucleotides. This is supported by the computed GOR IV secondary structure (Garnier *et al*. 1996), which predicts a β-sheet–α-helix–β-sheet motif at the C-terminus, a feature that is also seen in the overlaid secondary structure from the *Pseudomonas fragi* FadB protein. *Mt*-FadB2 has some sequence similarity to *Mt*-FadB3 and part of the *Mt*-FadB1 protein (scores of 44.8 % and 54.1 %, respectively). The identity between *Mt*-FadB2, -FadB4 and -FadB5 from *M. tuberculosis*, however, is much less (sequence similarity scores of 18.0 % and 16.1 % respectively) and *Mt*-FadB4 and -FadB5 do not share the same NAD^+ binding-site or hypothetical catalytic triad residues. This may indicate redundancy between *Mt*-FadB1, -FadB2 and -FadB3 but alternative role(s) for *Mt*-FadB4 and -FadB5.

4.3.2. Over-expression and purification of *Mt*-FadB2 and *Mt*-FadB3.

Sequencing confirmed that there were no errors in the pET28b-*Mt-fadB2* and pET28b-*Mt-fadB3* plasmids and that the PCR had added six histidine residues to both the N- and C-termini. *Mt*-FadB2 expressed well in *E. coli* C43 (DE3) cells following induction with 1 mM IPTG at 16 °C overnight, producing a high yield of His_6-tagged protein, as confirmed by Western blot (data not shown). Purification of *Mt*-FadB2 was a one-step process using a pre-packed Ni^{2+}-affinity column followed by dialysis against a 50 mM potassium phosphate (pH 7.9), 50 mM NaF buffer at 4 °C (Figure 4-4 A). The purity of the protein was seen by a large single band at ~32 kDa on SDS-PAGE and was correctly identified as *Mt*-FadB2 by trypsin digestion and mass spectrometry. *Mt*-FadB2 concentration was determined using a BCA Protein Assay kit (ThermoScientific) and a total of 18 mg of protein could be obtained from a 1-litre culture. A much lower yield of *Mt*-FadB3 was obtained, roughly 4 mg per litre of culture, but the one-step purification successfully removed all contaminants (Figure 4-4 B).

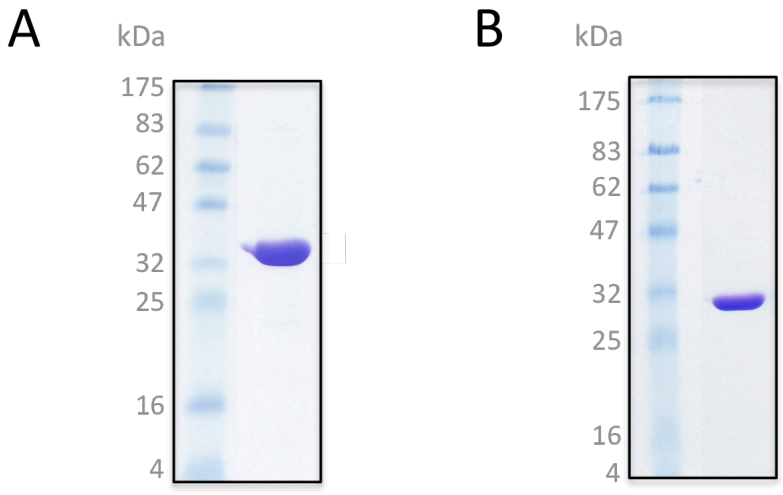

FIGURE 4-4. Purification of *Mt*-FadB2 and *Mt*-FadB3. The proteins were produced by IPTG-induction of *E. coli* C41 (DE3) transformants containing pET28b-*Mt-fadB2* or pET28b-*Mt-fadB3*. Following cell growth at 37 °C and after induction at 16 °C, the proteins were purified using a 5 ml Ni^{2+}-charged His-trap column and eluted with an increasing imidazole concentration. Fractions were visualised by Coomassie Blue staining after separation by electrophoresis on 12 % SDS-PAGE. (**A**) *Mt*-FadB2, (**B**) *Mt*-FadB3.

4.3.3. *Mt*-FadB2 is an enzymatically active β-hydroxybutyryl-CoA dehydrogenase.

In an effort to demonstrate enzymatic activity of *Mt*-FadB2, a spectrophotometric assay was developed, which involved monitoring the reduction of the co-factor NAD^+ at 340 nm (Figure 4-5 A). The His-tagged protein was found to be active both fresh and after being frozen without glycerol. The protein was highly stable, retaining its activity whilst being kept at 4 °C for over one week. The kinetic parameters calculated from the data using SigmaPlot 8.0 are displayed in Table 4-1.

TABLE 4-1. Kinetic parameters of *Mt*-FadB2 as determined by spectrophotometric assay and double-reciprocal plots. Values represent means ± standard error.

	K_M (μM)	V_{max} (nmol min^{-1} mg^{-1})	k_{cat} (min^{-1})
β-Hydroxybuyryl-CoA	43.5 ± 5.82	188.3 ± 7.4	0.723 ± 0.0284
Acetoactyl-CoA	65.6 ± 4.87	126.6 ± 8.6	0.677 ± 0.0330
NAD^+	29.5 ± 2.78	63.1 ± 1.7	0.242 ± 0.00653
NADH	50.0 ± 16.8	2,588.0 ± 200	11.36 ± 0.768

Only short-chain C_4 β-hydroxyacyl-CoA was tested as a substrate for FadB2, due to longer-chain molecules not being available commercially. However, a series of substrates of varying chain length were chemically synthesised by Dr V. Bhowruth (University of Birmingham), whereby the CoA is substituted with an *N*-acetylcysteamine (*N*-AC) group. It has been shown previously that some acyl-CoA dehydrogenases are capable of turning over such a mimic, a useful finding since it is far easier to synthesise *N*-AC-attached fatty acids than CoA (Kass *et al*. 1967, Shimakata *et al*. 1979, Williamson & Engel 1984). In order to solubilise the longer-chain fatty acids, tyloxpol (0.25 %) needed to be added to the reaction. Control assays were performed to ensure the detergent did not interfere with the spectrophotometric readings. Despite this, however, purified *Mt*-FadB2 did not appear to turn over C_{12}-*N*-AC (Figure 4-6).

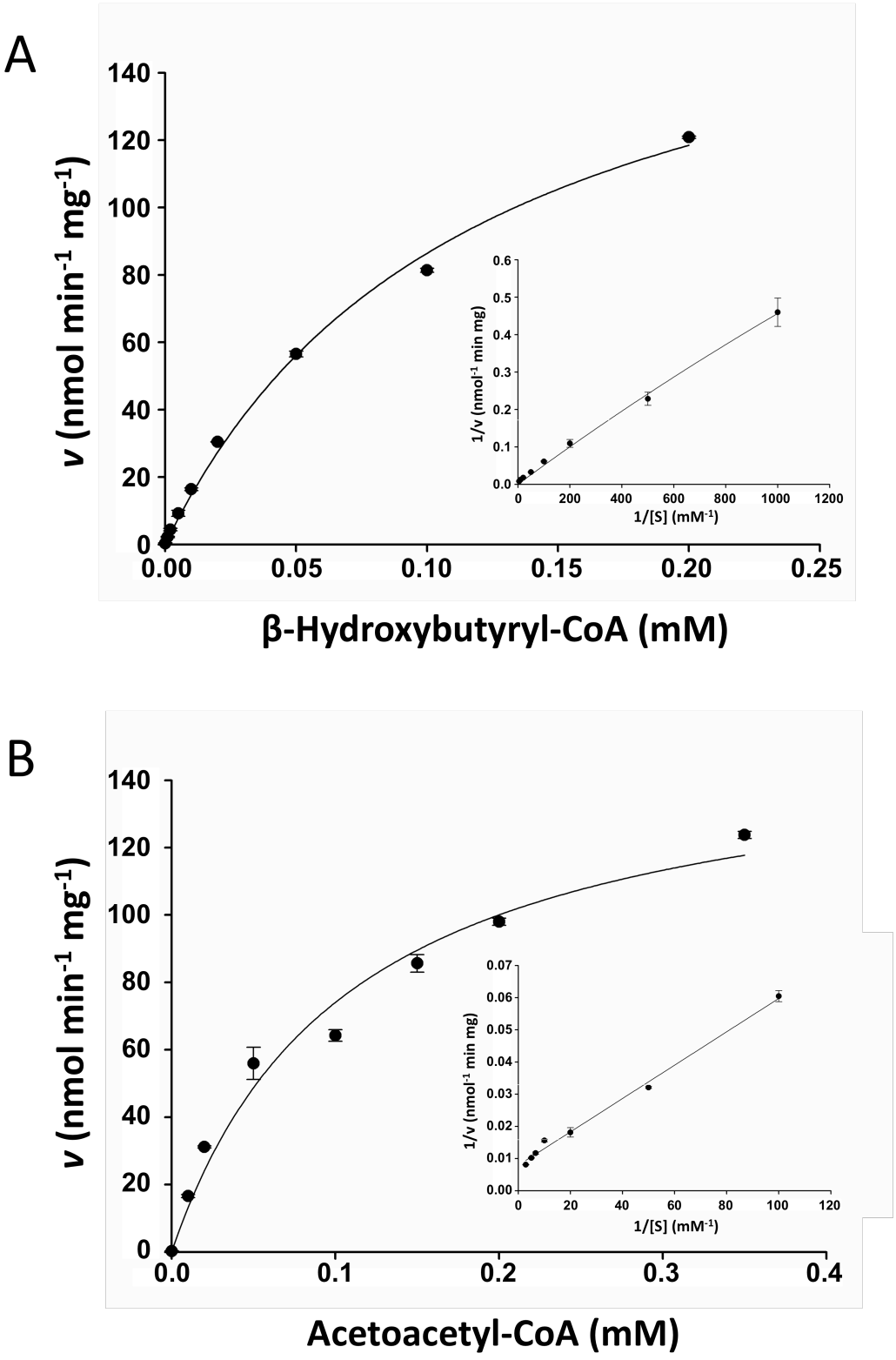

FIGURE 4-5. *Mt*-FadB2 enzyme kinetics. The reaction velocities were ascertained using increasing concentrations of substrate, β-hydroxybutyryl-CoA (**A**) and acetoacetyl-CoA (**B**). The data were fitted to the Michaelis-Menten equation using SigmaPlot 8.0 and by linear regression in the Lineweaver-Burke plot (insert). Points are the average of three replicates ± standard error.

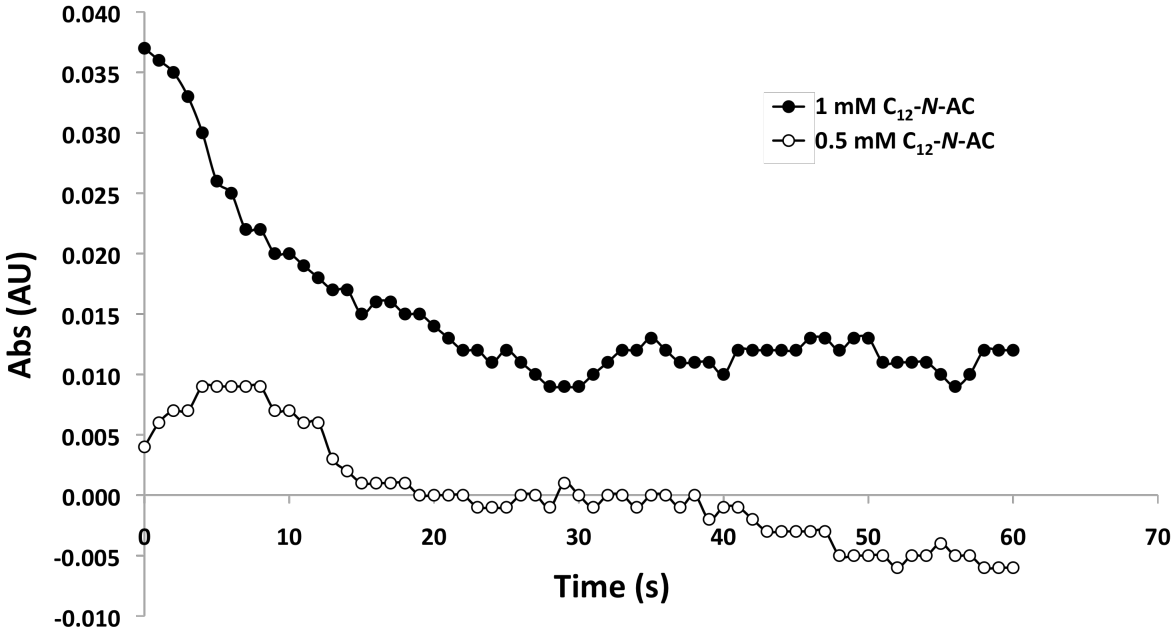

FIGURE 4-6. Raw data showing *Mt*-FadB2 enzyme activity using β-hydroxylauryl-*N*-acetylcysteamine (C_{12}-*N*-AC) as the substrate and NAD^+ as the co-factor. The reduction of NAD^+ to NADH was monitored spectrophotometrically. The standard 1 ml reaction contained 100 mM CAPS buffer (pH 9.5), 50 µM NAD^+, 1mM or 0.5 mM C_{12}-*N*-AC and 7 µg purified *Mt*-FadB2. The reaction mixture minus the protein was incubated at 30 °C before adding the enzyme to start the reaction.

The activity for the NAD^+-dependent dehydrogenase reaction was tested over a range of temperatures and pH values and the optima were found to be 37 °C and pH 10 (CAPS buffer), respectively (Figure 4-7 A, B). Not surprisingly, *Mt*-FadB2 was most active at the physiological temperature of the *M. tuberculosis* mammalian host, 37 °C. The pH data suggest that the enzyme appears to work best in alkaline conditions, the same as that obtained by Shimakata *et al*. (1979), who purified a protein fraction containing β-hydroxyacyl-CoA dehydrogenase activity from *M. smegmatis*. This, however, can be explained by the presence of protons in the enzyme reaction. Because of the release of H^+ upon oxidation of β-hydroxybutyryl-CoA and the fact that the reaction is reversible (Figure 4-1), the assay is very sensitive to changes in pH (He *et al*. 1989, Wakil *et al*. 1954).

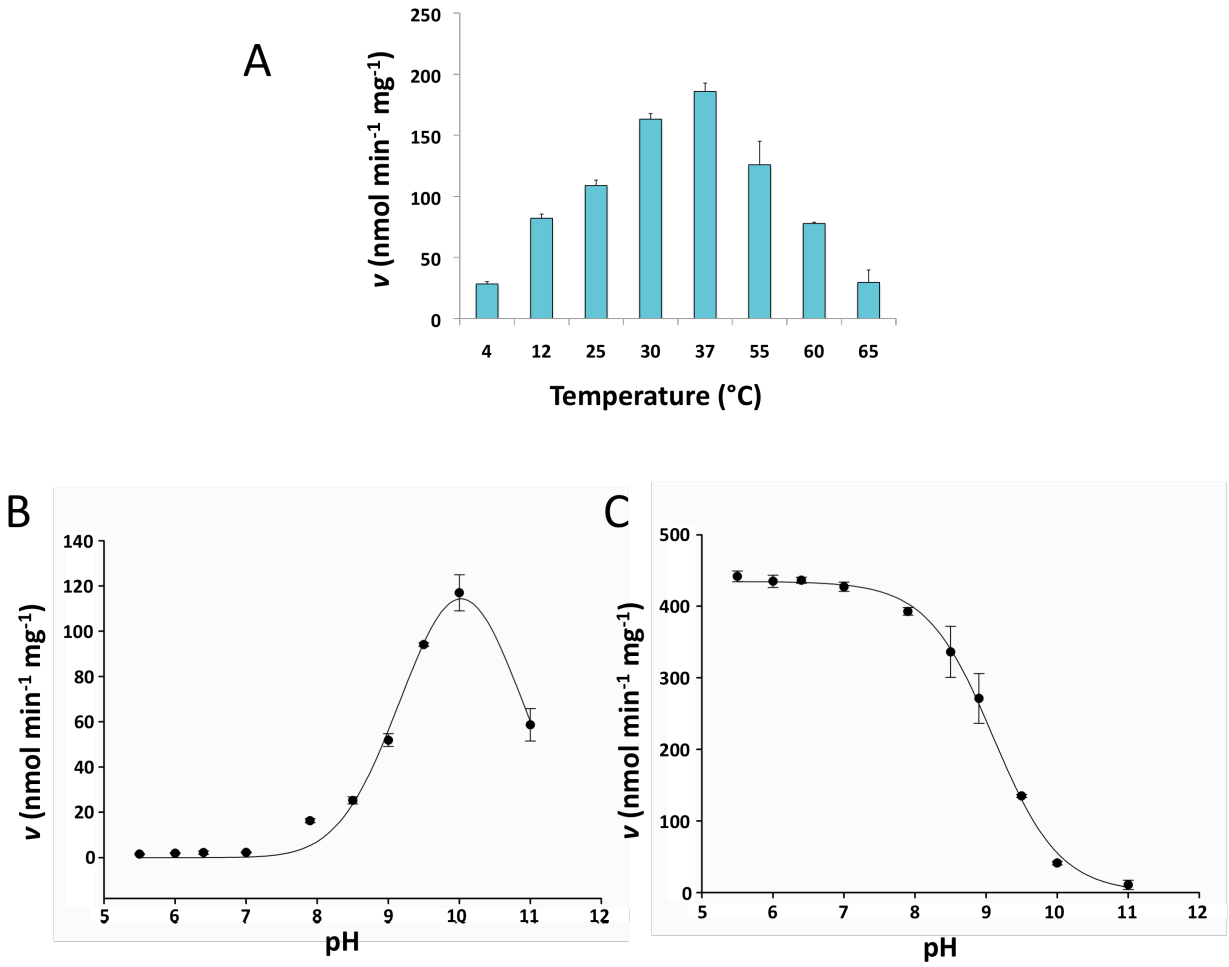

FIGURE 4-7. *Mt*-FadB2 enzyme activity. The activity of the *Mt*-FadB2 forward, NAD^+-dependent reaction was tested at different temperatures (**A**) and both the NAD^+- and NADH-dependent reactions were observed at different pHs (**B** and **C** respectively). Points are the average of three replicates ± standard error.

Wakil *et al*. (1954) studied the activity of a β-hydroxyacyl-CoA dehydrogenase isolated from beef liver mitochondria. The group found that the inflection point corresponding to 50 % β-hydroxybutyryl-CoA oxidation occurred at pH 8.2; at pH 9.0 or above oxidation is almost complete, and the equilibrium constant (K_{eq}) for β-hydroxybutyryl-CoA was calculated as 6.3×10^{-11}. By using this K_{eq} for the reaction assayed here, the effect of pH on the equilibrium can be explained (Figure 4-8).

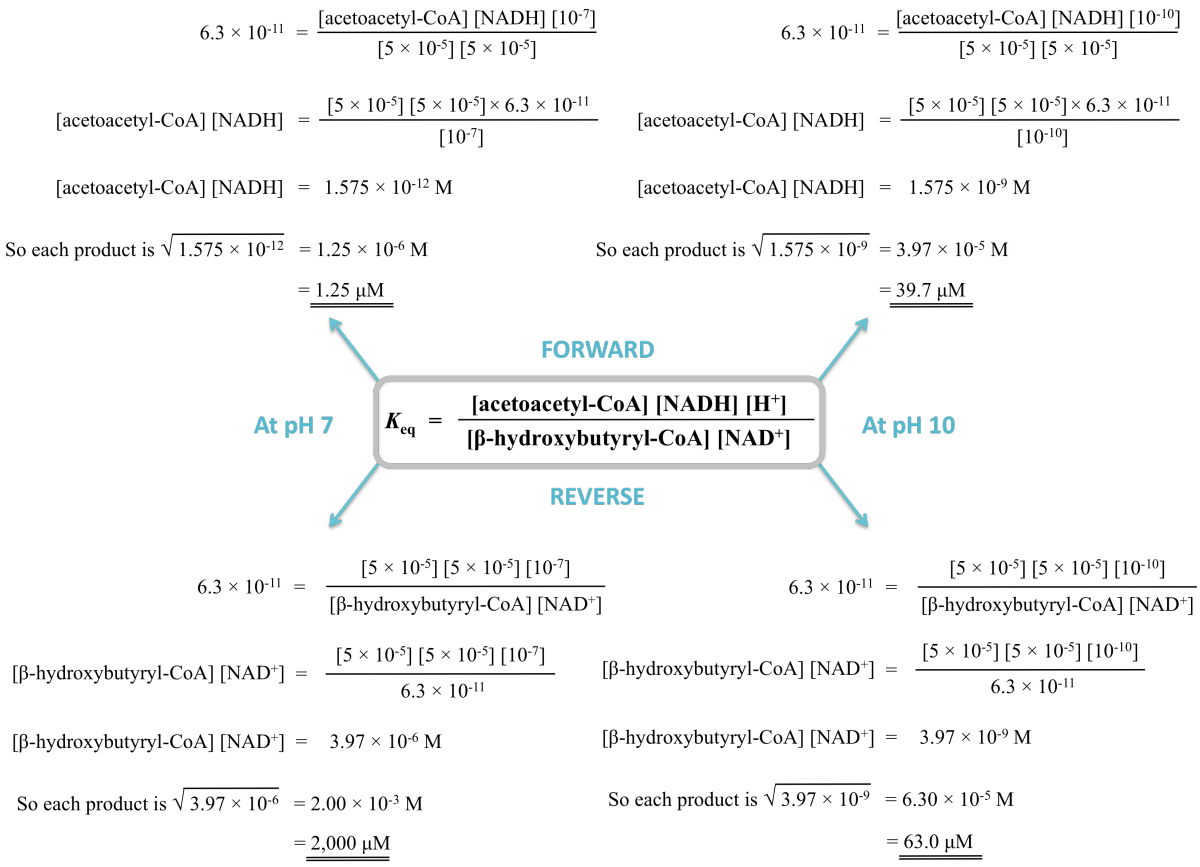

FIGURE 4-8. The effect of pH ($[H^+]$) on the position of the β-hydroxybutyryl-CoA dehydrogenase equilibrium. The equilibrium constant equation for the reaction is stated in the centre box. The forward, β-hydroxybutyryl-CoA oxidation reaction calculations are at the *top*; the reverse, NADH-dependent reaction calculations are at the *bottom*. Reactions at pH 7 are on the *left*; reactions at pH 10 are on the *right*. All values are molar unless otherwise stated. See text for details.

In the forward reaction, at pH 7, the proton concentration is such that equilibrium is pushed to the left (reactants) so very little acetoacetyl-CoA and NADH product is made. At pH 10, however, there are far fewer protons present and the reaction equilibrium is almost completely towards the product. This means that there is a higher yield of acetoacetyl-CoA and NADH product. The opposite is seen for the reverse NADH-dependent reaction (Figure 4-8).

CD spectra revealed that the protein is more susceptible to unfolding when in acidic conditions than at high pH values; the tertiary structure is maintained even at pH 10 (Figure 4-9 B). Nevertheless, it is likely that the optimal pH for *in vivo* activity may be different from those obtained with purified protein, especially knowing that the pI values of the native and recombinant protein are different.

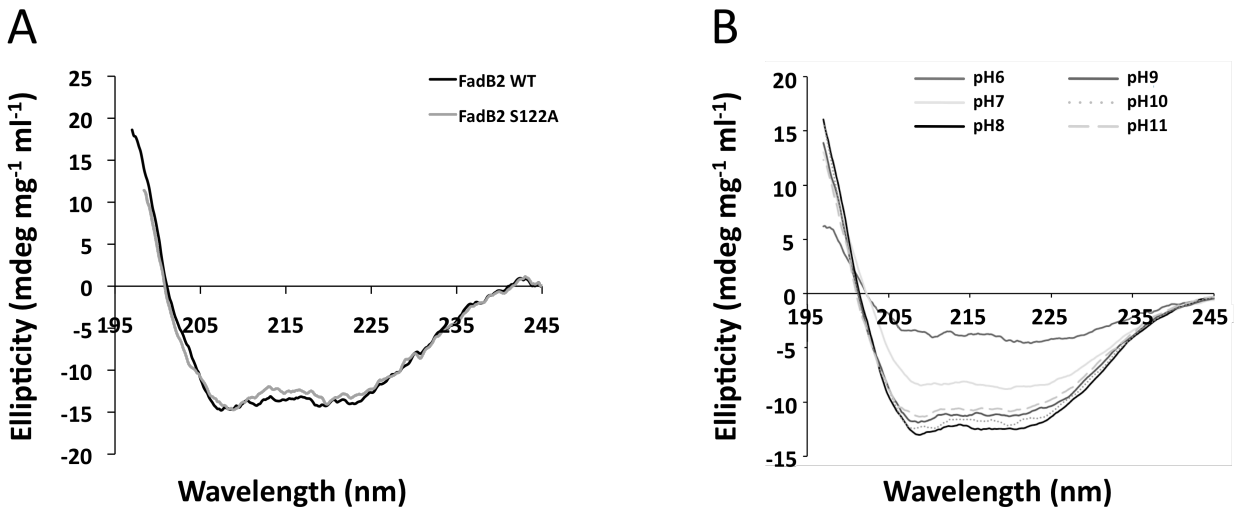

FIGURE 4-9. Circular dichroism (CD) spectra. (**A**) Superimposed CD spectra of wild-type *Mt*-FadB2 and S122A-mutated *Mt*-FadB2 in 50 mM potassium phosphate (pH 7.9), 50 mM NaF buffer. (**B**) Superimposed CD spectra of wild-type *Mt*-FadB2 in different pH buffers (50 mM potassium phosphate (pH 6, 7 or 8), 50 mM NaF or 50 mM CAPS (pH 9, 10 or 11), 50 mM NaF). Protein samples (1.1 mg/ml) were scanned in a 0.01 cm pathlength cell using a Jasco-J-715 spectropolarimeter. Spectra are averages of eight scans over a wavelength range of 197 to 245 nm, with a bandwidth of 2 nm. The results were normalised by subtracting the baseline buffer spectrum from each.

Furthermore, *Mt*-FadB2 NAD^+-reducing activity was found to be non-metal dependent, however various uni- and divalent cations were tested to see if their presence inhibited or activated the protein. Mg^{2+} and Ca^{2+} enhanced the activity of the enzyme, whereas Zn^{2+}, Ni^{2+} and Co^{2+} had an inhibitory effect (Figure 4-10). Wakil *et al*. (1954) found that the addition of Mg^{2+} to the forward β-hydroxybutyryl-CoA oxidation reaction also had the effect of increased activity. This could be explained by the di-cations forming a complex with the β-

oxoacyl-CoA product, in effect removing it from the reaction, resulting in a shift of equilibrium to the right (Wakil *et al*. 1954). The enzyme was not active when $NADP^+$ was used as a co-factor, even in the presence of $CaCl_2$.

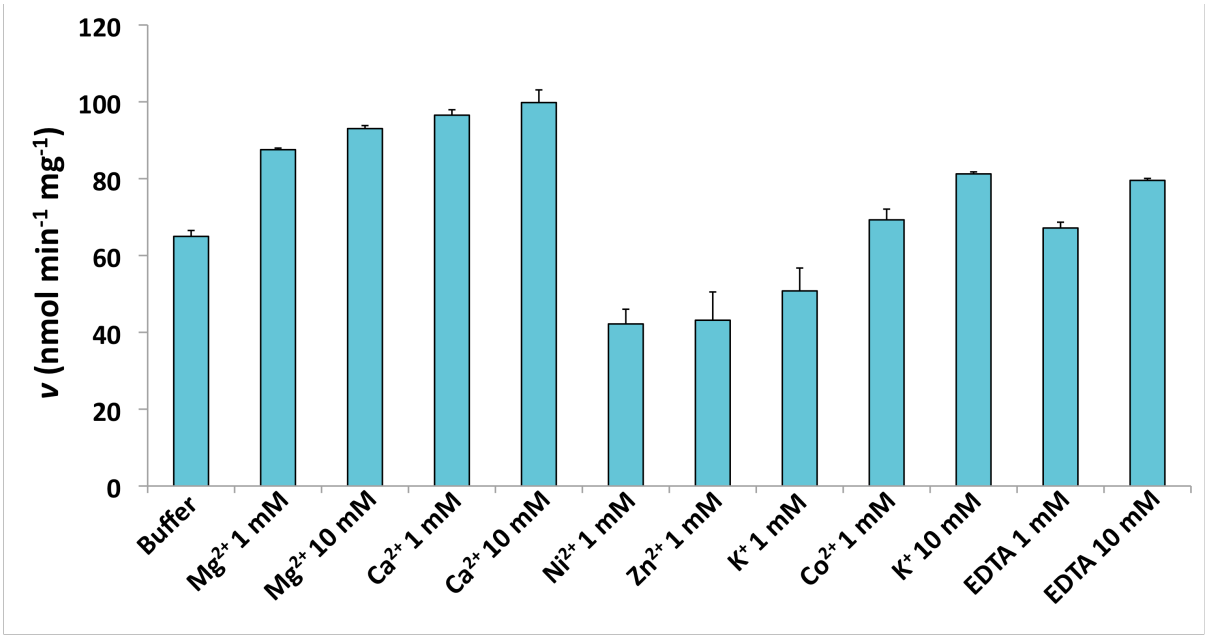

FIGURE 4-10. The effect of different uni- and divalent cations on the rate of reaction. Using β-hydroxybutyryl-CoA and NAD^+ as the substrate and co-factor respectively, different uni- and divalent cations were added to the reaction mix at a concentration of 1 mM or 10 mM. Bars represent the average of three replicates ± standard error.

Liu *et al*. (2004) found that, by substituting the Ser-137 residue with an alanine in rat mitochondrial β-hydroxyacyl-CoA dehydrogenase, the activity was greatly reduced, demonstrating that Ser-137 was a key catalytic residue. Generation of the equivalent mutation in *Mt*-FadB2 (Ser-122-Ala) abolished all activity, supporting the idea that *Mt*-FadB2 is indeed a β-hydroxyacyl-CoA dehydrogenase (data not shown). CD far-UV (197–245 nm) spectra of the wild-type and mutant protein were obtained to confirm the correct folding of both proteins (Figure 4-9 A). As well as showing that the mutation did not cause any changes to the secondary structure, this result strongly indicates that Ser-122 is a key active site residue of *Mt*-FadB2 that is directly involved in catalysis.

4.3.4. The NADH-dependent reverse reaction.

The ability of *Mt*-FadB2 to catalyse the reverse reaction, converting acetoacetyl-CoA to β-hydroxybutyryl-CoA, using NADH as the co-factor, was also investigated (Figure 4-5 B, Table 4-1). Shimakata *et al*. (1979) could not conclude that their protein with β-hydroxyacyl-CoA dehydrogenase activity was involved in fatty acid β-oxidation, but their results did show that the dehydrogenase was involved in the fatty acid elongation system. Wheeler *et al*. (1991) also implied the same conclusions in mycobacteria by showing that other enzymes of the β-oxidation pathway could catalyse both forward and reverse reactions. This reverse reaction was tested over a range of pH values and the optimum was found to be pH 5.5–6.5 (potassium phosphate buffer) (Figure 4-7 C, 4-8), a result that has been previously described for β-hydroxyacyl-CoA dehydrogenase (Shimakata *et al.* 1979). The enzyme kinetics for *Mt*-FadB2 indicate that the protein has a slightly greater affinity for β-hydroxybutyryl-CoA than acetoacetyl-CoA, *i.e.*, the fatty acid catabolism direction. It was also found that, whereas the forward reaction could not use $NADP^+$ as the co-factor, the reverse reaction was able to use NADPH as well as NADH. This therefore also indicates a role for *Mt*-FadB2 in lipid synthesis and fatty acid elongation.

4.3.5. Analytical ultracentrifugation of *Mt*-FadB2.

Analytical ultracentrifugation of *Mt*-FadB2 provided information about the state the protein adopts in buffered solution with NAD^+ and NADH co-factors and the substrate β-hydroxybutyryl-CoA. Absorbance data were not collected because the ligands absorb at the same wavelength as the protein, however, interference data of the native protein indicated that *Mt*-FadB2 exists in two forms, most likely as a monomer and dimer (Figure 4-11).

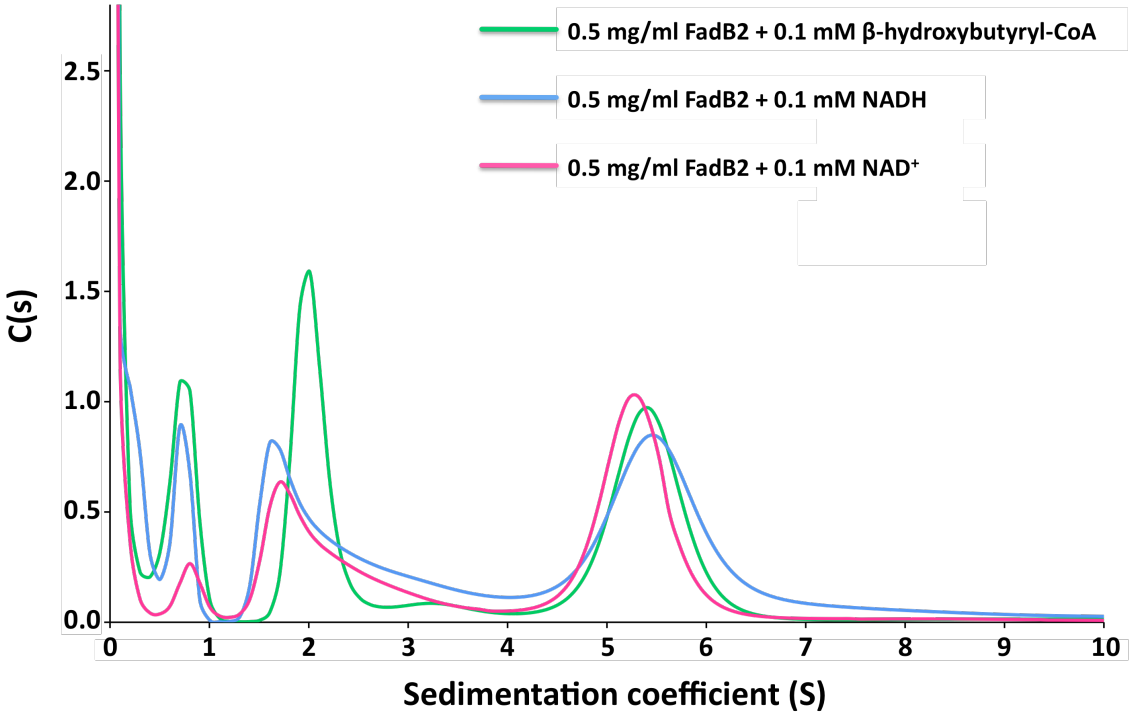

FIGURE 4-11. Analytical ultracentrifugation. The sedimentation mode indicates that *Mt*-FadB2 exists as both a monomer and dimer in buffered solution. Samples were centrifuged at 40,000 rpm at 4 °C for 8 h.

4.3.6. *Mt*-FadB2 crystallisation trials.

Attempts were made to crystallise native *Mt*-FadB2 and protein bound to NAD^+, NADH, β-hydroxybutyryl-CoA or acetoacetyl-CoA. Several buffers produced crystals sufficient for diffraction. The precipitant solution that yielded the best cube-shaped crystals was 0.1 M 4-(2-hydroxyethyl)-1-piperazineethanesulfonic acid (HEPES; pH 7.5), 12 % polyethylene glycol (PEG) 6000, 6 % 2-methyl-2,4-pentanediol (MPD) using native protein. Crystals were cryoprotected with 0.1 M HEPES (pH 7.5), 15 % PEG 6000, 20 mM NAD^+ and 15 % glycerol and soaked for 10 min before flash freezing in liquid nitrogen. The diffraction data were collected on the University of Birmingham X-ray diffractor. The best resolution obtained was 3.81 Å, which was not adequate to solve the structure of the protein (Figure 4-12 A).

From this, efforts were made to optimise the conditions further, by increasing the precipitant (PEG 6000) or salt (HEPES) concentration. Other initially promising conditions were also trialled and modified. Isomorphous replacement of the methionine residues in the protein with selenomethionine was also tried, in an attempt to improve phase determination to aid structure resolution. However, problems arose with selenium labelling: it was thought this may have been due to the massive over-production of protein, so firstly the IPTG concentration used for induction was reduced. When this strategy proved unsuccessful, the bacterial strain used was changed from *E. coli* C43 to Tuner™ cells, in which induction by IPTG concentration can be more tightly controlled. Only a slight improvement was made, however, with a maximum of three out of nine methionine residues being replaced. Attempts to crystallise *Mt*-FadB2 halted at this point. A simulation of *Mt*-FadB2 was instead generated using the SWISS-MODEL server (<http://swissmodel.expasy.org/>; Arnold *et al*. 2006, Kiefer *et al*. 2009, Peitsch 1995), based on the protein structure of human heart short-chain L-3-hydroxyacyl-CoA dehydrogenase (PBD entry, 3HAD; Barycki *et al*. 1999) (Figure 4-12 B).

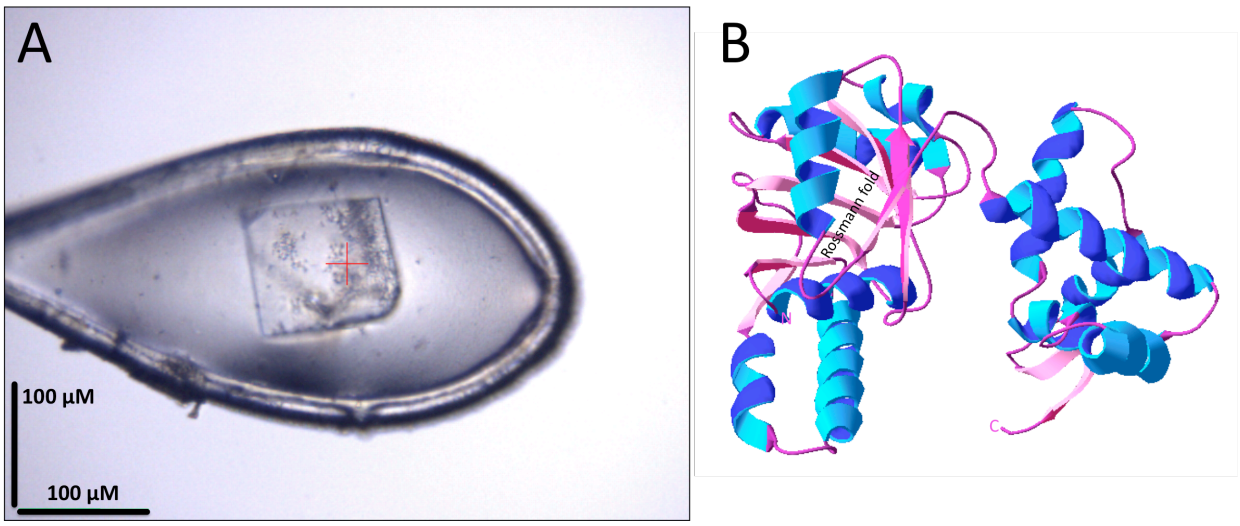

FIGURE 4-12. *Mt*-FadB2 crystallisation. (**A**) *Mt*-FadB2 protein crystal (**B**) The simulated structure of *Mt*-FadB2 based on human heart short-chain L-3-hydroxyacyl-CoA dehydrogenase, PBD entry: 3HAD (Barycki *et al*. 1999).

4.3.7. *M. smegmatis fadB2* and *fadB3* deletion mutant analysis.

The *Ms-fadB2*, *Ms-fadB3* and *Mb-fadB3* knock-out mutants were generated using specialised transduction (Bardarov *et al.* 2002) and confirmed by Southern blot (Figure 4-13). This verified that neither *fadB2* nor the *fadB3* homologue *MSME6791* are essential in *M. smegmatis*, as suggested by transposon data reported for *M. tuberculosis* (Sassetti *et al.* 2003). The same transposon data, however, reported that the *fadB3* gene in *M. tuberculosis* (*Mb1742-1743*) is essential. For this reason the generation of a mutant lacking the *fadB3* homologue in *M. bovis* BCG, a close relation to *M. tuberculosis*, is surprising. The best way of proving this, however, would be to attempt to generate the *Mt-fadB3* knock-out in *M. tuberculosis*.

There were no obvious differences were observed either in colony morphology or lipid profiles between the Δ*Ms-fadB2* and wild-type *M. smegmatis* strains (Figures 4-14, 4-15 and 4-16), except for a second species in the phopspholipid region visible in the Δ*Ms-fadB2*-pMV261-*Ms-fadB2* complemented strain (Figure 4-15 B). It would be interesting to identify what this potential phospholipid is. Also, better separation of the *M. smegmatis* MAMEs would provide more accurate information regarding the biosynthesis of α-, α′-and epoxy-mycolates (Figure 4-16 B).

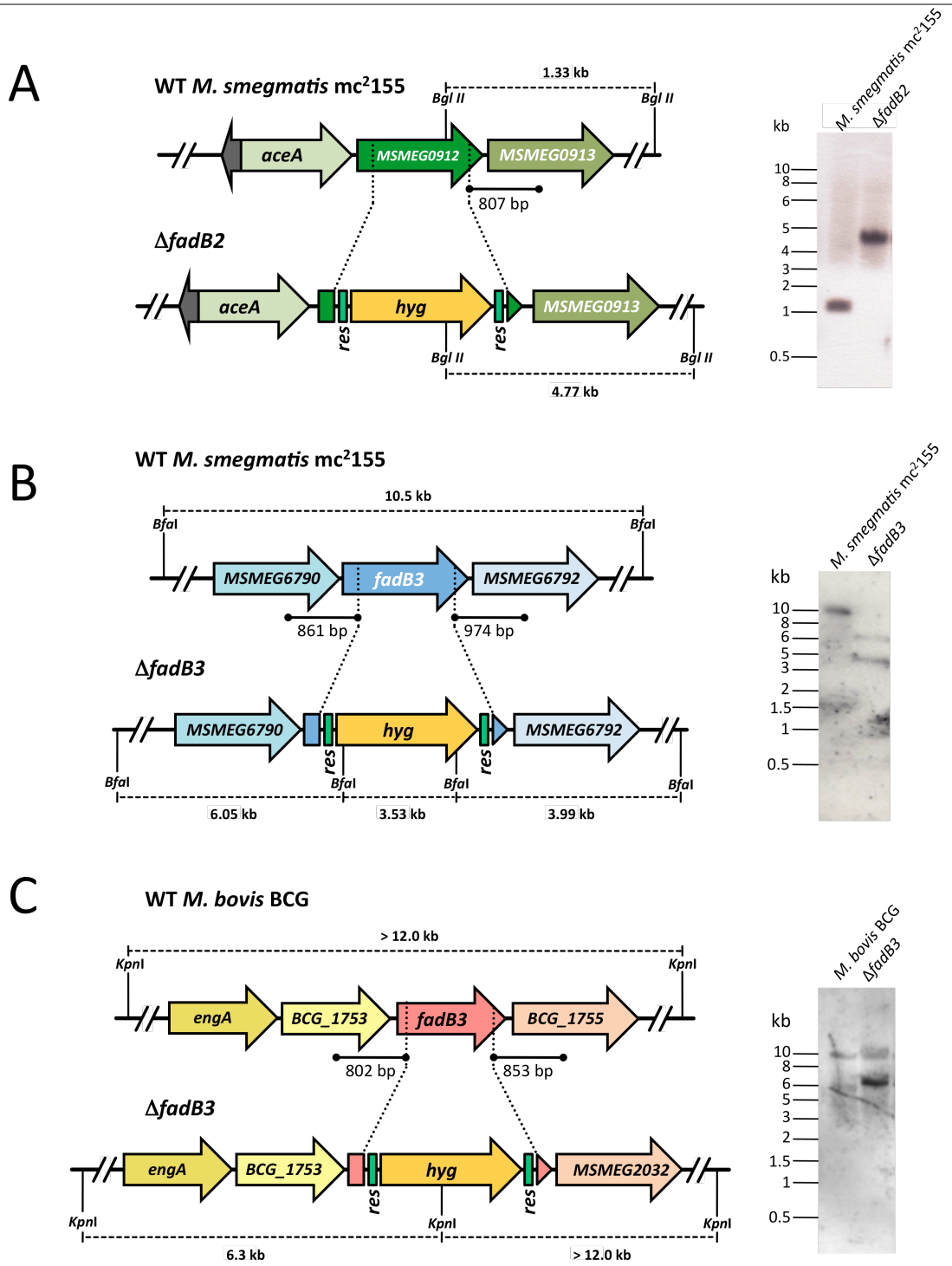

FIGURE 4-13. Generation of the *M. smegmatis fadB2* (*MSMEG0912*), *fadB3* (*MSMEG6791*) and *M. bovis* BCG *fadB3* (*Mb1742-1743*) knock-out mutants. *Left-hand panels* map the regions of the genes of interest in the *M. smegmatis* or *M. bovis* BCG genome and the corresponding regions in the mutant. *Right-hand panels* show Southern blot analyses of the PCR products obtained from genomic DNA isolated from wild-type *M. smegmatis* mc^{2}155 or mutant strains. (**A**) *M. smegmatis* Δ*fadB2*, (**B**) *M. smegmatis* Δ*fadB3* and (**C**) *M. bovis* BCG Δ*fadB3*. Regions where the right-hand PCR primer probe binds to the gDNA fragments are indicated by *solid lines* and expected sizes of the hybridised bands are indicated with *dashed lines*. *Hyg*, hygromycin resistance gene from *S. hygroscopicus*.

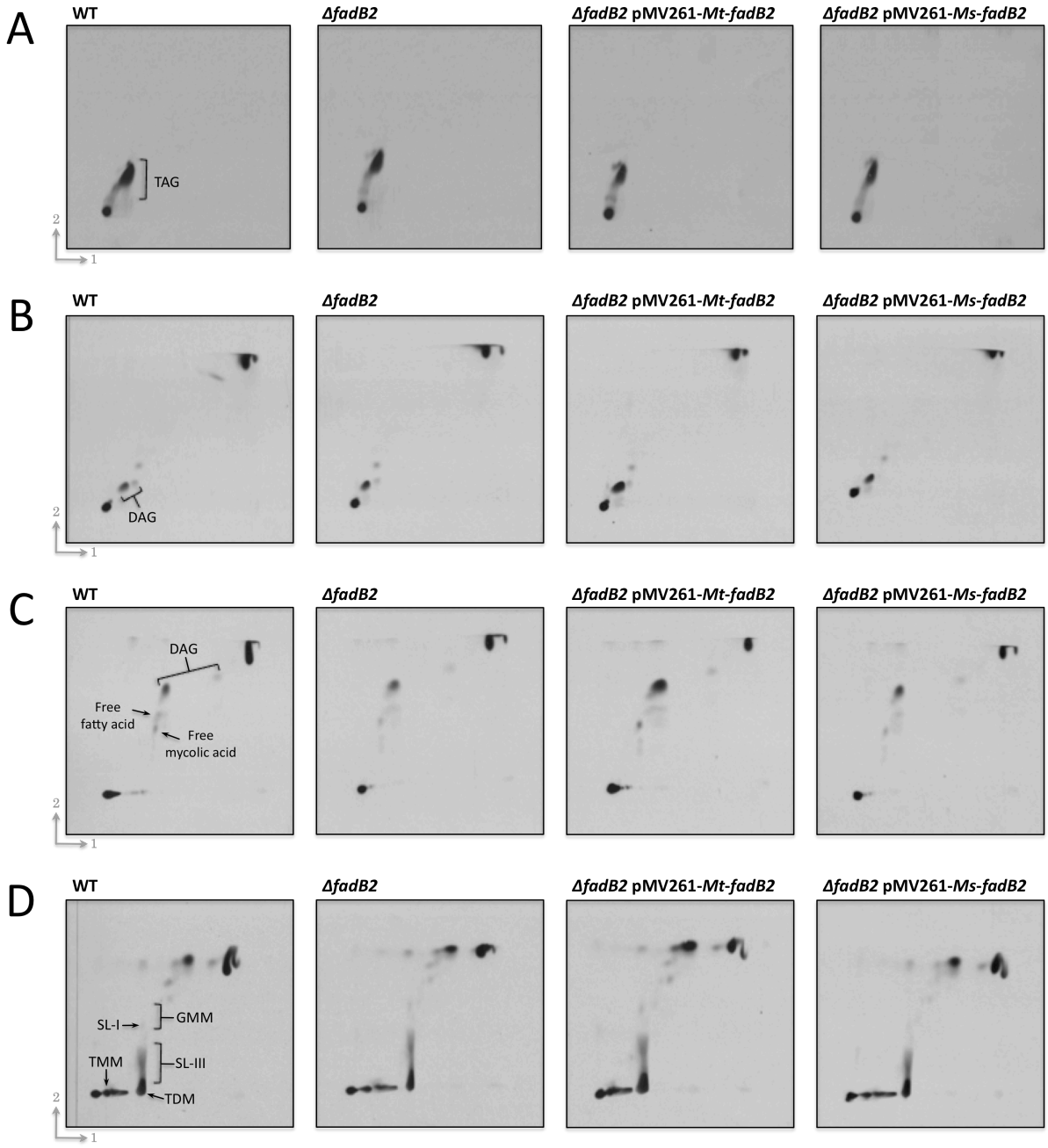

FIGURE 4-14. TLC autoradiography of [^{14}C]-labelled apolar lipid extracts from *M. smegmatis* Δ*fadB2* and complementing strains. Legend over page.

FIGURE 4-14. TLC autoradiography of [^{14}C]-labelled apolar lipid extracts from *M. smegmatis* Δ*fadB2* and complementing strains. Apolar lipids were extracted twice with 1 ml petroleum ether (60–80 °C) for 15 min. Extracts were pooled, dried and resuspended in 200 µl dichloromethane prior to TLC. Plates were developed using the following systems: (**A**) *direction 1*, petroleum ether / ethyl acetate (98 : 2, v/v) and *direction 2*, petroleum ether / acetone (98 : 2, v/v), (**B**) *direction 1*, petroleum ether / acetone (92 : 8, v/v) and *direction 2*, toluene / acetone (95 : 5, v/v), (**C**) *direction 1*, choroform / methanol (96 : 4, v/v) and *direction 2*, toluene / acetone (80 : 20, v/v), (**D**) *direction 1*, choroform / methanol / water (100 : 14 : 0.8, v/v/v) and *direction 2*, chloroform / acetone / methanol / water (50 : 60 : 2.5 : 3, v/v/v/v). Lipids were visualised by autoradiography (overnight exposure of Kodak X-Omat AR film to the TLC plates). *TAG*, triacyl glycerol; *DAG*, diacyl glycerol; *GMM*, glucose monomycolate; *SL*, sulfolipid; *TMM*, trehalose monomycolate, *TDM*, trehalose dimycolate.

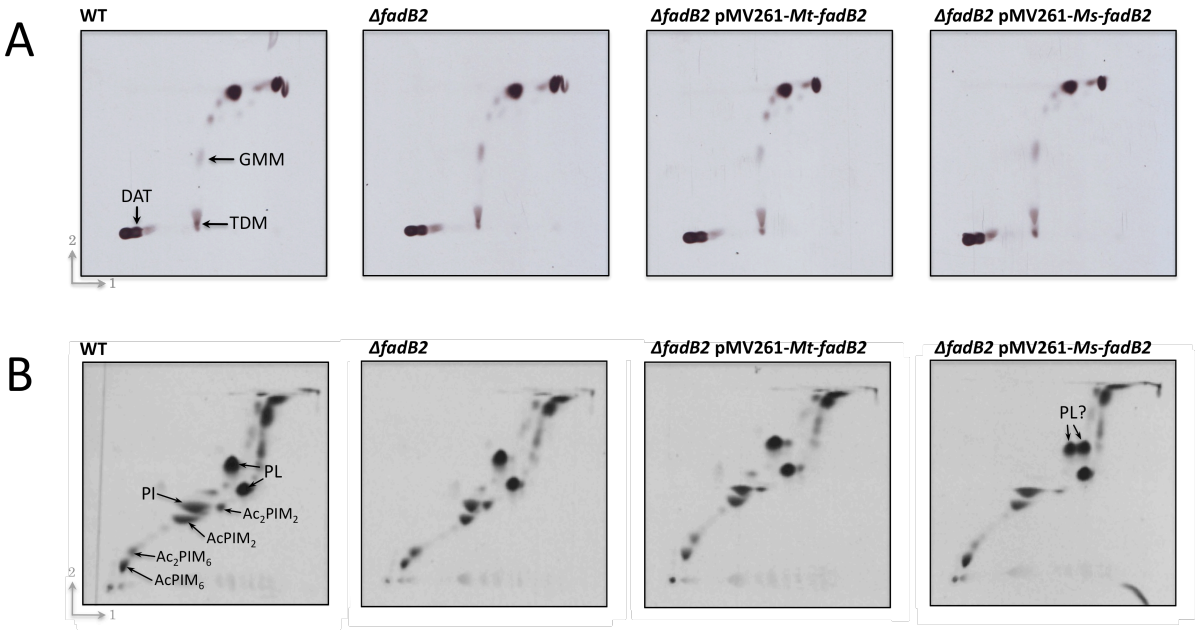

FIGURE 4-15. TLC autoradiography of [^{14}C]-labelled polar lipid extracts from *M. smegmatis* Δ*fadB2* and complementing strains. Polar lipids were extracted twice with 750 µl chloroform / methanol / 0.3 % NaCl (5 : 10 : 4, v/v/v) for 30 min, then again with 1.3 ml chloroform and 1.3 ml 0.3 % NaCl. Extracts were pooled, dried and resuspended in 200 µl chloroform / methanol (2 : 1, v/v) prior to TLC. Plates were developed using the following systems: (**A**) *direction 1*, chloroform / methanol / water (100 : 14 : 0.8, v/v/v) and *direction 2*, chloroform / acetone / methanol / water (50 : 60 : 2.5 : 3, v/v/v/v), (**B**) *direction 1*, chloroform / methanol / water (60 : 30 : 6, v/v/v) and *direction 2*, chloroform / acetic acid / methanol / water (40 : 25 : 3 : 6, v/v/v/v). *DAT*, diacyl trehalose; *GMM*, glucose monomycolate; *TDM*, trehalose dimycolate; *PL*, phospholipid; *PI*, phosphatidylinositol; Ac_xPIM_x, acylacted PIM(s).

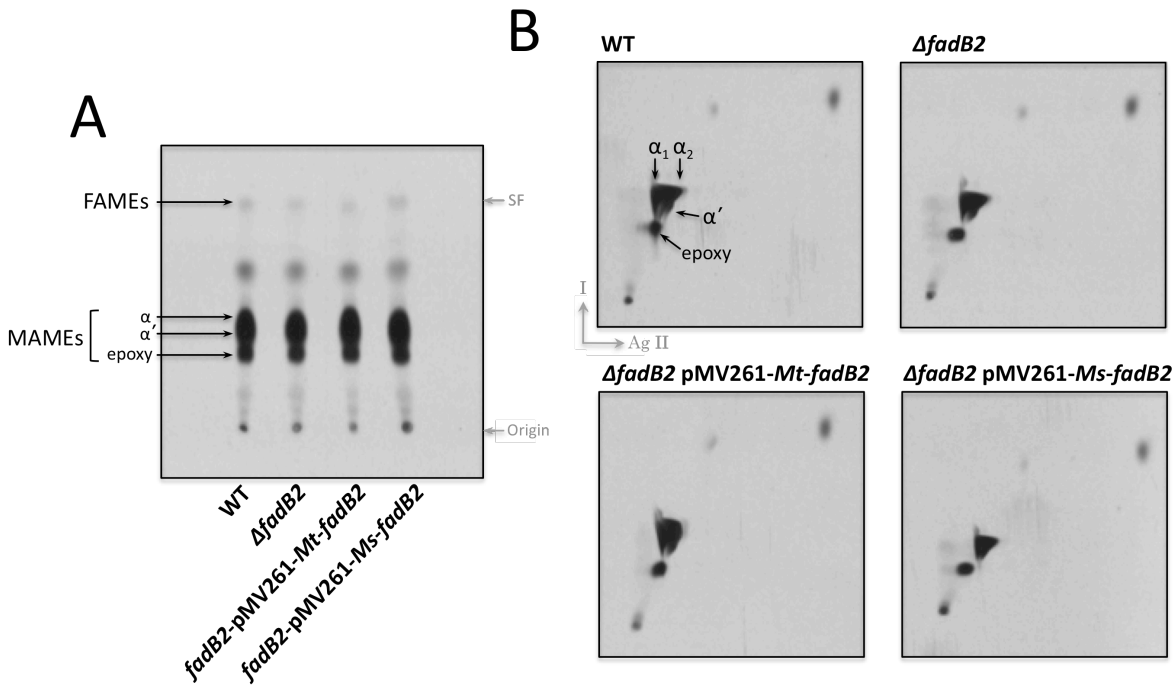

FIGURE 4-16. TLC autoradiography of [^{14}C]-labelled fatty acid methyl esters (FAMEs) and mycolic acid methyl esters (MAMEs) from *M. smegmatis* Δ*fadB2* and complementing strains. Cell wall-bound FAMEs and MAMEs were extracted from delipidated cells with TBAH, iodomethane and dichloromethane and washed three times with 2 ml deionised water. Extracts were pooled, dried and resuspended in 200 µl dichloromethane prior to TLC. Plates were developed using the following systems: (**A**) petroleum ether / acetone (95 : 5, v/v), (**B**) 2D aqueous silver nitrate (10 % w/v) *direction 1*, hexane / ethyl acetate (19 : 1, v/v) and *direction 2*, petroleum ether / diethyl ether (17 : 1, v/v). *SF*, solvent front; *FAMEs*, fatty acid methyl esters; *MAMEs*, mycolic acid methyl esters.

Growth of the Δ*Ms-fadB2* mutant on minimal medium containing a variety of carbon sources was compared to that of the wild-type and complemented strains. There was no difference in growth observed between any of the strains when grown on agar media containing glycerol, glucose, acetate, propionate, caprylic acid, capric acid, lauric acid, myristic acid, palmitic acid, oleic acid or linoleic acid as the sole carbon source (data not shown). Following the recent report on a mycobacterial FadA enzyme, which acts as a thiolase in cholesterol metabolism (Nesbitt *et al*. 2010), the growth of the *Ms-fadB2* deletion mutant on minimal medium containing cholesterol as the sole carbon source was also tested. However, in this

case too, no differences were observed in the growth of the wild-type and mutant strains (Figure 4-17).

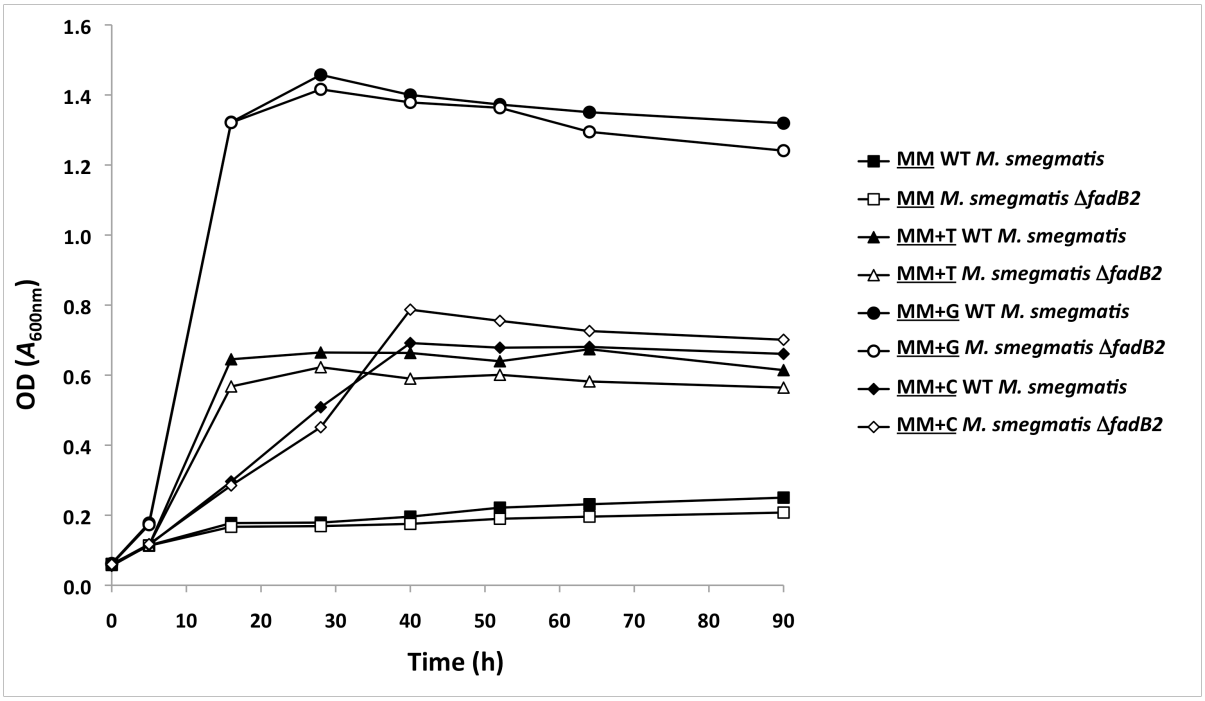

FIGURE 4-17. *M. smegmatis* Δ*fadB2* mutant growth analysis in cholesterol. Growth curves of *M. smegmatis* wild-type, Δ*fadB2*, and the *Mt-* and *Ms-fadB2* complemented strains in minimal medium (MM) with 0.2 % glycerol (MM+G), 0.1 % tyloxapol : ethanol (1 : 1 v/v) or 0.2 mM cholesterol (MM+C).

Previously, it has been shown that *Mt-fadB2* is up-regulated upon acid shock and SDS stress (Fisher *et al.* 2002, Manganelli *et al.* 2001). To test whether FadB2 conferred tolerance to these stresses, the Δ*Ms-fadB2* mutant was grown in media of various pH values or containing different concentrations of SDS. The findings, however, indicate that the deletion had no effect on cell growth rate and survival at physiological pH, acidic pH or under SDS stress (Figure 4-18).

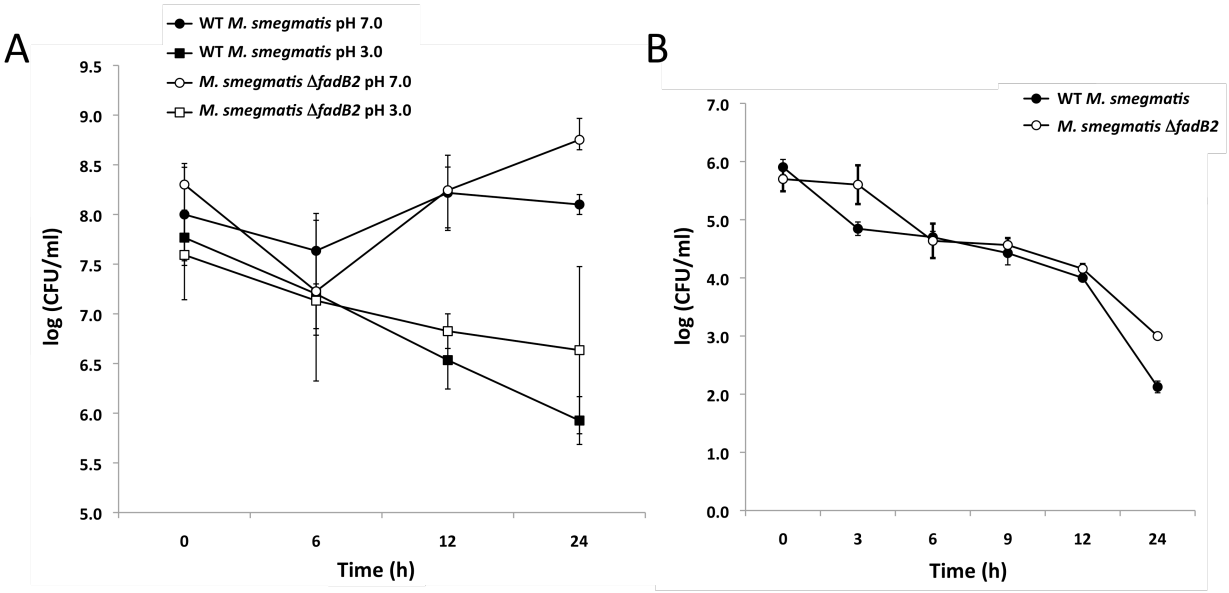

FIGURE 4-18. *M. smegmatis* Δ*fadB2* mutant growth analysis in acid and SDS. (**A**) Acid stress killing curve. (**B**) SDS stress killing curve. Cultures were grown to an OD_{600} of 0.4, washed and resuspended in 7H9 medium at pH 7 or pH 3 or containing 0.05 % SDS. Samples were taken over 24 h and viable counts were calculated as described in section 4.2.12.3. Bars represent the average of three replicates ± standard error.

The Bauer-Kirby disc diffusion method was also used to test how the *M. smegmatis* mutants responded to oxidative (30 % H_2O_2) and SDS (10 %) stress (Bauer *et al*. 1966). The zones of inhibition around the filter paper discs were measured and compared between the strains. Similarly, however, no statistically significant differences were observed between wild-type *M. smegmatis* and the Δ*Ms-fadB2* or Δ*Ms-fadB3* mutants (Figure 4-19).

The growth of the Δ*Ms-fadB2* and Δ*Ms-fadB3* mutants on isoniazid was also tested, by diluting increasing concentrations of the drug in TSB agar. Isoniazid blocks the FAS-II biosynthetic pathway, thus creating an excess of fatty acids. Without either FadB2 or FadB3, it is reasonable to suggest that the surplus lipids cannot be metabolised and therefore potentially have a toxic effect on top of that produced by the drug. This did not appear to be the case, however, with results showing that both the mutant strains and the wild-type behaved in the same way under this stress (Figure 4-19 C).

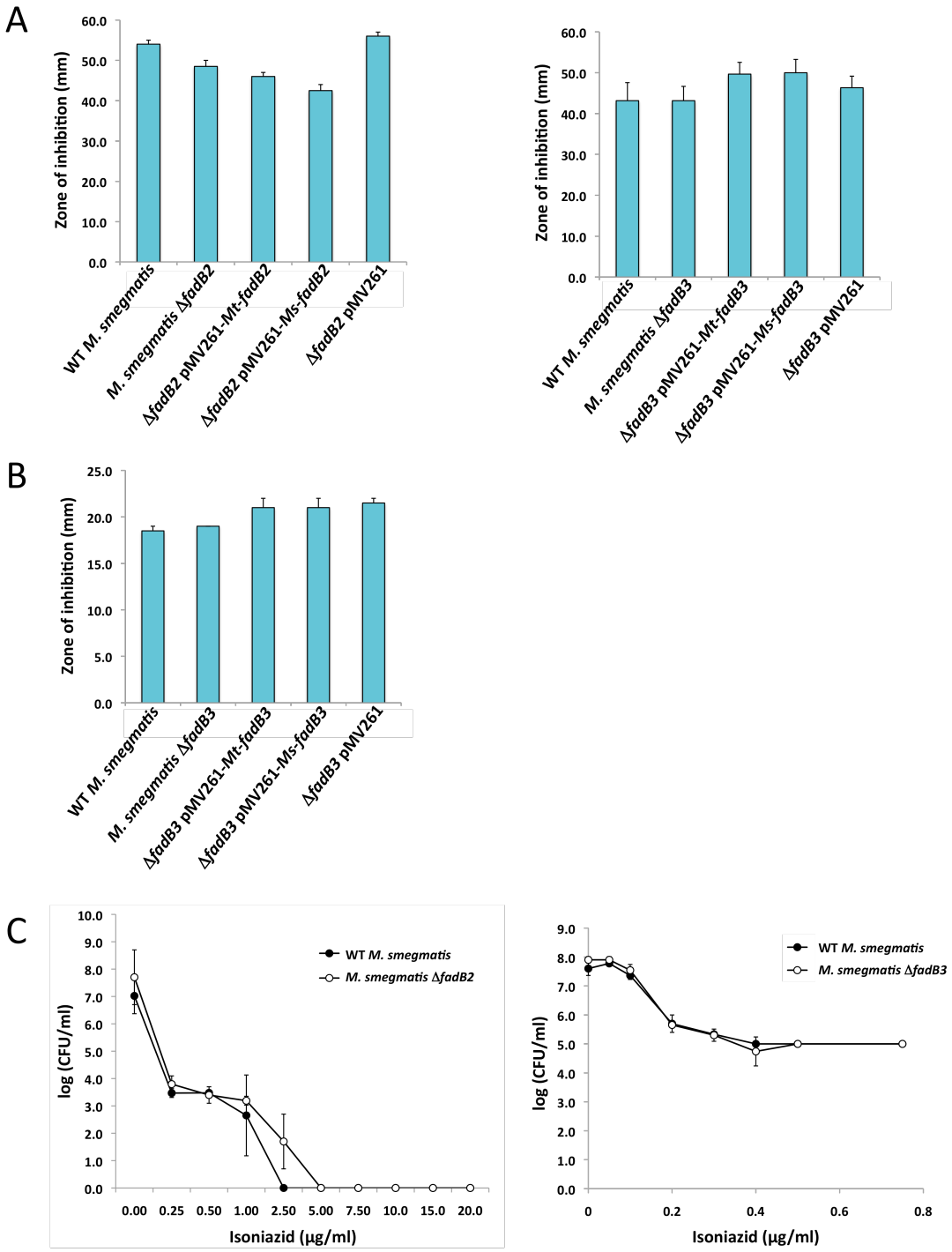

FIGURE 4-19. Toleration of *M. smegmatis* Δ*fadB2* and Δ*fadB3* mutants to stresses. (**A**) 30 % H_2O_2 (Δ*Ms-fadB2, left panel;* Δ*Ms-fadB3*, *right panel*) and (**B**) 10 % SDS. Sterile filter paper discs saturated with 6 µl of 30 % H_2O_2 or 10 % SDS were applied to the overlaid plates and incubated at 37 °C for 3 days. The diameters of the zones of inhibition surrounding the discs were then measured. Bars represent means of three replicates ± standard error. (**C**) Isoniazid. TSB agar plates supplemented with isoniazid (0–20 µg/ml or 0–0.8 µg/ml) were spotted with 10 µl of each mutant (Δ*Ms-fadB2, left panel;* Δ*Ms-fadB3*, *right panel*) and wild-type (WT) culture, serially diluted to 10^{-7}, in duplicate. After incubation at 37 °C for 3–4 days, the colonies were counted and converted to log(CFU/ml). Points represent the means of duplicates ± standard error.

4.3.8. *In silico* analysis of *Mt*-FadB4 and *Mt*-FadB5.

The *in silico* data, generated using the GOR IV and TMHMM protein secondary structure prediction servers (Garnier *et al*. 1996), indicate that both *Mt*-FadB4 and *Mt*-FadB5 are soluble proteins, with no evidence for any transmembrane-spanning helices. The lack of cysteine residues in both FadB4 and FadB5, and therefore no iron-sulfur cluster [4Fe-4S]-binding motifs (C-X-X-C-X-X-C), suggest that neither protein is an NDH-1 ion pump (Yagi *et al*. 2004). One study by Maruyama *et al*. (2003) identified two NQOs in *Staphylococcus aureus*, SA_1989 and SA_1988. SA_1989 contains an NAD(P)H-binding motif (A-X-X-G-X-X-G), whereas the second downstream gene, *SA_1988*, encodes a protein with an alcohol dehydrogenase-type NAD(P)H-binding motif (G-X-G-X-X-G), as found in horse liver alcohol dehydrogenase. A similar finding was made in *Streptococcus gordonii*, where Qor1 (SGO_1169) has the nuclotide-binding site and Qor2 (SGO_1170) has the alcohol dehydrogenase-type NAD(P)H-binding motif. Upon alignment of this section of both of these enzymes with the homologous portions from *E. coli* QorA, *A. thaliana* P1-zeta-crystallin, horse liver alcohol dehydrogenase, FadB4 and FadB5, it becomes apparent that all enzymes share the same conserved motifs (Figure 4-20). Both FadB4 and FadB5 have the same NAD(P)H-binding motifs, A-X-X-G-X-X-G, which is highly conserved across different quinone oxidoreductases in bacteria, plants and mammals.

4.3.9. Over-expression and purification of *Mt*-FadB4.

Initial expression studies in *E. coli* C43 (DE3) cells harbouring the pET28a-*Mt-fadB4* plasmid showed a very small amount of soluble protein when induced with 1 mM IPTG. A one-step purification protocol with increasing concentrations of imidazole failed to remove many contaminants and very little FadB4 protein remained. Over-expression was improved greatly by the use of *E. coli* Tuner™ cells, however the majority of the protein was insoluble. Purification was attempted with the addition of 0.1 % Triton-X 100 in the elution buffers, the

rationale for this being that the detergent would break down any inclusion bodies trapping the protein. More FadB4 protein was obtained but was found to degrade during the second step of purification with an anion exchange QHP column (GE Healthcare).

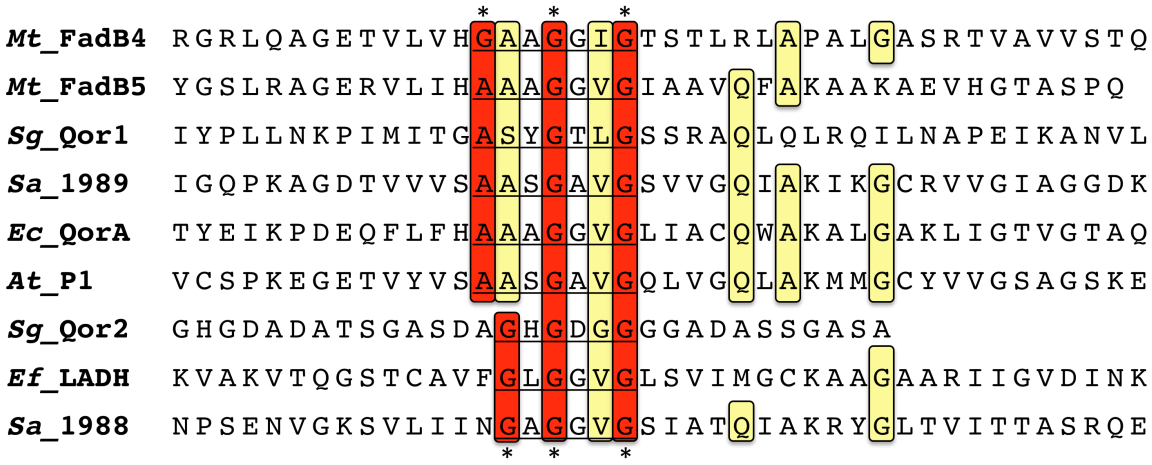

FIGURE 4-20. Sequence alignments. Multiple sequence alignment of NAD(P)H-binding motifs for Qor proteins. The amino acid sequences of *M. tuberculosis* FadB4 residues 132–174 (*Mt*_FadB4) and FadB5 residues 135–176 (*Mt*_FadB5) are compared with *Streptococcus gordonii* Qor1 96–138 (*Sg*_Qor1), *S. gordonii* Qor2 386–415 (*Sg*_Qor2), *Staphylococcus aureus* SA_1988 143–184 (*Sa*_1988), *S. aureus* SA_1989 139–180 (*Sa*_1989), *Escherichia coli* QorA 137–179 (*Ec*_QorA), *Arabidopsis thaliana* P1-ζ-crystallin 150–192 (*At*_P1) and horse liver alcohol dehydrogenase 186–228 (*Ef*_LADH). *Asterisks* indicate the NAD(P)H-binding motifs, *red boxes* indicate highly conserved residues and *yellow boxes* indicate conserved residues. Based on Maruyama *et al*. (2003).

The use of chaperones to improve soluble recombinant protein yield is well documented (de Marco *et al*. 2007, 2011a, 2011b, Gupta *et al*. 2006). Protein over-expression in *E. coli* cells often leads to mis-folding and aggregation, which can be due to a lack of endogenous chaperones or inadequate folding machinery in the cell. In certain cases if the recombinant protein is too alien to *E. coli* this species cannot be used, and a different over-expression species is chosen. Trigger factor, DnaK and the GroEL/ES systems are examples of enzymes used by *E. coli* to help fold newly synthesised proteins, re-fold those that have become denatured due to intrinsic instability or heat and solubilise aggregated proteins (de Marco *et al*. 2007). Therefore, *E. coli* BL21 (DE3) cells containing machinery for the expression of

GroES and CPN 60.2 chaperones were then used. Subsequently, soluble protein was produced that did not degrade during anion exchange chromatography and an estimated 0.7 mg of *Mt*-FadB4 could be obtained from 1 l of culture using this method (Figure 4-21).

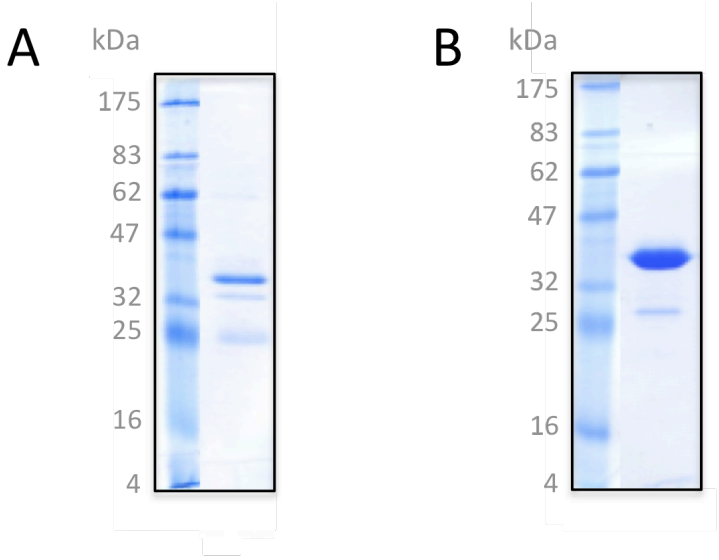

FIGURE 4-21. Purification of *Mt*-FadB4. The protein was produced by IPTG-induction of *E. coli* BL21 (DE3) transformants containing pET28a-*Mt-fadB4*. Following cell growth at 37 °C and after induction at 16 °C, the protein was purified using a 1 ml Ni^{2+}-charged His-trap column and eluted with an increasing imidazole concentration (**A**). After dialysis, the protein was further purified using a QHP anion exchange column (**B**). In both cases, fractions were visualised by Coomassie Blue staining after separation by electrophoresis on 12 % SDS-PAGE.

4.3.10. Growth analysis of the *Ms-fadB4* deletion mutant.

The *Ms-fadB4* (*MSMEG2033*) knock-out was generated using specialised transduction (Bardarov *et al.* 2002) and confirmed by Southern blot (Figure 4-22). This confirmed that the gene is not essential in *M. smegmatis*, as suggested by Himar1-based transposon mutagenesis reported for *M. tuberculosis* (Sassetti *et al.* 2003).

There were no obvious differences observed either in colony morphology or lipid profiles between the mutant and wild-type *M. smegmatis* strain mc^2155 (Figures 4-23, 4-24 and 4-25).

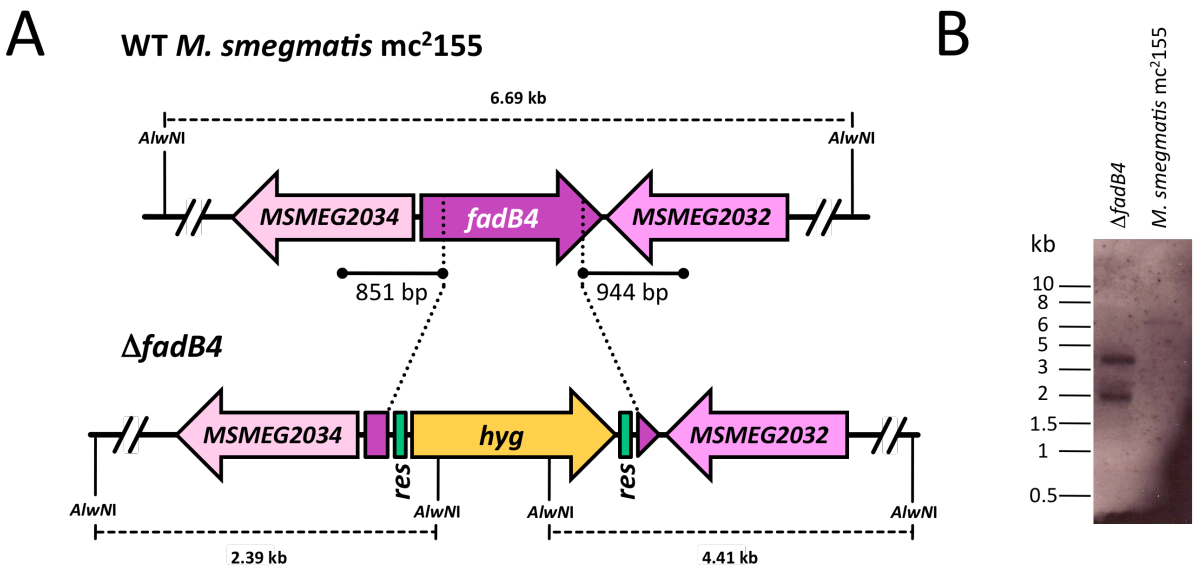

FIGURE 4-22. Generation of the *M. smegmatis fadB4* (*MSMEG2033*) knock-out mutant. (**A**) Map of the *fadB4* region in the *M. smegmatis* genome and its corresponding region in the mutant Δ*fadB4*. *Hyg*, hygromycin resistance gene from *S. hygroscopicus*. (**B**) Southern blot analysis of the PCR products obtained from genomic DNA isolated from wild-type *M. smegmatis* mc²155 or Δ*fadB4*. Regions where the right-hand PCR primer probe binds to the gDNA fragments are indicated by *solid lines* and expected sizes of the hybridised bands are indicated with *dashed lines*.

Growth of the Δ*Ms-fadB4* mutant on minimal medium containing a variety of carbon sources was compared to that of the wild-type and complemented strains. There was no difference in growth observed between any of the strains when grown on agar media containing glycerol, glucose, acetate, propionate, caprylic acid, capric acid, lauric acid, myristic acid, palmitic acid, oleic acid or linoleic acid as the sole carbon source (data not shown). The Bauer-Kirby disc diffusion experiment was used to investigate any altered sensitivity of the mutant to oxidative and SDS stress (Bauer *et al*. 1966). Results revealed that there was no difference between wild-type *M. smegmatis* and the Δ*Ms-fadB4* strain (Figure 4-26 A, B).

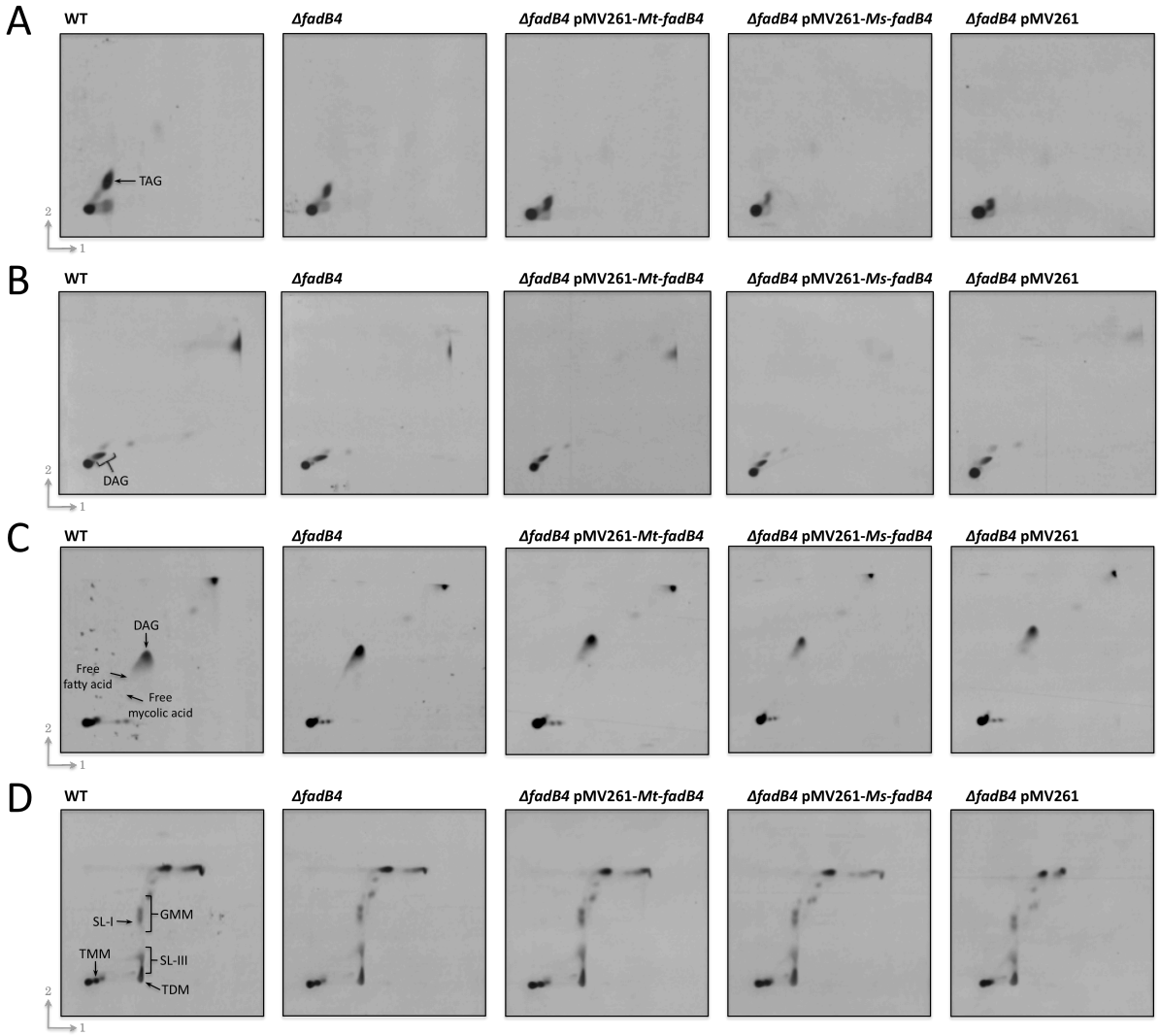

FIGURE 4-23. TLC autoradiography of [^{14}C]-labelled apolar lipid extracts from *M. smegmatis* Δ*fadB4* and complementing strains. Apolar lipids were extracted twice with 1 ml petroleum ether (60–80 °C) for 15 min. Extracts were pooled, dried and resuspended in 200 µl dichloromethane prior to TLC. Plates were developed using the following systems: (**A**) *direction 1*, petroleum ether / ethyl acetate (98 : 2, v/v) and *direction 2*, petroleum ether / acetone (98 : 2, v/v), (**B**) *direction 1*, petroleum ether / acetone (92 : 8, v/v) and *direction 2*, toluene / acetone (95 : 5, v/v), (**C**) *direction 1*, choroform / methanol (96 : 4, v/v) and *direction 2*, toluene / acetone (80 : 20, v/v), (**D**) *direction 1*, choroform / methanol / water (100 : 14 : 0.8, v/v/v) and *direction 2*, chloroform / acetone / methanol / water (50 : 60 : 2.5 : 3, v/v/v/v). Lipids were visualised by autoradiography (overnight exposure of Kodak X-Omat AR film to the TLC plates). *TAG*, triacyl glycerol; *DAG*, diacyl glycerol; *GMM*, glucose monomycolate; *SL*, sulfolipid; *TMM*, trehalose monomycolate, *TDM*, trehalose dimycolate.

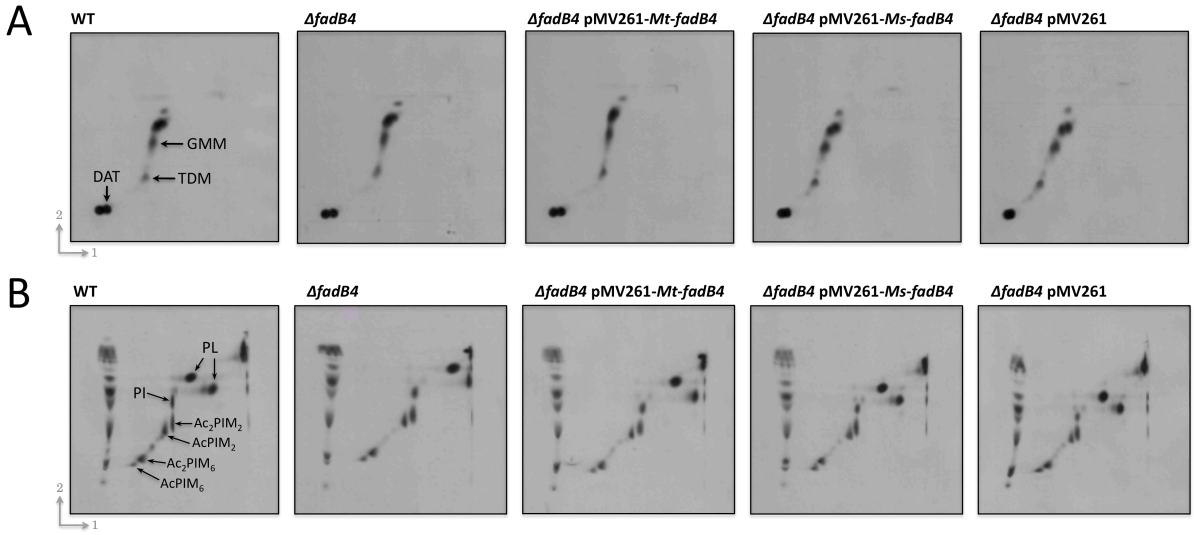

FIGURE 4-24. TLC autoradiography of [^{14}C]-labelled polar lipid extracts from *M. smegmatis* Δ*fadB4* and complementing strains. Polar lipids were extracted twice with 750 µl chloroform / methanol / 0.3 % NaCl (5 : 10 : 4, v/v/v) for 30 min, then again with 1.3 ml chloroform and 1.3 ml 0.3 % NaCl. Extracts were pooled, dried and resuspended in 200 µl chloroform / methanol (2:1, v/v) prior to TLC. Plates were developed using the following systems: (**A**) *direction 1*, chloroform / methanol / water (100 : 14 : 0.8, v/v/v) and *direction 2*, chloroform / acetone / methanol / water (50 : 60 : 2.5 : 3, v/v/v/v), (**B**) *direction 1*, chloroform / methanol / water (60 : 30 : 6, v/v/v) and *direction 2*, chloroform / acetic acid / methanol / water (40 : 25 : 3 : 6, v/v/v/v). *DAT*, diacyl trehalose; *GMM*, glucose monomycolate; *TDM*, trehalose dimycolate; *PL*, phospholipid; *PI*, phosphatidylinositol; Ac_xPIM_x, acylacted PIM(s).

A report by Prüß *et al*. (1994) showed how *E. coli* cells that are devoid of either of the two NQO genes are less able to metabolise the amino acids glutamate, glycine, threonine and alanine. In order to test if this is also the case for *M. smegmatis* lacking the putative NQO *fadB4*, cells were plated on minimal medium agar containing the amino acids (20 µg/ml and 100 µg/ml) alanine, asparagine, lysine, leucine, valine and threonine. No difference was observed, however, between the growth of the strains on glucose and on agar containing the amino acids (Figure 4-26 C).

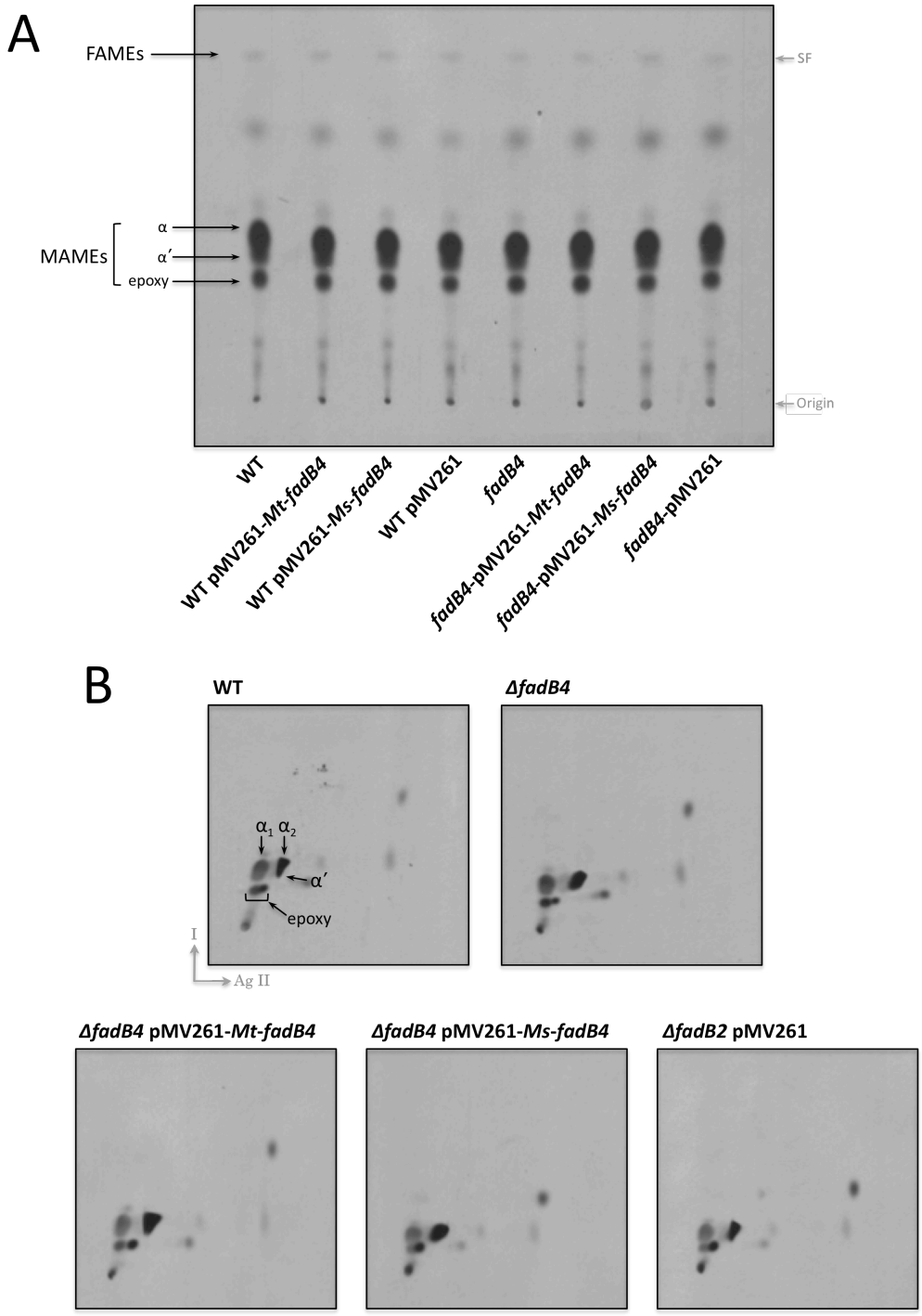

FIGURE 4-25. TLC autoradiography of [^{14}C]-labelled fatty acid methyl esters (FAMEs) and mycolic acid methyl esters (MAMEs) from *M. smegmatis* Δ*fadB4* and complementing strains. Cell wall-bound FAMEs and MAMEs were extracted from delipidated cells with TBAH, iodomethane and dichloromethane and washed three times with 2 ml deionised water. Extracts were pooled, dried and resuspended in 200 µl dichloromethane prior to TLC. Plates were developed using the following systems: (**A**) petroleum ether / acetone (95 : 5, v/v), (**B**) 2D aqueous silver nitrate (10 % w/v) *direction 1*, hexane / ethyl acetate (19 : 1, v/v) and *direction 2*, petroleum ether / diethyl ether (17 : 1, v/v). *SF*, solvent front; *FAMEs*, fatty acid methyl esters; *MAMEs*, mycolic acid methyl esters.

4.3.11. Construction of the *Mb-fadB5* deletion mutant.

As with the other deletion mutants, Δ*Mb-fadB5* (*Mb1947c*) was generated using specialised transduction (Bardarov *et al*. 2002) and the knock-out was confirmed by Southern blot (Figure 4-27). The successful deletion of the gene shows that *fadB5* is not required for cell growth or survival *in vitro*, as predicted by Sassetti and co-workers (2003).

4.4. Discussion

The work described here provides a detailed study of *Mt*-FadB2 and preliminary insights into three of the other mycobacterial *fadB* genes, *fadB3*, *fadB4* and *fadB5*. Investigation of the mycobacterial fatty acid β-oxidation pathway has been somewhat neglected, perhaps due to the assumed redundancy between the abundant *fad*-annotated genes. There is, however, an immense need to find new drug targets within *M. tuberculosis* in order to halt the spread of disease. By exploring novel genes, it is possible to isolate those essential to the bacillus, thus highlighting a potentially different pathway or system that can be inhibited by new drugs.

Here, evidence for the function of *Mt*-FadB2 (Rv0468) in converting both β-hydroxyacyl-CoA to acetoacetyl-CoA and acetoacetyl-CoA to β-hydroxyacyl-CoA has been provided. The NADH-oxidation 'reverse' reaction was found to be optimum at the pH inside the macrophage vacuole (pH 6–7), which could suggest that this reaction is favoured *in vivo* and that the dehydrogenase is utilised by the bacteria to synthesise, or elongate, fatty acids rather than degrade them, although this feature can also be explained by reaction equilibria. It was also shown, by gene deletion, that *Ms*-FadB2 is not essential in *M. smegmatis*. No differences could be found between the wild-type and deletion mutant strain in the lipid profile, although the presence of an extra phospholipid spot in the *Ms-fadB2*-complemented strain is of

potential interest. There were similarly no differences between strains in reaction to cellular stresses.

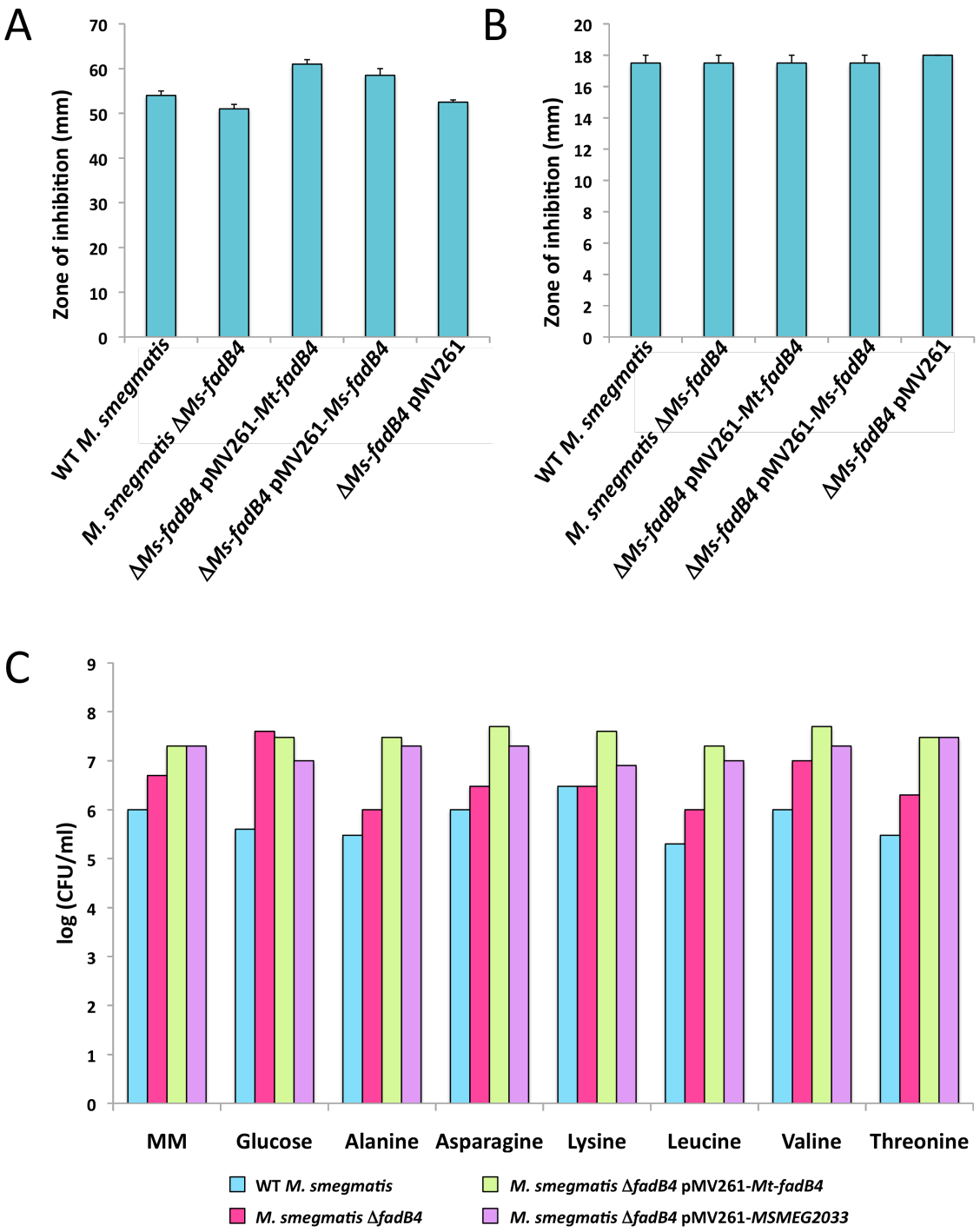

FIGURE 4-26. *M. smegmatis* Δ*fadB4* growth analysis. Survival of mutant cells on (**A**) 30 % H_2O_2 and (**B**) 10 % SDS. Sterile filter paper discs saturated with 6 µl of 30 % H_2O_2 or 10 % SDS were applied to the overlaid plates and incubated at 37 °C for 3 days. The diameters of the zones of inhibition surrounding the discs were then measured. Values are means of three replicates ± standard error. (**C**) The growth of *M. smegmatis* Δ*fadB4* on individual amino acids as the sole carbon source compared with wild-type and complementing strains.

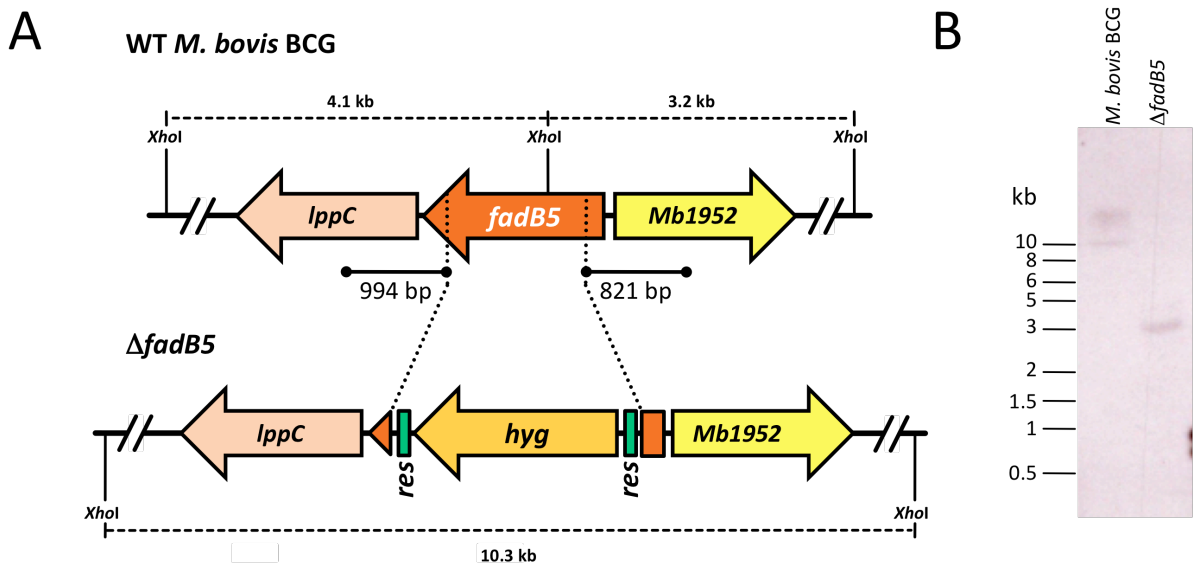

FIGURE 4-27. Generation of the *M. bovis* BCG *fadB5* (*Mb1947c*) knock-out mutant. (**A**) Map of the *fadB5* region in the *M. bovis* BCG genome and its corresponding region in the mutant Δ*fadB5*. *Hyg*, hygromycin resistance gene from *S. hygroscopicus*. (**B**) Southern blot analysis of the PCR products obtained from genomic DNA isolated from wild-type *M. bovis* BCG or Δ*fadB5*. Regions where the right-hand PCR primer probe binds to the gDNA fragments are indicated by *solid lines* and expected sizes of the hybridised bands are indicated with *dashed lines*.

Despite being unable to allocate a function to *Mt*-FadB3, the predicted role is the same as that of *Mt*-FadB2, a β-hydroxyacyl-CoA dehydrogenase. The spectrophotometric assay developed for *Mt*-FadB2 was tested with purified *Mt*-FadB3. The protein was unable to catalyse the NAD^+-dependent reduction of β-hydroxybutyryl-CoA to acetoacetyl-CoA, in the presence or absence of $CaCl_2$ or $MgCl_2$ (the cations found to increase the activity of *Mt*-FadB2), in acidic or basic conditions, nor with $NADP^+$ as the co-factor. The reverse reaction was also tested with the same acetoacetyl-CoA substrate in various conditions, with NADH or NADPH, but *Mt*-FadB3 was also unable to catalyse these reactions (data not shown). It could be hypothesised that *Mt*-FadB2 accepts short-chain molecules, such as β-hydroxybutyryl-CoA, and *Mt*-FadB3 takes longer chain CoAs. To test this, *N*-acetylcysteamine (*N*-AC) molecules that mimic CoA-attached molecules (synthesised by Dr. V. Bhowruth, University of

Birmingham) were tested as a substrate for both *Mt*-FadB2 and *Mt*-FadB3. Neither protein could turn over β-hydroxylauryl-*N*-AC (C_{12}) at physiological pH, nor in alkaline conditions as found to be favoured for the *Mt*-FadB2 β-hydroxybutyryl-CoA reaction, with NAD^+ as the co-factor. The addition of bovine serum albumin (50 μg) to the *Mt*-FadB3 reaction was also examined, to see if stabilising the enzyme would help activity. None of the conditions tested, however, resulted in NAD^+-reduction, indicating that the protein was either not active or it is not able to catalyse the reaction. The role of *Mt*-FadB3 was investigated *in vivo*, also by means of gene deletion, and was similarly found to be non-essential in both *M. smegmatis* and *M. bovis* BCG. This could potentially be of interest, since a previous genome-wide study suggested the gene is essential in *M. tuberculosis* (Sassetti *et al*. 2003). The deletion would have to be performed in this species, however, in order to identify the importance, be it for survival or virulence or not at all.

Mt-FadB4 and *Mt*-FadB5 are annotated as having NADH:quinone oxidoreductase activity. Despite this, and in order to test for functional redundancy, purified *Mt*-FadB4 was substituted into the *Mt*-FadB2 assay, but as predicted no activity was found. The *in silico* analysis of the proteins strongly indicates NQO function, since both have the highly conserved NAD(P)H-binding motifs A-X-X-G-X-X-G found in quinone oxidoreductases of bacteria, plants and mammals.

In this study, a viable *fadB4* gene deletion in *M. smegmatis* was generated, although no differences could be found when compared to the wild-type in the experiments completed. The homologous deletion in *M. tuberculosis* is also viable but was found to be hypervirulent during the initial two weeks of infection (Scandurra *et al*. 2008). The group proposed that this was due to changes in the composition of the *M. tuberculosis* Δ*fadB4* cell wall, whereby the ability to enter and infect macrophages was significantly increased. The *M. smegmatis fadB4*

mutant generated here, however, did not appear to have any alterations to cell wall composition. The antioxidant function of the mutants was also tested, since evidence suggests that NQO enzymes may act as antioxidants (Itoh *et al*. 1997, Shimada 2006, Triccas *et al*. 1999, Tumminia *et al*. 1993). No differences were observed between the mutant, wild-type and complemented strains when challenged with oxidative (H_2O_2) or SDS stress on agar (Bauer *et al*. 1966), although it would be interesting to repeat the experiment in liquid medium and in acidic conditions. It is, however, possible that *Mt*-FadB5 shares the same function, providing a back-up mechanism should FadB4 be lost. Genes important for survival are often duplicated, as found for mycobacterial resuscitation promotion factor (*rpf*) genes (Kana *et al*. 2008).

Under these circumstances, the generation of double or multiple *fadB* knock-out strains in surrogate species, but most valuably in *M. tuberculosis*, would be ideal for studying the roles of these genes in the biology of mycobacteria. This would provide an excellent tool for studying how the mutant(s) interact with the host and a plethora of further information, such as altered virulence, could be obtained.

CHAPTER 5

General Conclusions

With an estimated one third of the world's population infected with tuberculosis, it is imperative that progress is made to halt the spread of disease. The emergence of drug resistant strains of *M. tuberculosis* and the synergistic effects of HIV-1 co-infection has complicated the battle further. Bearing in mind that the majority of cases are found in poorer countries, it is also important to create therapeutics that are cheap to produce and distribute in order to reach those most at need. This project has aimed to address these issues, taking a two-pronged approach to (a) identify novel compounds based on both known chemotherapeutics and new scaffolds inhibiting enzymes previously determined as essential, and (b) characterise formerly unstudied genes and their protein products with the view of isolating new drug targets.

In **chapter 2** the first of these project aims was explored. The objective was inhibition of FAS-II cycle enzymes, *i.e.* those not found in mammals and that are known to be effective targets through the use of known drugs such as isoniazid and ethionamide. Three different groups of novel compounds were tested: platensimycin, thiolactomycin analogues and indole derivatives. Platensimycin is an excellent example of a natural product being discovered as a new scaffold with therapeutic potential. Here, the compound was established as an inhibitor of mycobacterial growth, specifically of *Mt*-KasA and *Mt*-KasB, the β-ketoacyl-AcpM synthase enzymes that repeatedly elongate the meromycolate chain, with *in vitro* IC_{50} values of 2.0 ± 0.1 and 4.2 ± 0.1 μg/ml, respectively. Platensimycin was also found to be active against the whole cell, both slow-growing *M. tuberculosis* CDC1551 and fast-growing *M. smegmatis* mc^2155, with MIC_{99} values of 12 and 14 μg/ml, respectively. Platencin is a congener of platensimycin that has activity against both FabF and FabH of Gram-positive bacteria (homologous to mycobacterial KasB and FabH, respectively) (Wang *et al*. 2007b). Given that platensimycin was found to be not active against *Mt*-FabH, it would be interesting to test platencin against this enzyme. Indeed, since this work, several analogues of both

compounds have been produced either naturally using *Streptomyces platensis* (Zhang *et al*. 2011) or synthesised chemically (Jang *et al*. 2010, Wang & Sintim 2011). Some preliminary work was undertaken at the end of this project, testing three of these latter compounds against mycobacterial FAS-II enzymes *in vitro* in collaboration with J. Wang and Prof. H. Sintim (University of Maryland). Although the structures of these compounds are currently undisclosed and biological testing is just beginning, initial results have revealed some promising IC_{50} values of 144.0–165.5 μg/ml against *Mt*-FabH, 35.5–186.7 μg/ml against *Mt*-KasA and 40.8–172.0 μg/ml against *Mt*-KasB.

The thiolactomycin analogues tested were designed to competitively inhibit the *Mt*-FabH active site. Three were found to be active against the enzyme, two of which showed better IC_{50} values than the parent compound itself: 1.04 ± 0.2 μg/ml (QAB-62) and 1.1 ± 0.1 μg/ml (QAB-62a) compared to 16.0 μg/ml of thiolactomycin (Kim *et al*. 2006). Disappointingly, however, these compounds were also active against *Ms*-FAS-I crude cell extracts, a system also found in mammals, and collaborative work by Dr. Al-Balas (University of Strathclyde) demonstrated that QAB-61 and QAB-62 were not active against *M. tuberculosis in vivo*. Interestingly, four of the compounds did inhibit the whole cell, albeit not through FAS-I/II, with QAB-4a being most potent, showing an MIC_{99} of 0.06 μg/ml (compared to 13.0 μg/ml for thiolactomycin). Having such a low MIC_{99} value, QAB-4a should be examined further and better understood. By acquired QAB-4a resistance experiments and genome sequencing, the target could be discerned and a completely new way of inhibiting *M. tuberculosis* could be identified.

Finally, work looking at derivatives of indole-containing compounds revealed four structures that displayed activity against *Ms*-FAS-II but not FAS-I. The compound showing most potential was WIUAKP-045, with an IC_{50} of 3.64 ± 0.02 μg/ml. It would be interesting to

assay this and the other four compounds against individual FAS-II enzymes in order to identify the precise target(s). Similarly, it would be worthwhile to generate molecules based on WIUAKP-045 to distinguish the active functional groups and potentially increase potency further. Another important additional experiment would be whole cell testing against *M. tuberculosis*. The lipid-rich cell wall often proves to be a highly impervious barrier, and, whilst the compounds may be active against FAS-II *in vitro*, they are generally useless unless they are able to enter the cell.

Overall, chapter 2 has demonstrated that work finding new anti-tubercular chemotherapeutics is very much underway and all three of the structural scaffolds examined hold promise. The undertaking, however, is very challenging, expensive with regard to time and money and the ever-evolving target bacillus ensures resistance to any new drug. For this reason, groups are starting to apply new therapeutic strategies in the fight against TB. One example is the use of synergistic drug combinations. Although combined drug regimens are currently used as part of the DOTS treatment, a new approach uses spectinomycin as a 'sensitiser' (Ramón-García *et al*. 2011). Alone, the antibiotic has little effect on *M. tuberculosis* but can be employed with other antibiotics to increase potency. The advantages are that all the compounds are already approved so therapy could be mobilised quickly, and that this could be an efficient way of treating XDR strains. The disadvantage is that adding another antibiotic to the regimen increases cost. In a similar vein, a recent report identified thiophen-2-yl-1,2,4-oxadiazoles as effective ethionamide boosters by not only increasing activity but also enhancing solubility and metabolic stability (Flipo *et al*. 2011). A second alternative mode of treatment is through augmenting and complementing the host's immune cells *i.e.* directing drugs at macrophages rather than the internalised bacilli (Martins 2011). One particular mechanism is the use of phenothiazines, organic compounds already used in some anti-psychotics and anti-histamines (Booth 2007). Phenothiazines act on both prokaryotic and

eukaryotic efflux pumps, ATPases and genes affecting cell permeability, thereby facilitating the killing by inactivated macrophages of both intracellular MDR and XDR *M. tuberculosis* (Amaral *et al*. 2010, Viveiros *et al*. 2010). As well as targeting XDR strains, by using this strategy the problem of developing drug resistance could be avoided. Betaglycan (transforming growth factor, beta receptor III; TGFβR3) has also been trialled in TB immunotherapy (Hernández-Pando *et al*. 2006). It is known that monocytes infected with *M. tuberculosis* express TGF-βI, which boosts the growth of ingested bacilli and inhibits the bacteristatic effects of TNF-α and IFN-γ (Hirsch *et al*. 1994). A potent TGF-β antagonist, betaglycan, has been shown to rapidly reduce bacillary load from the infected lungs of mice when administered in combination with niflumic acid, a peptidoglycan synthesis inhibitor (Hernández-Pando *et al*. 2006).

Chapter 3 turned attention to the regulation of FAS-II enzymes and the biosynthesis of mycolic acids. Understanding how these enzymes are switched on and off could provide another valuable tool in fighting tuberculosis. Previous reports have shown how InhA, the primary target of the highly successful drug isoniazid, is down-regulated by phosphorylation (Molle *et al*. 2010). The authors noted the importance of discerning how *M. tuberculosis* regulates mycolic acid content with regard to new anti-TB therapies.

Work here looked at the regulation of *Mt*-FabH by phosphorylation and revealed, not only that the enzyme is a substrate for mycobacterial serine/threonine protein kinases, but also is actually inhibited by phosphorylation of Thr-45. PknA and PknF were the most efficient kinases, with less phosphorylation by PknD, PknE and PknH. PknB, PknK and PknL failed to phosphorylate *Mt*-FabH, an interesting finding knowing that PknB phosphorylates the other KAS enzymes in *M. tuberculosis*, KasA and KasB (Molle *et al*. 2006). Using *Mt*-FabH(T45D) as a mimic of constitutive phosphorylation, activity was assessed and compared

to the wild-type enzyme and T45A, T45E, T45S and T45/47A point mutants. The enzyme reaction was broken down into three parts: (i) condensation, (ii) transacylation and (iii) decarboxylation. The 'phosphorylated' version of the enzyme (T45D) displayed reduced activity in all three part-reactions: 42 % of wild-type condensing activity, 62 % of wild-type transacylation activity and 10 % of wild-type decarboxylation activity. Since some activity is seen in all experiments, it may be reasonable to suggest that *Mt*-FabH is modulated by phosphorylation, rather than simply switched on or off.

Using the crystal structure of *Mt*-FabH (Alhamadsheh *et al*. 2007, Brown *et al*. 2005, Musayev *et al*. 2005, Scarsdale *et al*. 2001) and the mechanism of action proposed by Sachdeva *et al*. (2008a, 2008b), it was possible to locate the position of the phosphorylated residue and identify other residues that may be involved, and suggest how phosphorylation is used to tweak activity. Firstly, Thr-45 is close to the AcpM interaction site and, as such, addition of a phosphate group may be enough to prevent docking in the narrow binding channel. Secondly, the residue is ≤6 Å from Arg-46 and Trp-42, both of which are important in the binding of coenzyme A (work by Brown and co-workers (2005) found that mutations of Trp-42 significantly reduce KAS activity). In *Ec*-FabH, Arg-46 is the residue that co-ordinates the pyrophosphate of CoA and Trp-42 stacks on top of the adenine base (Qiu *et al*. 2001). By introducing a negatively charged group to this region, CoA substrate binding is directly hampered. The $[PO_4]^{3-}$ would present an alternative salt bridge to CoA for Arg-46 and may also impede the ability of Trp-42 to stack with the nucleobase.

The work described here provides the first report on regulation of *Mt*-FabH, the critical linker enzyme between FAS-I and FAS-II in mycobacteria. Several further experiments could provide more information, such as at what stage of cell growth FabH is phosphorylated and how the enzyme is phosphorylated under different growth conditions. Khan *et al*. (2010)

generated a conditional *inhA* knockout in *M. smegmatis* and tested whether a constitutively phosphorylated InhA could rescue the deletion. A similar experiment could be done using an *Ms*-FabH knockout to see how FabH phosphorylation affects the whole cell. Additional work could look at how the synthesis of complex lipids and thus virulence are affected by constitutive FabH phosphorylation.

The final section, **Chapter 4**, tackled the second project aim, to characterise new mycobacterial genes and identify potential drug targets. The focus was on the FadB enzymes, those involved in the fatty acid β-oxidation pathway. *M. tuberculosis* is able to survive intracellularly for very long periods of time and the importance of using host lipids to maintain this is well appreciated. There is, therefore, potential to produce new drugs that aim to halt this process, which could kill infecting bacilli essentially by starving them. Detailed research into the Fad enzymes has only taken hold within the last decade or so. Publication of the genome sequence in 1998 has helped the identification of these genes enormously (Cole *et al*. 1998). During this time, attention has mainly focussed on the thirty-six FadD genes, those annotated as fatty acyl-CoA synthetases, which activate fatty acids for metabolism. A wealth of data provides evidence for these genes being involved in a variety of important processes such as mycobactin (FadD33; LaMarca *et al.* 2004), phenolic glycolipid (FadD22; Ferreras *et al*. 2008, Siméone *et al*. 2010), PDIM (FadD26, FadD29 and FadD10; Hotter *et al*. 2005, Siméone *et al*. 2010) and sulfolipid (FadD23; Lynett & Stokes 2007) biosynthesis, mycolate recycling (FadD5; Dunphy *et al*. 2005), sterol metabolism (FadD19; Wilbrink *et al*. 2011), *M. avium* invasion of mucosal epithelial cells (FadD2; Dam *et al*. 2006) and intracellular survival (FadD13; Khare *et al*. 2009, Singh *et al*. 2005, and FadD33; Rindi *et al*. 2002, 2004). This shows how annotations made purely from the genome sequence and locations within the genome can be misleading. In contrast to FadD, of the five *Mt-fadA* genes only *fadA5* has so far been characterised (Nesbitt *et al*. 2010). Similarly, there is one

paper reporting on the affects of deleting *fadB4* in *M. tuberculosis* (Scandurra *et al*. 2008) and a very recent publication confirming the non-essentiality of *Mt*-FadB3 (Williams *et al*. 2011).

The gene explored in the most detail here was *fadB2*. Through the expression and purification of recombinant *Mt*-FadB2 the function of the enzyme was confirmed as a β-hydroxybutyryl-CoA dehydrogenase, which uses NAD^+ as the co-factor. Two reports from the 1970s describe a protein fraction from *M. smegmatis* containing a β-hydroxybutyryl-CoA dehydrogenase as being involved in fatty acid elongation, rather than β-oxidation (Shimakata *et al*. 1977, 1979). Although it is not known whether this group had isolated *Ms*-FadB2, the 'reverse' reaction was also tested here, *i.e.* whether *Mt*-FadB2 would convert acetoacetyl-CoA to β-hydroxybutyryl-CoA. Interestingly, not only did the enzyme catalyse the reaction, consistent with the reversible nature of mammalian mitochondrial β-hydroxybutyryl-CoA dehydrogenase, but it was also found that the pH-dependent activity was the same as that found over thirty years ago (Shimakata *et al*. 1979): the NAD^+ reaction was optimal at pH 10 and the NADH reaction optimal at pH 6. This is noteworthy knowing the acidic conditions bacilli are exposed to in macrophages. Perhaps, *in vivo*, the enzyme uses its dual functionality when the cell adapts and switches from lipid metabolism to biosynthesis. Despite being annotated as non-essential (Sassetti *et al*. 2003), it would be interesting to delete *fadB2* from the *M. tuberculosis* genome and monitor cell growth and survival in different conditions and within macrophages, especially since *Mt*-FadB2 is up-regulated in macrophage and mouse infection models (Manganelli *et al*. 2001, Schnappinger *et al*. 2003, Talaat *et al*. 2004), as well as in low pH and acid shock conditions (Fisher *et al*. 2002). Some progress was made in investigating this by generating an *M. smegmatis* Δ*fadB2* mutant. The cells were viable, confirming non-essentiality of the gene in this species, and no differences could be observed

between the knock-out and wild-type strains when treated with SDS, acid stress or isoniazid, nor were there any changes in lipid profile.

Mycobacterial FadB3 is predicted to have the same function as FadB2. This hypothesis was tested with purified *Mt*-FadB3 but it was found that the enzyme was unable to turn over either β-hydroxybutyryl-CoA or acetoacetyl-CoA. In an effort to probe this further, longer hydroxyacyl-CoA mimics were synthesised, with an *N*-acetylcysteamine group (*N*-AC) replacing the CoA. The paper by Shimakata *et al*. (1979) showed how their enzyme would accept this substrate as well as an alternative artificial thioester, acetoacetyl-pantetheine, albeit with higher K_M and lower V_{max} values. Neither *Mt*-FadB2 nor *Mt*-FadB3, however, showed any activity with C_{12}-*N*-AC, although in the case of recombinant FadB3 the purified protein might not have been active. Further experiments could be done to look into this, such as removing the His_6-tag to see if it was obstructing the active site, and using CD analysis to ensure the protein was correctly folded. By way of investigating the role of FadB3 *in vivo*, Δ*fadB3* mutants in both *M. smegmatis* and *M. bovis* BCG were generated. Both knock-outs were viable despite being one of only two *fad* genes annotated as being essential for *in vitro* growth in *M. tuberculosis* (Lamichhane *et al*. 2003, Sassetti *et al*. 2003). A recent report has further corroborated this finding, by producing a viable *fadB3* deletion mutant in *M. tuberculosis* (Williams *et al*. 2011). The group could find no altered phenotype in the mutant strain with regard to growth on different carbon sources, a similar finding to the research here, nor with respect to growth and survival in the mouse model of infection.

Preliminary results for two further deletion mutants were also produced, Δ*Ms-fadB4* and Δ*Mb-fadB5*. With regard to the former, no differences were observed between the mutant, wild-type and complemented strains with respect to growth on sole carbon sources, or media containing SDS or H_2O_2, nor regarding amino acid metabolism or lipid profile. The deletion

of *fadB5* in *M. bovis* BCG showed that the gene is not essential for *in vitro* growth, but unfortunately the strain was not explored further. It is clear from the literature that deleting single *fad* genes can have a big effect on the cell *in vivo*, such as the hypervirulent Δ*Mt-fadB4* mutant (Scandurra *et al*. 2008) and the seemingly attenuated Δ*Mt-fadD5* (Dunphy *et al*. 2010). It is therefore vital to see how deleting each of these *fadB* genes would affect *M. tuberculosis* growth and survival in macrophages and whole animal models.

Overall, this last chapter has given a significant indication that redundancy plays an enormous role in mycobacterial β-oxidation, signifying the importance of the pathway to the bacilli. It is evident that, in order for this essential process to be exploited as a drug target, much more biochemical analysis needs to be done and the effects of double and multiple deletion mutants need to be discerned. Allocating functions to the remaining FadB proteins would also be valuable, as has been done with many of the FadD enzymes.

CHAPTER 6

General Methods

6.1. Media

6.1.1. Luria-Bertani (LB) broth and agar.

To make 1 l of broth, dissolve 25 g Difco™ Middlebrook dehydrated LB in deionised H_2O (dH_2O) in a total volume of 1 litre. The medium contains peptone from casein, yeast extract and NaCl in the ratio 10 : 5 : 10 (v/v/v). For all the media described, solid agar versions can be made by adding 15 g agar (Oxoid Agar Technical; Agar No. 3) per 1 l liquid medium. Sterilisation is by autoclaving under high-pressure steam at approximately 123 °C for 15–20 min.

6.1.2. Terrific Broth.

This is a rich medium devised by Tartoff & Hobbs (1987) to specifically produce a high yield of recombinant *E. coli*. To make 1 litre of broth, dissolve 12 g tryptone, 24 g yeast extract and 4 ml glycerol in dH_2O in a total volume of 900 ml. In a separate flask, dissolve 2.31 g KH_2PO_4 and 12.54 g K_2HPO_4 in dH_2O to a total volume of 100 ml. This is the 10× terrific broth salt. Sterilise both by autoclaving and, when at room temperature, aseptically add the 100 ml 10× salts to the broth.

6.1.3. Tryptic soy broth (TSB).

TSB is a nutrient-rich medium used to grow *M. smegmatis* but not other mycobacteria. To make 1 litre of broth, dissolve 30 g Difco™ Middlebrook dehydrated TSB in dH_2O to a total volume of 1 l. The medium contains 17 g pancreatic digest of casein, 5 g NaCl, 3 g papaic digest of soybean, 2.5 g dextrose and 2.5 g K_2HPO_4.

6.1.4. 7H9 broth.

7H9 medium was developed by Middlebrook *et al*. (1954) and Middlebrook & Cohn (1958) for the growth of mycobacteria by including an essential high concentration of inorganic salts. When supplemented with glycerol or glycerol plus BBL™ Middlebrook ADC (100 ml per litre of 7H9 medium), growth is enhanced and suitable for supporting cultivation of *M. bovis* and *M. tuberculosis*. The medium contains (per 900 ml) 0.5 g ammonium sulfate, 0.5 g L-glutamic acid, 0.1 g sodium citrate, 1 mg pyridoxine, 0.5 mg biotin, 2.5 g Na_2HPO_4, 1 g KH_2PO_4, 40 mg ferric ammonium citrate, 50 mg $MgSO_4$, 0.5 mg $CaCl_2$, 1 mg $ZnSO_4$ and 1 mg $CuSO_4$. Sterilise by autoclaving. BBL™ Middlebrook ADC can be added aseptically once the medium has cooled to 45 °C. It contains (per litre) 8.5 g NaCl, 50 g bovine albumin to bind potentially toxic free fatty acids, 20 g dextrose and 0.03 g catalase, which removes any peroxides.

6.1.5. 7H11 agar.

7H11 medium was formulated by Cohn *et al*. (1968) for culturing fastidious mycobacteria, including drug-resistant strains of *M. tuberculosis*. The addition of malachite green is intended to supply limited inhibition of contaminating bacteria, an important factor when culturing slow-growing bacteria. The medium contains (per 900 ml) 1 g pancreatic digest of casein, 0.5 g L-glutamic acid, 0.4 g sodium citrate, 1 mg pyridoxine, 0.5 mg biotin, 40 mg ferric ammonium citrate, 0.5 g ammonium sulfate, 1.5 g Na_2HPO_4, 1.5 g KH_2PO_4, 0.05 g $MgSO_4$, 1 mg malachite green and 15 g agar. Similarly to 7H9, BBL™ Middlebrook ADC can be added aseptically to further enrich the medium.

6.1.6. Sauton's medium.

Sauton's medium is a liquid broth used for the growth of fastidious cultures, specifically *M. tuberculosis* and *M. bovis*. The medium is not available commercially but can be prepared in-house, containing (per litre) 0.5 g K_2HPO_4, 0.5 g $MgSO_4$, 4 g L-asparagine, 0.05 g ferric ammonium citrate, 60 ml glycerol, 2 g citric acid, 0.1 ml $ZnSO_4$ (1 % w/v), 5 ml Triton WR-1339 (5 %), pH 7.2.

6.1.7. Minimal media.

Minimal media contain the minimal amount of nutrients to support cell growth. Usually these media consist of various salts that provide nitrogen for protein synthesis along with essential ions such as potassium, sodium, phosphate, chloride and calcium.

6.1.7.1. Minimal medium for testing carbon sources in *M. smegmatis*.

Individual carbon sources can be added to this medium to test for any metabolic deficiencies in mutant strains. The medium used contains (per litre) 1.5 g KH_2PO_4, 1.0 g NH_4Cl, 0.2 g $MgSO_4 \cdot 7H_2O$, 20.0 mg $CaCl_2 \cdot 2H_2O$, 1.2 mg ferric ammonium citrate, 0.85 g NaCl and 8.99 g $Na_2HPO_4 \cdot 12H_2O$. Additional carbon sources are independently sterilised and added to the autoclaved medium after it has cooled.

6.1.7.2. Minimal medium for testing carbon sources in *M. bovis* BCG.

A modified Sauton's medium was used to test the growth of *M. bovis* BCG mutants on different carbon sources, as described by Keating *et al*. (2005). The medium contains (per litre) 4 g asparagine, 2 g citric acid, 0.5 g K_2HPO_4, 0.5 g $MgSO_4 \cdot 7H_2O$ and 0.05 g ferric ammonium citrate.

6.1.7.3. Minimal medium for seleno-methionine protein labelling.

To aid structure determination of *Mt*-FadB2, attempts were made to label the protein with selenium by replacing methionine residues with seleno-methionine. The minimal medium used during this procedure contains (per litre) 200 ml 5× M9 salts, 2 mM $MgSO_4$, 0.1 mM $CaCl_2$ and 0.4 % glucose. The 5× M9 salts are made by dissolving the following in 1 l *d*H_2O and sterilising by autoclaving: 83.9 g $Na_2HPO_4 \cdot 12H_2O$, 15 g KH_2PO_4, 2.5 g NaCl and 5.0 g NH_4Cl. The $MgSO_4$ and $CaCl_2$ solutions are prepared and sterilised separately and added after the 5× M9 salts have been diluted (Sambrook & Russell 2001).

6.2. Molecular biology protocols

6.2.1. DNA sequences used in molecular biology protocols (TubercuList).

6.2.1.1. *M. tuberculosis fadB2* (*Rv0468*).

```
gtgagcgatgcgatccagcgggtaggggttgtcggggccgggcagatggggtccggcatcgccgaggt
ctcggctcgcgccggcgtcgaagtgacggtgttcgagccggccgaggcgttgatcaccgcgggacgca
accgcatcgtgaagtcgctggagcgggccgtcagcgccggcaaggtaaccgagcgcgagcgtgaccgc
gccctcggcctgttgaccttcaccaccgacctcaacgacctatccgataggcaactggtgatcgaggc
cgttgtcgaggacgaggccgtcaagtccgagatcttcgccgagctcgaccgggtcgtcaccgatccgg
acgcggtgctggcgtcgaatacctccagcatcccgatcatgaaggtcgccgcggccaccaagcagccg
caacgggttcttggcctgcatttcttcaatccggtcccggtgctgccgctggtcgagttggtgcgcac
gctggtcaccgacgaagccgccgccgcgcgcacggaggagtttgccagtactgtgctgggcaaacagg
tcgtgcgttgctccgaccgctccggattcgtggtcaatgcgctcctggtgccgtatttgctgtcggcg
attcggatggtcgaggccgggtttgccaccgtcgaagatgtcgacaaggccgttgttgcggggttatc
gcacccgatgggtccgctgcggctttccgatcttgtcggcctagacaccctcaagctgatcgcggaca
agatgttcgaagaattcaaagaaccgcactacgggccccctccgctgttgctgcgtatggttgaggcg
ggccagttgggaaagaaatcgggtcgaggtttctacacgtactga
```

6.2.1.2. *M. smegmatis fadB2* (*MSMEG0912*).

```
gtgagcaatgcaatcgaacgagtaggtgtcgtcggagccggccagatgggcagcggcatcgccgaggt
gtccgcccgcgcgggcgtcgacgtcctggtctacgacaccactgacgccttcgtgacggccgggcgca
accgcatcacgaagtcgctggagcgcgccgtgagcgcgggcaaggtcaccgagcgtgagaaggacgag
gcgctgggccggctgcgcttcaccacgagcctcgccgacatggccgaccgtcagctggtcatcgaggc
cgtgatcgaggacgagaacatcaagggcgagatcttcgccgaactcgaccgcgtgatcaccgaccccg
acgcggtgctggcgtcgaacacgtcgagcatcccgatcatgaagatcgcggcgtccaccgagaacccc
gagcgcgtgctgggcctgcacttcttcaacccggtgcccgtcctgccactcgtcgagttggtgtccac
actcgtcacctccgaggcggcggccgaccgggtcgagcagttcgccggatcggtgctgggcaagcagg
tcgtgcggtgctccgaccggtccggcttcgtggtgaacttcctgctcgtgccgtacctgctctcggca
atccgcatggtcgaaggtggcgtcgccaccatcgaggacgtcgacaaggccgtggtggccgggttgtc
gcacccgatggggccgctgcgcctgtccgatctggtagggctcgacacgctgaagctgatcgccgaca
agatgttcgacgagttcaaggagcccctgtacgcggcgccgccactgctgctgcgcatggtcgaggcc
ggccagctcggcaagaaaacgggcaagggcttctatacctactga
```

6.2.1.3. *M. tuberculosis fadB3* (*Rv1715*).

```
atgctgacctcgcacgggttctcccgtgccgccgtcgtgggtgccgggctgatgggccggcgcatcgc
cggcgtgctggcctcggcgggcctggatgtcgccatcaccgacaccaacgctgagattctccacgccg
cagcggtggaggccgcccgggtagccggtgctggccgtggctcggtggccgcggcagccgacctagcc
gcggcgataccagacgccgacctggtgattgaggccgtcgtcgaaaacctggccgtcaagcaggaact
cttcgaacggctggcgacactcgcgcccgacgcggtgctggccaccaacacctcggtgctgccgatcg
gcgctgtcaccgaacgggtcgaggacggcagccgagtgatcgggacacactttggaaccgccggatc
ttatcccggtggtcgaggtggtgcccagcgcgcgcaccgccccagatacggcggatcgcgtcgtggcg
ctgctgacccaagtcggcaagctgccggtgcgggtcgggcgcacgtgccgggtttcatcggcaaccgg
ctgcagcacgcgctgtggcgcgaggcgatcgcgctggtcgccgagggtgtctgcgacccgaagacggt
agatctcgtggtacgcaacaccattgggctgcgactggccaccttggggccgctggaaaacgccgact
acatcgggttggacctcaccctggccatccacgacgcggtgatcccgagcctcaaccacgacccgcac
cccagcccgctgctgcgggaactggtcgccgccgggcaactcggggcgcgtaccggtcacggctttct
ggactggcccgcaggagcccgcgaggccaccaccgcccgacttgcccagcacatcgccgcgcaactcc
aagccaacgaaaaaggaaggggggacatag
```

6.2.1.4. *M. bovis* BCG *fadB3* (*Mb1742–1743*).

```
atgctgacctcgcacgggttctcccgtgccgccgtcgtgggtgccgggctgatgggccggcgcatcgc
cggcgtgctggcctcggcgggcctggatgtcgccatcaccgacaccaacgctgagattctccacgccg
cagcggtggaggccgcccgggtagccggtgctggccgtggctcggtggccgcggcagccgacctagcc
gcggcgataccagacgccgacctggtgattgaggccgtcgtcgaaaacctggccgtcaagcaggaact
cttcgaacggctggcgacactcgcgcccgacgcggtgctggccaccaacacctcggtgctgccgatcg
gcgctgtcaccgaacgggtcgaggacggcagccgagtgatcgggacacactttggaacccgccggat
cttatcccggtggtcgaggtggtgcccagcgcgcgcaccgccccagatacggcggatcgcgtcgtggc
gctgctgacccaagtcggcaagctgccggtgcgggtcgggcgcgacgtgccgggtttcatcggcaacc
ggctgcagcacgcgctgtga|gtggtacgcaacaccattgggctgcgactggccaccttggggccgct
ggaaaacgccgactacatcgggttggacctcaccctggccatccacgacgcggtgatcccgagcctca
accacgacccgcaccccagcccgctgctgcgggaactggtcgccgccgggcaactcggggcgcgtacc
ggtcacggctttctggactggcccgcaggagcccgcgaggccaccaccgcccgacttgcccagcacat
cgccgcgcaactccaagccaacgaaaaaggaaggggggacatag
```

6.2.1.5. *M. smegmatis fadB3* (*MSMEG6791*).

```
atgcgcaagatcaacaccgtcacagtcgtcggcgccgggtacatgggcggcggcatcgcccaggtgct
ggccctcaacggattcaaggtccagatcgccgacgtcaacgccgaggccacccaggaggcgctcaagc
gcctcgaccgggaggcacgggaattcgagcagcagggcctgttcggccccggcagcgccgacaccatc
atgagcaacctcacggccagcgacagcctggacgacgccgtctccgacgtcgactacgtgatggaggc
cgttttcgaagacgtcgacgtcaagaaggaagtgctggcgcgcgtgtgtgcgagcgctcgccccgaca
cgatcatcggcaccaacacctccaccatcccggtcaaggtgctggtcgacgcggtaacccacccggag
cggttcctcaccgtgcacttctccaacccggcaccgttcatccccggtgtggaactcgtcgcgggcga
ggccacgacccaagaggtgatcgactccgtcaaggacctcctggcacgtgccggacgtgagggcgccc
aggtggccgacaccccgggtatggcgctgaaccgcctgcagtacgcgctgctcaaggaggcgacgctg
atcgtcgaagagggcgtggccaccaaggaggacgtcgacaccatcgtccgcaccacgttcggcttccg
gctcgggttcttcggcccgttcgccatcgccgatcaggccgggctcgacgtgtacgtcaagggctacc
acaccttggagaacgcattcggtgagcgcatggccacccccaagctgctcacggacaacgtcgacgcc
ggccgttacggcaccaagaacggcaagggctggaccggcgacttcgacgacgaaaccaaggctgcggt
catcgcataccgcaacaaggcctactcgcgcatgggcgaactgctgcgcgaactcggaccggccccca
agggcgcctga
```

6.2.1.6. *M. tuberculosis fadB4* (*Rv3141*).

```
atgcgcgcggtacgggtgactcggctggagggaccagatgcggtcgaggtggccgaggtcgaggaacc
cacgagcgccggtgtggtcatcgaggtgcacgctgccggcgtggccttcccggacgcactgctaaccc
gtggccgttaccagtaccgcccggagccgccattcgtgctcggcgccgagatcgccggagtggttcga
tcggcgccggataacagccaagtgcgttccggagacagggttgtcggcctcacgatgctcaccggcgg
catggccgaagtcgcggtattgtcgcccgagcgcgtgttcaagctgccggacaacatgactttcgagg
cgggcgcgggcgtgctgttcaacgacctgacggtgtacttcgcgctggcggtccggggccggctgcag
gccggtgagacggtgctggtgcacggggcggcaggcgggatcggcacatcgacgttgcgactagcgcc
ggcgctcggggcgtctcgcaccgtcgcggtggtcagcacgcaggagaaggccgagcttgcgacagtgg
ccggggcgacagatgtggtgttggccgaggggttcaaggacgcggtacaggagctgacgaacggccgt
ggtgtcgacatcgtcgtagacccggtcggcggcgaccggttcaccgattcgctgcgctcgcttgctgc
gggaggacggctgttggtcatcggcttcactggcggcgagattcccaccgtgaaggtaaaccgccttc
tgctcaacaacattgacgttgtcggggtaggctggggcgcctggtcgctgacccaccccgatgcgctg
gcccagcagtggtcacaactcgagcggctgctacgctcgggcaagctgcctcctcccgaaccagtggt
ctacccactggaccaagccgctgcggcgattgcatcgctggagaatcgcaccgccaaggggaaggtcg
tactacgcgtgcgcgactaa
```

6.2.1.7. *M. smegmatis fadB4* (*MSMEG2033*).

```
atgcgcgctgcactgataacccgtctcgacggtcccgacgcggtggaagtggtcgaggtcgacgaacc
gtccggtgatgacgccgtcctgatcgacgtccacgccgcaggcgtggcgtttcccgacgcgctgctga
cgcgaggcctctaccagtacaagccggacctgccgttctcccccggcgccgaggtggccggtgtggtg
cgcagcgcaccggcaggcgcgtcggtcgcggcgggcgatcgtgtgctgggcctgacgatgctgtccgg
cggtatggcggaagtggttgcgctgcccgaggatcgcgtgttcaagctgcccgatgcggtgccgttcg
acgccggggcgggaatcctgttcaacgacatgaccgtgcacttcgtgctgcgcacccgcggcaggcta
tccggcggcgagacggttctggtgcacggcgccgctggcggaatcggttcgtcggtgctgcgcctggc
gcccgctttgggcgcggcccgcaccatcgcggtggtgtccaccgaggagaagggcgagatcgccaggg
ccgcaggcgcatccgatgtggtgctggccgacggtttccgtgacgcggtcaaggagttgaccgacggt
cgcggcgtcgacatggtggtcgaccccgtcggaggtgaccgcttcaccgattcgctgcgctcgctggc
ggtcggcgggcgcctgctggtggtcggcttcaccggcggcgagatcccccaggtgaaggtgaaccggt
tgctgctcaacaacatcgaggtgatcggcgcgggttggggtgcgtggactttcacgcacccgggttat
ctgcaggagcagtgggccgaactggagccgctgctggcctccggcgcggtcgccccgccgcaggtcga
ggtgtatccgttggagcaggccgcgcaggccatcgcgtcactggagaatcgcagcgccaagggcaagg
tggtgctcaaactgcgctga
```

6.2.1.8. *M. tuberculosis fadB5* (*Rv1912c*).

```
atgcgagcagtggtcatcaccaaacatggcgacccatcggtcttgcaggtgcggcagcgaccggaccc
gccgccaccgggcccgggccagctgcgggtcgccgtccgcgcagcaggggtgaacttcgctgaccatc
tcgcccgcgtcggcctgtacccagacgcgccgaaacttccggcggtggtcggatacgaagtcgctggg
acggtcgaggctgtcggtgatggggtcgacccgaaccgggtcggcgaacgagtcctggccggtacacg
atttggtggctactgcgagatcgtcaacgttgcggccaccgactcggttgtgctccccgatgcgctga
gcttcgaacagggtgccgcggtcccggtgaattacgcgaccgcctgggcggcgctgcacggctacgga
tcgttgcgcgccggtgagcgggtgctgattcacgccgcggccggtggagtcggcatcgcggcggtcca
attcgcgaaagcagccaaggccgaagtgcacggcaccgcatcaccccaaaaacatcagaagctggccg
agttcggtgtggaccgcgcgatcgactaccgccgggacggctggtggcagggattgggcccgtatgac
gtcgtgcttgacgcgctcggcggcacctcgctgcggcggtcctacactctgctgcgcccgggtggaag
gctggttggctacgggatttcgaatatgcagcacggcgagaaacgatcgatgcgcagggtggcgcccc
acgcgttgtcaatgctgcgcggctttaacctgatgaaacaactcgaggagtcgaaaaccgtgatcggt
cttaacatgctgcggttgtgggacgatcgccgcacccttgaaccctggatcgcgccgctgaccaaggc
gctcaacgacggaacgatcctgccgatcgttcatgcaatcgtgccgttcgccgaagctcctgaagcac
atcggattctggccgcacgggagaacgtcgacaaggtggtgctggtaccgtga
```

6.2.1.9. *M. bovis* BCG *fadB5* (*Mb1947c*).

```
atgcgagcagtggtcatcaccaaacatggcgacccatcggtcttgcaggtgcggcagcgaccggaccc
gccgccaccgggcccgggccagctgcgggtcgccgtccgcgcagcaggggtgaacttcgctgaccatc
tcgcccgcgtcggcctgtacccagacgcgccgaaacttccggcggtggtcggatacgaagtcgctggg
acggtcgaggctgtcggtgatggggtcgacccgaaccgggtcggcgaacgagtcctggccggtacacg
atttggtggctactgcgagatcgtcaacgttgcggccaccgactcggttgtgctccccgatgcgctga
gcttcgaacagggtgccgcggtcccggtgaattacgcgaccgcctgggcggcgctgcacggctacgga
tcgttgcgcgccggtgagcgggtgctgattcacgccgcggccggtggagtcggcatcgcggcggtcca
attcgcgaaagcagccaaggccgaagtgcacggcaccgcatcaccccaaaaacatcagaagctggccg
agttcggtgtggaccgcgcgatcgactaccgccgggacggctggtggcagggattgggcccgtatgac
gtcgtgcttgacgcgctcggcggcacctcgctgcggcggtcctacactctgctgcgcccgggtggaag
gctggttggctacgggatttcgaatatgcagcacggcgagaaacgatcgatgcgcagggtggcgcccc
acgcgttgtcaatgctgcgcggctttaacctgatgaaacaactcgaggagtcgaaaaccgtgatcggt
cttaacatgctgcggttgtgggacgatcgccgcacccttgaaccctggatcgcgccgctgaccaaggc
gctcaacgacggaacgatcctgccgatcgttcatgcaatcgtgccgttcgccgaagctcctgaagcac
atcggattctggccgcacgggagaacgtcggcaaggtggtgctggtaccgtga
```

6.2.2. Polymerase chain reaction (PCR).

6.2.2.1. The general PCR mix.

Two different DNA polymerases have been employed, Vent$_R$® and Phusion® (both New England Biolabs). The latter was used the majority of the time because it was found to be more successful. Four different conditions have been used throughout this project to optimise DNA amplification, which are as follows:

Constituent	Stock concentration	Volume			
		①	②	③	④
5' primer	100 pmol/µl	1 µl	1 µl	1 µl	1 µl
3' primer	100 pmol/µl	1 µl	1 µl	1 µl	1 µl
gDNA template	10 ng/µl	1 µl	1 µl	1 µl	1 µl
dNTP	25 mM	2 µl	2 µl	2 µl	2 µl
10× buffer		10 µl	10 µl	10 µl	10 µl
DNA polymerase		1 µl	1 µl	1 µl	1 µl
$MgSO_4$	100 mM	0 µl	1 µl	0 µl	1 µl
DMSO	100 %	0 µl	0 µl	8 µl	8 µl
H_2O		84 µl	83 µl	76 µl	75 µl
Total		100 µl			

6.2.2.2. PCR reaction steps.

A variety of conditions have been tested throughout this project to optimise PCR yield and reduce mis-priming. The following two-step PCR procedure (with no annealing step) has been the most successful and has therefore been used most routinely:

Temperature (°C)	Time	
98	30 s	
98	10 s	× 35 cycles
60.9 – 75.6	90 s	
72	10 min	
4	∞	

6.2.3. DNA electrophoresis and purification.

In order to separate DNA fragments according to size, electrophoresis is employed. The DNA samples with added loading dye (New England Biolabs) are pipetted into wells in an agarose gel (Bioline). An electric field is applied that causes the negatively-charged DNA to migrate towards the positive anode. The viscous medium of the agarose provides resistance for the DNA of varying degrees depending on the concentration. Generally, 1 % agarose gels have been used in this project, except when analysing larger fragments of DNA such as cosmids, when 0.8 % gels are used. The agarose is dissolved in TAE buffer (Sambrook & Russell 2001) by heating until boiling and is left to set in a gel cast. Once solid, the gel is completely submerged in TAE buffer within a HE33 Mini Submarine gel tank (Hoefer) and the DNA is loaded. The tank is connected to a power pack and the gel is run at 120–140 V, 400 mA for 40–50 min. At the end of the run, the gel is immersed for 10–20 min in ethidium bromide, a fluorescent tag that intercalates with double-stranded DNA. The DNA bands can then be analysed under a UV light.

1× DNA loading dye:

- 2.5 % Ficoll 400
- 11 mM EDTA
- 3.3 mM Tris·HCl
- 0.017 % SDS
- 0.015 % Bromophenol Blue
- pH 8.0 at 25 °C

1× TAE buffer:

- 40 mM Tris·acetate
- 1 mM EDTA
- pH 8.0 at 25 °C

Individual bands can be excised from the gel and purified using the QIAquick Gel Extraction Kit (Qiagen). Essentially, the gel is dissolved and the DNA is released. The dissolved gel is applied to a spin column with a silica membrane to which the DNA binds. Impurities are removed during the washing stages and the DNA is eluted with *d*H_2O or EB buffer (10 mM Tris·HCl, pH 8.5).

6.2.4. DNA digestion.

In order to sub-clone PCR products or plasmid DNA into vectors or to check the orientation of sub-cloned DNA, the DNA must be digested and analysed by agarose gel electrophoresis. Usually, a double digest is required, where a 20 µl cocktail is made containing 1 µl of each restriction enzyme, 2 µl of digest buffer suitable for both enzymes, 10 µl DNA and 6 µl *d*H_2O. The mix is incubated at 37 °C for 2 h, although this is enzyme-dependent; Van91*i* FastDigest enzyme only requires a 5 min incubation at 37 °C. For some restriction enzymes, when performing a double digest, a sequential digest is needed.

6.2.5. DNA ligation.

Sub-cloning requires DNA fragments to be ligated into plasmids that have been digested by the same enzymes. The 20 µl ligation cocktail consists of 1µl T4 ligase (New England Biolabs), 2 µl ligase buffer, 1 µl plasmid DNA, 10 µl fragment DNA that is to be inserted into the plasmid and 6 µl *d*H_2O. T4 ligase requires an incubation of 16 h at 16 °C. Generally

the number of plasmids containing the insert will be quite low, so *E. coli* cells are employed to make large numbers of plasmid. For this, the plasmid first has to be transformed into competent cells.

6.2.6. Preparation of competent cells for heat-shock transformation.

A glycerol stock of heat-shock competent *E. coli* cells is thawed on ice and 10 µl used to inoculate 5 ml LB broth. The culture is incubated with shaking at 37 °C overnight. Of this mini-culture, 500 µl is then used to inoculate 50 ml LB broth, which is incubated with shaking at 37 °C until the OD_{600} reaches 0.4–0.6. The culture is then centrifuged at 3,000 × *g* for 10 min at 4 °C and, having removed the supernatant, the resulting pellet is resuspended in 10 ml ice-cold $CaCl_2$ and left at 4 °C for 20 min. The cells are centrifuged again at 3,000 × *g* for 10 min at 4 °C, the supernatant is discarded and the pellet is resuspended in 2.5 ml ice-cold $CaCl_2$ + 15 % glycerol. The cells are then aliquotted and flash frozen using liquid nitrogen before storing immediately at -80 °C.

Heat shock transformation: Cells (50 µl) are thawed on ice, 1 µl of plasmid DNA is added, gently mixed and kept at 4 °C for 30 min. The tube is then submerged in a water bath at 42 °C for 45 sec with gentle agitation to equally distribute the heat. After this time, the tube is immediately put back on ice for 2 min before 200 µl LB broth is added. The cells are then incubated for 1 h at 37 °C without shaking (recovery time) and plated onto LB agar supplemented with selective antibiotic(s) as required.

6.2.7. Preparation of competent cells for electroporation.

A 5 ml culture of wild-type cells (*M. smegmatis* or *M. bovis* BCG) is grown from a glycerol stock in 7H9 broth (supplemented with BBL™ Middlebrook ADC for *M. bovis*) until the OD_{600} has reached 0.6–0.7. The culture is centrifuged at 3,000 × *g* for 10 min at 4 °C and the

supernatant is discarded. The cells are washed three times with 5 ml ice-cold 10 % glycerol, centrifuging and removing the supernatant between each wash. Finally, the cells are resuspended in 5 ml ice-cold 10 % glycerol and aseptically pipetted into 100 µl aliquots before flash freezing.

Electroporation: Cells (100 µl) are thawed on ice, 5 µl plasmid DNA is added to the cells, gently mixed and kept on ice for 10 min. The mix is then transferred to an electroporation cuvette (1 mm gap) and electroporated at 1,800 V, 1000 Ω, 25 µF in an Eppendorf electroporator 2510. 7H9 media (1 ml) is added to the cells and they are incubated at 37 °C static for 6 h (*M. smegmatis*) or 12 h (*M. bovis*) to recover. Following this time, the cells are spread onto 7H9 agar plates containing the appropriate selective antibiotic(s). Plates are incubated at 37 °C for 4–5 days (*M. smegmatis*) or 3–4 weeks (*M. bovis*), or until colonies are visible.

6.2.8. Plasmid extraction

To check that the fragment of DNA has been correctly inserted into the vector, the plasmid DNA needs to be purified away from the cell. This is done using a mini-prep kit (Qiagen). Colonies of transformed *E. coli* are used to inoculate 5 ml LB broth containing selective antibiotic and incubated overnight at 37 °C with shaking. The next day, the mini-cultures are centrifuged at 3,500 × *g* for 10 min to form a pellet. The cells are resuspended in 250 µl P1 buffer and transferred to a 1.5 ml eppendorf. P2 buffer (250 µl) is then added and mixed by inversion, immediately followed by the addition and mixing of 300 µl N3 buffer. The P2 buffer lyses the cells releasing the contents and the N3 buffer differentiates between the plasmid and genomic DNA. The insoluble components are pelleted by centrifugation (13,000 × *g*, 15 min) and the supernatant containing the DNA is applied to a QIAprep spin column. The column has a membrane onto which the plasmid DNA binds. The DNA is first washed

using 500 µl PB and 750 µl ethanol-containing PE buffer before eluting the DNA with 50 µl *d*H_2O or, for larger plasmids and cosmids, warm EB buffer.

6.2.9. Site-directed mutagenesis.

The Stratagene QuikChange® Multi Site-Directed Mutagenesis Kit has been used in this project to introduce mutations into genes of interest. The protocol is outlined below:

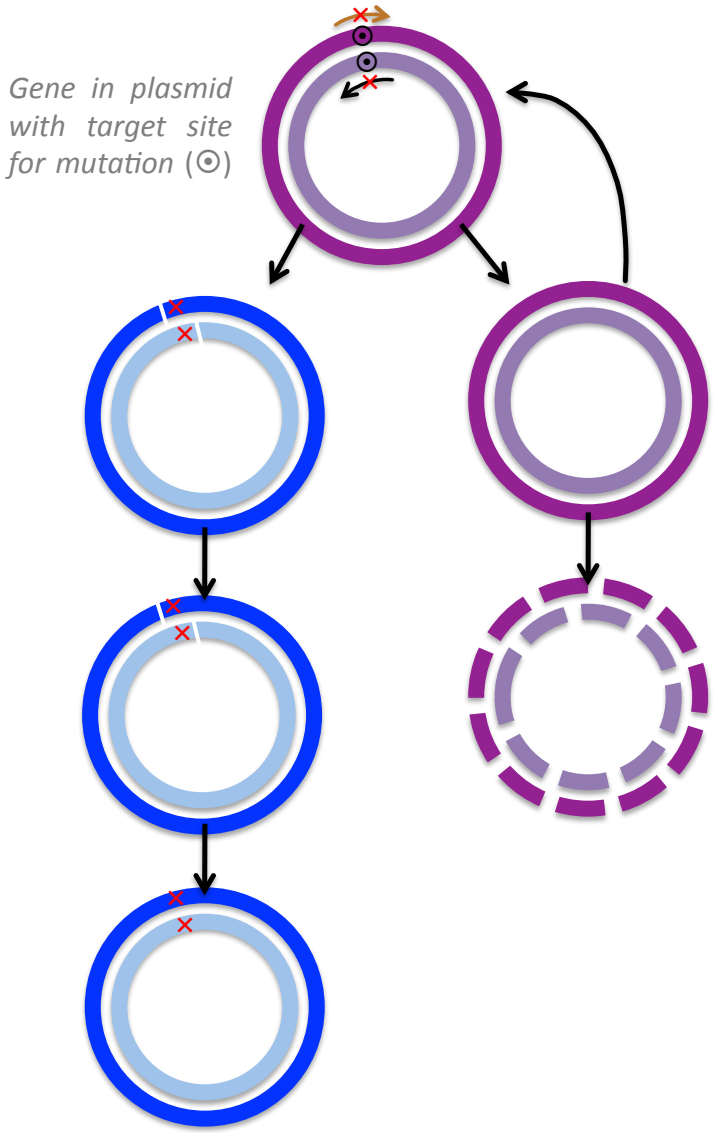

1. **Mutant strand synthesis:** PCR denatures the DNA template, anneals the mutagenic primers (arrows) and amplifies the plasmid with *PfuUltra* DNA polymerase. Results in nicked circular strands.

2. ***DpnI* digestion of template:** Digest methylated and hemimethylated non-mutated parental DNA with *Dpn*I.

3. **Transformation:** Mutated plasmid transformed into XL10-Gold® Ultracompetent *E. coli*. The cells repair the nicks in the plasmid.

6.2.10. Genomic DNA extraction.

Genomic DNA (gDNA) in this project has been extracted from whole cells in order to (i) use it as a template for PCR and cloning procedures in the case of WT species and (ii) in order to check if desired mutations have been made following specialised transduction. A 10 ml culture of the mycobacterium of interest is grown in 7H9 plus 0.05 % Tween®-80, plus any selective antibiotic, by incubation at 37 °C for 24 h with shaking (*M. smegmatis*) or 7–14 days static (*M. bovis* BCG). The cells are pelleted by centrifugation at 3,000 × *g* for 15 min and the supernatant is discarded. The pellet is washed with 500 µl PBS, transferred to a clean eppendorf and centrifuged again. The pellet is resuspended in 225 µl P1 buffer and 25 µl lysozyme (10 mg/ml) is added, mixed gently and incubated at 37 °C overnight. The next day, 50 µl SDS (10 %) and 25 µl proteinase K (10 mg/ml) are added, mixed gently and incubated at 55 °C for ≥ 6 h. One hundred µl NaCl (5 M) is then added to block binding of DNA to cetrimide. Then 500 µl chloroform is added, mixed by gentle inversion and centrifuged at 13,000 × *g* for 15 min. The top (aqueous) layer is aspirated into a clean tube making sure none of the interface debris is removed. To this supernatant, 280 µl isopropanol is added and mixed by inversion until the DNA can be seen to precipitate out of solution. After incubation at room temperature for 5 min, the tube is centrifuged to harvest the DNA. The supernatant is removed and the DNA pellet is washed with 70 % ethanol (500 µl). Following further centrifugation, the supernatant is again removed. The ethanol is allowed to evaporate before covering the DNA with 25 µl EB buffer. The pellet dissolves in the buffer overnight at 4 °C.

6.2.11. Southern blotting.

This technique, summarised in Figure 6-1, is used to identify fragments of DNA and, in the case of this project, to confirm gene knock-out mutants and is performed as per the kit manual (Roche Applied Science). The extracted gDNA of the wild-type bacteria and the mutant is first cut using a restriction enzyme that will produce different sized fragments in

both strains. Gel electrophoresis is used to separate the fragments, which will produce a ladder pattern (Figure 6-1 A). The gel is submerged in 0.25 N HCl to depurinate the DNA – this breaks it into smaller fragments allowing for better transfer later (Figure 6-1 B). The gel is then covered with a solution that denatures the double-stranded DNA – this will aid binding of the negative DNA to the positive membrane (Figure 6-1 C). The gel is returned to pH 7.4 before transferring the DNA to a positively charged nitrocellulose membrane by capillary action (Figure 6-1 D). Once complete, the DNA is covalently bound to the membrane by UV radiation. The hybridisation probe is a single DNA fragment with a specific sequence whose presence in the target DNA is to be determined. This can be the PCR fragments used to knock the gene out in the specialised transduction protocol. The probe is prepared by boiling, snap freezing and labelling with digoxigenin-dUTP (Figure 6-1 E). The membrane is exposed to the probe overnight at 65 °C. The next day the membrane is washed and the antibody is incubated with the membrane for 30 min at 25 °C (Figure 6-1 F). The antibody binds to the digoxigenin-dUTP on the probe and is conjugated to alkaline phosphatase. CSPD is then applied to the membrane (1 ml). The alkaline phosphatase on the antibody dephosphorylates the CSPD, which is a chemiluminescence reaction (Figure 6-1 G). The light emitted is visualised by exposing the membrane to film.

6.2.12. Specialised transduction.

Specialised transduction is a process used to create gene knock-out mutants in mycobacteria, first introduced by Bardarov *et al.* in 2002. Broadly, transduction is the transfer of genetic material from one bacterial cell to another *via* a viral vector. Specialised transduction is a result of the virus making a mistake when removing itself from the bacterial chromosome, *i.e.* when transitioning from the lysogenic to the lytic cycle. A small portion of bacterial DNA from either end of the viral DNA is mistakenly packaged into the capsid and injected into the next cell. There are several possible consequences of this, including recycling of the

DNA or insertion into the chromosome resulting in gene duplication. The outcome harnessed in genetic engineering, however, is homologous recombination. Regions shared by the transferred bacterial DNA and the host chromosome match up and the viral genetic material between the bacterial portions is exchanged. In essence, the gene of interest in replaced in the genome with a hygromycin-resistance cassette by homologous recombination. The transduced cells are then plated on hygromycin selective media to screen for mutant colonies.

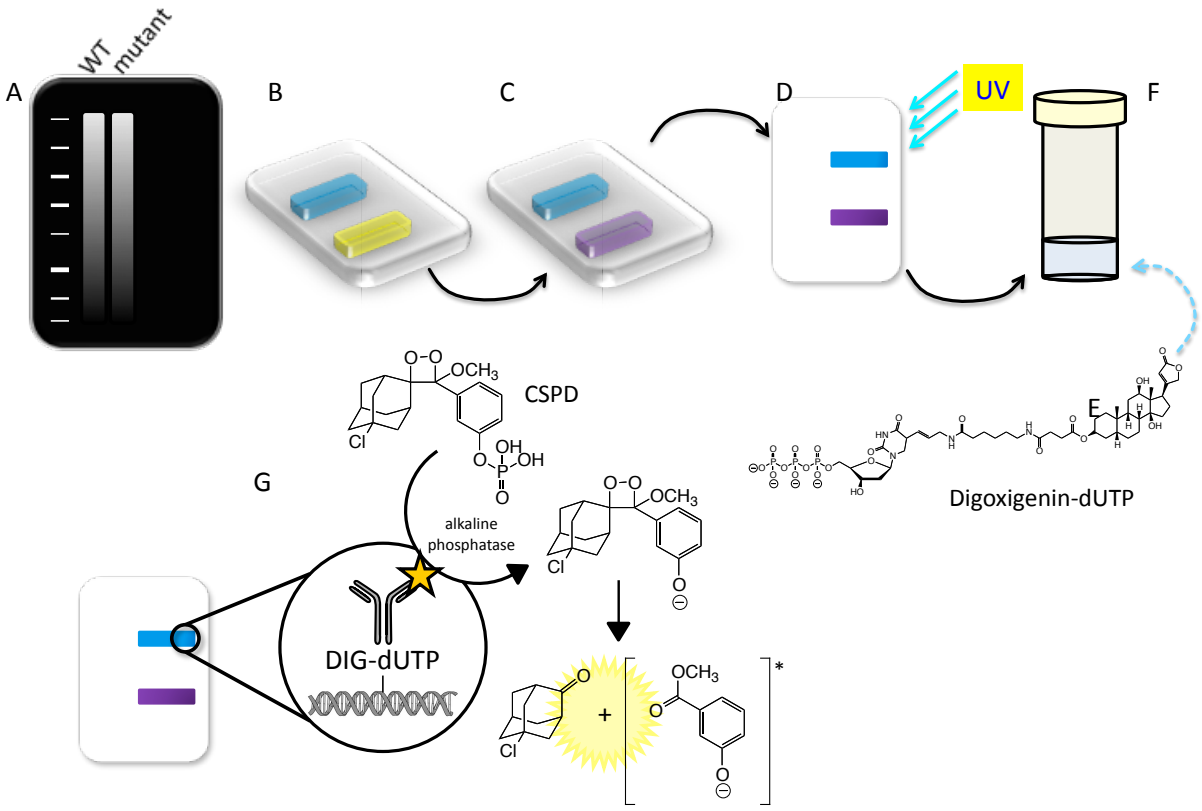

FIGURE 6-1. Southern blot procedure. (**A**) The gDNA is digested and fragments separated by gel electrophoresis, (**B**) DNA depurination, (**C**) DNA denaturation and neutralisation, (**D**) The DNA is transferred to a nitrocellulose membrane by capillary action and covalently bound by UV radiation, (**E**) The probe is labelled with DIG-dUTP and is hybridised with the membrane (**F**). (**G**) Immunodetection – the alkaline phosphatase conjugated to the anti-DIG-dUTP antibody catalyses the CSPD chemiluminescent reaction.

Methods used prior to Bardarov *et al*. (2002) used electroporation to deliver the hygromycin-resistant gene or allelic exchange substrate (AES). However, this was found to be inefficient

in slow-growing mycobacteria largely due to erroneous recombination events and the high tendency for cells to clump together, making it difficult to isolate successful transductants. A protocol was developed that employs mycobacteriophages to transfer the AES rather than electroporation (Figure 6-2).

1. AES and cosmid construction:

Fragments of DNA, roughly 800–900 bp in length, upstream (to the left) and downstream (to the right) of the gene of interest are first amplified by PCR. The primers used also include a restriction site for specific endonucleases, such as *Dra*III, *Alw*NI or *Bst*API. It is these fragments that will match up with the mycobacterial chromosome to allow homologous recombination to occur. The DNA products are then cloned into the p0004S plasmid, which contains a *Pac*I restriction site, a hygromycin resistance cassette and γδ resolvase recognition sites, regions that are capable of mediating site-specific recombination. The complete vector is transformed into *E. coli* Top10 cells and selected for by plating on hygromycin (150 μg/ml) agar. Following mini-prep, the plasmid is sequenced to check for errors. The p0004S vector is then linearised by *Pac*I digestion. The phage DNA, phAE159, is cut similarly with *Pac*I to remove the β-lactamase gene and provide a site in which to clone in the p0004S vector. Fragments are ligated using T4 ligase. The complete phAE159-p0004S phasmid is then packaged into phage particles, which are used to transfect *E. coli* HB101 cells. These cells are used because they have high transformation efficiency. Transfected cells are plated onto selective medium (150 μg/ml hygromycin) and transductant colonies are picked after overnight incubation and mini-prepped. A small sample is cut with *Pac*I and run on a 0.7 % agarose gel. The inserted p0004S DNA should appear on the gel as a drop-out band from the large phage plasmid.

2. Propagation of phage particles

The phasmid is electroporated into *M. smegmatis* mc^2155 cells regardless of the species in which the knock-out is being made. TSB media (1 ml, devoid of Tween®-80) is added and the cells are incubated at 30 °C for 6 h. The phage particles are temperature-sensitive and are unable to replicate at 37 °C. The electroporated cells are mixed with wild-type *M. smegmatis* mc^2155 and overlaid on 7H9 plates containing no Tween®-80 or antibiotic. Plates are incubated at 30 °C for 2–3 days. After this time phage plaques should be visible on the lawn of *M. smegmatis* cells, forming a lacy pattern. Sterile MP buffer (4 ml) is applied to the surface of the bacterial lawn and the plates are left at room temperature for 4–6 h to soak up the phage particles. The MP buffer is then pooled and filtered (0.2 μm) to remove any *M. smegmatis* cells. The concentration of phage particles is assessed by serially diluting the pooled buffer and spotting 10 μl on 7H9 plates (devoid of antibiotic) overlaid with wild-type *M. smegmatis*. Phage plaques at each dilution are totalled and the titre is calculated. A titre of ~10^{10} particles is required for transduction.

3. Transduction

Wild-type cells in which the knock-out is being made (*M. smegmatis*, *M. bovis* BCG, *M. marinum*) are cultured to an OD_{600} of 0.8–1.0 in appropriate medium containing 0.05 % Tween®-80. The cells are then pelleted and washed with sterile MP buffer to remove the Tween®-80, as the surfactant can impede transduction. The cells are resuspended in MP buffer to give a concentration of 10^9 cells per ml. Roughly 10^8 phages are added to the cells and gently mixed. The transduction mixture is incubated at 37 °C overnight. The next day the cells are pelleted, resuspended in 2 ml fresh medium and the mixture is left to recover at 37 °C for 6 h. Following this, the cells are resuspended again in fresh medium and plated on selective agar, 100 μg/ml hygromycin for *M. smegmatis* or 75 μg/ml hygromycin for *M.*

bovis BCG. Transductants should appear after 6–7 days for *M. smegmatis* or 3–4 weeks for *M. bovis* BCG.

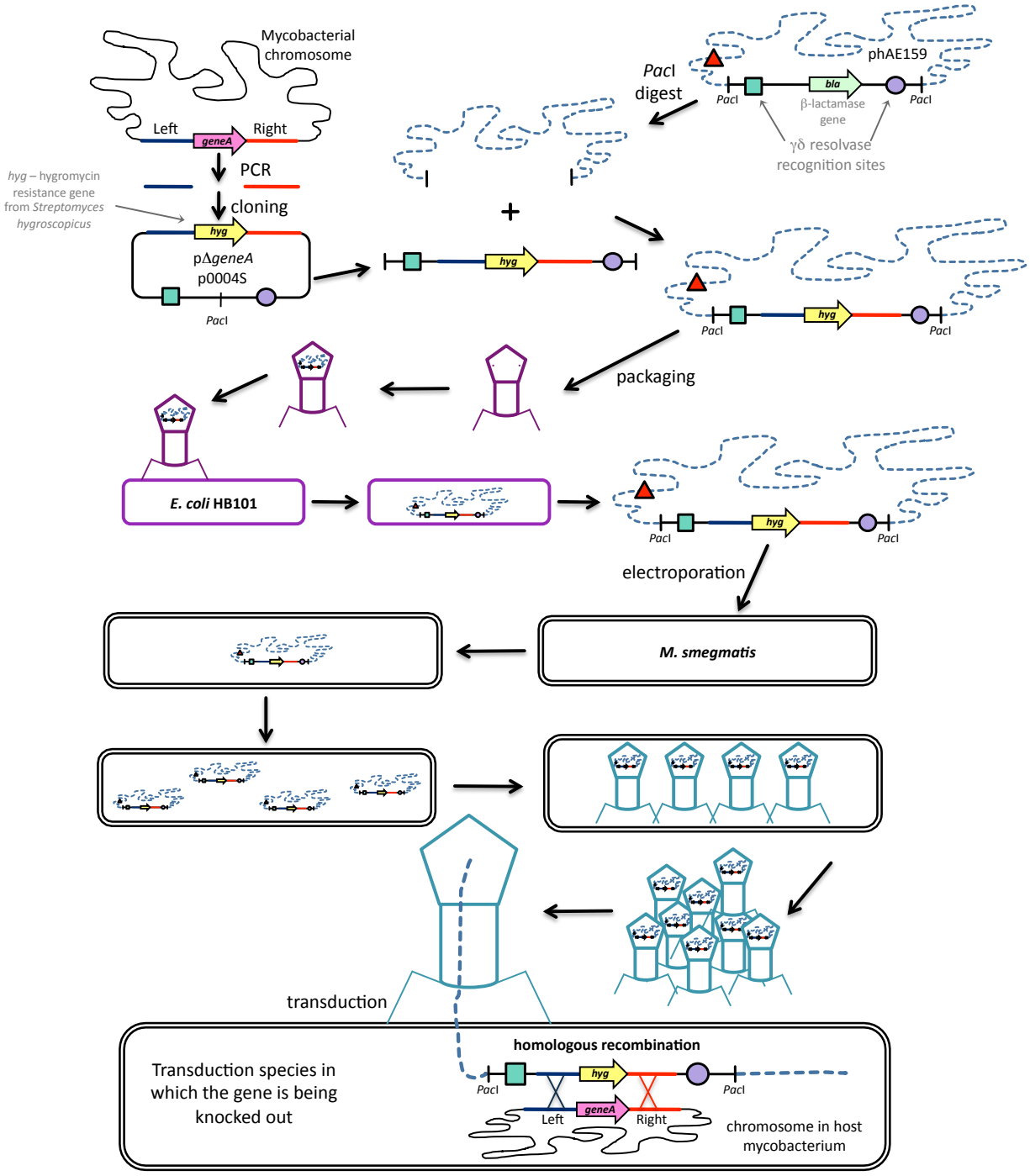

FIGURE 6-2. Specialised transduction. See text above (section 6.2.12.) for full description.

6.2.13. Bacterial strains.

6.2.13.1. *E. coli* strains used for plasmid propagation.

The following *E. coli* strains have been used to increase plasmid copy number. The strains have been developed to have very high transformation efficiency.

Top10

Source: Invitrogen

Genotype: F^- *mcrA* Δ(*mrr-hsd*RMS-*mcrBC*) φ80*lacZ*ΔM15 Δ*lac*X74 *nupG recA1 araD*139 Δ(ara-leu)7697 galE15 galK16 *rps*L(Str^R) *endA1* λ^-

Characteristics: Has high transformation efficiency and allows the stable replication of high copy number plasmids. Deletion of *hsd*R and *mrcA* allow the transformation of both methylated and unmethylated DNA and Δ*endA1* abolishes non-specific digestion of DNA by endonuclease I.

HB101

Source: Invitrogen

Genotype: F^- *mcr*B *mrr hsd*S_{20} (r_B^-, m_B^-) *recA13 sup*E44 *ara*14 *gal*K2 *lac*Y1 *pro*A2 *rps*L20(Smr) *xy15* λ^- *leu mtl*1.

Characteristics: Hybrid of *E. coli* K12 and *E. coli* B strains. Has very high transformation efficiency. The Δ*recA* phenotype helps to minimise recombination events.

XL-10 Gold

Source: Stratagene

*Genotype: endA1 gln*V44 *rec*A1 thi-1 *gyrA*96 *relA*1 *lac The* Δ(*mcrA*)183 Δ(*mcrCB-hsdSMR-mrr*)173 tet^R F′[proAB $lacI^q$ZΔM15 Tn10(Tet^R Amy Cm^R)]

Characteristics: Δ*Hte* phenotype allows cells to accept large or ligated plasmids much better. It dramatically increases transformation efficiency and cells grow faster producing larger colonies.

6.2.13.2. *E. coli* strains used for protein over-expression.

These *E. coli* strains differ from those above by having the IPTG inducible T7 RNA polymerase. This polymerase, from the T7 bacteriophage, synthesises RNA in the 5′→3′ direction in the presence of a DNA template, Mg^{2+} ions and, very specifically, the upstream T7 promoter. T7 promoter-driven expression is repressed until IPTG addition. This molecule acts as a mimic for lactose, which binds to the repressor inactivating it and initiating *lac* operon transcription. There are three genes in the *lac* operon, *lacZ*, *lacY* and *lacA*, which encode β-galactosidase, β-galactoside permease and β-galactoside transacetylase respectively. In protein over-expression systems, it is the *lacZ* gene that is replaced by the gene of interest.

BL21 (DE3)

Genotype: F^- *ompT gal dcm lon hsd*$S_B(r_B^- m_B^-)$ λ(DE3 [lacI lacUV5-T7 gene 1 ind1 sam7 nin5])

Characteristics: E. coli B strain containing the lambda prophage DE3, which harbours a single copy of the T7 RNA polymerase gene under the control of the *lac*UV5 promoter. *lac*UV5 is a mutated *lac* operon that is less sensitive to cyclic AMP, a molecule known to derepress the *lac* promoter. Addition of 1 % glucose to the culture medium also reduces 'leaky' expression by increasing repression at the promoter. In combination with the pET vector system as well, which also has a T7/*lac* promoter, basal expression is minimal and target protein expression is greatly improved. BL21 cells are also protease deficient (lon^-, $ompT^-$), improving protein yield further.

C41 (DE3)

Genotype: F⁻ *ompT gal dcm hsd*S_B(r_B^- m_B^-)(DE3)

Characteristics: Derived from BL21, C41 cells have at least one mutation such that over-expression of toxic proteins is tolerated and the cells remain viable. C41 are also used for over-expressing membrane proteins. Both transformation efficiency and protein expression are better than in BL21.

C43 (DE3)

Genotype: F⁻ *ompT gal dcm hsd*S_B(r_B^- m_B^-)(DE3)

Characteristics: Derived from C41 cells, C43 cells are mutated so that a different set of toxic proteins from C41 can be expressed.

Tuner™

Genotype: F⁻ *ompT hsdSB* (r_B^- m_B^-) gal *dcm lacY*1(DE3)

Characteristics: Also derived from BL21, Tuner™ cells are deficient in the *lacY* gene. This allows the level of expression to be regulated by altering IPTG concentration. The Δ*lacY* phenotype also provides uniform levels of target gene induction through consistent entry of IPTG into all cells.

6.2.13.3. Mycobacterial strains.

***M. smegmatis* mc²155**

M. smegmatis mc²155 is a mutant of *M. smegmatis* originally isolated in 1990 (Snapper *et al.* 1990). Unlike the parental strain, mc²155 has very high electroporation transformation efficiency. The genome was sequenced by the J. Craig Venter Institute in 2004 and was found to have one circular chromosome of 6.98 Mb and high G+C content (67.4 %).

***M. bovis* BCG str. Pasteur 1173P2**

The avirulent BCG (Bacille Calmette-Guérin) strain was originally derived from *M. bovis* by serial passage on glycerol-ox bile-saturated potato slices from 1908 to 1921. The source of attenuation is due to the loss of the RD1 locus (Belley *et al*. 2004, Keller *et al*. 2008), a 9.5 kb region found to regulate numerous loci (Mahairas *et al*. 1996). The Pasteur strain 1173P2 was passaged a further 1,173 times at the Pasteur Institute in Paris (ExPasy HAMAP) and was sequenced by the Pasteur Institute in 2009. The genome is 4.37 Mb and also has a high G+C content (65.6 %).

***M. tuberculosis* CDC1551**

Sequenced by the J. Craig Venter Institute in 2000, the CDC1551 strain was first identified in 1995 in the USA (Manca *et al*. 1999). The strain had a very high transmission rate but a subsequent study showed that it is no more virulent than other *M. tuberculosis* strains but does induce a greater host response. Like all mycobacteria, CDC1551 has a high G+C content of 65.6 % and is 4.40 Mb.

6.2.14. CellTiter-Blue® cell viability assay.

The CellTiter-Blue® (Promega) assay kit has been used in this project for testing the efficacy of compounds against whole cell *M. smegmatis* and *M. bovis* BCG. The method was first used with mycobacteria by Franzblau *et al*. in 1998. The reagent contains resazurin, a compound that is reduced to resorufin in the mitochondria of viable cells. Resorufin is bright pink in colour and, unlike resazurin, is highly fluorescent (Figure 6-3).

Cells are grown to an OD_{600} of 0.4 before being diluted 1 : 25 with fresh medium. The culture is aliquotted into a 96-well plate and the inhibitor is added at the desired concentration(s). The plate is sealed with parafilm to reduce evaporation and incubated at 37 °C without

shaking for 24 h. A 1:1 mixture of CellTiter-Blue® and Tween-80 (0.05 %) is made and 50 µl is added to a control well containing culture with no drug. The plate is re-sealed and incubated at 37 °C until the well has turned pink indicating live metabolising cells. At this point, the same mixture of CellTiter-Blue® is added to the remaining wells and incubated similarly for a further 6–8 h. The fluorescence is then measured using a plate reader at $560_{Ex}/590_{Em}$. Because only the resorufin fluoresces, a high value indicates live cells and a low reading indicates non-viable cells.

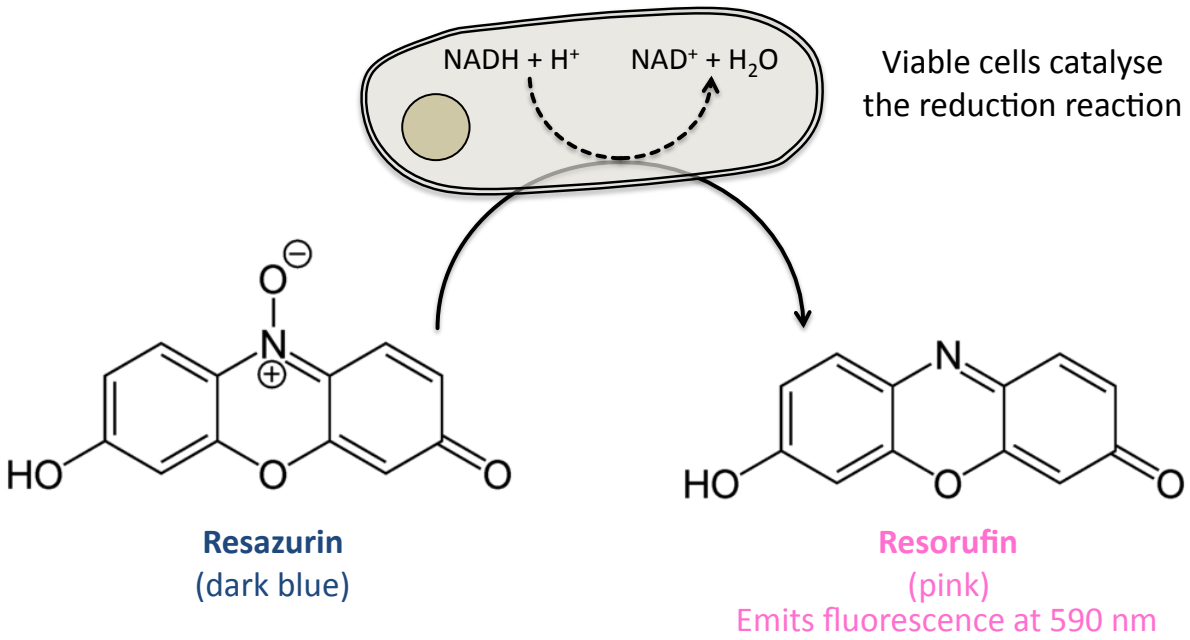

FIGURE 6-3. The principal of CellTiter-Blue® for cell viability testing. See text above (section 6.2.14.) for full description.

6.3. Protein biochemistry protocols

6.3.1. SDS-PAGE.

Sodium dodecyl sulfate polyacrylamide gel electrophoresis is used to separate proteins according to their molecular weight. Samples are initially diluted 1:1 with 2× Laemmli loading buffer and boiled for 10 min to denature the protein (leaving only the primary

structure) and to give all the proteins a negative charge (Figure 6-4). The gel consists of two parts, the lower resolving gel and the upper stacking gel in the approximate ratio 5 : 1:

2× Laemmli loading buffer:

- 0.125 M Tris·HCl (pH 6.8)
- 20 % Glycerol
- 4 % SDS
- 10 % β-mercaptoethanol

Laemmli running buffer:

- 3.03 % Tris
- 1.44 % Glycine
- 0.1 % SDS

Constituent	Volume
Acrylamide	0.65 ml
Water	3.05 ml
TEMED*	15 µl
10 % APS† (w/v)	75 µl
4× Stacking buffer: • 0.5 M Tris·HCl (pH 6.8) • 0.4 % SDS	1.25 ml

Constituent	Volume
Acrylamide-water mix (7–14 %)	11.25 ml
TEMED*	30 µl
10 % APS† (w/v)	75 µl
4× Resolving buffer: • 1.5 M Tris·HCl (pH 8.8) • 0.4 % SDS	3.75 ml

Gel (%)	7	8	9	10	11	12	13	14
Acrylamide (ml)	3.5	4.0	4.5	5.0	5.5	6.0	6.5	7.0
Water (ml)	7.75	7.25	6.75	6.25	5.75	5.25	4.75	4.25

*Tetramethylethylenediamine, †ammonium persulfate: added to the mixture just before pouring into the gel cast. All volumes are sufficient for two gels.

The gels are assembled in a SE200 Mighty Small vertical slab gel electrophoresis unit (Hoefer) and submerged in running buffer. The tank is connected to a power pack and the gels are run at 300 V, 20 mA per gel for 45 min to 1 h.

When the run has finished, the gels are stained by immersion for 15–30 min in Coomassie Brilliant Blue, a dye that binds to arginine, histidine and aromatic residues of the proteins on the gel. To remove all the non-specific binding, the gel is gently washed with *d*H_2O and immersed in destain solution until protein bands can be clearly seen.

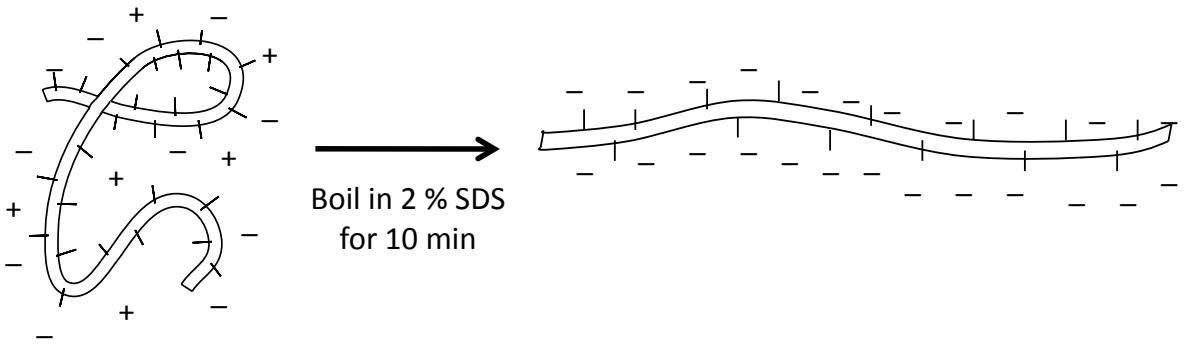

FIGURE 6-4. The effect of SDS and heating on proteins.

6.3.2. Western blotting

This technique, summarised in Figure 6-5, allows for the identification of His-tagged proteins. The protein sample is initially run on a SDS-PAGE gel of the appropriate acrylamide concentration. The proteins are then transferred electrophoretically onto a nitrocellulose membrane in a Transblot tank (Bio-Rad), submerged in transfer buffer. The tank is connected to a power pack and run at 10 V, 300 mA for 1 h. The membrane is removed to blocking buffer for 30 min to help prevent any non-specific binding before the mouse monoclonal Penta-His antibody (Qiagen), diluted 1 : 1,000 with 50 ml BSA-TBS-T buffer, is added for a further 30 min. The membrane is then washed with TBS-T buffer before adding the anti-mouse antibody. The membrane is washed again with TBS-T then TBS buffer before finally being immersed in BCIP reagent. This chemical reacts with the alkaline phosphatase on the anti-mouse antibody to produce an insoluble blue-black precipitate.

1. Transfer buffer (2 l):

- 6.06 g Tris
- 28.8 g Glycine
- 200 ml Methanol

2. Blocking buffer:

- TBS-T + 5 % (w/v) BSA powder

3. BSA-TBS-T buffer:

- TBS-T + 0.1 % (w/v) BSA powder

4. TBS-T buffer:

- TBS + 0.05 % Tween®-20

5. TBS buffer:

- 20 mM Tris·HCl
- 150 mM NaCl

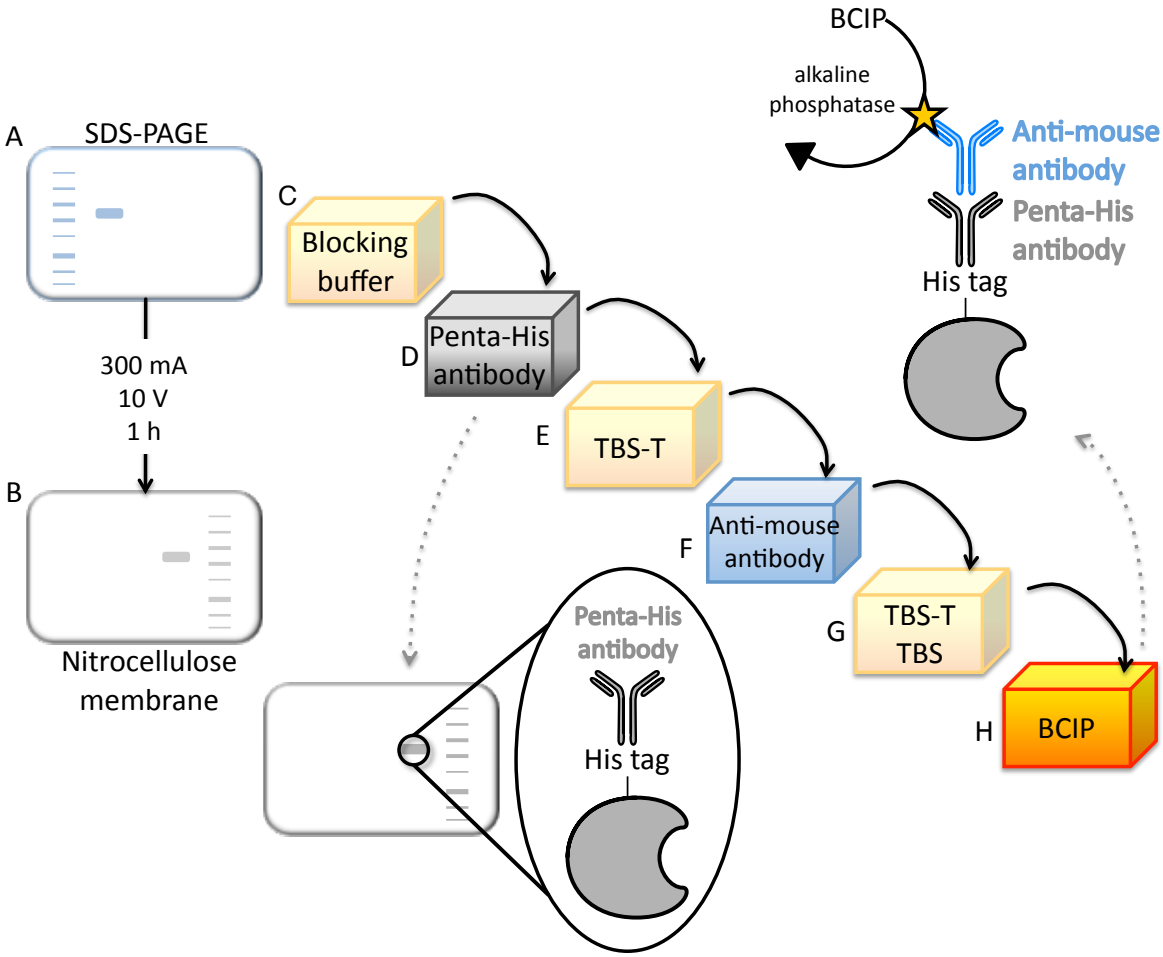

FIGURE 6-5. Western blot procedure. (**A**) The proteins are loaded and separated on an SDS-PAGE gel, (**B**) the proteins are transferred to a nitrocellulose membrane electrophoretically, (**C**) the membrane is covered with blocking buffer before the Penta-His antibody is added (**D**). (**E**) The membrane is washed before covering with anti-mouse antibody (**F**). (**G**) The membrane is washed again before immunodetection, where the alkaline phosphatase conjugated to the anti-mouse antibody catalyses the BCIP chemiluminescent reaction.

6.3.3. Isomorphous replacement of methionine residues with seleno-methionine.

The pET28b-*Mt-fadB2* plasmid was transformed into *E. coli* Tuner™ cells and incubated on LB agar containing 25 μg/ml kanamycin overnight at 37 °C. One colony was used to inoculate LB broth (5 ml) containing kanamycin (25 μg/ml) and cultures were incubated on a rotary incubator at 37 °C overnight. This mini-culture was used to inoculate 1 l LB broth containing kanamycin (25 μg/ml) and incubated on a rotary incubator (180 rpm) at 37 °C until the OD_{600} had reached 0.4. At this point, the cells were pelleted by centrifugation at 4,500 × *g* for 12 min. The supernatant was removed and the cells were resuspended in minimal medium (see section 6.1.7.3.) before further centrifugation to wash the cells. The cells were resuspended in the same minimal medium (1 l) plus kanamycin (25 μg/ml). Cell growth was then continued at 37 °C with shaking until an OD_{600} of 0.5 where upon the following amino acids were added: lysine, phenylalanine and threonine (0.1 mg/ml), isoleucine, leucine and valine (0.05 mg/ml) and L-selenomethionine (0.06 mg/ml). Growth was continued for a further hour at 37 °C before lowering the incubation temperature to 20 °C. At this point protein over-production was induced with 0.5 mM IPTG and the cells were incubated at 20 °C with shaking overnight until the OD_{600} had reached ~2.0. Cells were harvested and the protein was purified and dialysed as per the wild-type *Mt*-FadB2 protein (see section 4.2.5.).

MALDI-TOF mass spectrometry was used to identify the number of methionine residues replaced. The protein was prepared for this analysis using a $ZipTip_{C18}$™ (Millipore™), equilibrated firstly with 50 % acetonitrile and then 1 % acetic acid. The protein (10 μl, 1.0 mg/ml) was aspirated and dispensed 10× allowing it to bind to the chromatography medium inside the tip. The protein is eluted with 50 % acetonitrile / 1 % acetic acid (10 μl).

6.4. Biophysical techniques

6.4.1. Circular dichroism.

Circular dichroism (CD) is a means of investigating the secondary structure of proteins. The principal behind the technique is based on the difference in absorption of left and right circularly polarised light of the ultra-violet range. Proteins are chiral molecules, meaning that they do not have superimposable mirror images. It is because of this chirality that the protein interacts differently with left and right circularly polarised light. Whereas photons of linearly polarised light oscillate in the same plane, circularly polarised light beams trace out a helix (Figure 6-6).

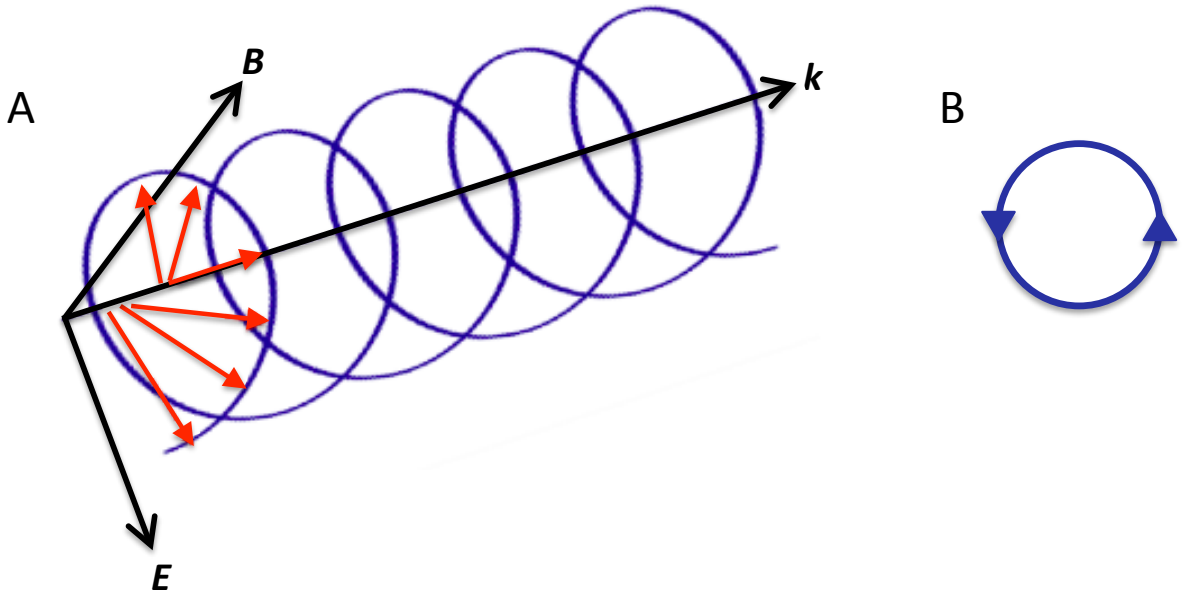

FIGURE 6-6. The principal of circular dichroism. (**A**) Right circularly polarised light traces out a vector field in an anti-clockwise circle (**B**). The magnetic field, *B*, is perpendicular to the electric field so that *k*, *E* and *B* form the right-handed system. Adapted from Rodger & Nordén (1997).

There are several advantages of using CD as a structural probe, including the quickness and simplicity of performing the experiment, the relatively low concentration of sample protein required and the fact that any size molecule can be studied, unlike NMR and crystallography, which can only provide detailed information for smaller proteins. The UV light is divided

into two groups: 'near' UV is the 250–300 nm region, where the aromatic residues (phenylalanine, tryptophan, tyrosine) and cysteine-cysteine disulfide bonds absorb. The amide backbones of proteins absorb in the 'far' UV region (~190–250 nm). Standard spectra have been identified for the α-helix, β-sheet, β-turn and random coil conformations (Figure 6-7).

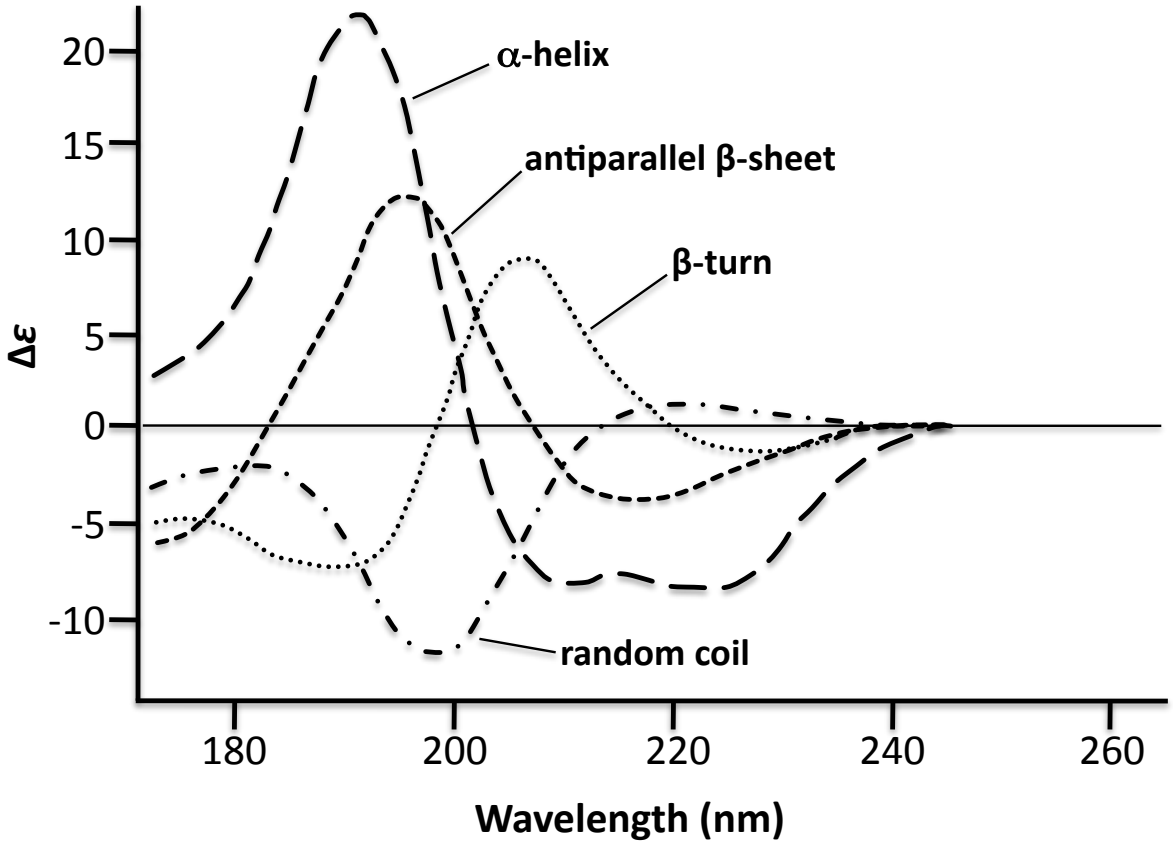

FIGURE 6-7. The standard CD spectra identifying the different secondary conformations of proteins observable. Adapted from Rodger & Nordén (1997).

6.4.2. Analytical ultracentrifugation.

Analytical ultracentrifugation (AUC) is a technique that can reveal several pieces of information about a solubilised protein, including size and shape, oligomerisation and protein-protein interactions (Balbo *et al*. 2009). The basic principle is that a protein sample is

monitored digitally as it is spun using ultra-violet light absorption and/or interference optical scanning. Sedimentation velocity (SV) and sedimentation equilibrium (SE) experiments are both widely performed with an AUC machine, however only the former was used in this project. SV is a time-course experiment that monitors the protein sample as it sediments. Results can disclose the shape and molecular mass of the sample as well as the non-covalent complexes that proteins form. SE cannot report on molecular shape but can provide molar mass and information on chemical equilibrium constants for reacting samples.

The protein sample needs to be around 99 % pure, however relatively low sample concentrations (0.1–5 mg/ml) and volumes (~500 µl) are required. The sample is loaded into a cell alongside a reference cell containing the buffer in which the protein is dissolved (Figure 6-8 A). When a strong centrifugal force is applied a moving boundary is formed. The distance moved by the boundary is recorded as a function of time (Figure 6-8 B). Computer data analysis programs, such as SEDFIT, are used to interpret the data obtained. For this project the analyses were kindly performed by Dr. T. Dafforn (University of Birmingham).

6.4.3. Crystallography.

6.4.3.1. Protein crystallisation.

In specific conditions, proteins can be forced to crystallise, whereby the purified protein slowly precipitates out from an aqueous buffered solution whilst not becoming denatured. During the process, individual protein molecules form a crystalline lattice by aligning in repeating unit cells, held together by non-covalent bonds. The objective behind crystallisation is to produce adequate crystals for X-ray diffraction, so that the tertiary structure of the protein can be obtained.

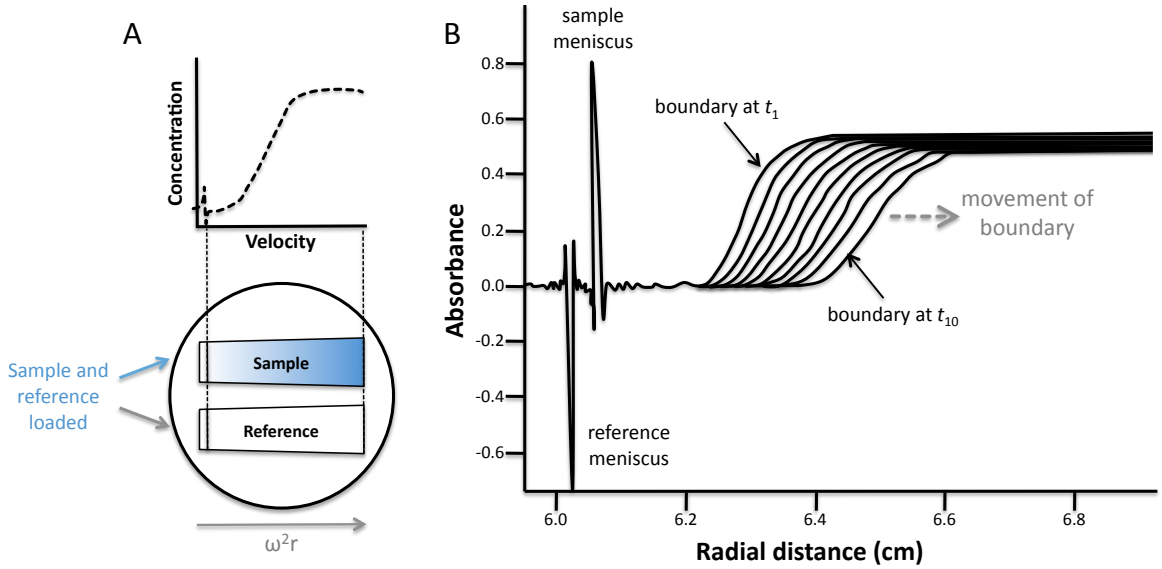

FIGURE 6-8. Analytical ultracentrifugation. (**A**) Sedimentation velocity cell. The sample is loaded into the top and the reference buffer into the bottom section. When centrifuged, the centrifugal force pushes the boundary towards the bottom of the cell. (**B**) Example of sedimentation velocity data. Ten scans are shown, t_1 being the first, t_{10} being the last. A larger volume of reference buffer is added than sample so the meniscuses can be distinguished. Adapted from Cole & Hansen (2000).

The most common method of crystallisation is to dissolve the protein (of at least 97 % purity) in a buffer solution that contains a precipitant, such as ammonium sulfate or polyethylene glycol (PEG). Over a period of time the water is removed, increasing both the protein and precipitant concentrations until crystals start to grow (Figure 6-9 A). One of the most common methods of crystallisation is vapour diffusion. Here, the protein/precipitant solution equilibrates with the reservoir solution, a larger volume containing an optimal precipitant concentration for crystallisation. Two examples of this method, both of which have been used in this project, are hanging-drop and sitting-drop vapour diffusion (Figure 6-9 B). With the hanging-drop system, the protein/precipitant droplet is suspended on the underside of a siliconised cover slip, which is then sealed to the top of the well containing the reservoir solution with air-tight vacuum grease. In the sitting-drop vapour diffusion technique, the droplet is pipetted directly onto a small plinth within or to the side of the reservoir well. The

wells are then covered with air-tight sealing tape.

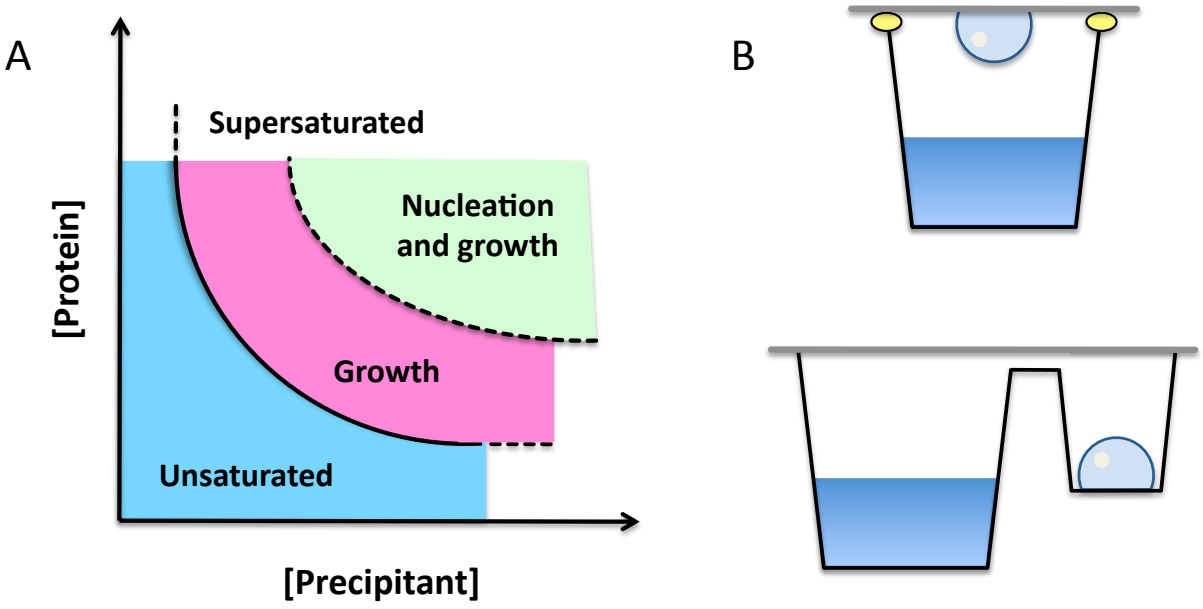

FIGURE 6-9. Conditions promoting protein crystallisation. (**A**) Phase diagram for protein crystallisation. (**B**) Hanging-drop vapour diffusion (*top*) and sitting-drop vapour diffusion (*bottom*). Adapted from Rhodes (2006).

The first stage of crystallisation is 'nucleation', where protein aggregates start to form. If this stage continues it is likely that many small crystals are made in a relatively short space of time, using up the source of soluble protein before large crystals form. The second stage is 'growth', which should result in crystals large enough to diffract. It is possible to 'streak seed' small but good quality crystals into new droplets by stroking the crystals with a hair and passing the hair through the new droplet. This is a faster way of obtaining crystals and it is more likely that more soluble protein makes up fewer bigger crystals (Rhodes 2006).

Before diffraction, the crystals are individually mounted in tiny loops (<1 mm diameter). Collecting X-ray data at very low temperatures is thought to improve diffraction by increasing molecular order, a process known as 'cryocrystallisation'. However, to protect the crystals from the intense cold of flash freezing in liquid nitrogen (–196 °C) and to prevent the

formation of ice crystals, which can interfere with the diffraction pattern, a cryoprotectant needs to first be applied. Within the original droplet the crystals are soaked in the cryoprotectant solution. This is the same as the precipitant solution but containing a concentration of glycerol, xylitol, glucose or PEG. The crystal is then scooped up in the loop, where it remains suspended in the cryoprotectant solution. The loop is dipped into liquid nitrogen and is kept at this low temperature until loaded onto the X-ray diffractor.

6.4.3.2. X-ray diffraction.

The principal behind X-ray diffraction is detecting the X-rays that have scattered after hitting the protein crystal. By then analysing the position of dots and their intensities formed by the scattered rays, a three-dimensional structure of the protein can be constructed. The crystal is mounted under a continuous stream of nitrogen gas (-100 °C) between the source of X-rays producing a narrow beam of rays and the detector (Figure 6-10). The detector could be an X-ray film, however in this project an optical scanner linked to a computer was used. All the analysis work for this project was kindly performed by Dr. K. Fütterer (University of Birmingham).

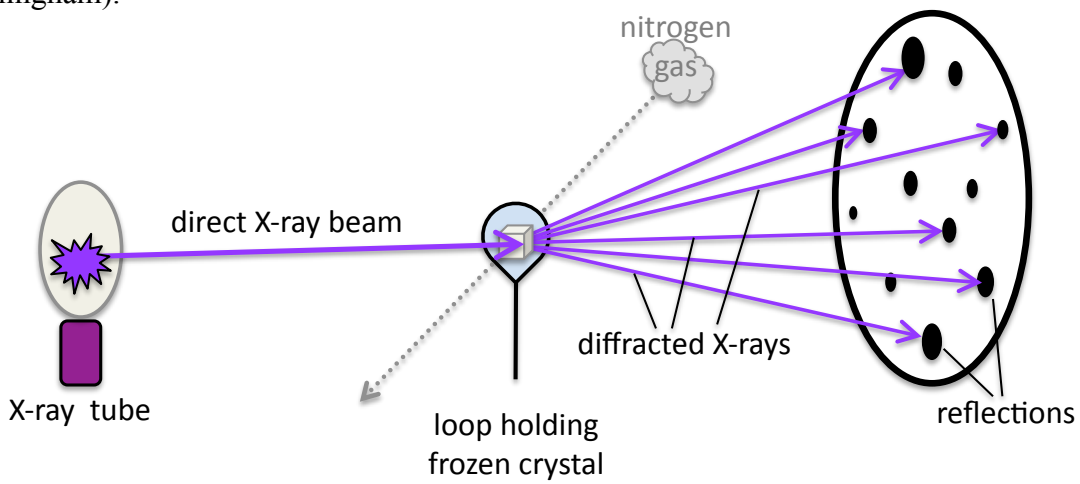

FIGURE 6-10. Schematic of X-ray crystallography. The crystal is held in suspension in cryoprotectant under a stream of nitrogen gas. X-ray beams are scattered by the crystal and data is collected electronically. Adapted from Rhodes 2006.

CHAPTER 7

References

Abdallah AM, Gey van Pittius NC, Champion PA, Cox J, Luirink J, Vandenbroucke-Grauls CM Appelmelk BJ, Bitter W (2007) Type VII secretion – mycobacteria show the way. **Nature Reviews Microbiology** 5: 883–891

Al-Balas Q, Anthony NG, Al-Jaidi B, Alnimr A, Abbott G, Brown AK, Taylor RC, Besra GS, McHugh TD, Gillespie SH, Johnston BF, Mackay SP, Coxon GD (2009) Identification of 2-aminothiazole-4-carboxylate derivatives active against *Mycobacterium tuberculosis* H_{37}Rv and the beta-ketoacyl-ACP synthase *mt*FabH. **PLoS One** 4: e5617

Alderwick LJ, Birch HL, Mishra AK, Eggeling L, Besra GS (2007) Structure, function and biosynthesis of the *Mycobacterium tuberculosis* cell wall: arabinogalactan and lipoarabinomannan assembly with a view to discovering new drug targets. **Biochemical Society Transactions** 35: 1325–1328

Alhamadsheh MM, Musayev F, Komissarov AA, Sachdeva S, Wright HT, Scarsdale N, Florova G, Reynolds KA (2007) Alkyl-CoA disulfides as inhibitors and mechanistic probes for FabH enzymes. **Chemistry and Biology** 14: 513–524

Altaf M, Miller CH, Bellows DS, O'Toole R (2010) Evaluation of the *Mycobacterium smegmatis* and BCG models for the discovery of *Mycobacterium tuberculosis* inhibitors. **Tuberculosis (Edinburgh)** 90: 333–337

Amar C, Vilkas E (1973) Isolation of arabinose phosphate from the walls of *Mycobacterium tuberculosis* H37Ra. **Comptes Rendus Hebdomadaires des Séances de l'Académie des Sciences. Série D: Sciences Naturelles** 277: 1949–1951

Amaral L, Martins A, Molnar J, Kristiansen JE, Martins M, Viveiros M, Rodrigues L, Spengler G, Couto I, Ramos J, Dastidar S, Fanning S, McCusker M, Pages JM (2010) Phenothiazines, bacterial efflux pumps and targeting the macrophage for enhanced killing of intracellular XDRTB. ***In vivo*** 24: 409–424

Ani A, Okpe S, Akambi M, Ejelinonu E, Yakubu B, Owolodun O, Ekeh P, Oche A, Tyen D, Idoko J (2009) Comparison of a DNA based PCR method with conventional methods for the detection of *M. tuberculosis* in Jos, Nigeria. **Journal of Infection in Developing Countries** 3: 470–475

Anthony LS, Chatterjee D, Brennan PJ, Nano FE (1994) Lipoarabinomannan from *Mycobacterium tuberculosis* modulates the generation of reactive nitrogen intermediates by gamma interferon-activated macrophages. **Federation of European Microbiological Societies Immunology and Medical Microbiology** 8: 299–305

API Consensus Expert Committee (2006) API TB Consensus Guidelines 2006: Management of pulmonary tuberculosis, extra-pulmonary tuberculosis and tuberculosis in special situations. **Journal of the Association of Physicians of India** 54: 219–234

Arnold K, Bordoli L, Kopp J, Schwede T (2006) The SWISS-MODEL Workspace: A web-based environment for protein structure homology modelling. **Bioinformatics** 22: 195–201

Aronson JD (1926) Spontaneous tuberculosis in salt water fish. **Journal of Infectious Diseases** 39: 314–320

Av-Gay Y, Everett M (2000) The eukaryotic-like Ser/Thr protein kinase of *Mycobacterium tuberculosis*. **Trends in Microbiology** 8: 238–244

Balbo A, Zhao H, Brown PH, Schuck P (2009) Assembly, loading, and alignment of an analytical ultracentrifuge sample cell. **Journal of Visualized Experiments** 5: 1530

Banerjee A, Dubnau E, Quémard A, Balasubramanian V, Um KS, Wilson T, Collins D, de Lisle G, Jacobs WR Jr. (1994) *inhA*, a gene encoding a target for isoniazid and ethionamide in *Mycobacterium tuberculosis*. **Science** 263: 227–230

Banerjee A, Sugantino M, Sacchettini JC, Jacobs WR Jr. (1998) The *mabA* gene from the *inhA* operon of *Mycobacterium tuberculosis* encodes a 3-ketoacyl reductase that fails to confer isoniazid resistance. **Microbiology** 144: 2697–2704

Bardarov S, Bardarov S Jr., Pavelka MS Jr., Sambandamurthy V, Larsen M, Tufariello J, Chan J, Hatfull G, Jacobs WR Jr. (2002) Specialized transduction: an efficient method for generating marked and unmarked targeted gene disruptions in *Mycobacterium tuberculosis*, *M. bovis* BCG and *M. smegmatis*. **Microbiology** 148: 3007–3017

Barton A, Breukelman SP, Kaye PT, Meakins DG, Morgan DJ (1982) The preparation of thiazole-4- and -5-carboxylates, and an infrared study of their rotational isomers. **Journal of the Chemical Society** 1: 159–164

Barycki JJ, O'Brien LK, Bratt JM, Zhang R, Sanishvili R, Strauss AW, Banaszak LJ (1999) Biochemical characterization and crystal structure determination of human heart short chain L-3-hydroxyacyl-CoA dehydrogenase provide insights into catalytic mechanism. **Biochemistry** 38: 5786–5798

Bauer QW, Kirby WM, Sherris JC, Turck M (1966) Antibiotic susceptibility testing by a standardized single disk method. **Journal of Clinical Pathology** 45: 493–496

Baulard AR, Betts JC, Engohang-Ndong J, Quan S, McAdam RA, Brennan PJ, Locht C, Besra GS (2000) Activation of the pro-drug ethionamide is regulated in mycobacteria. **Journal of Biological Chemistry** 275: 28326–28331

Beharka AA, Gaynor CD, Kang BK, Voelker DR, McCormack FX, Schlesinger LS (2002) Pulmonary surfactant protein A up-regulates activity of the mannose receptor, a pattern recognition receptor expressed on human macrophages. **Journal of Immunology** 169: 3565–3573

Belanger AE, Besra GS, Ford ME, Mikusova K, Belisle JT, Brennan PJ, Inamine JM (1996) The *embAB* genes of *Mycobacterium avium* encode an arabinosyl transferase involved in cell wall arabinan biosynthesis that is the target for the antimycobacterial drug ethambutol. **Proceedings of the National Academy of Sciences of the United States of America** 93: 11919–11924

Belisle JT, Vissa VD, Sievert T, Takayama K, Brennan PJ, Besra GS (1997) Role of the major antigen of *Mycobacterium tuberculosis* in cell wall biosynthesis. **Science** 276: 1420–1422

Belley A, Alexander D, Di Pietrantonio T, Girard M, Jones J, Schurr E, Liu J, Sherman DR, Behr MA (2004) Impact of methoxymycolic acid production by *Mycobacterium bovis* BCG vaccines. **Infection and Immunity** 72: 2803–2809

Beran V, Matlova L, Dvorska L, Svastova P, Pavlik I (2006) Distribution of mycobacteria in clinically healthy ornamental fish and their aquarium environment. **Journal of Fish Diseases** 29: 383–393

Bhamidi S, Scherman MS, Rithner CD, Prenni JE, Chatterjee D, Khoo KH, McNeil MR (2008) The identification and location of succinyl residues and the characterization of the interior arabinan region allow for a model of the complete primary structure of *Mycobacterium tuberculosis* mycolyl arabinogalactan. **Journal of Biological Chemistry** 283: 12992–13000

Bhargava HN, Leonard PA (1996) Triclosan: applications and safety. **American Journal of Infection Control** 24: 209–218

Bhatt A, Kremer L, Dai AZ, Sacchettini JC, Jacobs WR Jr. (2005) Conditional depletion of KasA, a key enzyme of mycolic acid biosynthesis, leads to mycobacterial cell lysis. **Journal of Bacteriology** 187: 7596–7606

Bhatt A, Molle V, Besra GS, Jacobs WR Jr., Kremer L (2007a) The *Mycobacterium tuberculosis* FAS-II condensing enzymes: their role in mycolic acid biosynthesis, acid fastness, pathogenesis and in future drug development. **Molecular Microbiology** 64: 1442–1454

Bhatt A, Fujiwara N, Bhatt K, Gurcha SS, Kremer L, Chen B, Chan J, Porcelli SA, Kobayashi K, Besra GS, Jacobs WR Jr. (2007b) Deletion of *kasB* in *Mycobacterium tuberculosis* causes loss of acid-fastness and subclinical latent tuberculosis in immunocompetent mice. **Proceedings of the National Academy of Sciences of the United States of America** 104: 5157–5162

Bhatt A, Brown AK, Singh A, Minnikin DE, Besra GS (2008) Loss of a mycobacterial gene encoding a reductase leads to an altered cell wall containing beta-oxo-mycolic acid analogs and accumulation of ketones. **Chemistry and Biology** 15: 930–939

Bhowruth V, Brown AK, Senior SJ, Snaith JS, Besra GS (2007) Synthesis and biological evaluation of a C5-biphenyl thiolactomycin library. **Bioorganic and Medicinal Chemistry Letters** 17: 5643–5646

Bhowruth V, Brown AK, Besra GS (2008) Synthesis and biological evaluation of NAS-21 and NAS-91 analogues as potential inhibitors of the mycobacterial FAS-II dehydratase enzyme Rv0636. **Microbiology** 154: 1866–1875

Birkness KA, Deslauriers M, Bartlett JH, White EH, King CH, Quinn FD (1999) An *in vitro* culture bilayer model to examine early events in *Mycobacterium tuberculosis* infection. **Infection and Immunity** 67: 653–658

Bishai W (2000) Microbiology: Lipid lunch for persistent pathogen. **Nature** 406: 683–685

Black PN, DiRusso CC (1994) Molecular and biochemical analyses of fatty acid transport, metabolism, and gene regulation in *Escherichia coli*. **Biochimica et Biophysica Acta** 1210: 123–145

Bloch H, Segal W (1956) Biochemical differentiation of *Mycobacterium tuberculosis* grown *in vivo* and *in vitro*. **Journal of Bacteriology** 72: 132–141

Booth RG (2007) Psychotherapeutic drugs: Antipsychotic and Anxiolytic Agents *in* **Foye's Principles of Medicinal Chemistry** pp. 601–630. Edited by Foye WO, Lemke TL, Williams DA, Roche VF, Zito SW. USA: Lippincott Williams & Wilkins

Briken V, Porcelli SA, Besra GS, Kremer L (2004) Mycobacterial lipoarabinomannan and related lipoglycans: from biogenesis to modulation of the immune response. **Molecular Microbiology** 53: 391–403

Brown AK, Sridharan S, Kremer L, Lindenberg S, Dover LG, Sacchettini JC, Besra GS (2005) Probing the mechanism of the Mycobacterium tuberculosis beta-ketoacyl-acyl carrier protein synthase III *mt*FabH: factors influencing catalysis and substrate specificity. **Journal of Biological Chemistry** 280: 32539–32547

Brown AK, Bhatt A, Singh A, Saparia E, Evans AF, Besra GS (2007a) Identification of the dehydratase component of the mycobacterial mycolic acid-synthesizing fatty acid synthase-II complex. **Microbiology** 153: 4166–4173

Brown AK, Papaemmanouil A, Bhowruth V, Bhatt A, Dover LG, Besra GS (2007b) Flavonoid inhibitors as novel antimycobacterial agents targeting Rv0636, a putative dehydratase enzyme involved in *Mycobacterium tuberculosis* fatty acid synthase II. **Microbiology** 153: 3314–3322

Brown AK, Taylor RC, Bhatt A, Fütterer K, Besra GS (2009) Platensimycin activity against mycobacterial beta-ketoacyl-ACP synthases. **PLoS One** 4: e6306

Brünger AT (2007) Version 1.2 of the Crystallography and NMR system. **Nature Protocols** 2: 2728–2733

Buist PH (2007) Exotic biomodification of fatty acids. **Natural Products Reports** 24: 1110–1127

Camacho LR, Ensergueix D, Perez E, Gicquel B, Guilhot C (1999) Identification of a virulence gene cluster of *Mycobacterium tuberculosis* by signature-tagged transposon mutagenesis. **Molecular Microbiology** 34: 257–267

Camacho LR, Constant P, Raynaud C, Lanéelle MA, Triccas JA, Gicquel B, Daffé M, Guilhot C (2001) Analysis of the phthiocerol dimycocerosate locus of *Mycobacterium tuberculosis*. Evidence that this lipid is involved in the cell wall permeability barrier. **Journal of Biological Chemistry** 276: 19845–19854

Campbell EA, Korzheva N, Mustaev A, Murakami K, Nair S, Goldfarb A, Darst SA (2001) Structural mechanism for rifampicin inhibition of bacterial RNA polymerase. **Cell** 104: 901–912

Campbell IA, Bah-Sow O (2006) Pulmonary tuberculosis: diagnosis and treatment. **British Medical Journal (Clinical Research Edition)** 332: 1194–1197

Canova MJ, Veyron-Churlet R, Zanella-Cléon I, Cohen-Gonsaud M, Cozzone AJ, Bacchi M, Kremer L, Molle V (2008) The *Mycobacterium tuberculosis* serine/threonine kinase PknL phosphorylates Rv2175c: mass spectrometric profiling of the activation loop phosphorylation sites and their role in the recruitment of Rv2175c. **Proteomics** 8: 521–533

Castell A, Johansson P, Unge T, Jones TA, Bäckbro K (2005) Rv0216, a conserved hypothetical protein from *Mycobacterium tuberculosis* that is essential for bacterial survival during infection, has a double hotdog fold. **Protein Science** 14: 1850–1862

Chan J, Fan XD, Hunter SW, Brennan PJ, Bloom BR (1991) Lipoarabinomannan, a possible virulence factor involved in persistence of *Mycobacterium tuberculosis* within macrophages. **Infection and Immunity** 59: 1755–1761

Chang JC, Miner MD, Pandey AK, Gill WP, Harik NS, Sassetti CM, Sherman DR (2009) *igr* genes and *Mycobacterium tuberculosis* cholesterol metabolism. **Journal of Bacteriology** 191: 5232–5239

Chatterjee D, Khoo KH (1998) Mycobacterial lipoarabinomannan: an extraordinary lipoheteroglycan with profound physiological effects. **Glycobiology** 8: 113–120

Chaudhuri RR, Loman NJ, Snyder LA, Bailey CM, Stekel DJ, Pallen MJ (2008) *x*BASE2: a comprehensive resource for comparative bacterial genomics. **Nucleic Acids Research** 36: D543–546

Chung DK, Hubbard WW (1969) Hyponatremia in untreated active pulmonary tuberculosis. **American Review of Respiratory Disease** 99: 595–597

Choi KH, Kremer L, Besra GS, Rock CO (2000) Identification and substrate specificity of beta-ketoacyl (acyl carrier protein) synthase III (*mt*FabH) from *Mycobacterium tuberculosis*. **Journal of Biological Chemistry** 275: 28201–28207

Cohen-Gonsaud M, Ducasse S, Hoh F, Zerbib D, Labesse G, Quémard A (2002) Crystal structure of MabA from *Mycobacterium tuberculosis*, a reductase involved in long-chain fatty acid biosynthesis. **Journal of Molecular Biology** 320: 249–261

Cohen-Gonsaud M, Barthe P, Pommier F, Harris R, Driscoll PC, Keep NH, Roumestand C (2004) (1)H, (15)N, and (13)C chemical shift assignments of the resuscitation promoting factor domain of Rv1009 from *Mycobacterium tuberculosis*. **Journal of Biomolecular NMR** 30: 373–374

Cohen-Gonsaud M, Barthe P, Bagnéris C, Henderson B, Ward J, Roumestand C, Keep NH (2005) The structure of a resuscitation-promoting factor domain from *Mycobacterium tuberculosis* shows homology to lysozymes. **Nature Structural & Molecular Biology** 12: 270–273

Cohn ML, Waggoner RF, McClatchy JK (1968) The 7H11 medium for the cultivation of mycobacteria. **American Review of Respiratory Disease** 98: 295–296

Colditz GA, Berkey CS, Mosteller F, Brewer TF, Wilson ME, Burdick E, Fineberg HV (1995) The efficacy of bacillus Calmette-Guérin vaccination of newborns and infants in the prevention of tuberculosis: meta-analyses of the published literature. **Pediatrics** 96: 29–35

Cole JL, Hansen JC (2000) Analytical ultracentrifugation as a contemporary biomolecular research tool. **Methods and Reviews** *at* **The Association of Biomolecular Resourse Facilities** <http://www.abrf.org>

Cole ST, Brosch R, Parkhill J, Garnier T, Churcher C, Harris D, Gordon SV, Eiglmeier K, Gas S, Barry CE 3rd, Tekaia F, Badcock K, Basham D, Brown D, Chillingworth T, Connor R, Davies R, Devlin K, Feltwell T, Gentles S, Hamlin N, Holroyd S, Hornsby T, Jagels K, Krogh A, McLean J, Moule S, Murphy L, Oliver K, Osborne J, Quail MA, Rajandream M-A, Rogers J, Rutter S, Seeger K, Skelton J, Squares R, Squares S, Sulsto JE, Taylor K, Whitehead S, Barrell BG (1998) Deciphering the biology of *Mycobacterium tuberculosis* from the complete genome sequence. **Nature** 393: 537–544

Cole ST, Eiglmeier K, Parkhill J, James KD, Thomson NR, Wheeler PR, Honore N, Garnier T, Churcher C, Harris D, Mungall K, Basham D, Brown D, Chillingworth T, Connor R, Davies RM, Devlin K, Duthoy S, Feltwell T, Fraser A, Hamlin N, Holroyd S, Hornsby T, Jagels K, Lacroix C, Maclean J, Moule S, Murphy L, Oliver K, Quail MA, Rajandream MA, Rutherford KM, Rutter S, Seeger K, Simon S, Simmonds M, Skelton J, Squares R, Squares S, Stevens K, Taylor K, Whitehead S, Woodward JR, Barrell BG (2001) Massive gene decay in the leprosy bacillus. **Nature** 409: 1007–1011

Colston MJ, Cox, RA (1999) Mycobacterial growth and dormancy *in* **Mycobacteria: Molecular Biology and Virulence** pp. 198–219. Edited by Ratledge C, Dale J. Great Britain: Blackwell Science Ltd.

Côtes K, Bakala N'goma JC, Dhouib R, Douchet I, Maurin D, Carrière F, Canaan S (2008) Lipolytic enzymes in *Mycobacterium tuberculosis*. **Applied Microbiology and Biotechnology** 78: 741–749

Cottin V, Van Linden A, Riches DW (1999) Phosphorylation of tumor necrosis factor receptor CD120a (p55) by p42(mapk/erk2) induces changes in its subcellular localization. **Journal of Biological Chemistry** 274: 32975–32987

Cowley S, Ko M, Pick N, Chow R, Downing KJ, Gordhan BG, Betts JC, Mizrahi V, Smith DA, Stokes RW, Av-Gay Y (2004) The *Mycobacterium tuberculosis* protein serine/threonine kinase PknG is linked to cellular glutamate/glutamine levels and is important for growth *in vivo*. **Molecular Microbiology** 52: 1691–1702

Cox JS, Chen B, McNeil M, Jacobs WR Jr. (1999) Complex lipid determines tissue-specific replication of *Mycobacterium tuberculosis* in mice. **Nature** 402: 79–83

Cox H, Kebede Y, Allamuratova S, Ismailov G, Davletmuratova Z, Byrnes G, Stone C, Niemann S, Rüsch-Gerdes S, Blok L, Doshetov D (2006) Tuberculosis recurrence and mortality after successful treatment: Impact of drug resistance. **PLoS ONE** 3: e384

Crick DC, Mahapatra S, Brennan PJ (2001) Biosynthesis of the arabinogalactan-peptidoglycan complex of *Mycobacterium tuberculosis*. **Glycobiology** 11: 107R–118R

Cronan JE Jr., Waldrop GL (2002) Multi-subunit acetyl-CoA carboxylases. **Progress in Lipid Research** 41: 407–435

Curry JM, Whalan R, Hunt DM, Gohil K, Strom M, Rickman L, Colston MJ, Smerdon SJ, Buxton RS (2005) An ABC transporter containing a forkhead-associated domain interacts with a serine-threonine protein kinase and is required for growth of *Mycobacterium tuberculosis* in mice. **Infection and Immunity** 73: 4471–4477

Daffé M, Draper P (1998) The envelope layers of mycobacteria with reference to their pathogenicity. **Advances in Microbial Physiology** 39: 131–203

Dam T, Danelishvili L, Wu M, Bermudez LE (2006) The *fadD2* gene is required for efficient *Mycobacterium avium* invasion of mucosal epithelial cells. **Journal of Infectious Diseases** 193: 1135–1142

Daniel J, Oh TJ, Lee CM, Kolattukudy PE (2007) AccD6, a member of the FasII locus, is a functional carboxyltransferase subunit of the acyl-coenzyme A carboxylase in *Mycobacterium tuberculosis*. **Journal of Bacteriology** 189: 911–917

Dasgupta A, Datta P, Kundu M, Basu J (2006) The serine/threonine kinase PknB of *Mycobacterium tuberculosis* phosphorylates PBPA, a penicillin-binding protein required for cell division. **Microbiology** 152: 493–504

Davies C, Heath RJ, White SW, Rock CO (2000) The 1.8 Å crystal structure and active site architecture of β-ketoacyl-acyl carrier protein synthase III (FabH) from *Escherichia coli*. **Structure** 8: 185–195

Davies RPO, Tocque K, Bellis MA, Remmington T, Davies PDO (1999) Historical declines in tuberculosis in England and Wales: improving social conditions or natural selection? **Vesalius: Acta Internationales Historiae Medicinae** 5: 25–29

DeBarber AE, Mdluli K, Bosman M, Bekker LG, Barry CE 3rd (2000) Ethionamide activation and sensitivity in multidrug-resistant *Mycobacterium tuberculosis*. **Proceedings of the National Academy of Sciences of the United States of America** 97: 9677–9682

De la Rua-Domenech R (2006) Human *Mycobacterium bovis* infection in the United Kingdom: Incidence, risks, control measures and review of the zoonotic aspects of bovine tuberculosis. **Tuberculosis (Edinburgh)** 86: 77–109

de Marco A, Deuerling E, Mogk A, Tomoyasu T, Bukau B (2007) Chaperone-based procedure to increase yields of soluble recombinant proteins produced in *E. coli*. **BMC Biotechnology** 7: 32

de Marco A (2011a) Molecular and chemical chaperones for improving the yields of soluble recombinant proteins. **Methods in Molecular Microbiology** 705: 31–51

de Marco A (2011b) Strategies for boosting the accumulation of correctly folded recombinant proteins expressed in *Escherichia coli*. **Methods in Molecular Microbiology** 752: 1–15

De Rossi E, Aínsa JA, Riccardi G (2006) Role of mycobacterial efflux transporters in drug resistance: an unresolved question. **Federation of European Microbiological Societies Microbiology Reviews** 30: 36–52

de Souza MVN (2009) Promising candidates in clinical trials against multidrug-resistant tuberculosis (MDR-TB) based on natural products. **Filoterapia** 80: 453–460

Deol P, Vohra R, Saini AK, Singh A, Chandra H, Chopra P, Das TK, Tyagi AK, Singh Y (2005) Role of *Mycobacterium tuberculosis* Ser/Thr kinase PknF: implications in glucose transport and cell division. **Journal of Bacteriology** 187: 3415–3420

Dillon SC, Bateman A (2004) The Hotdog fold: wrapping up a superfamily of thioesterases and dehydratases. **BMC Bioinformatics** 5: 109

DiRusso (1990) Primary sequence of the *Escherichia coli fadBA* operon, encoding the fatty acid-oxidizing multienzyme complex, indicates a high degree of homology to eucaryotic enzymes. **Journal of Bacteriology** 172: 6459–6468

DiRusso CC, Heimert TL, Metzger AK (1992) Characterization of FadR, a global transcriptional regulator of fatty acid metabolism in *Escherichia coli*. Interaction with the *fadB* promoter is prevented by long chain fatty acyl coenzyme A. **Journal of Biological Chemistry** 267: 8685–8691

Dobson G, Minnikin DE, Minnikin SM, Parlett JH, Goodfellow M, Ridell M, Magnusson M (1985) Systematic analysis of complex mycobacterial lipids *in* **Chemical Methods in Bacterial Systematics** pp. 237–265. Edited by Goodfellow M, Minnikin DE. London: Academic Press

Doetsch RN (1978) Benjamin Marten and his "New Theory of Consumptions". **Microbiological Reviews** 42: 521–528

Dommes V, Kunau WH (1984) 2,4-Dienoyl coenzyme A reductases from bovine liver and *Escherichia coli*. **Journal of Biological Chemistry** 259: 1781–1788

Dosanjh DP, Hinks TS, Innes JA, Deeks JJ, Pasvol G, Hackforth S, Varia H, Millington KA, Gunatheesan R, Guyot-Revol V, Lalvani A (2008) Improved diagnostic evaluation of suspected tuberculosis. **Annals of Internal Medicine** 148: 325–336

Dover LG, Corsino PE, Daniels IR, Cocklin SL, Tatituri V, Besra GS, Fütterer K (2004) Crystal structure of the TetR/CamR family repressor *Mycobacterium tuberculosis* EthR implicated in ethionamide resistance. **Journal of Molecular Biology** 340: 1095–1105

Ducasse-Cabanot S, Cohen-Gonsaud M, Marrakchi H, Nguyen M, Zerbib D, Bernadou J, Daffé M, Labesse G, Quémard A (2004) *In vitro* inhibition of the *Mycobacterium tuberculosis* beta-ketoacyl-acyl carrier protein reductase MabA by isoniazid. **Antimicrobial Agents and Chemotherapy** 48: 242–249

Dunphy KY, Senaratne RH, Masuzawa M, Kendall LV, Riley LW (2010) Attenuation of *Mycobacterium tuberculosis* functionally disrupted in a fatty acyl-coenzyme A synthetase gene *fadD5*. **Journal of Infectious Diseases** 201: 1232–1239

Dyer DH, Lyle KS, Rayment I, Fox BG (2005) X-ray structure of putative acyl-ACP desaturase DesA2 from *Mycobacterium tuberculosis* H37Rv. **Protein Science** 14: 1508–1517

Ebrahim O, Folb PI, Robson SC, Jacobs P (2009) Blunted erythropoietin response to anaemia in tuberculosis. **Haematology** 55: 251–254

El-Fakhri M, Middleton B (1982) The existence of an inner-membrane-bound, long acyl-chain-specific 3-hydroxyacyl-CoA dehydrogenase in mammalian mitochondria. **Biochimica et Biophysica Acta** 713: 270–279

Emmart EW (1945) The tuberculostatic action of streptothricin and streptomycin with special reference to the action of streptomycin on the chorioallantoic membrane of the chick embryo. **US Public Health Service, Public Health Reports** 60: 1415–1421

Ernst JD (1998) Macrophage receptors for *Mycobacterium tuberculosis*. **Infection and Immunity** 66: 1277–1281

Escalante P, Ramaswamy S, Sanabria H, Soini H, Pan X, Valiente-Castillo O, Musser JM (1998) Genotypic characterization of drug-resistant *Mycobacterium tuberculosis* isolate from Peru. **Tubercle and Lung Disease** 79: 111–118

Esko JD, Doering TL, Raetz CRH (2009) Organismal Diversity: Eubacteria and Archaea *in* **Essentials of Glycobiology** Edited by Varki A, Cummings RD, Esko JD, Freeze HH, Stanley P, Bertozzi CR, Hart GW, Etzler ME. New York: Cold Spring Harbor Laboratory Press. Accessed *via* NCBI Bookshelf, ID: NBK1945

Ezekiel DH, Hutchins JE (1968) Mutations affecting RNA polymerase associated with rifampicin resistance in *Escherichia coli*. **Nature** 220: 276–277

FASgen, Inc. (2005) FASgen compound FAS20013 demonstrates remarkable killing effect against TB. **FASgen Press Releases** May 12 <http://www.fasgen.com/pr-january122005.html>

Fernandez P, Saint-Joanis B, Barilone N, Jackson M, Gicquel B, Cole ST, Alzari PM (2006) The Ser/Thr protein kinase PknB is essential for sustaining mycobacterial growth. **Journal of Bacteriology** 188: 7778–7784

Ferreras JA, Stirrett KL, Lu X, Ryu JS, Soll CE, Tan DS, Quadri LE (2008) Mycobacterial phenolic glycolipid virulence factor biosynthesis: mechanism and small-molecule inhibition of polyketide chain initiation. **Chemistry and Biology** 15: 51–61

Fisher MA, Plikaytis BB, Shinnick TM (2002) Microarray analysis of the *Mycobacterium tuberculosis* transcriptional response to the acidic conditions found in phagosomes. **Journal of Bacteriology** 184: 4025–4032

Fiuza M, Canova MJ, Zanella-Cléon I, Becchi M, Cozzone AJ, Mateos LM, Kremer L, Gil JA, Molle V (2008) From the characterization of the four serine/threonine protein kinases (PknA/B/G/L) of *Corynebacterium glutamicum* toward the role of PknA and PknB in cell division. **Journal of Biological Chemistry** 283: 18099–18112

Flipo M, Desroses M, Lecat-Guillet N, Dirie B, Carette X, Leroux F, Piveteau C, Demirkaya F, Lens Z, Rucktooa P, Villeret V, Christophe T, Jeon HK, Locht C, Brodin P, Deprez B, Baulard AR, Willand N (2011) Ethionamide boosters: synthesis, biological activity, and structure-activity relationships of a series of 1,2,4-oxadiazole EthR inhibitors. **Journal of Medicinal Chemistry** 54: 2994–3010

Franzblau SG, Witzig RS, McLaughlin JC, Torres P, Madico G, Hernandez A, Degnan MT, Cook MB, Quenzer VK, Ferguson RM, Gilman RH (1998) Rapid, low-technology MIC determination with clinical *Mycobacterium tuberculosis* isolates by using the microplate Alamar Blue assay. **Journal of Clinical Microbiology** 36: 362–366

Fujita Y, Matsuoka H, Hirooka K (2007) Regulation of fatty acid metabolism in bacteria. **Molecular Microbiology** 66: 829–839

Galeotti F, Barile E, Curir P, Dolci M, Lanzotti V (2008) Flavonoids from carnation (*Dianthus caryophyllus*) and their antifungal activity. **Phytochemistry Letters** 1: 44–48

Gande R, Gibson KJ, Brown AK, Krumbach K, Dover LG, Sahm H, Shioyama S, Oikawa T, Besra GS, Eggeling L (2004) Acyl-CoA carboxylases (accD2 and accD3), together with a unique polyketide synthase (*Cg*-pks), are key to mycolic acid biosynthesis in Corynebacterianeae such as *Corynebacterium glutamicum* and *Mycobacterium tuberculosis*. **Journal of Biological Chemistry** 279: 44847–44857

Garnier JG, Gibrat JF, Robson B (1996) GOR secondary structure prediction method version IV. **Methods in Enzymology** 266: 540–553

Gasteiger E, Hoogland C, Gattiker A, Duvaud S, Wilkins MR, Appel RD, Bairoch A (2005) Protein identification and analysis tools on the ExPASy server *in* **The Proteomics Protocols Handbook**, pp. 571–607. Edited by Walker JM. Totowa, NJ: Humana Press

Gatfield J, Pieters J (2000) Essential role for cholesterol in entry of mycobacteria into macrophages. **Science** 288: 1647–1650

Gaud RS, Gupta GD (2008) Identification of Micro-organisms *in* **Practical Microbiology**, pp. 27–28. Pune: Nirali Prakashan

Gavalda S, Léger M, van der Rest B, Stella A, Bardou F, Montrozier H, Chalut C, Burlet-Schiltz O, Marrakchi H, Daffé M, Quémard A (2009) The Pks13/FadD32 crosstalk for the biosynthesis of mycolic acids in *Mycobacterium tuberculosis*. **Journal of Biological Chemistry** 284: 19255–19264

Ghadbane H, Brown AK, Kremer L, Besra GS, Futterer K (2007) Structure of *Mycobacterium tuberculosis mt*FabD, a malonyl-CoA:acyl carrier protein transacylase (MCAT). **Acta Crystallographica Section F: Structural Biology and Crystallization Communications** 63: 831–835

Geoffroy C, Gaillard JL, Alouf JE, Berche P (1987) Purification, characterization, and toxicity of the sulfhydryl-activated hemolysin listeriolyin O from *Listeria monocytogenes*. **Infection and Immunity** 55: 1641–1646

Glickman MS, Jacobs WR Jr. (2001) Microbial pathogenesis of *Mycobacterium tuberculosis*: dawn of a discipline. **Cell** 104: 477–485

Glickman MS, Cox JS, Jacobs WR Jr. (2000) A novel mycolic acid cyclopropane synthetase is required for cording, persistence, and virulence of *Mycobacterium tuberculosis*. **Molecular Cell** 5: 717–727

Glickman MS, Cahill SM, Jacobs WR Jr. (2001) The *Mycobacterium tuberculosis cmaA2* gene encodes a mycolic acid *trans*-cyclopropane synthetase. **Journal of Biological Chemistry** 276: 2228–2233

Gouet P, Courcelle E, Stuart DI, Metoz F (1999) ESPript: analysis of multiple sequence alignments in PostScript. **Bioinformatics** 15: 305–308

Greenwood D, Finch R, Davey P, Wilcox M (2007) General properties of antimicrobial agents: Inhibitors of bacterial protein synthesis *in* **Antimicrobial Chemotherapy** pp. 35–54. Edited by Greenwood D. Great Britain: Oxford University Press

Grogan DW, Cronan JE Jr. (1997) Cyclopropane ring formation in membrane lipids of bacteria. **Microbiology and Molecular Biology Reviews** 61: 429–441

Guérardel Y, Maes E, Elass E, Leroy Y, Timmerman P, Besra GS, Locht C, Strecker G, Kremer L (2002) Structural study of lipomannan and lipoarabinomannan from *Mycobacterium chelonae*. Presence of unusual components with alpha 1,3-mannopyranose side chains. **Journal of Biological Chemistry** 277: 30635–30648

Gupta P, Aggarwal N, Batra P, Mishra S, Chaudhuri TK (2006) Co-expression of chaperonin GroEL/GroES enhances *in vivo* folding of yeast mitochondrial aconitase and alters the growth characteristics of *Escherichia coli*. **International Journal of Biochemistry and Cell Biology** 38: 1975–1985

Gurvitz A, Hiltunen JK, Kastaniotis AJ (2008) Identification of a novel mycobacterial 3-hydroxyacyl-thioester dehydratase, HtdZ (Rv0130), by functional complementation in yeast. **Journal of Bacteriology** 190: 4088–4090

Gurvitz A (2009) The essential mycobacterial genes, *fabG1* and *fabG4*, encode 3-oxoacyl-thioester reductases that are functional in yeast mitochonidrial fatty acid synthase type 2. **Molecular Genetics and Genomics** 282: 407–416

Gurvitz A, Hiltunen JK, Kastaniotis AJ (2009) Heterologous expression of mycobacterial proteins in *Saccharomyces cerevisiae* reveals two physiologically functional 3-hydroxyacyl-thioester dehydratases, HtdX and HtdY, in addition to HadABC and HtdZ. **Journal of Bacteriology** 191: 2683–2690

Gutierrez MC, Brisse S, Brosch R, Fabre M, Omaïs B, Marmiesse M, Supply P, Vincent V (2006) Ancient origin and gene mosaicism of the progenitor of *Mycobacterium tuberculosis*. **PLoS Pathogens** 2: e98

Hachani A, Biskri L, Rossi G, Marty A, Ménard R, Sansonetti P, Parsot C, Van Nhieu GT, Bernardini ML, Allaoui A (2008) IpgB1 and IpgB2, two homologous effectors secreted via the Mxi-Spa type III secretion apparatus, cooperate to mediate polarized cell invasion and inflammatory potential of *Shigella flexenri*. **Microbes and Infection** 10: 260–268

Hanks SK, Quinn AM, Hunter T (1988) The protein kinase family: conserved features and deduced phylogeny of the catalytic domains. **Science** 241: 42–52

Hanna LE, Bose JC, Nayak K, Subramanyam S, Swaminathan S (2005) Short communication: Influence of active tuberculosis on chemokine and chemokine receptor expression in HIV-infected persons. **AIDS Research and Human Retroviruses** 21: 997–1002

He XY, Yang SY, Schultz H (1989) Assay of L-3-hydroxyacyl-coenzyme A dehydrogenase with substrates of different chain lengths. **Analytical Biochemistry** 180: 105–109

He XY, Yang SY, Schulz H (1997) Cloning and expression of the *fadH* gene and characterization of the gene product 2,4-dienoyl coenzyme A reductase from *Escherichia coli*. **European Journal of Biochemistry** 248: 516–520

Health Protection Agency (2009) TB figures continue to increase. <www.hpa.nhs.uk/web/HPAwebFile/HPAweb_C/1259152020077>

Heath RJ, Rock CO (1996a) Roles of the FabA and FabZ beta-hydroxyacyl-acyl carrier protein dehydratases in *Escherichia coli* fatty acid biosynthesis. **Journal of Biological Chemistry** 271: 27795–27801

Heath RJ, Rock CO (1996b) Inhibition of beta-ketoacyl-acyl carrier protein synthase III (FabH) by acyl-acyl carrier protein in *Escherichia coli*. **Journal of Biological Chemistry** 271: 10996–11000

Heath RJ, Yu YT, Shapiro MA, Olson E, Rock CO (1998) Broad spectrum antimicrobial biocides target the FabI component of fatty acid synthesis. **Journal of Biological Chemistry** 273: 30316–30320

Heath RJ, Rock CO (2004) Fatty acid biosynthesis as a target for novel antibacterials. **Current Opinion in Investigative Drugs** 5: 146–153

Hernández-Pando R, Orozco-Esteves H, Maldonado HA, Aguillar-León D, Vilchis-Landeros MM, Mata-Espinosa DA, Mendoza V, López-Casillas F (2006) A combination of a transforming growth factor-beta antagonist and an inhibitor of cyclooxygenase is an effective treatment for murine pulmonary tuberculosis. **Clinical and Experimental Immunology** 144: 264–272

Herzog H (1998) History of tuberculosis. **Respiration** 65: 5–15

Hirsch CS, Yoneda T, Averill L, Ellner JJ, Toossi Z (1994) Enhancement of intracellular growth of *Mycobacterium tuberculosis* in human monocytes by transforming growth factor-beta 1. **Journal of Infectious Diseases** 170: 1229–1237

Hoffmann C, Leis A, Niederweis M, Plitzko JM, Engelhardt H (2008) Disclosure of the mycobacterial outer membrane: cryo-electron tomography and vitreous sections reveal the lipid bilayer structure. **Proceedings of the National Academy of Sciences of the United States of America** 105: 3963–3967

Hotter GS, Wards BJ, Mouat P, Besra GS, Gomes J, Singh M, Bassett S, Kawakami P, Wheeler PR, de Lisle GW, Collins DM (2005) Transposon mutagenesis of Mb0100 at the *ppe1-nrp* locus in *Mycobacterium bovis* disrupts phthiocerol dimycocerosate (PDIM) and glycosylphenol-PDIM biosynthesis, producing an avirulent strain with vaccine properties at least equal to those of *M. bovis* BCG. **Journal of Bacteriology** 187: 2267–2277

Huang YS, Ge J, Zhang HM, Lei JQ, Zhang XL, Wang HH (2006) Purification and characterization of the *Mycobacterium tuberculosis* FabD2, a novel malonyl-CoA:AcpM transacylase of fatty acid synthase. **Protein Expression and Purification** 45: 393–399

Hughes AL, Friedman R, Murray M (2002) Genomewide pattern of synonymous nucleotide substitution in two complete genomes of *Mycobacterium tuberculosis*. **Emerging Infectious Diseases** 8: 1342–1346

Hunter T (1995) Protein kinases and phosphatases: the yin and yang of protein phosphorylation and signalling. **Cell** 80: 225–236

Itoh K, Chiba T, Takahashi S, Ishii T, Igarashi K, Katoh Y, Oyake T, Hayashi N, Satoh K, Yamamotot M, Nabeshima Y (1997) An Nrf2/small Maf heterodimer mediates the induction of phase II detoxifying enzyme genes through antioxidant response elements. **Biochemical and Biophysical Research Communications** 236: 313–322

Jackson M, Raynaud C, Lanéelle MA, Guilhot C, Laurent-Winter C, Ensergueix D, Gicquel B, Daffé M (1999) Inactivation of the antigen 85C gene profoundly affects the mycolate content and alters the permeability of the *Mycobacterium tuberculosis* cell envelope. **Molecular Microbiology** 31: 1573–1587

Jackson M, Crick DC, Brennan PJ (2000) Phosphatidylinositol is an essential phospholipid of mycobacteria. **Journal of Biological Chemistry** 275: 30092–30099

Jackson M, Stadthagen G, Gicquel B (2007) Long-chain multiple methyl-branched fatty acid-containing lipids of *Mycobacterium tuberculosis*: Biosynthesis, transport, regulation and biological activities. **Tuberculosis** 87: 78–86

Jang KP, Kim CH, Na SW, Jang DS, Kim H, Kang H, Lee E (2010a) 7-Phenylplatensimycin and 11-methyl-7-phenylplatensimycin: more potent analogs of platensimycin. **Bioorganic and Medicinal Chemistry Letters** 20: 2156–2158

Jang, J, Stella A, Boudou F, Levillain F, Darthuy E, Vaubourgeix J, Wang C, Bardou F, Puzo G, Gilleron M, Burlet-Schiltz O, Monsarrat B, Brodin P, Gicquel B, Neyrolles O (2010b) Functional characterization of the *Mycobacterium tuberculosis* serine/threonine kinase PknJ. **Microbiology** 156: 1619–1631

Jayakumar D, Jacobs WR Jr., Narayanan S (2008) Protein kinase E of *Mycobacterium tuberculosis* has a role in the nitric oxide stress response and apoptosis in a human macrophage model of infection. **Cellular Microbiology** 10: 365–374

Jones D, Metzger HJ, Schatz A, Waksman SA (1944) Control of Gram-negative bacteria in experimental animals by streptomycin. **Science** 100: 103–105

Jones SM, Urch JE, Brum R, Harwood JL, Berry C, Gilbert IH (2004) Analogues of thiolactomycin as potential anti-malarial and anti-trypanosomal agents. **Bioorganic and Medicinal Chemistry** 12: 683–692

Kana BD, Gordhan BG, Downing KJ, Sung N, Vostroktunova G, Machowski EE, Tsenova L, Young M, Kaprelyants A, Kaplan G, Mizrahi V (2008) The resuscitation-promoting factors of *Mycobacterium tuberculosis* are required for virulence and resuscitation from dormancy but are collectively dispensable for growth *in vitro*. **Molecular Microbiology** 67: 672–684

Kang CM, Abbott DW, Park ST, Dascher CC, Cantley LC, Husson RN (2005) The *Mycobacterium tuberculosis* serine/threonine kinases PknA and PknB: substrate identification and regulation of cell shape. **Genes and Development** 19: 1692–1704

Kang CM, Nyayapathy S, Lee JY, Suh JW, Husson RN (2008a) Wag31, a homologue of the cell division protein DivIVA, regulates growth, morphology and polar cell wall synthesis in mycobacteria. **Microbiology** 154: 725–735

Kang Y, Nguyen DT, Son MS, Hoang TT (2008b) The *Pseudomonas aeruginosa* nutrient acquisition and pathogenesis in the lungs of cystic fibrosis patients. **Microbiology** 154: 1584–1598

Kang Y, Zarzycki-Siek J, Walton CB, Norris MH, Hoang TT (2010) Multiple FadD acyl-CoA synthetases contribute to differential fatty acid degradation and virulence in *Pseudomonas aeruginosa*. **PLoS One** 5: e13557

Kappelman J, Alçiçek MC, Kazanci N, Schultz M, Ozkul M, Sen S (2008) First *Homo erectus* from Turkey and implications for migrations into temperate Eurasia. **American Journal of Physical Anthropology** 135: 110–116

Kass LR, Brock DJH, Bloch K (1967) β-Hydroxydecanoyl thioester dehydrase. I. Purification and properties. **Journal of Biological Chemistry** 242: 4418–4431

Kaye K, Frieden TR (1996) Tuberculosis control: the relevance of classic principles in an era of acquired immunodeficiency syndrome and multidrug resistance. **Epidemiologic Reviews** 18: 52–63

Keating LA, Wheeler PR, Mansoor H, Inwald JK, Dale J, Hewinson RG, Gordon SV (2005) The pyruvate requirement of some members of the *Mycobacterium tuberculosis* complex is due to an inactive pyruvate kinase: implications for *in vivo* growth. **Molecular Microbiology** 56: 163–174

Keller PM, Böttger EC, Sander P (2008) Tuberculosis vaccine strain *Mycobacterium bovis* BCG Russia is a natural *recA* mutant. **BioMed Central Microbiology** 8: 120

Khan S, Nagarajan SN, Parikh A, Samantaray S, Singh A, Kumar D, Roy RP, Bhatt A, Nandicoori VK (2010) Phosphorylation of enoyl-acyl carrier protein reductase InhA impacts mycobacterial growth and survival. **Journal of Biological Chemistry** 285: 37860–37871

Khare G, Gupta V, Gupta RK, Gupta R, Bhat R, Tyagi AK (2009) Dissecting the role of critical residues and substrate preference of a fatty acyl-CoA synthetase (FadD13) of *Mycobacterium tuberculosis*. **PLoS One** 4: e8387

Kiefer F, Arnold K, Kunzli M, Bordoli L, Schwede T (2009) The SWISS-MODEL Repository and associated resources. **Nucleic Acids Research** 37: D387–392

Kikuchi S, Kusaka T (1984) Purification of NADPH-dependent enoyl-CoA reductase involved in the malonyl-CoA dependent fatty acid elongation system of *Mycobacterium smegmatis*. **Journal of Biochemistry (Tokyo)** 96: 841–848

Kim P, Zhang YM, Shenoy G, Hguyen QA, Boshoff HI, Manjunatha UH, Goodwin MB, Lonsdale J, Price AC, Miller DJ, Duncan K, White SW, Rock CO, Barry CE 3rd, Dowd CS (2006) Structure-activity relationships at the 5-position of thiolactomycin: An intact (5R)-isoprene unit is required for activity against the condensing enzymes from *Mycobacterium tuberculosis* and *Escherichia coli*. **Journal of Medicinal Chemistry** 49: 159–171

Kimber MS, Martin F, Lu Y, Houston S, Vedadi M, Dharamsi A, Fiebig KM, Schmid M, Rock CO (2004) The structure of (3R)-hydroxyacyl-acyl carrier protein dehydratase (FabZ) from *Psuedomonas aeruginosa*. **Journal of Biological Chemistry** 279: 52593–52604

Kirkpatrick AS, Yokoyama T, Choi KJ, Yeo HJ (2009) *Campylobacter jejuni* fatty acid synthase II: structural and functional analysis of beta-hydroxyacyl-ACP dehydratase (FabZ). **Biochemical and Biophysical Research Communications** 380: 407–412

Klenk HP, Clayton RA, Tomb JF, White O, Nelson KE, Ketchum KA, Dodson RJ, Gwinn M, Hickey EK, Peterson JD, Richardson DL, Kerlavage AR, Graham DE, Kyrpides NC, Fleischmann RD, Quackenbush J, Lee NH, Sutton GG, Gill S, Kirkness EF, Dougherty BA, McKenney K, Adams MD, Loftus B, Peterson S, Reich CI, McNeil LK, Badger JH, Glodek A, Zhou L, Overbeek R, Gocayne JD, Weidman JF, McDonald L, Utterback T, Cotton MD, Spriggs T, Artiach P, Kaine BP, Sykes SM, Sadow PW, D'Andrea KP, Bowman C, Fujii C, Garland SA, Mason TM, Olsen GJ, Fraser CM, Smith HO, Woese CR, Venter JC (1997) The complete genome sequence of the hyperthermophilic, sulphate-reducing archaeon *Archaeoglobus fulgidus*. **Nature** 390: 364–370

Kolattukudy PE, Fernandes ND, Azad AK, Fitzmaurice AM, Sirakova TD (1997) Biochemistry and molecular genetics of cell-wall lipid biosynthesis in mycobacteria. **Molecular Microbiology** 24: 263–270

Kremer L, Besra GS (2002) Current status and future development of antitubercular chemotherapy. **Expert Opinion on Investigational Drugs** 11: 1033–1049

Kremer L, Douglas JD, Baulard AR, Morehouse C, Guy MR, Alland D, Dover LG, Lakey JH, Jacobs WR Jr., Brennan PJ, Minnikin DE, Besra GS (2000a) Thiolactomycin and related analogues as novel anti-mycobacterial agents targeting KasA and KasB condensing enzymes in *Mycobacterium tuberculosis*. **Journal of Biological Chemistry** 275: 16857–16864

Kremer L, Baulard AR, Besra GS (2000b) Genetics of Mycolic Acid Biosynthesis *in* **Molecular Genetics of Mycobacteria** pp. 173–190. Edited by Hatfull GF, Jacobs WR Jr. Washington DC: American Society for Microbiology Press

Kremer L, Dover LG, Morehouse C, Hitchin P, Everett M, Morris HR, Dell A, Brennan PJ, McNeil MR, Flaherty C, Duncan K, Besra GS (2001a) Galactan biosynthesis in *Mycobacterium tuberculosis*. Identification of a bifunctional UDP-galactofuranosyltransferase. **Journal of Biological Chemistry** 276: 26430–26440

Kremer L, Nampoothiri KM, Lesjean S, Dover LG, Graham S, Betts J, Brennan PJ, Minnikin DE, Locht C, Besra GS (2001b) Biochemical characterization of acyl carrier protein (AcpM) and malonyl-CoA:AcpM transacylase (*mt*FabD), two major components of *Mycobacterium tuberculosis* fatty acid synthase II. **Journal of Biological Chemistry** 276: 27967–27974

Kremer L, Dover LG, Carrère S, Nampoothiri KM, Lesjean S, Brown AK, Brennan PJ, Minnikin DE, Locht C, Besra GS (2002a) Mycolic acid biosynthesis and enzymic characterization of the beta-ketoacyl-ACP synthase A-condensing enzyme from *Mycobacterium tuberculosis*. **Biochemical Journal** 364: 423–430

Kremer L, Guerardel Y, Gurcha SS, Locht C, Besra GS (2002b) Temperature-induced changes in the cell-wall components of *Mycobacterium thermoresistibile*. **Microbiology** 148: 3145–3154

Kremer L, Maughan WN, Wilson RA, Dover LG, Besra GS (2002c) The *M. tuberculosis* antigen 85 complex and mycolyltransferase activity. **Letters in Applied Microbiology** 34: 233–237

Krithika R, Marathe U, Saxena P, Ansari MZ, Mohanty D, Gokhale RS (2006) A genetic locus required for iron acquisition in *Mycobacterium tuberculosis*. **Proceedings of the National Academy of Sciences of the United States of America** 103: 2069–2074

Kruh NA, Borgaro JG, Ruzsicska BP, Xu H, Tonge PJ (2008) A novel interaction linking the FAS-II and phthiocerol dimycocerosate (PDIM) biosynthetic pathways. **Journal of Biological Chemistry** 283: 31719–31725

Kubica G (1976) *M. tuberculosis* colonies (photograph). National Institute for Medical Research <www.nimr.mrc.ac.uk/mycobact/davis/>

Kuo MR, Morbidoni HR, Alland D, Sneddon SF, Gourlie BB, Staveski MM, Leonard M, Gregory JS, Janjigian AD, Yee C, Musser JM, Kreiswirth B, Iwamoto H, Perozzo R, Jacobs WR Jr., Sacchettini JC, Fidock DA (2003) Targeting tuberculosis and malaria through inhibition of enoyl reductase: compound activity and structural data. **Journal of Biological Chemistry** 278: 20851–20859

Labarga A, Valentin F, Anderson M, Lopez R (2007) Web services at the European bioinformatics institute. **Nucleic Acids Research** 35: W6-11

LaMarca BB, Zhu W, Arceneaux JE, Byers BR, Lundrigan MD (2004) Participation of *fad* and *mbt* genes in synthesis of mycobactin in *Mycobacterium smegmatis*. **Journal of Bacteriology** 186: 374–382

Lamichhane G, Zignol M, Blades NJ, Geiman DE, Dougherty A, Grosset J, Broman KW, Bishai WR (2003) A postgenomic method for predicting essential genes at subsaturation levels of mutagenesis: application to *Mycobacterium tuberculosis*. **Proceedings of the National Academy of Sciences of the United States of America** 100: 7213–7218

Larsen MH, Vilcheze C, Kremer L, Besra GS, Parsons L, Salfinger M, Heifets L, Hazbon MH, Alland D, Sacchettini JC, Jacobs WR Jr. (2002) Over-expression of *inhA*, but not *kasA*, confers resistance to isoniazid and ethionamide in *Mycobacterium smegmatis*, *M. bovis* BCG and *M. tuberculosis*. **Molecular Microbiology** 46: 453–466

Lawn SD, Griffin GE (2008) Infection – bacterial *in* **Mechanisms of Disease: An Introduction to Clinical Science** pp. 136–159. Edited by Tomlinson S, Heagerty AM, Weetman AP. Cambridge University Press

Lea-Smith DJ, Pyke JS, Tull D, McConville MJ, Coppel RL, Crellin PK (2007) The reductase that catalyzes mycolic motif synthesis is required for efficient attachment of mycolic acids to arabinogalactan. **Journal of Biological Chemistry** 282: 11000–11008

Lechat P, Hummel, Rousseau S, Moszer I (2008) GenoList: an integrated environment for comparative analysis of microbial genomes. **Nucleic Acids Research** 36: D469–474

Li Z, Huang Y, Ge J, Fan H, Zhou X, Li S, Bartlam M, Wang H, Rao Z (2007) The crystal structure of MCAT from *Mycobacterium tuberculosis* reveals three new catalytic models. **Journal of Molecular Biology** 371: 1075–1083

Lindqvist Y, Huang W, Schneider G, Shanklin J (1996) Crystal structure of Δ9 stearoyl-acyl carrier protein desaturase from castor seed and its relationship to other di-iron proteins. **European Molecular Biology Organization Journal** 15: 4081–4092

Liu J, Rosenberg EY, Nikaido H (1995) Fluidity of the lipid domain of the cell wall from *Mycobacterium chelonae*. **Proceedings of the National Academy of Sciences of the United States of America** 92: 11254–11258

Liu J, Barry CE 3rd, Besra GS, Nikaido H (1996) Mycolic acid structure determines the fluidity of the mycobacterial cell wall. **Journal of Biological Chemistry** 271: 29545–29551

Liu X, Chu X, Yu W, Li P, Li D (2004) Expression and purification of His-tagged rat mitochondrial short-chain 3-hydroxyacyl-CoA dehydrogenase wild-type and Ser137 mutant proteins. **Protein Expression and Purification** 37: 344–351

Linell F, Norden A (1954) *Mycobacterium balnei*, a new acid-fast bacillus occurring in swimming pools and capable of producing skin lesions in humans. **Acta Tuberculosea Scandinavica Supplementum** 33: 1–84

Loo CY, Mitrakul K, Jaafar S, Gyurko C, Hughes CV, Ganeshkumar N (2004) Role of a *nosX* homologue in *Streptococcus gordonii* in aerobic growth and biofilm formation. **Journal of Bacteriology** 186: 8193–8206

Lorenz MC, Fink GR (2001) The glyoxylate cycle is required for fungal virulence. **Nature** 412: 83–86

Lu XY, Chen YD, You QD (2010) 3D-QSAR studies of acylcarboxamides with inhibitory activity on InhA using pharmacophore-based alignment. **Chemical Biology & Drug Design** 75: 195–203

Luckner SR, Machutta CA, Tonge PJ, Kisker C (2009) Crystal structures of *Mycobacterium tuberculosis* KasA show mode of action within cell wall biosynthesis and its inhibition by thiolactomycin. **Structure** 17: 1004–1013

Luthra A, Malik SS, Ramachandran R (2008) Cloning, purification and comparative structural analysis of two hypothetical proteins from *Mycobacterium tuberculosis* found in the human granuloma during persistence and highly up-regulated under carbon-starvation conditions. **Protein Expression and Purification** 62: 64–74

Lynett J, Stokes RW (2007) Selection of transposon mutants of *Mycobacterium tuberculosis* with increased macrophage infectivity identifies *fadD23* to be involved in sulfolipid production and association with macrophages. **Microbiology** 153: 3133–3140

Mahairas GG, Sabo PJ, Hickey MJ, Singh DC, Stover CK (1996) Molecular analysis of genetic differences between *Mycobacterium bovis* BCG and virulent *M. bovis*. **Journal of Bacteriology** 178: 1274–1282

Mahapatra S, Basu J, Brennan PJ, Crick DC (2005) Structure, biosynthesis, and genetics of the mycolic acid-arabinogalactan-peptidoglycan complex *in* **Tuberculosis and the Tubercle Bacillus** pp. 275–285. Edited by Cole ST, Eisenach KD, McMurray DN, Jacobs WR Jr. ASM Press, Washington DC

Manca C, Tsenova L, Barry CE 3rd, Bergtold A, Freeman S, Haslett PAJ, Musser JM, Freedman VH, Kaplan G (1999) *Mycobacterium tuberculosis* CDC1551 induces a more vigorous host response *in vivo* and *in vitro*, but is not more virulent than other clinical isolates. **Journal of Immunology** 162: 6740–6746

Manganelli R, Voskuil MI, Schoolnik GK, Smith I (2001) The *Mycobacterium tuberculosis* ECF sigma factor sigmaE: role in global gene expression and survival in macrophages. **Molecular Microbiology** 41: 423–437

Mann FM, Xu M, Chen X, Fulton DB, Russell DG, Peters RJ (2009) Edaxadiene: a new bioactive diterpene from *Mycobacterium tuberculosis*. **Journal of the Americal Chemical Society** 131: 17526–17527

Mann FM, VanderVen BC, Peters RJ (2011) Magnesium depletion triggers production of an immune modulating diterpenoid in *Mycobacterium tuberculosis*. **Molecular Microbiology** 79: 1594–1601

Mano J, Babiychuk E, Belles-Boix E, Hiratake J, Kimura A, Inzé D, Kushnir S, Asada K (2000a) A novel NADPH:diamide oxidoreductase activity in *Arabidopsis thaliana* P1 zeta-crystallin. **European Journal of Biochemistry** 267: 3661–3671

Mano J, Yoon H, Asada K, Babiychuk E, Inzé D, Mikami B (2000b) Crystallization and preliminary X-ray crystallographic analysis of NADPH: azodicarbonyl/quinone oxidoreductase, a plant zeta-crystallin. **Biochimica et Biophysica Acta** 1480: 374–376

Mano J, Torii Y, Hayashi S, Takimoto K, Matsui K, Nakamura K, Inzé D, Babiychuk E, Kushnir S, Asada K (2002) The NADPH:quinone oxidoreductase P1-zeta-crystallin in Arabidopsis catalyzes the alpha,beta-hydrogenation of 2-alkenals: detoxication of the lipid peroxide-derived reactive aldehydes. **Plant and Cell Physiology** 43: 1445–1455

Marks F (1996) Protein phosphoryation in prokaryotes in **Protein Phosphorylation** p. 12. Edited by Marks F. Wiley-VCH

Marrakchi H, Ducasse S, Labesse G, Montrozier H, Margeat E, Emorine L, Charpentier X, Daffé M, Quémard A (2002) MabA (FabG1), a *Mycobacterium tuberculosis* protein involved in the long-chain fatty acid elongation system FAS-II. **Microbiology** 148: 951–960

Martins M (2011) Targeting the human macrophage with combinations of drugs and inhibitors of Ca^{2+} and K^{+} transport to enhance the killing of intracellular multi-drug resistant *Mycobacterium tuberculosis* (MDR-TB) – a novel, patentable approach to limit the emergence of XDR-TB. **Recent Patents on Anti-Infective Drug Discovery** 6: 110–117

Maruyama A, Kumagai Y, Morikawa K, Taguchi K, Hayashi H, Ohta T (2003) Oxidative-stress-inducible *qorA* encodes an NADPH-dependent quinone oxidoreductase catalysing a one-electron reduction in *Staphylococcus aureus*. **Microbiology** 149: 389–398

Mazurek GH, Jereb J, LoBue P, Iademarco MF, Metchock B, Vernon A (2005) Guidelines for Using the QuantiFERON®-TB Gold Test for Detecting *Mycobacterium tuberculosis* Infection, United States. **Centers for Disease Control and Prevention Morbidity and Mortality Weekly Report** 54(RR15): 49–55

McClure WR, Cech CL (1978) On the mechanism of rifampicin inhibition of RNA synthesis. **Journal of Biological Chemistry** 253: 8949–8956

McGuire BS, Carroll JE, Chancey VF, Howard JC (1990) Mitochondrial enzymes responsible for oxidizing medium-chain fatty acids in developing rat skeletal muscle, heart, and liver. **Journal of Nutritional Biochemistry** 1: 410–414

McKeown T, Lowe CR (1977) **An Introduction to Social Medicine** pp. 8–9. Great Britain: Blackwell Scientific Publications

McKinney JD, Höner zu Bentrup K, Muñoz-Elias EJ, Miczak A, Chen B, Chan WT, Swenson D, Sacchettini JC, Jacobs WR Jr., Russell DG (2000) Persistence of *Mycobacterium tuberculosis* in macrophages and mice requires the glyoxylate shunt enzyme isocitrate lyase. **Nature** 406: 735–738

McNeil M, Daffé M, Brennan PJ (1990) Evidence for the nature of the link between the arabinogalactan and peptidoglycan of mycobacterial cell walls. **Journal of Biological Chemistry** 265: 18200–18206

Mdluli K, Slayden RA, Zhu Y, Ramaswamy S, Pan X, Mead D, Crane DD, Musser JM, Barry CE 3rd (1998) Inhibition of a *Mycobacterium tuberculosis* beta-ketoacyl ACP synthase by isoniazid. **Science** 280: 1607–1610

Middlebrook G, Cohn ML, Schaefer WB (1954) Studies on isoniazid and tubercle bacilli. III. The isolation, drug-susceptibility, and catalase-testing of tubercle bacilli from isoniazid-treated patients. **American Review of Tuberculosis** 70: 852–872

Middlebrook G, Cohn ML (1958) Bacteriology of tuberculosis: laboratory methods. **American Journal of Public Health and the Nation's Health** 48: 844–853

Mikusova K, Yagi T, Stern R, McNeil MR, Besra GS, Crick DC, Brennan PJ (2000) Biosynthesis of the galactan component of the mycobacterial cell wall. **Journal of Biological Chemistry** 275: 33890–33897

Miller LG, Asch SM, Yu EI, Knowles L, Gelberg L, Davidson P (2000) A population-based survey of tuberculosis symptoms: How atypical are atypical presentations? **Clinical Infectious Diseases** 30: 293–299

Minnikin DE (1982) Lipids: Complex lipids, their chemistry, biosynthesis and roles *in* **The Biology of the Mycobacteria: Physiology, Identification and Classification, Vol. 1** pp. 95–184. Edited by Ratledge C, Stanford J. London: Academic Press

Minnikin DE, Kremer L, Dover LG, Besra GS (2002) The methyl-branched fortifications of *Mycobacterium tuberculosis*. **Chemistry and Biology** 9: 545–553

Mishra AK, Driessen NN, Appelmelk BJ, Besra GS (2011) Lipoarabinomannan and related glycoconjugates: structure, biogenesis and role in *Mycobacterium tuberculosis* physiology and host-pathogen interaction. **Federation of European Microbiological Societies Microbiology Reviews** 35: 1126–1157

Miyakawa S, Suzuki K, Noto T, Harada Y, Okazaki H (1982) Thiolactomycin, a new antibiotic. IV. Biological properties and chemotherapeutic activity in mice. **Journal of Antibiotics (Tokyo)** 35: 411–419

Molle V, Kremer L, Girard-Blanc C, Besra GS, Cozzone AJ, Prost JF (2003a) An FHA phosphoprotein recognition domain mediates protein EmbR phosphorylation by PknH, a Ser/Thr protein kinase from *Mycobacterium tuberculosis*. **Biochemistry** 42: 15300–15309

Molle V, Girard-Blanc C, Kremer L, Doublet P, Cozzone AJ, Prost JF (2003b) Protein PknE, a novel transmembrane eukaryotic-like serine-threonine kinase from *Mycobacterium tuberculosis*. **Biochemical and Biophysical Research Communications** 308: 820–825

Molle V, Brown AK, Besra GS, Cozzone AJ, Kremer L (2006) The condensing activities of the *Mycobacterium tuberculosis* type II fatty acid synthase are differentially regulated by phosphorylation. **Journal of Biological Chemistry** 281: 30094–30103

Molle V, Gulten G, Vilchèze C, Veyron-Churlet R, Zanella-Cléon I, Sacchettini JC, Jacobs WR Jr., Kremer L (2010) Phosphorylation of InhA inhibits mycolic acid biosynthesis and growth of *Mycobacterium tuberculosis*. **Molecular Microbiology** 78: 1591–1605

Moreno C, Mehlert A, Lamb J (1988) The inhibitory effects of mycobacterial lipoarabinomannan and polysaccharides upon polyclonal and monoclonal human T cell proliferation. **Clinical and Experimental Immunology** 74: 206–210

Morlock GP, Metchock B, Sikes D, Crawford JT, Cooksey RC (2003) *ethA*, *inhA*, and *katG* loci of ethionamide-resistant clinical *Mycobacterium tuberculosis* isolates. **Antimicrobial Agents and Chemotherapy** 47: 3799–3805

Muñoz S, Rivas-Santiago B, Enciso JA (2009) *Mycobacterium tuberculosis* entry into mast cells through cholesterol-rich membrane microdomains. **Scandinavian Journal of Immunology** 70: 256–263

Musayev F, Sachdeva S, Scarsdale JN, Reynolds KA, Wright HT (2005) Crystal structure of a substrate complex of *Mycobacterium tuberculosis* beta-ketoacyl-acyl carrier protein synthase III (FabH) with lauroyl-coenzyme A. **Journal of Molecular Biology** 346: 1313–1321

Nelson RT, Hua J, Pryor B, Lodge JK (2001) Identification of virulence mutants of the fungal pathogen *Cryptococcus neoformans* using signature-tagged mutagenesis. **Genetics** 157: 935–947

Nemeria N, Yan Y, Zhang Z, Brown AM, Arjunan P, Furey W, Guest JR, Jordan F (2001) Inhibition of the *Escherichia coli* pyruvate dehydrogenase complex E1 subunit and its tyrosine 177 variants by thiamin 2-thiazolone and thiamin 2-thiothiazolone diphosphates. Evidence for reversible tight-binding inhibition. **Journal of Biological Chemistry** 276: 45969–45978

Nesbitt NM, Yang X, Fontán P, Kolesnikova I, Smith I, Sampson NS, Dubnau E (2010) A thiolase of *Mycobacterium tuberculosis* is required for virulence and production of androstenedione and androstadienedione from cholesterol. **Infection and Immunity** 78: 275–282

Nguyen L, Scherr N, Gatfield J, Walburger A, Pieters J, Thompson CJ (2007) Antigen 84, an effector of pleiomorphism in *Mycobacterium smegmatis*. **Journal of Bacteriology** 189: 7896–7910

Nigou J, Gilleron M, Puzo G (2003) Lipoarabinomannans: from structure to biosynthesis. **Biochimie** 85: 153–166

Nomura S, Horiuchi T, Hata T, Omura S (1972) Inhibition of sterol and fatty acid biosyntheses by cerulenin in cell-free systems of yeast. **Journal of Antibiotics (Tokyo)** 25: 365–368

Obermeyer Z, Abbott-Klafter J, Murray CJL (2008) Has the DOTS strategy improved case finding or treatment success? An empirical assessment. **PLoS ONE** 3: e1721

Oh TJ, Daniel J, Kim HJ, Sirakova TD, Kolattukudy PE (2006) Identification and characterization of Rv3281 as a novel subunit of a biotin-dependent acyl-CoA Carboxylase in *Mycobacterium tuberculosis* H_{37}Rv. **Journal of Biological Chemistry** 281: 3899–3908

Ohlrogge J, Browse J (1995) Lipid biosynthesis. **Plant Cell** 7: 957–970

Oishi H, Noto T, Sasaki H, Suzuki K, Hayashi T, Okazaki H, Ando K, Sawada M (1982) Thiolactomycin, a new antibiotic. I. Taxonomy of the producing organism, fermentation and biological properties. **Journal of Antibiotics (Tokyo)** 35: 391–395

Okamoto S, Tamaru A, Nakajima K, Tanaka Y, Yokuyama S, Suzuki Y, Ochi K (2007) Loss of a conserved 7-methylguanosine modification in 16S rRNA confers low-level streptomycin resistance in bacteria. **Molecular Microbiology** 63: 1096–1106

Orhan DD, Ozçelik B, Ozgen S, Ergun F (2009) Antibacterial, antifungal, and antiviral activities of some flavonoids. **Microbiological Research** 165: 496–504

Orhan I, Sener B, Kaiser M, Brum R, Tasdemir D (2010) Inhibitory activity of marine sponge-derived natural products against parasitic protozoa. **Marine Drugs** 8: 47–58

Pallen M, Chaudhuri R, Khan A (2002) Bacterial FHA domains: neglected players in the phospho-threonine signalling game? **Trends in Microbiology** 10: 556–563

Palomino JC, Ramos DF, da Silva PA (2009) New anti-tuberculosis drugs: strategies, sources and new molecules. **Current Medicinal Chemistry** 16: 1898–1904

Papavinasasundaram KG, Chan B, Chung JH, Colston MJ, Davis EO, Av-Gay Y (2005) Deletion of the *Mycobacterium tuberculosis pknH* gene confers a higher bacillary load during the chronic phase of infection in BALB/c mice. **Journal of Bacteriology** 187: 5751–5760

Parish T, Roberts G, Laval F, Schaeffer M, Daffé M, Duncan K (2007) Functional complementation of the essential gene *fabG1* of *Mycobacterium tuberculosis* by *Mycobacterium smegmatis fabG* but not *Escherichia coli fabG*. **Journal of Bacteriology** 189: 3721–3728

Peirs P, De Wit L, Braibant M, Huygen K, Content J (1997) A serine/threonine protein kinase from *Mycobacterium tuberculosis*. **European Journal of Biochemistry** 244: 604–612

Peirs P, Parmentier B, De Wit L, Content J (2000) The *Mycobacterium bovis* homologous protein of the *Mycobacterium tuberculosis* serine/threonine protein kinase Mbk (PknD) is truncated. **Federation of European Microbiological Societies Microbiology Letters** 188: 135–139

Peitsch MC (1995) Protein modeling by E-mail. **Bio/Technology** 13: 658–660

Pérez J, Garcia R, Bach H, de Waard JH, Jacobs WR Jr., Av-Gay Y, Bubis J, Takiff HE (2006) *Mycobacterium tuberculosis* transporter MmpL7 is a potential substrate for kinase PknD. **Biochemical and Biophysical Research Communications** 348: 6–12

Pethe K, Swenson DL, Alonso S, Anderson J, Wang C, Russell DG (2004) Isolation of *Mycobacterium tuberculosis* mutants defective in the arrest of phagosome maturation. **Proceedings of the National Academy of Sciences of the United States of America** 101: 13642–13647

Phetsuksiri B, Jackson M, Scherman H, McNeil M, Besra GS, Baulard AR, Slayden RA, DeBarber AE, Barry CE 3rd, Baird MS, Crick DC, Brennan PJ (2003) Unique mechanism of action of the thiourea drug isoxyl on *Mycobacterium tuberculosis*. **Journal of Biological Chemistry** 278: 53123–53130

Pommerville JC (2007) The Genus *Mycobacterium in* **Alcamo's Laboratory Fundamentals of Microbiology** pp. 154–156. Edited by Pommerville JC. Sudbury, Massachusetts: Jones and Bartlett Publishers

Portevin D, de Sousa-D'Auria C, Houssin C, Grimaldi C, Chami M, Daffé M, Guilhot C (2004) A polyketide synthase catalyzes the last condensation step of mycolic acid biosynthesis in mycobacteria and related organisms. **Proceedings of the National Academy of Sciences of the United States of America** 101: 314–319

Portevin D, de Sousa-D'Auria C, Montrozier H, Houssin C, Stella A, Lanéelle MA, Bardou F, Guilhot C, Daffé M (2005) The acyl-AMP ligase FadD32 and AccD4-containing acyl-CoA carboxylase are required for the synthesis of mycolic acids and essential for mycobacterial growth: identification of the carboxylation product and determination of the acyl-CoA carboxylase components. **Journal of Biological Chemistry** 280: 8862–8874

Porth CM, Matfin G (2010) Respiratory tract infections *in* **Essentials of Pathophysiology: Concepts of Altered Health States** pp. 549–554. Edited by Porth CM. Philadelphia: Lippincott Williams & Wilkins

Prach L, Kirby J, Keasling JD, Alber T (2010) Diterpene production in *Mycobacterium tuberculosis*. **Federation of European Biochemical Societies Journal** 277: 3588–3595

Price AC, Choi KH, Heath RJ, Li Z, White SW, Rock CO (2001) Inhibition of beta-ketoacyl-acyl carrier protein synthases by thiolactomycin and cerulenin. Structure and mechanism. **Journal of Biological Chemistry** 276: 6551–6559

Prüß BM, Nelms JM, Park C, Wolfe AJ (1994) Mutations in NADH:ubiquinone oxidoreductase of *Escherichia coli* affect growth on mixed amino acids. **Journal of Bacteriology** 176: 2143–2150

Qiu X, Janson CA, Smith WW, Head M, Lonsdale J, Konstantinidis AK (2001) Refined structures of beta-ketoacyl-acyl carrier protein synthase III. **Journal of Molecular Biology** 307: 341–356

Quémard A, Sacchettini JC, Dessen A, Vilchèze C, Bittman R, Jacobs WR Jr., Blanchard JS (1995) Enzymatic characterization of the target for isoniazid in *Mycobacterium tuberculosis*. **Biochemistry** 34: 8235–8241

Qureshi N, Sathyamoorthy N, Takayama K (1984) Biosynthesis of C30 to C56 fatty acids by an extract of *Mycobacterium tuberculosis* H_{37}Ra. **Journal of Bacteriology** 157: 46–52

Radmacher E, Alderwick LJ, Besra GS, Brown AK, Gibson KJ, Sahm H, Eggeling L (2005) Two functional FAS-I type fatty acid synthases in *Corynebacterium glutamicum*. **Microbiology** 151: 2421–2427

Ramakrishnan L, Tran HT, Federspiel NA, Falkow S (1997) A *crtB* homolog essential for photochromogenicity in *Mycobacterium marinum*: isolation, characterization, and gene disruption via homologous recombination. **Journal of Bacteriology** 179: 5862–5868

Raman K, Rajagopalan P, Chandra N (2007) Hallmarks of mycolic acid biosynthesis: a comparative genomics study. **Proteins** 69: 358–368

Ramón-García S, Martín C, De Rossi E, Aínsa JA (2007) Contribution of the Rv2333c efflux pump (the Stp protein) from *Mycobacterium tuberculosis* to intrinsic antibiotic resistance in *Mycobacterium bovis* BCG. **Journal of Antimicrobial Chemotherapy** 59: 544–547

Ramón-García S, Ng C, Anderson H, Chao JD, Zheng X, Pfeifer T, Av-Gay Y, Roberge M, Thompson CJ (2011) Synergistic drug combinations for tuberculosis therapy indentified by a novel high-throughput screen. **Antimicrobial Agents and Chemotherapy** 55: 3861–3869

Rastogi N (2003) An introduction to mycobacterial taxonomy, structure, drug resistance, and pathogenesis *in* **Textbook-Atlas of Intestinal Infections in AIDS** pp. 89–115. Edited by Dionisio D. Milan: Springer-Verlag

Rhee KH, Lee KS, Priyadarshi A, Kim EE, Hwang KY (2005) Crystallization and preliminary X-ray crystallographic studies of fatty acid-CoA racemase from *Mycobacterium tuberculosis* H_{37}Rv. **Acta Crystallographica Section F: Structural Biology and Crystallization Communications** 61: 1017–1019

Rhodes G (2006) An Overview of Protein Crystallography *in* **Crystallography made Crystal Clear** pp. 7–30. Edited by Rhodes G. Canada: Academic Press

Rindi L, Fattorini L, Bonanni D, Iona E, Freer G, Tan D, Dehò G, Orefici G, Garzelli C (2002) Involvement of the *fadD33* gene in the growth of *Mycobacterium tuberculosis* in the liver of BALB/c mice. **Microbiology** 148: 3873–3880

Rindi L, Bonanni D, Lari N, Garzelli C (2004) Requirement of the gene *fadD33* for the growth of *Mycobacterium tuberculosis* in a hepatocyte cell line. **New Microbiologica** 27: 125–131

Rodger A, Nordén B (1997) Spectroscopy, chirality and oriented systems *and* Circular dichroism of biomolecules *in* **Circular Dichroism and Linear Dichroism** pp.1–32. Edited by Compton RG, Davies SG, Evans J. Oxford University Press

Rousseau C, Neyrolles O, Bordat Y, Giroux S, Sirakova TD, Prevost MC, Kolattukudy PE, Gicquel B, Jackson M (2003) Deficiency in mycolipenate- and mycosanoate-derived acyltrehaloses enhances early interactions of *Mycobacterium tuberculosis* with host cells. **Cellular Microbiology** 5: 405–415

Rubins JB (2003) Alveolar macrophages – Wielding the double-edged sword of inflammation. **American Journal of Respiratory and Critical Care Medicine** 167: 103–104

Sacco E, Covarrubias AS, O'Hare HM, Carroll P, Eynard N, Jones TA, Parish T, Daffé M, Bäckbro K, Quémard A (2007) The missing piece of the type II fatty acid synthase system from *Mycobacterium tuberculosis*. **Proceedings of the National Academy of Sciences of the United States of America** 104: 14628–14633

Sachdeva S, Musayev FN, Alhamadsheh MM, Scarsdale JN, Wright HT, Reynolds KA (2008a) Separate entrance and exit portals for ligand traffic in *Mycobacterium tuberculosis* FabH. **Chemistry and Biology** 15: 402–412

Sachdeva S, Musayev FN, Alhamadsheh MM, Scarsdale JN, Wright HT, Reynolds KA (2008b) Probing reactivity and substrate specificity of both subunits of the dimeric *Mycobacterium tuberculosis* FabH using alkyl-CoA disulfide inhibitors and acyl-CoA substrates. **Bioorganic Chemistry** 36: 85–90

Saint-Joanis B, Demangel C, Jackson M, Brodin P, Marsollier L, Boshoff H, Cole ST (2006) Inactivation of Rv2525c, a substrate of the twin arginine translocation (Tat) system of *Mycobacterium tuberculosis*, increases beta-lactam susceptibility and virulence. **Journal of Bacteriology** 188: 6669–6679

Sambrook J, Russell DW (2001) **Molecular Cloning: A Laboratory Manual.** Cold Spring Harbor, NY Cold Spring Harbor Laboratory

Sassetti CM, Boyd DH, Rubin EJ (2003) Genes required for mycobacterial growth defined by high density mutagenesis. **Molecular Microbiology** 48: 77–84

Sassetti CM, Rubin EJ (2003) Genetic requirements for mycobacterial survival during infection. **Proceedings of the National Academy of Sciences of the United States of America** 100: 12989–12994

Scandurra GM, Britton WJ, Triccas JA (2008) Inactivation of the *Mycobacterium tuberculosis fadB4* gene results in increased virulence in host cell and mice. **Microbes and Infection** 10: 38–44

Scarsdale JN, Kazanina G, He X, Reynolds KA, Wright HT (2001) Crystal structure of the *Mycobacterium tuberculosis* beta-ketoacyl-acyl carrier protein synthase III. **Journal of Biological Chemistry** 276: 20516–20522

Schaeffer ML, Agnihotri G, Volker C, Kallender H, Brennan PJ, Lonsdale JT (2001) Purification and biochemical characterization of the *Mycobacterium tuberculosis* beta-ketoacyl-acyl carrier protein synthases KasA and KasB. **Journal of Biological Chemistry** 276: 47029–47037

Schatz A, Waksman SA (1944) Effect of streptomycin and other antibiotic substances upon *Mycobacterium tuberculosis* and related organisms. **Proceedings of the Society for Experimental Biology and Medicine** 57: 244–248

Scherr N, Pieters J (2009) The eukaryotic-like serine/threonine protein kinase family in mycobacteria *in* **Mycobacterium: Genomics and Molecular Biology** pp. 171–192. Edited by Parish T, Brown A. Norfolk: Caister Academic Press

Schnappinger D, Ehrt S, Voskuil MI, Liu Y, Mangan JA, Monahan IM, Dolganov G, Efron B, Butcher PD, Nathan C, Schoolnik GK (2003). Transcriptional adaptation of *Mycobacterium tuberculosis* within macrophages: insights into the phagosomal environment. **Journal of Experimental Medicine** 198: 693–704

Seefeld MA, Miller WH, Newlander KA, Burgess WJ, DeWolf WE Jr., Elkins PA, Head MS, Jakas DR, Janson CA, Keller PM, Manley PJ, Moore TD, Payne DJ, Pearson S, Polizzi BJ, Qiu X, Rittenhouse SF, Uzinskas IN, Wallis NG, Huffman WF (2003) Indole naphthyridinones as inhibitors of bacterial enoyl-ACP reductases FabI and FabK. **Journal of Medicinal Chemistry** 46: 1627–1635

Sharma SK, Kapoor M, Ramya TNC, Kumar S, Kumar G, Modak R, Sharma S, Surolia N, Surolia A (2003) Identification, characterization, and inhibition of *Plasmodium falciparum* β-hydroxyacyl carrier protein dehydratase (FabZ). **Journal of Biological Chemistry** 278: 45661–45671

Sharma K, Gupta M, Pathak M, Gupta N, Koul A, Sarangi S, Baweja R, Singh Y (2006) Transcriptional control of the mycobacterial *embCAB* operon by PknH through a regulatory protein, EmbR, *in vivo*. **Journal of Bacteriology** 188: 2936–2944

Shiloh MU, DiGiuseppe Champion PA (2009) To catch a killer. What can mycobacterial models teach us about *Mycobacterium tuberculosis* pathogenesis? **Current Opinion in Microbiology** 13: 86–92

Shimada T (2006) Xenobiotic-metabolizing enzymes involved in activation and detoxification of carcinogenic polycyclic aromatic hydrocarbons. **Drug Metabolism and Pharmacokinetics** 21: 257–276

Shimakata T, Fujita Y, Kusaka T (1977) Acetyl-CoA-dependent elongation of fatty acids in *Mycobacterium smegmatis*. **Journal of Biochemistry** 82: 725–732

Shimakata T, Fujita Y, Kusaka T (1979) Purification and characterization of 3-hydroxyacyl-CoA dehydrogenase of *Mycobacterium smegmatis*. **Journal of Biochemistry** 86: 1191–1198

Shimomura Y, Kakuta Y, Fukuyama K (2003) Crystal structures of the quinone oxidoreductases from *Thermus thermophilus* HB8 and its complex with NADPH: implication for NADPH and substrate recognition. **Journal of Bacteriology** 185: 4211–4218

Shimono N, Morici L, Casali N, Cantrell S, Sidders B, Ehrt S, Riley LW (2003) Hypervirulent mutant of *Mycobacterium tuberculosis* resulting from disruption of the *mce1* operon. **Proceedings of the National Academy of Sciences of the United States of America USA** 100: 15918–15923

Shorrosh BS, Savage LJ, Soll J, Ohlrogge JB (1996) The pea chloroplast membrane-associated protein, IEP96, is a subunit of acetyl-CoA carboxylase. **Plant Journal: for Cell and Molecular Biology** 10: 261–268

Sibley LD, Hunter SW, Brennan PJ, Krahenbuhl JL (1988) Mycobacterial lipoarabinomannan inhibits gamma interferon-mediated activation of macrophages. **Infection and Immunity** 56: 1232–1236

Siméone R, Léger M, Constant P, Malaga W, Marrakchi H, Daffé M, Guilhot C, Chalut C (2010) Delineation of the roles of FadD22, FadD26 and FadD29 in the biosynthesis of phthiocerol dimycocerosates and related compounds in *Mycobacterium tuberculosis*. **Federation of European Biochemical Societies Journal** 277: 2715–2725

Sinai AP, Joiner KA (1997) Safe haven: The cell biology of nonfusogenic pathogen vacuoles. **Annual Review of Microbiology** 51: 415–462

Singh A, Gupta R, Vishwakarma RA, Narayanan PR, Paramasivan CN, Ramanathan VD, Tyagi AK (2005) Requirement of the *mymA* operon for appropriate cell wall ultrastructure and persistence of *Mycobacterium tuberculosis* in the spleens of guinea pigs. **Journal of Bacteriology** 187: 4173–4186

Singh SB, Jayasuriya H, Ondeyka JG, Herath KB, Zhang C, Zink DL, Tsou NN, Ball RG, Basilio A, Genilloud O, Diez MT, Vicente F, Pelaez F, Young K, Wang J (2006) Isolation, structure, and absolute stereochemistry of platensimycin, a broad spectrum antibiotic discovered using an antisense differential sensitivity strategy. **Journal of the American Chemical Society** 128: 11916–11920

Singh SB, Tota MR, Wang J (2008) Method of treatment using fatty acid synthesis inhibitors. **US: World Intellectual Property Organization** pp. 1–49, PCT/US2007/020226

Skeiky YAW, Sadoff JC (2006) Advances in tuberculosis vaccine strategies. **Nature Reviews Microbiology** 4: 469–476

Slama N, Leiba J, Eynard N, Daffé M, Kremer L, Quémard A, Molle V (2011) Negative regulation by Ser/Thr phosphorylation of HadAB and HadBC dehydratases from *Mycobacterium tuberculosis* type II fatty acid synthase system. **Biochemical and Biophysical Research Communications** 412: 401–406

Slayden RA, Lee RE, Armour JW, Cooper AM, Orme IM, Brennan PJ, Besra GS (1996) Antimycobacterial action of thiolactomycin: an inhibitor of fatty acid and mycolic acid synthesis. **Antimicrobial Agents and Chemotherapy** 40: 2813–2819

Slayden RA, Barry CE 3rd (2002) The role of KasA and KasB in the biosynthesis of meromycolic acids and isoniazid resistance in *Mycobacterium tuberculosis*. **Tuberculosis (Edinburgh)** 82: 149–160

Smith MI, McClosky WT (1945) Chemotherapeutic action of streptomycin and promin in experimental tuberculosis. **US Public Health Service, Public Health Reports** 60: 1129–1138

Snapper SB, Melton RE, Mustafa S, Kieser T, Jacobs WR Jr. (1990) Isolation and characterization of efficient plasmid transformation mutants of *Mycobacterium smegmatis*. **Molecular Microbiology** 4: 1911–1919

Søballe B, Poole RK (1999) Microbial ubiquinones: multiple roles in respiration, gene regulation and oxidative stress management. **Microbiology** 145: 1817–1830

Sridharan S, Wang L, Brown AK, Dover LG, Kremer L, Besra GS, Sacchettini JC (2007) X-ray crystal structure of *Mycobacterium tuberculosis* beta-ketoacyl-acyl carrier protein synthase II (*mt*KasB). **Journal of Molecular Biology** 366: 469–480

Srivastava SK, Dube D, Kukshal V, Jha AK, Hajela K, Ramachandran R (2007) NAD^+-dependent DNA ligase (Rv3014c) from *Mycobacterium tuberculosis*: novel structure-function relationship and identification of a specific inhibitor. **Proteins** 69: 97–111

Stock JB, Ninfa AJ, Stock AM (1989) Protein phosphorylation and regulation of adaptive responses in bacteria. **Microbiological Reviews** 53: 450–490

Stover CK, de la Cruz VF, Fuerst TR, Burlein JE, Benson LA, Bennett LT, Bansal GP, Young JF, Lee MH, Hatfull GF, Snapper SB, Barletta RG, Jacobs WR Jr., Bloom BR (1991) New use of BCG for recombinant vaccines. **Nature** 351: 456–460

Sturgill-Koszycki S, Schlesinger PH, Chakraborty P, Haddix PL, Collins HL, Fok AK, Allen RD, Gluck SL, Heuser J, Russell DG (1994) Lack of acidification in *Mycobacterium* phagosomes produced by exclusion of the vesicular proton-ATPase. **Science** 263: 678–681

Sukhova EV (2004) Need for psychological correction in patients with pulmonary tuberculosis. **Problemy Tuberculeza i Bolezneĭ Legkikh** 10: 34–36

Surolia N, Surolia A (2001) Triclosan offers protection against blood stages of malaria by inhibiting enoyl-ACP reductase of *Plasmodium falciparum*. **Nature Medicine** 7: 167–173

Takayama K, Kilburn JO (1989) Inhibition of synthesis of arabinogalactan by ethambutol in *Mycobacterium smegmatis*. **Antimicrobial Agents and Chemotherapy** 33: 1493–1499

Takayama K, Wang L, David HL (1972) Effect of isoniazid on the *in vivo* mycolic acid synthesis, cell growth, and viability of *Mycobacterium tuberculosis*. **Antimicrobial Agents and Chemotherapy** 2: 29–35

Takayama K, Wang C, Besra GS (2005) Pathway to synthesis and processing of mycolic acids in *Mycobacterium tuberculosis*. **Clinical Microbiology Reviews** 18: 81–101

Talaat AM, Lyons R, Howard ST, Johnston SA (2004) The temporal expression profile of *Mycobacterium tuberculosis* infection in mice. **Proceedings of the National Academy of Sciences of the United States of America** 101: 4602–4607

Tartoff KD, Hobbs CA (1987) Improved media for growing plasmid and cosmid clones. **Focus** 9: 12

Tasdemir D, Lack G, Brun R, Rüedi P, Scapozza L, Perozzo R (2006) Inhibition of *Plasmodium falciparum* fatty acid biosynthesis: evaluation of FabG, FabZ, and FabI as drug targets for flavonoids. **Journal of Medicinal Chemistry** 49: 3345–3353

Tchilian EZ, Desel C, Forbes EK, Bandermann S, Sander CR, Hill AV, McShane H, Kaufmann SH (2009) Immunogenicity and protective efficacy of prime-boost regimens with recombinant (delta)*ureC hly*$^{+}$ *Mycobacterium bovis* BCG and modified vaccinia virus ankara expressing M. tuberculosis antigen 85A against murine tuberculosis. **Infection and Immunity** 77: 622–631

Thakur M, Chakraborti PK (2008) Ability of PknA, a mycobacterial eukaryotic-type serine/threonine kinase, to transphosphorylate MurD, a ligase involved in the process of peptidoglycan biosynthesis. **Biochemical Journal** 415: 27–33

Thorn JM, Barton JD, Dixon NE, Ollis DL, Edwards KJ (1995) Crystal structure of *Escherichia coli* QOR quinone oxidoreductase complexed with NADPH. **Journal of Molecular Biology** 249: 785–799

Tobin DM, Ramakrishnan L (2008) Comparative pathogenesis of *Mycobacterium marinum* and *Mycobacterium tuberculosis*. **Cellular Microbiology** 10: 1027–1039

Toossi Z (2003) Virological and immunological impact of tuberculosis on human immunodeficiency virus type 1 disease. **Journal of Infectious Diseases** 188: 1146–1155

Triccas JA, Berthet FX, Pelicic V, Gicquel B (1999) Use of fluorescence induction and sucrose counterselection to identify *Mycobacterium tubercuosis* genes expressed within host cells. **Microbiology** 145: 2923–2930

Tripathi RP, Tewari N, Dwivedi N, Tiwari VK (2004) Fighting tuberculosis: An old disease with new challenges. **Medicinal Research Reviews** 25: 93–131

Trivedi OA, Arora P, Sridharan V, Tickoo R, Mohanty D, Gokhale RS (2004) Enzymic activation and transfer of fatty acids as acyl-adenylates in mycobacteria. **Nature** 428: 441–445

TubercuList World-Wide Web Server <http://genolist.pasteur.fr/TubercuList/>

Tuberculosis Research Section, scanning electron micrograph of *M. tuberculosis* cells <www.pasteur-guadeloupe.fr/tb/projects/NATO/>

Tumminia SJ, Rao PV, Zigler JS Jr., Russell P (1993) Xenobiotic induction of quinone oxidoreductase activity in lens epithelial cells. **Biochimica et Biophysica Acta** 1203: 251–259

Tyagi AK, Singh R, Gupta V (2008) The role of mycobacterial kinases and phosphatases in growth, pathogenesis, and cell wall metabolism *in* **The Mycobacterial Cell Envelope** pp. 323–344. Edited by Daffé M, Reyrat JM. Washington DC: American Society for Microbiology Press

United Nations Children's Fund (UNICEF; 2010) **Expanded Immunization Coverage** <www.unicef.org/immunization/index_coverage>

van Roermund CWT, Hettterna EH, Kal AJ, van den Berg M, Tabak HF, Wanders RJA (1998) Peroxisomal b-oxidation of polyunsaturated fatty acids in *Saccharomyces cerevisiae*: isocitrate dehydrogenase provides NADPH for reduction of double bonds at even positions. **European Molecular Biology Organization Journal** 17: 677–687

Vanzembergh F, Peirs P, Lefevre P, Celio N, Mathys V, Content J, Kalai M (2010) Effect of PstS sub-units or PknD deficiency on the survival of *Mycobacterium tuberculosis*. **Tuberculosis (Edinburgh)** 90: 338–345

Veyron-Churlet R, Guerrini O, Mourey L, Daffé M, Zerbib D (2004) Protein-protein interactions within the fatty acid synthase-II system of *Mycobacterium tuberculosis* are essential for mycobacterial viability. **Molecular Microbiology** 54: 1161–1172

Veyron-Churlet, Bigot S, Guerrini O, Verdoux S, Malaga W, Daffé M, Zerbib D (2005) The biosynthesis of mycolic acids in *Mycobacterium tuberculosis* relies on multiple specialized elongation complexes interconnected by specific protein-protein interactions. **Journal of Molecular Biology** 353: 847–858

Veyron-Churlet R, Molle V, Taylor RC, Brown AK, Besra GS, Zanella-Cléon I, Fütterer K, Kremer L (2009) The *Mycobacterium tuberculosis* beta-ketoacyl-acyl carrier protein synthase III activity is inhibited by phosphorylation on a single threonine residue. **Journal of Biological Chemistry** 284: 6414–6424

Veyron-Churlet R, Zanella-Cléon I, Cohen-Gonsaud M, Molle V, Kremer L (2010) Phosphorylation of the *Mycobacterium tuberculosis* beta-ketoacyl-acyl carrier protein reductase MabA regulates mycolic acid biosynthesis. **Journal of Biological Chemistry** 285: 12714–12725

Vilchèze C, Morbidoni HR, Weisbrod TR, Iwamoto H, Kuo M, Sacchettini JC, Jacobs WR Jr. (2000) Inactivation of the *inhA*-encoded fatty acid synthase II (FASII) enoyl-acyl carrier protein reductase induces accumulation of the FASI end products and cell lysis of *Mycobacterium smegmatis*. **Journal of Bacteriology** 182: 4059–4067

Vilchèze C, Wang F, Arai M, Hazbón MH, Colangeli R, Kremer L, Weisbrod TR, Alland D, Sacchettini JC, Jacobs WR Jr. (2006) Transfer of a point mutation in *Mycobacterium tuberculosis inhA* resolves the target of isoniazid. **Nature Medicine** 12: 1027–1029

Viveiros M, Martins M, Couto I, Rodrigues L, Machado D, Portugal I, Amaral L (2010) Molecular tools for rapid identification and novel effective therapy against MDRTB/XDRTB infections. **Expert Review of Anti-Infective Therapy** 8: 465–480

Vordermeier HM, Villarreal-Ramos B, Cockle PJ, McAulay M, Rhodes SG, Thacker T, Gilbert SC, McShane H, Hill AV, Xing Z, Hewinson RG (2009) Viral booster vaccines improve *Mycobacterium bovis* BCG-induced protection against bovine tuberculosis. **Infection and Immunity** 77: 3364–3373

Wakil SJ, Green DE, Mii S, Mahler HR (1954) Studies on the fatty acid oxidizing system of animal tissues. VI: β-Hydroxyacyl coenzyme A dehydrogenase. **Journal of Biological Chemistry** 207: 631–638

Walburger A, Koul A, Ferrari G, Nguyen L, Prescianotto-Baschong C, Huygen K, Klebl B, Thompson C, Bacher G, Pieters J (2004) Protein kinase G from pathogenic mycobacteria promotes survival within macrophages. **Science** 304: 1800–1804

Wang J, Soisson SM, Young K, Shoop W, Kodali S, Galgoci A, Painter R, Parthasarathy G, Tang YS, Cummings R, Ha S, Dorso K, Motyl M, Jayasuriya H, Ondeyka J, Herath K, Zhang C, Hernandez L, Allocco J, Basilio A, Tormo JR, Genilloud O, Vicente F, Pelaez F, Colwell L, Lee SH, Michael B, Felcetto T, Gill C, Silver LL, Hermes JD, Bartizal K, Barrett J, Schmatz D, Becker JW, Cully D, Singh SB (2006) Platensimycin is a selective FabF inhibitor with potent antibiotic properties. **Nature** 441: 358–361

Wang F, Langley R, Gulten G, Dover LG, Besra GS, Jacobs WR Jr., Sacchettini JC (2007a) Mechanism of thioamide drug action against tuberculosis and leprosy. **Journal of Experimental Medicine** 204: 73–78

Wang J, Kodali S, Lee SH, Galgoci A, Painter R, Dorso K, Racine F, Motyl M, Hernandez L, Tinney E, Colletti SL, Herath K, Cummings R, Salazar O, González I, Basilio A, Vicente F, Genilloud O, Pelaez F, Jayssuriya H, Young K, Cully DF, Singh SB (2007b) Discovery of platencin, a dual FabF and FabH inhibitor with *in vivo* antibiotic properties. **Proceedings of the National Academy of Sciences of the United States of America** 104: 7612–7616

Wang J, Sintim HO (2011) Dialkylamino-2,4-dihydroxybenzoic acids as easily synthesized analogues of platensimycin and platencin with comparable antibacterial properties. **Chemistry** 17: 3352–3357

Watanabe M, Aoyagi Y, Ridell M, Minnikin DE (2001) Separation and characterization of individual mycolic acids in representative mycobacteria. **Microbiology** 147: 1825–1837

Watanabe M, Aoyagi Y, Mitome H, Fujita T, Naoki H, Ridell M, Minnikin DE (2002) Location of functional groups in mycobacterial meromycolate chains; the recognition of new structural principles in mycolic acids. **Microbiology** 148: 1881–1902

Wehenkel A, Bellinzoni M, Graña M, Duran R, Villarino A, Fernandez P, Andre-Leroux G, England P, Takiff H, Cerveñansky C, Cole ST, Alzari PM (2008) Mycobacterial Ser/Thr protein kinases and phosphatases: physiological roles and therapeutic potential. **Biochimica et Biophysica Acta** 1784: 193–202

Wen L, Chmielowski JN, Bohn KC, Huang JK, Timsina YN, Kodali P, Pathak AK (2009) Functional expression of *Francisella tularensis* FabH and FabI, potential antibacterial targets. **Protein Expression and Purification** 65: 83–91

Wheeler PR, Bulmer K, Ratledge C (1990) Enzymes for biosynthesis *de novo* and elongation of fatty acids in mycobacteria grown in host cells: is *Mycobacterium leprae* competent in fatty acid biosynthesis? **Journal of General Microbiology** 136: 211–217

Wheeler PR, Bulmer K, Ratledge C (1991) Fatty acid oxidation and the beta-oxidation complex in *Mycobacterium leprae* and two axenically cultivable mycobacteria that are pathogens. **Journal of General Microbiology** 137: 885–893

Wheeler PR, Ratledge C (1994) Metabolism of *Mycobacterium tuberculosis in* **Tuberculosis: Pathogenesis, Protection and Control** pp. 353–385. Edited by Bloom BR. Washington DC: American Society for Microbiology

Wiker HG, Harboe M (1992) The antigen 85 complex: a major secretion product of *Mycobacterium tuberculosis*. **Microbiological Reviews** 56: 648–661

Wilbrink MH, Petrusma M, Dijkhuizen L, van der Geize R (2011) FadD19 of *Rhodococcus rhodochrous* DSM43269, a steroid-coenzyme A ligase essential for degradation of C-24 branched sterol side chains. **Applied and Environmental Microbiology** 77: 4455–4464

Williams KJ, Boshoff HI, Krishnan N, Gonzales J, Schnappinger D, Robertson BD (2011) The *Mycobacterium tuberculosis* β-oxidation genes *echA5* and *fadB3* are dispensible for growth *in vitro* and *in vivo*. **Tuberculosis (Edinburgh).** 91: 549–555

Williamson G, Engel PC (1984) Butyryl-CoA dehydrogenase from *Megasphaera elsdenii*. Specificity of the catalytic reaction. **Journal of Biochemistry** 218: 521–529

Wilson M, DeRisi J, Kristensen H, Imboden P, Rane S, Brown PO, Schoolnik GK (1999) Exploring drug-induced alterations in gene expression in *Mycobacterium tuberculosis* by microarray hybridization. **Proceedings of the National Academy of Sciences of the United States of America** 96: 12833–12838

Winkler U, Säftel W, Stabenau H (2003) A new type of multifunctional beta-oxidation enzyme in euglena. **Plant Physiology** 131: 753–762

Wolinsky E, Steenken W Jr. (1947) Effect of streptomycin on the tubercle bacillus. **American Review of Tuberculosis** 55: 281–288

World Health Organisation (WHO; 2009) Global tuberculosis control – epidemiology, strategy, financing. **Programmes and Projects** WHO Report 2009

World Health Organisation (WHO; 2010) Tuberculosis. **Media Centre:** Factsheet No. 104

Wright A, Bai G, Barrera L, Boulahbal F, Martín-Casabona N, Gilpin C Drobniewski F, Havelková M, Lepe R, Lumb R, Metchock B, Portaels F, Rodrigues M, Rüsch-Gerdes S, van Deun A, Vincent V, Leimane V, Riekstina V, Skenders G, Holtz T, Pratt R, Laserson K, Wells, C, Cegielski P, Shah NS (2006) Emergence of *Mycobacterium tuberculosis* with extensive resistance to second-line drugs-worldwide, 2000-2004. **MMWR Morbidity and Mortality Weekly Report** 55: 301–305

Xu S, Cooper A, Sturgill-Koszycki S, van Heyningen T, Chatterjee D, Orme I, Allen P, Russell DG (1994) Intracellular trafficking in *Mycobacterium tuberculosis* and *Mycobacterium avium*-infected macrophages. **Journal of Immunology** 153: 2568–2578

Yagi T, Di Bernardo S, Nakamaru-Ogiso E, Kao MC, Seo BB, Matsuno-Yagi A (2004) NADH Dehydrogenases (NADH-Quinone Oxidoreductase) *in* **Respiration in Archaea and Bacteria** pp. 15–40. Edited by Zannoni D. Dordrecht: Kluwer Academic Publishers

Yang JK, Yoon HJ, Ahn HJ, Lee BI, Cho SH, Waldo GS, Park MS, Suh SW (2002) Crystallization and preliminary X-ray crystallographic analysis of the Rv2002 gene product from *Mycobacterium tuberculosis*, a beta-ketoacyl carrier protein reductase homologue. **Acta Crystallographica Section D: Biological Crystallography** 58: 303–305

Youmans GP (1945) The effect of streptomycin *in vitro* on *M. tuberculosis* var. *hominis*. **Quarterly Bulletin of the Northwestern University Medical School** 20: 420

Yuan Y, Lee RE, Besra GS, Belisle JT, Barry CE 3rd (1995) Identification of a gene involved in the biosynthesis of cyclopropanated mycolic acids in *Mycobacterium tuberculosis*. **Proceedings of the National Academy of Sciences of the United States of America** 92: 6630–6634

Yuan Y, Barry CE 3rd (1996) A common mechanism for the biosynthesis of methoxy and cyclopropyl mycolic acids in *Mycobacterium tuberculosis*. **Proceedings of the National Academy of Sciences of the United States of America** 93: 12828–12833

Zampieri D, Grazia Mamolo M, Laurini E, Scialino G, Banfi E, Vio L (2009) 2-Aryl-3-(1*H*-azol-1-yl)-1*H*-indole derivatives: A new class of antimycobacterial compounds – conventional heating in comparison with MW-assisted synthesis. **Archiv der Pharmazie** 342: 716–722

Zhang C, Ondeyka J, Herath K, Jayasuriya H, Guan Z, Zink DL, Dietrich L, Burgess B, Ha SN, Wang J, Singh SB (2011) Platensimycin and platencin congeners from *Streptomyces platensis*. **Journal of Natural Products** 74: 329–340

Zhang G, Campbell EA, Minakhin L, Richter C, Severinov K, Darst SA (1999) Crystal structure of *Thermus aquaticus* core RNA polymerase at 3.3 Å resolution. **Cell** 98: 811–824

Zheng X, Papavinasasundaram KG, Av-Gay Y (2007) Novel substrates of *Mycobacterium tuberculosis* PknH Ser/Thr kinase. **Biochemical and Biophysical Research Communications** 355: 162–168

Zhang Y, Heym B, Allen B, Young D, Cole S (1992) The catalase-peroxidase gene and isoniazid resistance of *Mycobacterium tuberculosis*. **Nature** 358: 591–593

Zhang Y, Young DB (1993) Molecular mechanisms of isoniazid: a drug at the front line of tuberculosis control. **Trends in Microbiology** 1: 109–113

Zhang Y, Vilcheze C, Jacobs WR Jr. (2005) Mechanisms of drug resistance in *Mycobacterium tuberculosis* in **Tuberculosis and the Tubercle Bacillus** pp. 115–140 Edited by Cole ST, Davis Eisenbach K, McMurray DN, Jacobs WR Jr. Washington DC: American Society for Microbiology

Zhang Y, Yew WW (2009) Mechanisms of drug resistance in *Mycobacterium tuberculosis*. **International Journal of Tuberculosis and Lung Disease** 13: 1320–1330

Zimhony O, Cox JS, Welch JT, Vilchèze C, Jacobs WR Jr. (2000) Pyrazinamide inhibits the eukaryotic-like fatty acid synthetase I (FASI) of *Mycobacterium tuberuclosis*. **Nature Medicine** 6: 1043–1047

Zimhony O, Vilchèze C, Arai M, Welch JT, Jacobs WR Jr. (2007) Pyrazinoic acid and its *n*-propyl ester inhibit fatty acid synthase type I in replicating tubercle bacilli. **Antimicrobial Agents and Chemotherapy** 51: 752–754

Zink AR, Sola C, Reischl U, Grabner W, Rastogi N, Wolf H, Nerlich AG (2003) Characterization of *Mycobacterium tuberculosis* complex DNAs from Egyptian mummies by spoligotyping. **Journal of Clinical Microbiology** 41: 359–367

Zuber B, Chami M, Houssin C, Jacques D, Griffiths G, Daffé M (2008) Direct visualization of the outer membrane of *Mycobacteria* and *Corynebacteria* in their native state. **Journal of Bacteriology** 190: 5672–5680